

NQ

3 9 6 1 0

U M I
MICROFILMED 1999

INFORMATION TO USERS

This manuscript has been reproduced from the microfilm master. UMI films the text directly from the original or copy submitted. Thus, some thesis and dissertation copies are in typewriter face, while others may be from any type of computer printer.

The quality of this reproduction is dependent upon the quality of the copy submitted. Broken or indistinct print, colored or poor quality illustrations and photographs, print bleedthrough, substandard margins, and improper alignment can adversely affect reproduction.

In the unlikely event that the author did not send UMI a complete manuscript and there are missing pages, these will be noted. Also, if unauthorized copyright material had to be removed, a note will indicate the deletion.

Oversize materials (e.g., maps, drawings, charts) are reproduced by sectioning the original, beginning at the upper left-hand corner and continuing from left to right in equal sections with small overlaps. Each original is also photographed in one exposure and is included in reduced form at the back of the book.

Photographs included in the original manuscript have been reproduced xerographically in this copy. Higher quality 6" x 9" black and white photographic prints are available for any photographs or illustrations appearing in this copy for an additional charge. Contact UMI directly to order.

UMI[®]

Bell & Howell Information and Learning
300 North Zeeb Road, Ann Arbor, MI 48106-1346 USA
800-521-0600

UNIVERSITY OF ALBERTA

AN AUTOMATED DIRECT SAMPLE INSERTION-INDUCTIVELY COUPLED
PLASMA SPECTROMETER FOR ENVIRONMENTAL SAMPLE ANALYSIS

by

LISHI YING ©

A Thesis Submitted to the Faculty of Graduate Studies and Research in Partial Fulfillment
of the Requirements for the Degree of Doctor of Philosophy

DEPARTMENT OF CHEMISTRY

EDMONTON, ALBERTA

SPRING, 1999



National Library
of Canada

Acquisitions and
Bibliographic Services

395 Wellington Street
Ottawa ON K1A 0N4
Canada

Bibliothèque nationale
du Canada

Acquisitions et
services bibliographiques

395, rue Wellington
Ottawa ON K1A 0N4
Canada

Your file Votre référence

Our file Notre référence

The author has granted a non-exclusive licence allowing the National Library of Canada to reproduce, loan, distribute or sell copies of this thesis in microform, paper or electronic formats.

The author retains ownership of the copyright in this thesis. Neither the thesis nor substantial extracts from it may be printed or otherwise reproduced without the author's permission.

L'auteur a accordé une licence non exclusive permettant à la Bibliothèque nationale du Canada de reproduire, prêter, distribuer ou vendre des copies de cette thèse sous la forme de microfiche/film, de reproduction sur papier ou sur format électronique.

L'auteur conserve la propriété du droit d'auteur qui protège cette thèse. Ni la thèse ni des extraits substantiels de celle-ci ne doivent être imprimés ou autrement reproduits sans son autorisation.

0-612-39610-X

Canada

UNIVERSITY OF ALBERTA
RELEASE FORM

NAME OF AUTHOR: Lishi Ying

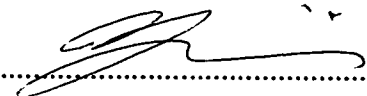
TITLE OF THESIS: An Automated Direct Sample Insertion-Inductively Coupled
Plasma Spectrometer for Environmental Sample Analysis.

DEGREE: DOCTOR OF PHILOSOPHY

YEAR THIS DEGREE GRANTED: 1999

Permission is hereby granted to the University of Alberta Library to reproduce single copies of this thesis and to lend or sell such copies for private, scholarly or scientific research purposes only.

The author reserves all other publication and other right in association with the copyright in the thesis, and except as hereinbefore provided neither the thesis nor any substantial portion thereof may be printed or otherwise reproduced in any material form whatever without the author's prior written permission.



.....

(Student's Signature)

Permanent Address:

7403 - 182 street

Edmonton, Alberta

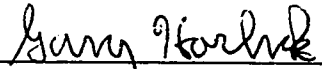
Canada T5T 2G8

Date: Jan. 18, 1999

UNIVERSITY OF ALBERTA

FACULTY OF GRADUATE STUDIES AND RESEARCH

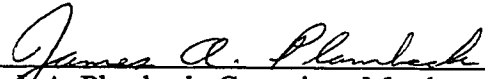
The undersigned certify that they have read, and recommend to the **Faculty of Graduate Studies and Research** for acceptance, a thesis entitled AN AUTOMATED DIRECT SAMPLE INSERTION - INDUCTIVELY COUPLED PLASMA SPECTROMETER FOR ENVIRONMENTAL SAMPLE ANALYSIS submitted by LISHI YING in partial fulfillment of the requirements for the degree of Doctor of Philosophy.



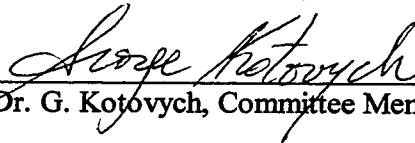
Dr. G. Horlick, Supervisor



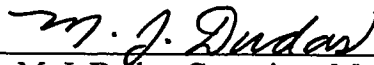
Dr. B. G. Kratochvil, Committee Chairman



Dr. J. A. Plambeck, Committee Member



Dr. G. Kotovych, Committee Member



Dr. M. J. Dudas, Committee Member



Dr. V. Karanassios, External Examiner

Date: Jan 18, 1999

To Ross, George and Dawn

Abstract

Simultaneous multielement determinations were carried out on microgram portions of environmental samples by direct sample insertion - inductively coupled plasma emission spectrometry (DSI-ICP-AES). The success of the determination was mainly due to the use of oxygen (20%) in the plasma operation. As a result, the samples were burned into the plasma facilitated the direct determination of elements with different volatilities in hard to vaporize matrices. The samples used in the study included stack flyash, kiln slag, and landfill cell leachate from a hazardous waste treatment plant. The results of these analyses obtained from DSI-ICP were compared with the results obtained from conventional solution nebulization ICP after microwave acid digestion.

An automatic sample insertion system with a 24- sample holder tray was developed for the DSI system in order to speed up the analysis and provide consistency for each insertion. A simple car antenna was employed as the insertion driver. Insertion positions were controlled by a magnet and a Hall sensor. A dedicated computer with Window based custom software was developed to control the autosampler and synchronize data acquisition operation.

A dual mode torch was developed to accommodate both conventional solution nebulization operation and direct sample insertion. By placing or removing a cap on the central tube of the torch, either solution or solid sample analysis could be performed on a single torch. The sensitivity and stability for the solution operation on the dual mode torch were equivalent to the original set-up.

The new DSI sub-system was mounted on a LECO Plasma-Array spectrometer. Linear calibration curves for As, Cd, Cu, Mn, Pb and Zn were obtained. The average relative standard deviation for multiple analyses of solution residues was around 6 %.

The system was then used for the determination of volatile elements in different NIST SRMs that included soil, ash, food and leaves. The results indicated that the partial matrix matched solution residues were valid for calibration in the determination of volatile elements in solid samples. In general, the results obtained with DSI were in good agreement with NIST certified values.

Acknowledgements

I would like to thank my supervisor, Professor Gary Horlick for his invaluable advice and very patient guidance throughout this work. I would also like to thank all members of the research group for their assistance and thoughtful discussions.

I thanks to the staff of the Chemistry Department Electronics, Machine and Glass shops for their help.

Finally, I would like to acknowledge the Department of Chemistry for financial support.

GLOSSARY OF ABBREVIATIONS

ADC	Analog-to-Digital Converter
APDC	Ammonium Pyrolidine DithioCarbamate
ASCI	American Standard Code for Information and Interchange
BAS	Bureau of Analysed Samples (U. K.)
BCR	Community Bureau of Reference (U. K.)
CBNM	Central Bureau for Nuclear Measurement
CCD	Charge Coupled Device
CID	Charge Injection Device
CRM	Certified Reference Material
CTD	Charge Transferred Device
D/A	Digital to Analog Conversions
DSI	Direct sample insertion
EDM	Electrical Discharge Machining
EPA	Environmental Protection Agency
ETV	Electrothermal Vaporization
EU	European Union
FAAS	Flame Atomic Absorption spectroscopy
FAES	Flame Atomic Emission spectroscopy
GFAAS	Graphite Furnace Atomic Absorption spectroscopy
HDPE	High Density PolyEthylene
ICP	Inductively coupled plasma
ICP-AES	Inductively Coupled Plasma Atomic Emission Spectroscopy
ICP-MS	Inductively Coupled Plasma Mass Spectroscopy
INAA	Instrumental Neutron Activation Analysis
I/O	Digital Input and Output transfers
IR	Infrared
ITV	In-Touch Vaporization
LA	laser Ablation
NAA	Neutron Activation Analysis
NIST	National Institute of Standards and Technology (U. S.)
NRC	National Research Council of Canada
PA	Power Amplifier
PCBs	PolyChlorinated Biphenyls
PDA	PhotoDiode Array
PMT	PhotoMultiplier Tube
PSP	Pre-Selection Polychromator
RCRA	Resource Conservation and Recovery Act
RF	Radio Frequency
RM	Reference Material
RSD	Relative Standard Deviation
S/N	Signal to Noise ratio
SRM	Standard Reference Materials

SS	Solid Sampling
TCLP	Toxicity Characteristic Leaching Procedure
TOF	Time of Flight
TTL	Transistor Transistor Logic
USGS	U. S. Geological Survey
UV	Ultraviolet
VDA	Verband der Automobilindustrie
VRWR	Variable Standard Waveform Ratio
XRF	X-Ray Fluorescence
ZAAS	Zeeman Atomic Absorption Spectrometry
BCR CRM142R	Light Sandy Soil
BCR CRM143R	Sewage Sludge Amended Soil
BCR CRM145R	Sewage Sludge
BCR CRM 176	City Waste Incineration Ash
BCR CRM185	Bovine Liver
BCR CRM 422	Cod Muscle
NIST SRM 679	Brick Clay
NIST SRM1515	Apple Leaves
NIST SRM 1547	Peach Leaves
NIST SRM 1566a	Oyster Tissue
NIST SRM 1568a	Rice Flour
NIST SRM 1570a	Spinach Leaves
NIST SRM 1571	Orchard Leaves
NIST SRM 1572	Citrus Leaves
NIST SRM 1573a	Tomato Leaves
NIST SRM 1577a	Bovine Liver
NIST SRM 1632b	Trace Elements in Coal (bituminous)
NIST SRM 1633a	Trace Elements in Coal Fly Ash
NIST SRM 1633b	Trace Elements in Coal Fly Ash
NIST SRM 1635	Trace Elements in Coal (Sub-bituminous)
NIST SRM 1648	Urban Particulate,
NIST SRM 2689	Coal Fly Ash (Low Calcium Concentration)
NIST SRM 2690	Coal Fly Ash (Medium Calcium Concentration)
NIST SRM 2691	Coal Fly Ash (High Calcium Concentration)
NIST SRM 2704	Buffalo River Sediment
NIST SRM 2709	San Joaquin Soil Baseline Trace Element Concentrations
NIST SRM 2710	Montana Soil Highly Elevated Traces Element Concentrations
NIST SRM 2711	Montana Soil Moderately Elevated Trace Element Concentrations
NIST SRM 4355	Peruvian Soil

TABLE OF CONTENTS

CHAPTER	PAGE
1 General Introduction.....	1
1.1 Background.....	1
1.2 Current Status of Direct Solids Analysis for Elemental Determination by ICP Spectrometry.....	2
1.21 Direct Sample Insertion (DSI).....	2
1.22 Electrothermal Vaporization (ETV).....	11
1.23 Laser Ablation (LA).....	13
1.24 Slurry Sampling.....	16
1.3 Recent Developments in Standard Reference Materials.....	18
1.31 Soil, Sediment and Ash Materials.....	18
1.32 Botanical, Biological and Food Materials.....	22
1.4 Sample Homogeneity Issues for Direct Solids Analysis.....	24
1.5 Objectives of This Research Work.....	29
References.....	31
2 Environmental Sample Analysis by Ar-O ₂ Mixed Gases DSI-ICP.....	35
2.1 Brief Overview.....	35
2.11 The DSI-ICP Instrument Setup.....	36
2.12 The Drive Assembly.....	36
2.13 Computer with Control Board.....	38
2.14 The Torch and Gases.....	40
2.15 The Probe.....	41
2.16 Software.....	43
2.17 DSI Sample Analysis.....	44
2.2 Sample Analysis by Conventional ICP.....	45
2.21 Conventional ICP Used in this Study.....	45
2.22 Microwave Sample Digestion.....	49

2.23 Chemicals and Reagents.....	52
2.24 Standard Reference Materials.....	53
2.3 Source of Sample - An Industrial Waste Treatment Plant.....	54
2.31 Introduction of Waste Process in a Hazardous Waste Plant.....	54
2.32 Flyash and Slag (Bottom Ash).....	54
2.33 Landfill Cell.....	57
2.4 Sample Analysis by Ar-O ₂ -Ar Mixed Gas DSI-ICP.....	59
2.41 Analysis Procedure.....	59
2.411 Calibration Curve.....	59
2.412 Instrument Stability and Sample Homogeneity.....	63
2.42 Leachate Analysis.....	68
2.421 Background.....	68
2.422 Results and Discussion.....	70
2.43 Slag and Flyash Analysis.....	71
2.431 Background.....	71
2.432 Results and Discussion.....	75
2.44 Standard Reference Materials Analysis.....	80
2.441 Background.....	80
2.442 Results and Discussion.....	80
2.45 NIST Wear Metal Oil Analysis.....	82
2.451 Background.....	82
2.452 Results and Discussion.....	91
2.5 Limitations and Future Work.....	91
References.....	95

3 Development of an Automated

Solid/Liquid Interchangeable DSI-ICP System.....	97
3.1 Introduction.....	97
3.2 Objectives.....	98
3.3 Leco Spectrometer.....	98

3.31 Optics.....	98
3.32 Mask.....	103
3.33 RF Generator.....	104
3.34 Plasma.....	107
3.35 Detector.....	107
3.36 Detection System.....	108
3.4 Autosampler for DSI.....	108
3.41 Background.....	108
3.42 Torch.....	109
3.43 Antenna.....	114
3.44 Position Sensor.....	119
3.45 Shutter.....	125
3.46 Carousel.....	125
3.47 Turn Table.....	131
3.48 Mounting.....	131
3.49 Sample Plug Insertion and Retraction.....	133
3.410 Data Acquisition Board.....	134
3.411 Synchronization.....	136
3.5 Software.....	139
3.51 Background.....	139
3.52 DSID Program Windows Application.....	139
3.6 Summary.....	151
References.....	152
4 Basic Performance of An Automated DSI-ICP with a Dual-mode Torch.....	154
4.1 Introduction.....	154
4.2 Principle of Non Cross-Dispersive Echelle Spectrometer.....	154
4.3 Characterization of Dual-Mode Torch for Solution Analysis.....	156
4.4 Characterization of Dual-Mode Torch for DSI.....	165
4.41 DSI Ar -O ₂ Mixed Gas Plasma.....	165

4.42 Chemical Modifier.....	165
4.43 DSI Ar Plasma.....	168
4.5 Conclusion.....	174
References.....	182
5 Direct Analysis of NIST Standard Reference Materials by an Automated DSI-ICP.....	183
5.1 Introduction.....	183
5.2 Soil and Ash.....	185
5.21 Background.....	185
5.22 Results and Discussion.....	188
5.3 Food.....	201
5.31 Background.....	201
5.32 Results and Discussion.....	201
5.4 Leaves.....	209
5.41 Background.....	209
5.42 Results and Discussion.....	213
5.5 Replicate Analysis of Spinach Leaves.....	218
5.6 Summary.....	221
References.....	222
6 Summary and Future Work.....	224
6.1 Summary.....	224
6.2 Future Work.....	226
References.....	228

FIGURE	PAGE
1.1 Schematic diagram of a typical direct sample insertion system.....	4
2.1 Schematic diagram of an Ar-O ₂ (20%) mixed gas DSI-ICP-AES.....	37
2.2 Graphite sample probes (a) before burning and (b) after burning.....	42
2.3 Leeman Labs. ICP Echelle optics.....	47
2.4 Microwave digestion system diagram with a control vessel diagram.....	51
2.5 Hazardous waste plant process diagram.....	55
2.6 Slagging rotary kiln incineration system.....	56
2.7 Landfill cell.....	58
2.8 Nine element log-log calibration curves.....	60
2.9 Signals at 1ppm concentration for nine elements.....	61
2.10 Signals at 10ppm concentration for nine elements.....	62
2.11 Sampling study of Cr in five different matrices.....	65
2.12 Cr peak profiles in five different matrices.....	66
2.13 Six element peak profiles in leachate.....	73
2.14 Four element peak profiles in slag.....	77
2.15 Three element peak profiles in stack ash.....	79
2.16 Fe calibration curves by standard reference materials.....	83
2.17 Cu calibration curves by standard reference materials.....	84
2.18 Cr calibration curves by standard reference materials.....	85
2.19 Zn calibration curves by standard reference materials.....	86
2.20 Fe signals in different SRM matrices.....	87
2.21 Cu signals in different SRM matrices.....	88
2.22 Cr signals in different SRM matrices.....	89
2.23 Zn signals in different SRM matrices.....	90
2.24 100 ppm Cr, Cu, Pb and V in NIST wear metal oil.....	93
3.1 Schematic diagram of an automated direct sample insertion device for ICP-AES.....	99
3.2 Leco optical diagram.....	101
3.3 Six element mask.....	105

3.4	Twenty four element mask.....	106
3.5	A typical Fassel type torch (a), dual-mode torch (b) and a cap (c).....	111
3.6	Diagram of the torch set-up with a spray chamber.....	112
3.7	Automated direct sample insertion system.....	113
3.8	Schematic diagram of car antenna	115
3.9	Interface box.....	116
3.10	DT707 screw terminal panel.....	117
3.11	Diagram of antenna head part.....	118
3.12	Hall effect sensor.....	120
3.13	Sensor electronic diagram.....	121
3.14	Hall effect sensor holder.....	124
3.15	Diagram of shutter.....	128
3.16	Diagram of the solid sample autosampler.....	129
3.17	Sample plug with electrode.....	130
3.18	Carousel organizer.....	132
3.19	Autosampler fifteen pin connector.....	137
3.20(a)	The flow chart of DSI window application - main menu.....	141
3.20(b)	The flow chart of DSI window application - carousel.....	142
3.20(c)	The flow chart of DSI window application - antenna.....	143
3.21(a)	Screen copy of DC Motor program for MS Windows. The carrousel control dialog box is shown.....	144
3.21(b)	Screen copy of DC Motor program for MS Windows. The cup positions control dialog box is shown.....	146
3.21(c)	Screen copy of DC Motor program for MS Windows. The run status dialog box is shown.....	147
3.21(d)	Screen copy of DC Motor program for MS Windows. The warning dialog box is shown.....	148
3.21(e)	Screen copy of DC Motor program for MS Windows. The warning pop up window is shown.....	149

3.21(f)	Screen copy of DC Motor program for MS Windows.	
	The Tune up dialog box is shown.....	150
4.1	Diagram of a mask.....	155
4.2	Lateral scan of ICP torch.....	160
4.3	(a) Spectrum of super solution: original LECO ICP torch	
	(b) Spectrum of super solution: dual-mode torch.....	161
4.4	Sample take up time and wash time for solution nebulization.....	163
4.5	Signal stability of Leco ICP with a dual-mode torch.....	164
4.6	Pb, Zn, Ni Cr, and Cu spectrum of flyash in Ar-O ₂ mix gas plasma.....	166
4.7	NaF effect on SRM 2704 Buffalo River Sediment in Ar plasma.....	167
4.8	Pb, Zn Ni, Cr and Cu spectrum of 10 ppm solution residue in Ar plasma....	172
4.9	Pb, Zn, Ni Cr and Cu spectrum of flyash in Ar plasma.....	173
4.10	Lateral scan of DSI-ICP torch.....	174
4.11	Power effect on DSI signal.....	175
4.12	Calibration curves for super solution.....	176
4.13	Al, Cd, Cu, Mg and Zn spectrum of solution residue at different calibration concentrations.....	177
4.14	Calibration curves for As, Mn and Pb.....	178
4.15	Replicate measurement of 1/5 Leco super solution in Ar plasma.....	179
4.16	Replicate measurement of 10 ppm standard solution in Ar plasma.....	180
5.1	Pb concentrations in NIST Coal Ash SRMs.....	190
5.2	Pb concentrations in NIST Soil SRMs.....	191
5.3	Pb concentrations in NIST Ash and Soil SRMs.....	192
5.4	Zn concentrations in NIST Ash and Soil SRMs.....	193
5.5	Pb and Zn spectrum of SRM 2704 Buffalo River Sediment.....	196
5.6	As concentrations in NIST Ash and Soil samples.....	197
5.7	Cd concentrations in NIST Ash and Soil samples.....	198
5.8	As spectra of SRM 1633b Coal Flyash.....	199
5.9	Cd spectra of NIST Soils.....	200
5.10	Zn concentrations in NIST Food SRMs.....	204

5.11	Cu concentrations in NIST Food SRMs.....	205
5.12	Mn concentrations in NIST Food SRMs.....	206
5.13	Zn and Cu spectra for Food SRMs.....	207
5.14	Zn and Cu spectrum of SRM Oyster Tissues.....	208
5.15	Mn spectra for two NIST Food SRMs.....	210
5.16	Zn concentrations in NIST Leaf SRMs.....	215
5.17	Cu concentrations in NIST Leaf SRMs.....	216
5.18	Zn and Cu spectra of NIST Leaf SRMs.....	217
5.19	Variability of results for replicate determinations of Zn and Cu in NIST Spinach Leaves (SRM 1570a).....	219
5.20	Variability of results for replicate determinations of Zn and Cu in NIST Spinach Leaves (SRM 1570).....	220

TABLE	PAGE	
2.1	Hardware specifications and typical operating conditions for the Ar-O ₂ mixed gas DSI-ICP system.....	39
2.2	Specifications of Leeman Labs. ICP.....	46
2.3	Specification of MDS-2000 microwave oven	50
2.4	Operation parameters of microwave digestion oven.....	53
2.5	RSD summary of replicate analyses.....	64
2.6	Sampling data summary.....	67
2.7	Summary of leachate results.....	72
2.8	Bottom ash (slag) data summary.....	76
2.9	Stack ash data summary.....	78
2.10	Metal concentrations of standard reference materials.....	81
2.11	DSI-ICP analysis results of NIST wear metal oil.....	92
3.1	Leco ICP Technical Specifications.....	102
3.2	Hall Effect Digital Switch Maximum Ratings.....	122
3.3	Carousel tray specifications.....	126
3.4	Specifications of DT2801-A Digital I/O Subsystem.....	135
3.5	Synchronized operation parameters for DSI operation.....	138
4.1	Metal concentrations (ppm) in super solution and its series dilution.....	157
4.2	MEM6 wavelength positions on camera.....	158
4.2	MEM24 wavelength positions on camera.....	169
4.4	Typical operating conditions of ICP in the experiment.....	171
5.1	Pb and Zn concentrations of NIST SRM Ash and Soil.....	189
5.2	As and Cd concentrations of NIST SRM Ash and Soil.....	195
5.3	Zn, Cu and Mn concentrations of NIST SRM Food.....	203
5.4	Zn and Cu concentrations of NIST SRM Leaves.....	214

Chapter 1

General Introduction

1.1 Background

In the continuing development of analytical atomic spectroscopy there is emphasis on the establishment of reliable and robust methods. A constantly expanding area is that of sampling and sample preparation. Partly this reflects the sustained realization of the need to use robust and valid methodology, and partly it reflects the continued search for simple, low cost and safe methods.

A number of research projects in our group are aimed at the development of simple and robust methodology. Direct sample insertion (DSI) for inductively coupled plasma (ICP) spectrometry is one of such techniques. It provides a simple way to analyze a solid sample and several theses have been completed on this subject. This research project is focused on further development of the DSI device and validation of real world application.

Standard Reference Materials (SRM) are widely used for quality control and method validation in analytical chemistry. One of the difficulties in direct solids analysis is lack of suitable solid standards for calibration. Sometimes, even when the SRM is available for the analysis, the homogeneity of the material may not be good enough for direct calibration due to the fact that a small quantity of material is used by most direct solids analysis methods. Recent developments in direct solids analysis methods for elemental determinations and developments in SRMs will be reviewed in this chapter to provide a background for the work to follow.

1.2 Current status of direct solids analysis for elemental determinations by ICP Spectrometry

Inductively coupled plasmas (ICPs) possess exceptional characteristics that make them excellent sources for vaporization, atomization, ionization and excitation. If there is a shortcoming in their universal analytical application, it is the general requirement that the sample be in liquid form for analysis. This requirement derives from the vast experience in nebulization of liquids that facilitated the initial development of the analytical utilization of ICPs. There is, however, no fundamental limitation preventing the use of these plasmas for the analysis of solids. Because many samples occur naturally in solid form, a number of analytical and practical advantages can be realized when solid samples are introduced directly into the ICP, without pretreatment or conversion to liquid. Ideally, when sample is analyzed in its natural state; contamination from reagents is minimized; dilution errors are eliminated; sample transfer losses arising from sample handling steps are avoided; the time delay between sample collection and analysis is diminished; reagent and labour costs are reduced; the potential for improved absolute detection limits is enabled; analysis of microsamples or localized segments of samples is facilitated; and sample vaporization, atomization, and excitation steps may be separated and optimized.

Direct solid sample analysis for elemental determination using inductively coupled plasma atomic emission spectrometry or mass spectrometry (ICP-AES/MS) is an area of growth. One of the reasons for this is that a multi-element determination can be made very quickly if the sample can be analyzed without pre-treatment. There are several approaches for delivering solid samples. These approaches include direct sample insertion (DSI), electrothermal vaporization (ETV), laser ablation (LA), arc and spark discharges, and slurry nebulization. Each method has its own strengths and limitations, and is used for certain specific applications.

1.21 Direct sample insertion (DSI)

The direct sample insertion device was first introduced in 1979 by Salin and Horlick [1]. Subsequent systems have been developed based on this concept since then within Horlick's group [2-6]. At the same time, other groups around world have also developed their own version of DSI devices [7-9]. A schematic diagram of a typical DSI system is shown in Figure 1.1. It consists of a torch, a sample probe and an insertion mechanism (usually a motor). A sample, either solution or solid, is placed on the top of the probe. Then the probe is inserted into the central tube of the torch. Before the sample probe enters the plasma, it may stop below the plasma for drying and/or ashing. Once the probe is driven into the core of the plasma, the sample is rapidly vaporized, atomized, excited and ionized.

The DSI device has been improved dramatically from the original version of two decades ago. These improvements include the insertion mechanism, data acquisition, sample treatment, sample probe and automation. A thorough review of these reports were summarized by Karanassios and Horlick up until 1990 [10]. In the following section recent DSI-ICP developments and applications are reviewed.

A method using pellet direct sample insertion for ICP-AES was developed by Blain and Salin [11-13]. A sediment standard reference material, PACS-1 (National Research Council of Canada) was mixed with graphite powder at a 1:5 ratio to form a pellet which was inserted into the plasma. The rationale behind using pellets instead of graphite cups was to increase the mass of sample inserted in the plasma and to improve the contact between the sample and the plasma. Sharp and intense peaks were recorded for elements of high and intermediate volatility (As, Cd, Cu, Hg, Mn, Pb, Se, Sn, Zn). It was found that internal standardization compensated for variations in volatilization interferences and changes in excitation conditions between sediment standards. It was also found that the method of standard additions allowed accurate calibration of the technique. Sub-ppm detection limits were typical for these elements.

The use of thermochemical additives to enhance the vaporization of refractory elements was also investigated by Blain and Salin [11-13]. It was found that chloride releasing reagents were preferable to fluoride salts, because the fluorides caused a sudden

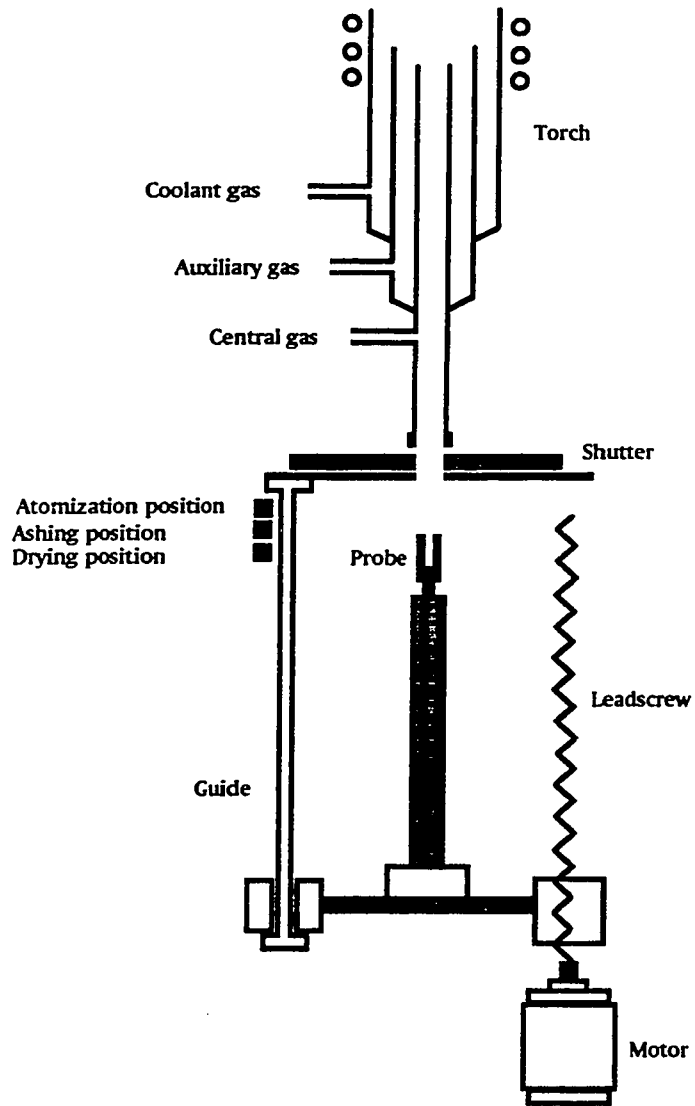


Figure 1.1 Schematic diagram of a typical direct sample insertion system

massive release of Si into the plasma, which resulted in severe physical and spectral interferences. A 1:1 AgCl/sediment mixture was used to enhance volatilization. The method of standard additions was used for calibration. It was found that powdered metal oxide standards (SPEX g-standards) were adequate spiking standards for Co, Cr, Ni, V in PACS-1. The reproducibility of the measurements was between 10 and 25 % RSD. The accuracy of the determinations was fair below $50 \mu\text{g g}^{-1}$, with typical errors falling below 10%, but accuracy degraded at the higher concentrations to errors of approximately 20%.

Recently, Page and co-workers adopted the above approach in the determination of four critically important lanthanides, Dy, Eu, Gd, and Sm in nuclear fuel materials [14]. A buffer-carrier mixture of graphite-silver chloride (4+1) was used to facilitate the volatilization of chemically separated lanthanides from UO_2 and PuO_2 into the ICP. A 20 μl volume of lanthanide solution was loaded on 20 mg of carrier-buffer mixture placed in the crater of an electrode, evaporated under an IR lamp and introduced into the running argon plasma. Graphite helps not only in minimizing the changes in ionization equilibrium arising from the presence of low ionization potential analytes but also in stabilizing the plasma temperature. It also serves as a base material for loading the solution, therefore preventing its seepage into the electrode walls; however, graphite alone cannot facilitate the volatilization of the analytes and hence graphite mixed with an appropriate amount of a suitable carrier enhances the selective volatilization of the impurities. The use of halide carriers helps in thermochemical reactions for the conversion of analyte oxide into halides which facilitates their volatilization into the plasma.

The viewing position of the plasma, one of the critical parameters influencing the signal intensity, was also studied by monitoring the analyte signal at various axial and radial positions. The viewing position was studied in the range 5 - 20 mm above the top of the load coil. At a viewing position 5 mm above the top of the electrode, the analytes produced maximum signal intensity. Beyond this a decrease in intensity was observed. This indicated that analyte intensities reached a maximum very close to the electrode as compared to the viewing position in conventional ICP spectrometers, where the viewing position is normally 15 mm above the load coil. This is because the high density analyte vapour was released as soon as the electrode experienced the high temperature.

Rattray and Salin [15] reported an approximately 500-fold reduction in the detection limit for ICP-AES by deposition of the primary aerosol from a nebulizer directly into an inductively heated DSI probe. This method involves deposition of the sample solution as an aerosol into an inductively heated, graphite, direct sample insertion probe. The aerosol was generated with a conventional Meinhard nebulizer and the preconcentration factor could be varied by changing the length of time over which the sample was deposited. The load coil of the ICP was used as the source of the induction field. The nebulizer was mounted on a swing arm inside the plasma box, with a mechanical stop that allowed reproducible positioning. The procedure involved first preheating the probe for 1 min with the outer argon gas flow on. This outer flow served to prevent any oxidation of the graphite and, more importantly, acted as a sheath to avoid any contamination from the atmosphere. Next, the sample was nebulized into the probe for the length of time desired, and the probe was maintained at the drying temperature for an additional 15 seconds. After retracting the probe into an enclosed chamber, the plasma was ignited and the probe was fully inserted. The DSI probes were reusable. No memory effect was observed. With a deposition time of 2 min and a sample volume of 0.5 ml, detection limits for Cu, Zn, Cd, and Pb were 0.05, 0.12, 0.10 and 0.07 ppb, respectively. Calibration curves for Cu, Zn, Cd and Pb were linear over the range studied, up to 200 ppb. The relative standard deviation was < 5% at the 10 ppb level.

The authors also compared the peak shape obtained by aerosol deposition with that obtained when the sample was introduced drop wise into the graphite cup. The signal observed with aerosol deposition DSI was narrower, for the same total mass of analyte. The trend was consistent for all elements studied. The reduced peak width might be due to the fact that the aerosol dries on contact with surface, and the analyte solution does not have time to soak into the graphite probe.

Further experiments performed on an automated version of this approach for ICP-MS were reported two years later [16]. The results were even more encouraging. A two minute deposition at 0.25 ml min^{-1} resulted in 3σ detection limits ranging from 0.06 to 1.8 pg ml^{-1} (0.03-0.9 pg) for eight elements studied. These limits represent an element specific improvement averaging two orders of magnitude over the nebulizer/spray

chamber-based sample introduction detection limits on the same instrument. The deposition and insertion procedure was automated, providing RSDs of approximately 5% at 1 ng ml^{-1} level. Analytical accuracy was assessed by replicate measurements of a Riverine Water Reference Material for Trace Metals (SLRS-2, National Research Council of Canada). Good agreement between calculated and certified values was obtained. This method holds great promise for the ultra-trace determination of these environmentally important elements (Cu, Cd, Zn, Hg, Tl, In, Bi, As and Sb) by ICP spectrometry.

The geometry of the DSI probe was modified to a narrower size in the above ICP-MS experiment. This modification would confine the plume of analyte to a tight region, thereby enhancing the signal. In addition, use of a narrower probe in ICP-MS obviated problems that arose from the probe touching the sides of the torch on insertion.

Unexpected results were found when the RF power was varied. As the RF power was increased, at a fixed insertion distance and sampling depth, lower signals were observed for the volatile elements studied, which was contrary to a previous report [17]. This suggested that the observation is due to lower electron density at lower power, and therefore less ion-electron recombination, and consequently higher ion signal.

Effects for sodium as a concomitant were also studied in the above experiment. The signal generated at m/z 63 from a $100 \text{ } \mu\text{g ml}^{-1}$ Na solution (i.e. NaAr^+) is equivalent to about 4 ng ml^{-1} Cu. In general, enhanced signal was observed for solutions containing sodium concentrations of $10 \text{ } \mu\text{g ml}^{-1}$ and greater. Peak appearance times were slightly earlier than the solution with Na concentration $10 \text{ } \mu\text{g ml}^{-1}$ or less, but the peak widths did not seem to be affected.

The same authors also did an experiment to pre-concentrate Cd, Cu, Pb and Zn on Chelex-100 resin and then inserted the analyte-laden resin directly into the plasma [18]. For both Cu and Zn the ratio of the signal before and after pre-concentration approached the theoretical pre-concentration factor, but this was not achieved for the other two analytes. This failure was attributed to the adverse effect of the remains of the resin after ashing on the excitation properties of the plasma. The performance of the technique was improved by increasing the forward power to the plasma.

An electrically heated wire-loop, in-torch vaporization sample introduction system for ICP-AES with photodiode array detector was developed by Karanassios and Bateman [19]. The system consists of an electrically heated W wire-loop which is attached to a thermocouple ceramic insulator. Ceramic and wire-loop are inserted manually into the central tube of a modified ICP torch. Unlike the typical DSI-ICP, the top of the wire-loop is positioned about 10 cm below the plasma; a separate power supply is used for sample vaporization. To help form a well-defined central channel, the diameter of the central tube near the top is reduced and the bottom of the torch is sealed. This in-torch vaporization (ITV) sample introduction system was characterized using an ICP optical emission spectrometer with a photodiode array detector. Calibration curves were linear for over three orders of magnitude for Sr, Y and Be. Non-linear calibration curves obtained for Cu were attributed to contamination from the power transfer cables, for Mg to contamination from ceramic and for Ca to airborne particles adhering to the wire-loop. Percent relative standard deviations were determined from six replicate measurements of 1 ng of a single element solution residues and were 1.9% for Sr, 2.0% for Be and 4.5% for Y, and estimated absolute detection limits were (10 μ l injection of single element standards in pg) Zn (710pg), V(20 pg), Mn (10 pg), Y (10 pg), Sc (9 pg), Be (1 pg) and Sr(0.4 pg). These results compare favorably with DSI and ETV systems.

The same system was also found to be useful to determine Hg^0 vapor in air [20]. Mercury vapor will form an amalgam with Au coated on a Tungsten wire-loop. Calibration of the system was done by passing known amounts of Hg^0 vapor through a quartz cell. The linear range was about two-and-a-half orders of magnitude. Mercury vapor levels determined close to a polarography apparatus compared favorably with measurements taken at the same location using cold vapor atomic absorption spectrometry.

Liu and Horlick described a computer controlled direct solid sample insertion device for the introduction of solid samples to an ICP [21-22]. The system was tested on Al_2O_3 , Al metal, oil, and botanical samples. The key operational feature that allowed the successful direct determination of trace elements in these materials, with essentially no pre-treatment, was the utilization of an argon-oxygen mixed gas plasma. By adding

enough O₂ (20%) into the plasma the samples were vaporized into the plasma which facilitated the direct analysis of elements with different volatilities in hard to vaporize matrices. Some of the most difficult elements such as Zr, Ti, V, and Ni were tested. For the aluminum alloys, the study indicated that the matrix effect was small and a single calibration curve could be applied to the different aluminum samples. An observation height of about 14 mm above the top of the load coil was chosen. The final probe position in the plasma of about 2 mm above the top load coil was selected for all the elements tested. During a run the graphite cup was consumed within 60 seconds. A plasma power from 1.8 kw to 2.0 kw was used, and observation time varied from 80 seconds to 120 seconds. The calibration curves were linear over a dynamic range of 3 to 4 orders of magnitude and detection limits were in the range of 10's of picograms. The use of the Ar-O₂ mixed gas DSI-ICP effectively extended the DSI-ICP technique to difficult to vaporize elements, refractory compounds, and refractory samples. It is expected that the Ar-O₂ mixed gas DSI-ICP-AES system can be readily used for a wide variety of applications in elemental analysis which could be difficult and time consuming for other methods.

Ying and Kratochvil used the above system for the determination of Al, Fe, Cu, Zn and Mn in agricultural materials [23]. Several NIST standard reference materials were analyzed and the results were in good agreement with the certified values.

Umemoto and Kubota summarized the main parameters that govern the characteristics of ICP - AES with graphite cup sample introduction as compared with a pneumatic nebulizer sample introduction [24]. The DSI plasma had a doughnut structure, and the linear dynamic range was roughly four orders of magnitude, which is smaller than that for nebulization. It did not have two distinct zones in the axial emission profiles, a thermal zone and a non-thermal zone, as observed with nebulization. The electron number density of the DSI plasma, as observed laterally, was a factor of 4.5 lower than that in the case of nebulization. The background intensities at 440 nm and 230 nm were inversely proportional to the outside diameter of the cup, while that for a cup with 0.5 mm wall thickness was a factor of 1.7 smaller than that in the case of nebulization. For Pb and Cu, the intensity ratios of ionic to atomic lines for the DSI were close to those for

the nebulization plasma, whereas, for Cd and Zn, these ratios were a factor of 3-4 smaller. The difference is related to the marked dependence of the ionic and atomic line intensities on the cup position for Cd and Zn in the DSI. It is then advantageous to use atomic lines for the analysis of Cd and Zn.

Recently, Skinner and Salin took some plasma images during direct sample insertion using a charge coupled device camera [25]. This revealed how the analyte behaves in the plasma. Graphite cups, graphite tubes and wire loops were used as sample carrying probes. The plasma was imaged from the region directly above the DSI probe to well above the normal analytical viewing zone.

The diameter of the graphite cup had a dramatic effect on the plasma and calcium emission. The dramatic increase in signal from the large (8.3 mm) to the narrow diameter cup (3.1 mm) was probably due to three sources: the narrower cups heat more quickly, reach a higher temperature and release more calcium into the plasma per unit time; the smaller cup also places a smaller load on the plasma, allowing greater efficiency of excitation; and the narrower cup keeps the calcium confined to a narrower plume in the center of the plasma. A narrow plume is advantageous because it increases the analyte signal intensity in the viewing zone and minimizes the impact of the sample on the plasma. If large amounts of sample are added to the plasma, interferences become possible. In addition, the narrow cups disturb the plasma the least. The medium diameter cup (5.2 mm) caused the plasma to fluctuate on insertion but the plasma stabilized quickly. The large cup was difficult to insert into the plasma without the plasma being extinguished.

The use of a carrier gas through a graphite tube and hollow stem cup showed that a dark central channel was established. The use of a central gas in combination with Freon-12 yields a performance comparable to that of wire loops, which produces the shortest transient signals.

In the case of a deep and narrow graphite cup (12 mm \times 3.1 mm) the analyte appears to emerge into the plasma along the walls of the cup. However, when the radial intensity maps from standard length cups (6.3 mm) were examined (both medium and narrow diameter), no evidence of this annular emission was found. It seems probable that

the shorter cups disturb the flow of the gases in the plasma so that there is rapid mixing of the calcium as it emerges from the cup.

Finally, Ohls gave his personal view of the development of solid sampling emission spectrochemical analysis [26]. He concluded that the DSI-ICP is comparable to the old dc arc spectrographic techniques with respect to power of information, when simultaneous reading instruments are used.

1.22 Electrothermal Vaporization (ETV)

A way to separate sample vaporization from atomization, ionization/excitation, and to facilitate independent optimization is by using an ETV-device. Using a programmed vaporization to control rates, times and temperatures of heating steps, allows for the selection of an optimum sequence of drying, ashing, and vaporization of the sample components. A measured weight or volume of sample, solid or liquid, is placed on the vaporizer surface and stepped through a controlled heating sequence that produces a highly dispersed aerosol. The aerosol is subsequently swept into the plasma by the injector gas, usually argon, where it undergoes decomposition, atomization, ionization, and excitation. By employing the ETV device, the analytical capability of ICP for solid analysis is extended and improved. It provides high sample transport efficiency for samples such as those in organic solvent or those having high total dissolved solids. It also results in an increase in sensitivity, reduced background because of the removal of the solvent, selective volatilization of matrix components, in situ chemistry (modified sample matrix) and the ability to analyze microliter volumes of solutions.

Salin and co-worker used Freon gases to assist the vaporization of refractory analytes [27-28]. One percent of aluminum oxide, silicon oxide and zirconium oxide slurry were analyzed with the assistance of the Freon gases. In all cases, the boiling point decreased when the sample was converted from the oxide to a halide. Four marine sediments reference materials and one coal fly ash reference material were analyzed for eight elements. The precision obtained for the analysis was between 3 and 15%.

Ren and Salin made modifications to a commercial ETV furnace by using sheath and cooling gas to increase the analyte transport efficiency and reduce matrix interferences [29]. It is believed that chemical reactions and cooling of the analyte vapour are necessary for the elimination of matrix interferences on analyte vaporization and transport efficiency. The sheath gas provides a thin sheath layer between the analyte vapour and the wall of the transport tube to prevent vapour condensation, and the cooling gas cools the analyte vapour to promote aggregate formation. This system could be very useful for direct solid sample analysis using ETV-ICP-AES.

The above system combined with Freon-12 gases was also used for zeolite slurry analysis [30]. The signals of the refractory elements of chromium and vanadium were improved dramatically. Detection limits of $1.4 \mu\text{g g}^{-1}$ and $0.3 \mu\text{g g}^{-1}$ were obtained respectively. The precision of determination for the zeolite sample varied from 3% for cadmium, to 6% for lead.

Bitterli et al. developed a method to trap airborne particles into a graphite tube by electrostatic precipitation and then coupled with ICP-MS for metal analysis [31]. Calibration was performed with dried aerosol produced by the nebulization of a standard solution. For Cr, Fe, Mn, Cu, Zn, Sr, Cd, Sb, Ba and Pb, the absolute detection limits were in the picogram range. The precision was 10-15%. The addition of $5 \mu\text{g g}^{-1}$ of Na (as NaNO_3) to the standards improved the signal intensities and reduced the curvature of the calibration curves. The influence of CHF_3 was investigated but subsequently abandoned owing to a general increase not only of the signals but also of the background. The NIST SRM 1648, Urban particulate matter, was analyzed for the above elements. The results for Fe, Pb and Sb were in fairly good agreement with the certified values, but not for Cu, Zn and Cr. In real air samples, Fe, Pb, Mn and Sb were always detected.

Vanhaecke et al. studied the direct determination of As in solid samples of plant origin using ETV-ICP-MS [32]. The signal profiles (signal intensity as a function of time) of As in tomato leaves showed a similar behavior to the liquid spike dried in the sample boat. An absolute limit of detection of approximately 1 pg was established for As, corresponding to a relative limit of detection of approximately 1 ng g^{-1} for a typical sample mass of 1 mg. Results obtained for the As content in the samples analyzed were

not deteriorated by the presence of Cl, as even on addition of amounts of Cl exceeding the Cl content of the samples, no $^{40}\text{Ar}^{35}\text{Cl}^+$ interference on the $^{75}\text{As}^+$ signal could be established. For the determination of As in these reference materials of plant origin, several methods of calibration were investigated, including external calibration using both liquid and solid standards and single standard addition. Single standard addition was assessed to be the most practicable and straight forward method.

Moens reviewed some of the literature concerning solid sampling ETV-ICP-AES/MS and presented analysis results of SRMs using SS-ETV-ICP-MS [33]. The conclusions were that the hardware and software of SS-ETV were fulfilled and the method was used for trace element determinations in a variety of materials, predominantly for the analysis of biological and environmental samples and of ceramics and other hard to dissolve materials. Accurate standardization can be performed using standard addition or external calibration with standard reference materials with composition similar to that of the sample. The precision of the method is typically around 10% (RSD%) but is limited by the sample inhomogeneity since the maximum sample weight could not exceed 10 mg. The SS-ETV-ICP methods can produce accurate results after careful study and optimization. Because it is fast and simple to use, SS-ETV will probably turn out to be most useful in the routine analysis of large numbers of similar solid samples.

1.23 Laser Ablation (LA)

A main area of growth in the solid sampling field in the last few years has been in the application of laser ablation techniques. Liu and Horlick have described an *in situ* laser sampling system [34]. The sample was placed within the torch immediately below the plasma discharge via a direct sample insertion probe. A Q-switched Nd:YAG laser was focused on the sample by a lens above the plasma. The ablated material entered the plasma directly, eliminating the need for an aerosol transport step. The emission signal had a duration of 0.7 ms in comparison with conventional LA, where the signal may last for several seconds. As a consequence, sample-transport efficiency into the plasma is

virtually 100%, yielding an extremely intense but brief signal. The sensitivity for several analytes in aluminum alloy, steel and brass reported in the range from $0.015 \mu\text{g g}^{-1}$ for Ca to $12 \mu\text{g g}^{-1}$ for Mo.

Baker et al. used a compact and inexpensive Nd:YAG laser for LA-ICP-MS analysis of NIST aluminum and glass samples [35]. These lasers, which were developed primarily for the ophthalmic market, offer a simple, low-cost solid sampling option for ICP users. The device, which measures approximately four inches in length, is permanently aligned and thus requires no manual adjustments. The system costs below \$7,000 compared to most laser ablation system where costs are often prohibitively high. This laser provides nominal pulse energies of 20 mJ, pulse widths of 4 ns, and a beam diameter of around 3 mm. It operates at its fundamental wavelength 1064 nm, or its harmonics 532 nm, 355 nm and 266 nm. It can be powered from a 12-V dc power source and has an operational life in excess of 300,000 shots. It can either be operated in a manual firing mode or repetitively fired at a maximum repetition rate of 1 Hz. A linear calibration plot ($R=0.99$) for Ti in an aluminum sample was obtained. The precision of the normalized measurements ($n=5$) ranged from 10 to 13%. The detection limit for Ti in the aluminum sample was 0.3 ppm. A linear calibration was also obtained for Sr ($R=0.9999$) in the glasses. The precision of the measurements ($n=5$) ranged from 2 to 10%. The detection limit for Sr was 0.1 ppm.

Mermet and co-worker used a Q-switched Nd:YAG laser coupled with ICP-AES to study depth profiling of thick layers of graded metal-zirconia ceramic coatings [36]. Several hundred micrometers of depth profiling was achieved. Five elements (Zr, Y, Cr, Ni and Al) were chosen for the study. The same research group compared the use of contained and added internal standards in LA-ICP-AES for silicate and limestones analysis [37]. Glass disks obtained by fusion of rocks with lithium tetraborate were sampled by the laser (355 nm, 10 Hz, 10 mJ per shot) and analyzed by an ICP with a segmented charge-coupled device detector. On the basis of the use of Li and B as internal standards, linear calibrations were obtained for Si, Al, Ca, Mg, Fe, Ti, Na, and K by using reference geological materials. The possibility of using flux elements overcomes

the need to have prior knowledge of the concentration when a contained element is being used as an internal standard.

Figg and Kahr [38] studied the effect of irradiance and wavelength upon elemental fractionation of glass using LA-ICP-MS. Three laser wavelengths (1064, 532 and 266 nm) were employed. It is suggested that 1064-nm (IR) and 532-nm (green) radiation produced elemental fractionation that relates to the melting point of the elemental oxide, whereas with 266-nm (UV) ablation the response was independent of the elemental oxide melting point. At high laser powers (2.4 - 3 mJ/pulse), ablation at 266 nm produced an elemental bias based upon the mass of the elements. These observations suggest the use of ultraviolet radiation at low pulse energies (200 - 400 μ J/pulse) to obtain improved analytical results.

Chan and Yip developed a preconcentration technique for laser ablation ICP-AES using ion-exchange polymer film [39]. Ammonium pyrrolidine dithiocarbamate (APDC)-polystyrene films were coated on glass plates for analyte preconcentration. After immersing the sample probe in a solution for 5 min, the ICP emission intensity for laser ablation of the polymer film is a few times larger than that after solution nebulization. The sample probe removes only a small fraction of the sample solution and, therefore, in principle, does not disturb the original solution significantly. Single-pulse laser ablation of the polymer film shows that the ion-exchanged metal ion concentration in the film reduces exponentially as a function of depth within the polymer film. Ion exchange to the polymer film is probably limited by the rate of metal ion diffusion into the film. Calibration curves for Cu, Hg, Pb, and Zn show a linear dynamic range of 1-2 orders of magnitude. The linear dynamic range for Cu increases to > 3 orders of magnitude when using Pb as an internal standard. RSDs of the ICP emission intensity are about 8%.

Soil analysis by LA-ICP-AES could save the time normally required for acid digestion and avoid sample contamination. Moenke-Blankenburg, Schumann and Nolte used a Q-switched Nd:YAG laser to ablate a blade pressed soil surface to generate an aerosol for ICP-AES analysis [40]. Internal standard solutions were mixed with soil sample before the soil was pressed into a steel ring. Relative standard deviations of 4.9 - 12.7 % and an accuracy of 0.3 - 12.4% were obtained for Fe, Mn, Cu, Pb, Cr, Zn and Ni.

D'Silva and co-worker at the Ames Laboratory used a LA-ICP-AES in a mobile laboratory for conducting a survey analysis of uranium in soil at a contaminated site [41]. In their system, the laser beam from a Nd:YAG laser (320 mJ/pulse, 532 nm, 20 Hz, 7 ns pulsewidth) was coupled into a 25-m long 600 μm core diameter silica clad, fiber optic cable that is routed out of the mobile lab to the soil surface. The ablated analytes were swept out by argon gas (flowing at a rate of 1 L/min, through a 15-m length of 3/16-in. i.d. polyvinyl tubing) into the ICP torch. The amount of Si in the soil was assumed to be constant across the sampling area and equal to that in the calibration standard samples. Therefore, the concentrations can be reported as the intensity ratio from the U (II) 409.014/Si (I)288.158. For 15 sites, the uranium concentrations determined by LA-ICP-AES ranged from <20 ppm to 102 ppm (95% CI of approximately 50 ppm). The same samples analyzed using microwave dissolution and subsequent standard addition through solution nebulization ICP-AES were found to contain 19-124 ppm uranium (95% CI of approximately 10 ppm).

1.24 Slurry Sampling

Slurry nebulization is a popular sample introduction route for powdered materials. Interest in the technique is undoubtedly due to the convenience of sample presentation (the only additional requirement for ICP analysis is the use of a high-solids nebulizer) and the possibility of using aqueous solutions for calibration. The validity of calibration based on aqueous standards critically depends on factors such as particle size, nature of the sample, nebulizer-spray chamber design, and operating conditions.

Slurry nebulization efficiency and its relationship with particle size has been studied by Goodall et al. [42]. It was concluded that the maximum particle size permissible to enable representative sampling depended on the density of the material. The maximum particle size for a material with density of 1 g cm^{-3} was $2.9 \mu\text{m}$ but this decreased to $1.5 \mu\text{m}$ for a material with density of 7 g cm^{-3} . It was also stated that for some carbonaceous materials micro-flocculation may occur, i.e., a loose assembly of 5-10 particles would form. This could behave in a similar manner to single particles of a much

greater diameter. This would inevitably lead to lower transport efficiency and lower recovery. This micro-flocculation problem was overcome by the use of a more concentrated dispersant. The work was validated by the successful analysis of a number of different Certified Reference Materials (CRMs).

The problem of particle size control and analytical recovery has also been tackled by Chen and McCreary [43]. A fundamental difference was observed between conversion of slurry and solution droplets to gas phase atoms. It was demonstrated that there was a reduction in the emission signal of refractory analytes in a slurry when compared with the same concentration in an aqueous solution. It was concluded that unit transport was not necessarily guaranteed to produce unit recovery.

Slurry nebulization of geological materials into Argon, Argon-Nitrogen and Argon-Oxygen ICP-AES was investigated by Verbeek and Brenner [44]. The study found that the slurry nebulization of geological materials into an ICP is more complicated and less amenable to generalization than that of aqueous solutions. One might expect the signal to background ratios to appear at a greater height in the ICP when analyzing geological materials, as presumably a longer residence time would be required to atomize refractory and larger particles. This is usually true, but with exceptions. The most apparent difference between the vertical emission profiles obtained from aqueous solutions and from slurries of homogeneous glasses is the irregularity of the latter. These irregularities cannot be related to specific chemical and mineralogical species undergoing decomposition in the plasma, because the elements are homogeneously dispersed in the glass particles.

Atomization of slurry samples in electrothermal atomizers is a well established technique, especially for relatively easily atomized elements and applications of this approach to the analysis of powdered samples continue to be published. The effect of particle size in the analysis of botanical samples by slurry sampling and fluorination-electrothermal vaporization ICP-AES was investigated by Jiang and co-workers [45]. Four refractory elements, B, Cr, Ti and Mo were among those studied. The signal intensity from slurry particle sizes less than 170 μm showed identical signal compared to aqueous solutions. The linear dynamic range of the calibration curves was 0.01 - 10 μg

ml⁻¹. The relative standard deviations were less than 5% at a concentration of 0.2 µg ml⁻¹ (n=9), and the results obtained were in good agreement with certified values of reference samples. The results also indicated that particle size effects can be reduced by high temperature *in situ* fluorination in the graphite furnace.

1.3 Recent Developments in Standard Reference Materials

Reference materials are well-characterized, stable, homogeneous materials having one or more physical or chemical properties determined within stated measurement uncertainties. These properties are sufficiently well-established to be used for the calibration of an apparatus or the assessment of a measurement method. Reference materials thus play an essential role in analytical chemistry. They are used to evaluate the accuracy of new analytical methods and to maintain the quality of established measurement procedures.

New issued standard reference materials are significantly improved over previous materials in terms of the number of elements certified, uncertainties of certified concentrations and sample homogeneity. These improvements are mainly due to advances in technology and better quality control in procedures. Since SRMs are so important for method development and validation in this thesis, recent developments in SRMs will be reviewed.

1.31 Soil, Sediment and Ash Materials

Environmental pollution from coal-burning can occur through direct stack emissions, as well as from the leaching of toxic metals from ash which is disposed in landfills. Well characterized, certified reference materials are required for quality assurance purposes when analyzing such materials. This has twice led to the renewal of NIST SRM 1633, Coal Fly Ash. In June 1993 NIST released the third version of "Constituent Elements in Coal Fly Ash" Standard Reference Material (SRM1633b) [46]. This material is intended for quality assurance purposes in evaluating the analytical

methods used for the determination of constituent elements in coal fly ash or in materials with similar matrices. It has been certified for 23 major, minor and trace elements using ten different analytical techniques. For an element to be certified in a NIST SRM, its concentration is usually determined by at least two independent analytical techniques. The concentrations of an additional 24 elements are provided for "information only" purposes in the new fly ash.

This SRM 1633b represents the fly ash generated by burning bituminous Pennsylvania and West Virginia (Appalachian Range) coals, and is a composite, rather than the ash which would result from burning any one specific coal. Prior to bottling, the material was sieved through a normal sieve opening of 90 μm (170 mesh) and then blended to assure homogeneity. Homogeneity testing was accomplished using instrumental neutron activation analysis and X-ray fluorescence.

The collection, processing and certification of SRM 2704 (Buffalo River Sediment) is described by Gills [47]. Collected from the bottom of the Buffalo River in New York State during the fall of 1986, SRM 2704 is certified for 25 elements with information provided on another 22 elements. Improvements in analytical methods as well as the application of well defined quality control procedures for collection, processing and analysis have resulted in a reference material that is more completely characterized than previous NIST sediment reference materials.

Inorganic constituents were characterized by using lithium metaborate fusion for sample preparation, and analysis by ICP and DCP spectrometry, FAAS and FAES. SRM 2704 was readily brought into solution after a lithium metaborate fusion. However, several analysts reported that acid digestion in an open vessel, with a combination of hydrofluoric, nitric and perchloric acids, left a small residue of dark particles. These particles were examined by several analytical methods. Arc emission spectroscopy reported Ti as the major component, Al, Ca, Fe, Mg, Mn, Si, Zr as minor components, and Cu as a trace component. Electron microprobe showed rutile (TiO_2), zircon (ZrSiO_4), chromite (FeCr_2O_4), and unknown particles which were possibly coal and glass. X ray diffraction indicated dispore and boehmite ($\text{AlO}(\text{OH})$), rutile and anatase (TiO_2), zircon (ZrSiO_4) and corundum (Al_2O_3).

Noncertified values are given for a large number of elements. There are several reasons why a concentration value may not be certified. If a bias is suspected in one or more of the methods required for certification, or if two independent methods are not available, the element concentration cannot be certified.

The uncertainty reported for each certified element reflects the material inhomogeneity and random and systematic errors among methods used for certification. As the certified concentrations decrease, the uncertainties increase. The highest concentration range, greater than 1000 $\mu\text{g/g}$, represents measurement by classical analytical techniques capable of high precision and by instrumental methods used in high precision modes. At the lowest concentrations, where the detection limits of the techniques are approached, random and systematic error due to fundamental instrument processes become significant, and the number of useful techniques becomes limited.

The confidence limits for certified values at all concentration levels decrease by a factor of almost two for the SRM 2704 as compared to last generation of SRM sediments. This improvement at high concentrations can be attributed to experience gained in the collection and processing of previous sediment materials as well as improved quality control and analytical procedures. At low concentrations, much of the improvement is due to the developments in analytical methodology for trace analysis that have occurred in the last decade.

Concern over the possible health and ecological effects of the ever increasing accumulation of heavy metal contaminants in the environment has prompted NIST to release three new soil SRMs. It is now well recognized that the development of effective strategies to solve the problems of contaminated land will depend greatly on our knowledge of the mobility and bioavailability of heavy metals in soils and sediments.

The three new SRMs are intended primarily for use in the analysis of soil, sediments, or other similar materials, SRM 2709 is an agricultural soil from a plowed field in San Joaquin Valley in central California which has baseline trace element concentrations. SRM 2710 is a highly contaminated soil from pasture land along Silver Bow Creek in the Butte, Montana area. The sampling site periodically floods depositing sediment with high concentrations of Cu, Mn, Pb and Zn from the settling ponds of a

local industrial plant. SRM 2711 is a moderately contaminated agricultural soil collected in the till layer of a wheat field [48-50]. There is an addendum to these three SRMs. Leachable concentrations using U.S. EPA Method 3050 for FAAS and ICP-AES are also provided as additional information. For a number of environmental monitoring purposes, the concentrations of labile or extractable fractions of elements are more useful than total concentrations. Concentrations of labile or extractable fractions are generally determined using relatively mild leach conditions which are unlikely to totally decompose the sample. It should be noted that results obtained using mild leach conditions are often erroneously depicted in reports as total concentrations. However, reported concentrations of labile or extractable fractions of elements are generally lower than total concentrations. Recovery can be total if an element in a given sample is completely labile. Results are often presented as measured concentration in the leachate in comparison to the total or certified concentration. The recovery of an element as a percent of total concentration is a function of several factors such as the mode of occurrence in the sample, leach medium, leach time and temperature conditions, and pH of the sample-leach medium mixture.

These new NIST standard reference materials (2709-2711) have been analyzed by a sequential chemical extraction method to provide analyte levels that are particularly useful for the characterization of contaminated soils [51]. All three soils were oven-dried, sieved and ground to pass through a 74 μm screen. The extraction solutions resulting from the five steps have been analyzed for 15 elements (Al, Ca, Cd, Co, Cu, Fe, K, Mn, Ni, P, Pb, Sr, Ti, V and Zn) using ICP-AES. The over-all recovery rates (the sum concentrations from the five steps/the certified total concentrations) were observed to lie between 90 and 105% for most of the elements. The total precision was estimated to be approximately 5% (2σ) for most extraction steps. The high concentrations and proportions of trace elements in the exchangeable fraction (first step) in NIST 2710 suggest that this reference material can be especially appropriate for studies of mobility and bioavailability of heavy metals in contaminated soils.

Three replacement Certified Reference Materials CRM142R Light Sandy Soil, CRM143R Sewage Sludge Amended Soil and CRM145R Sewage Sludge were produced by the Measurement and Testing Program (BCR) of the Commission of the European

Communities [52]. These materials were very similar to the exhausted ones. Nine laboratories from different EU countries were involved in element concentration certification, homogeneity and stability studies. In addition to the certification of total metal concentration, these material were also certified for their aqua regia soluble fraction.

1.32 Botanical, Biological and Food Materials

NIST issued the first botanical reference material certified for elemental content in January 1971, as standard reference material 1571, orchard leaves. In the following years a total of nine additional botanical certified reference materials have been issued by NIST. Botanical SRMs issued since 1991 are significantly improved over previous materials in a number of ways [53]. Probably the most significant change is the use of a jet milling process to grind them to extremely fine particles. This has resulted in botanical SRMs with significantly improved homogeneity.

For these jet-milled materials, it was expected that a high degree of homogeneity would be obtained. Prior to this, all botanical SRMs were certified only for sample sizes of 250 mg or larger. Since the Apple Leaves(SRM1515) and Peach Leaves(SRM 1547) were the first jet-milled botanical SRMs developed by NIST, these materials were studied to determine whether acceptable homogeneity could be established for 100 mg samples of these two materials [54-55]. This study employed instrumental neutron activation analysis to determine concentrations of 12 different elements (Al, Ca, Cl, Cr, Co, Fe, K, La, Mn, Na, Sc, Sm) in 15 samples of each SRM. The results showed remarkable homogeneity for such small samples of a natural matrix material, with seven elements showing less than 1.5% variability (1σ) for the Apple Leaves and six elements for the Peach Leaves. Only one element in one of the materials showed greater than three times the expected variability due to statistical counting uncertainty; this was scandium in the Peach Leaves, with a total analytical precision of 2.62% (1σ).

Recent improvements in production techniques have made the newer botanical SRMs even more useful. It may also be interesting to note that average uncertainties for

the certified values have continued to decrease with time, with the Tomato Leaves renewal SRM 1573a (1993) having the lowest uncertainties of all the botanical SRMs issued to date (all 15 elements above 1 mg/kg average +/- 2.65% relative uncertainty; all six elements below 1 mg/kg average +/- 5.85% relative uncertainty (both 1 σ)).

Ihnat and Wolynetz summarized the results of elemental composition in a series of agricultural/food reference materials [56]. Ten Agricultural/Food Reference Materials (RMs) were characterized with respect to their elemental compositions via an interlaboratory characterization (certification) campaign. Chemical analyses were conducted in 73 cooperating laboratories applying 13 major classes of independently different analytical methods. A total of 213 best estimate values, and 65 informational values were obtained for Al, As, B, Ba, Br, Ca, Cd, Cl, Co, Cr, Cs, Cu, F, Fe, Hg, I, K, Mg, Mn, Mo, N, Na, Ni, P, Pb, S, Sb, Se, Sr, Ti, V, W, and Zn in the following RMs: Bovine Muscle Powder (NIST RM 8414), Whole Egg Powder (NIST RM 8415), Microcrystalline Cellulose (NIST RM 8416), Wheat Gluten (NIST RM 8418), Corn Starch (NIST RM 8432), Corn Bran (NIST RM 8433), Whole Milk Powder (NIST RM 8435), Durum Wheat Flour (NIST RM 8436), Hard Red Spring Wheat Flour (NIST RM 8437) and Soft Winter Wheat Flour (NIST RM 8438). This interlaboratory characterization campaign led to the extensive chemical characterization of 10 new RMs for 34 major, minor and trace elemental constituents of nutritional, toxicological and environmental significance. These RMs, providing a significant addition to the world repertoire of biological RMs, are available from the Standard Reference Materials Program, National Institute of Standard and Technology, Gaithersburg, MD 20899, USA.

The total concentrations of Cu, Mo, and Se in the above ten RMs were also determined using isotope dilution ICP-MS [57]. The study found that ID-ICP-MS yielded highly reliable analytical results.

Different strategies are pursued by producers of reference material to arrive at reference or certified concentrations for analytes. While a few can rely on a single reference laboratory with a number of analytical techniques being used in-house as reference or definitive methods, most producers depend on results from cooperating laboratories, either through voluntary contributions or specific contracts. The approach

of the NIST reference materials program is to use selected and established in-house reference or definitive methods. This procedure has many obvious advantages for quality control of the certification process and traceability of the results. In contrast, the International Atomic Energy Agency's Analytical Quality Control Services AQCS uses intercomparison runs that are open to all laboratories in member states who volunteer their participation in the intercomparison.

A worldwide laboratory intercomparison was organized by (AQCS) involving the determination of trace elements in plant materials used for human consumption [58]. The NIST SRM program donated 5 kg of spinach designated for the production of the future SRM 1570a to this intercomparison; AQCS provided a similar amount of cabbage. For the study, 150 units of each material were distributed and 114 laboratories reported results on both materials to AQCS. The results for the spinach, encompassing more than forty elements, have been compiled and evaluated. Estimates of the elemental concentrations were made based on statistical evaluations, principles of analytical procedures and the laboratory performance indicated by the results on the cabbage material. Satisfactory estimates were obtained for 27 elements. Comparison with IAEA laboratory and NIST reference data did not reveal any significant bias that might have been introduced by the intercomparison approach or its evaluation. The evaluation showed that the results from this intercomparison should allow the establishment of 34 reference values in the spinach material. Comparing the 95% confidence intervals with the reference data, there is excellent agreement. In fact, the deviations within these data are in most instances smaller than 5% relative.

A series of interlaboratory studies has been organized by the Community Bureau of Reference, BCR to improve the quality of the determinations of selected trace metals in estuarine water samples. The improvement achieved allowed production of a reference material (CRM 505) which was certified for its content of Cd, Cu, Ni and Zn [59].

1.4 Sample Homogeneity Issues for Direct Solids Analysis

Homogeneity is considered to be the most vital pre-requisite for a candidate reference material, and therefore related testing methods deserve great attention. Environmental reference materials, such as soils, sediments, waste materials, plant and tissue materials typically consist of many different solid phases with characteristic physical properties such as size, density and geometrical form and widely varying contents of trace elements, which in some cases may cover four orders of magnitude. Even reference materials of high quality are more or less inhomogeneous [60]. For this reason the manufacturers prescribe a minimum mass which has to be used to perform chemical analysis in a proper way. Otherwise, the certified values of element concentrations are not warranted. Usually, this minimum mass is 200 mg or 250 mg, but sometimes also less or more.

Solid sampling graphite furnace ZAAS is very efficient for homogeneity testing because of the low sample intake (upper μg to lower mg) with this method. A number of biological reference materials were investigated for heterogeneity with respect to laboratory sampling error. [61]. It was observed that in some cases the investigated material appears to contain a distinct particle fraction of much higher trace element content ("nuggets") than in the average particles. The measured homogeneity constants for certain elements in each material give an excellent way of calculating the minimum sample mass necessary for reliable element determination. It is proposed to include this testing method in the certification of new CRMs.

It had been observed that conventional homogeneity testing, as introduced into candidate reference material production practices, can overlook micro-heterogeneities in otherwise perfectly homogenized materials and cause serious problems. With luck such heterogeneity may be detected during certification analysis as encountered during the certification of a series of meat materials for metal contents. Pig kidney, bovine liver and bovine muscle were tested and occasionally high lead contents, well above the average level, were found at low subsample sizes. Detailed investigation showed that few, but rather large cleavage fragments of calcium oxalate, just below the 125 μm particle size, occurred in the sample and that these crystals contained approximately 1% lead. Such micro-heterogeneities would escape detection by classical homogeneity testing methods

due to the relative high sample intake requirements. Solid sample Zeeman Atomic Absorption Spectrometry (SS-ZAAS) with a graphite furnace operating at a sub-milligram sample intake level, shows correspondingly enhanced detection power for the identification of particles carrying extremely high analyte contents.

The existence of nuggets in ground mineralogical and geological samples is to be expected and can be explained by the geochemical composition. The particles with extreme analyte content sometimes have an unexpected or surprising origin.

For the bovine muscle, Luckner et al. have shown the endogenous source of the nugget material [62]. The calcificated capsules of dead cysticercus (large stage of the "ox tapeworm") accumulate lead up to a 500 times higher content compared to the surrounding muscle tissue. These are ideal nugget-forming conditions; a very small mass fraction contains a large analyte portion.

The exogenous origin of nuggets in spruce needles was explained by Wyttenbach et al. [63]. The inclusion of particles from anthropogenic aerosols leads to a significant increase of the material content. Although it was shown only for some elements that are detectable with neutron activation analysis (e. g. aluminum), lead would also have a similarly considerable effect (external>endogenous). It seems to be impossible to determine and to describe exactly the physical parameters of real biological samples; the evaluation of the solid sampling data by the method presented gave the most detailed look yet into the distribution of trace elements in real powders of biological origin.

The choice of reference materials used for calibration influences the values of analytes obtained for a sample[64]. Determination of Cd, Cu, Pb and Zn in BCR Bovine Liver CRM185 was carried out using two ways of calibration: calibration with a reference material of the same matrix (NIST Bovine Liver SRM 1577a) and with materials of a different matrix, such as mussel tissue, milk powder and aquatic plant material. The deviation of results for copper and zinc was very small. The calibration with a reference material of a different matrix has led to cadmium results being about 20 % lower than the certified value. Both results of lead determination were clearly lower than the certified value. However, it is peculiar that calibration with material of the same matrix has led to lower results than calibration with material of a different matrix. Probably, the reason for

this phenomenon can be seen in the certification procedure of BCR CRM 185 as well as in a micro-inhomogeneity (Nugget Effect) of the material. Thus, the assumption seems to be justified that for calibration, reference materials of the same matrix should be preferentially used. These materials should be of high quality, i.e. very homogeneous and well characterized.

Four types of plastic with four different nominal Cd concentrations in the range of 40 to 400 mg/kg were sampled, homogenized and certified at Central Bureau for Nuclear Measurement (CBNM) in Belgium on the behalf of VDA (Verband der Automobilindustrie) [65]. The homogeneity of the materials as well as the evaluation of the minimum sample size for which the certified confidence intervals are valid were evaluated on the basis of microhomogeneity studies using SS-GF-ZAAS. On each of the four materials 60 analyses were carried out on microsamples (60 to 250 µg per analysis) taken from 60 different cuts of plastic wire. Analyses were carried out at 326.1 nm. Pyrolytically coated graphite was used for both furnace tubes and L'vov platforms. Peak evaluation was done by measuring the height of the peaks. Calibration was carried out using four sewage sludge BCR certified reference materials (CRM-143: 31.1mg/kg; CRM-144 4.82 mg/kg; CRM-145: 18.0 mg/kg; CRM-146:77.7 mg/kg). Each homogeneity study was preceded by a calibration based on 9 to 17 analyses spread over the whole calibration range. The minimum sample mass to be used in measurement were determined: VDA-001:27mg; VDA-002: 18mg; VDA-003: 13mg; VDA-004:1g.

BCR CRM-422 (cod muscle) was prepared at CBNM by cryogrinding and subsequent freeze-drying, mixing and bottling under controlled conditions [66]. After completion of the production process, the material was examined for microhomogeneity by solid sampling Zeeman atomic absorption spectrometry on 85 to 138 microsamples for five elements: Pb, Cd, Hg, Fe, Zn. The minimum representative sample mass for mercury is 416 mg; for iron is 68.7 mg; for zinc is 20.8 mg; for lead is 11.6 mg and for cadmium is 24.0 mg.

Neutron activation analysis (NAA) plays a very important role in the certification of reference materials and their characterization, including homogeneity testing. Byrne reviewed the application of NAA in standard reference materials and radionuclide

reference materials [67]. The advantages of NAA are, in brief: its sensitivity and wide applicability, especially for trace elements; its virtual absence of an analytical blank; its relative freedom from matrix and interference effects; its nondestructive nature in many cases; its high specificity. In addition, NAA is isotopic based and the method is theoretically simple and well understood, which means that sources of uncertainty can be modelled easily and accurately estimated.

The distribution homogeneities of 13 elements (As, Ce, Co, Cr, Cs, Eu, Fe, Hf, La, Rb, Sc, Sm and Th) in the esturine sediment NIST SRM 1646 have been evaluated by INAA and synchronous radiation -based X-ray fluorescence spectrometry in the range of sampling amounts from 10 μg to 20 mg [68]. The experimental results reveal that the homogeneities of the elements studied relate to their species and sampling amount. The sampling constants of 13 elements of SRM 1646 were also calculated.

The esturine sediment SRM 1646 is significant for the environmental monitoring and sand movement investigations of coast and harbor areas. But no information on its homogeneity is available. Thus, it was selected as a research specimen. From 10 μg to 20 mg, 9 fractions of different sampling weight were used. Each fraction has 3 to 5 samples. All samples were weighed by a photoelectric balance with a precision of $\pm 1\mu\text{g}$, except the samples for synchronous radiation SRXRF, whose sampling amount was estimated by beam currency size. On the basis of the experimental results the following conclusions were drawn:

1. The homogeneity of the elemental distribution was related to its chemical species.
2. The relative deviation of almost all the elements increased with a decrease of the sampling amount.
3. The experimental errors were very small in comparison with the sampling error.

A method for the quantitative determination of the minimum representative sample mass of a solid reference material is described and illustrated by Pauwels and Vandecasteele [69]. If CRMs are to be used to calibrate microtechniques, the uncertainty which should be assigned to the certified value in that case, can also be evaluated. The method is applied in the preparation and certification of several reference materials with which Central Bureau for Nuclear Measurements (CBNM) was involved.

To determine the minimum sample mass of a CRM to be used in an analysis, the term "unit" in the above statements should be replaced by "subsample". The size of this subsample is then decreased to such an extent that one moves from homogeneous material to heterogeneous material, i.e. that if the CRM would be subdivided in progressively smaller subsamples, the uncertainty quoted on the certificate (in general the 95% confidence interval) must be replaced by a 95%/95% statistical interval.

Two single-cell algal materials IAEA-392 and IAEA-393 and one urban dust, IAEA-396 were used for a micro-homogeneity study [70]. Solid sampling Zeeman effect AAS was applied to the determination of trace elements on the bases of 10^{-6} - 10^{-3} g amounts of the selected materials. From the experiment results, it seems that the algal materials IAEA-392 and IAEA-393 are extremely homogeneous biological materials for Cu and Pb with an extraordinarily sharp particle size distribution below 10^{-5} m. A similar situation seems to hold for the urban dust material IAEA-396, which had been air-jet milled to a particle size distribution of around 4×10^{-6} m. The introduction of these materials as CRMs with very small amounts needed to determine the certified concentrations will help to meet the needs of micro-analytical techniques for natural matrix reference materials.

1.5 Objective of this Research Work

Direct sample insertion is accomplished, as the name suggests, by inserting the sample on a probe directly into the ICP. A number of studies have demonstrated the analytical capabilities of the direct sample insertion (DSI) technique coupled with ICP spectrometry [1-24]. Energy transfer results in rapid heating of the sample probe and vaporization of analyte species into the ICP. The extremely efficient sample introduction process ensures high sensitivity and low detection limits for DSI measurements.

Most of the samples used in the initial development of instrumentation and techniques were liquid. In the case of solids, the sample usually was a powder form of a standard reference material. The recent success in the utilization of an argon-oxygen mixed gas plasma has extended the DSI-ICP capability for the difficult to vaporize

elements and refractory samples. Sample matrices such as aluminum oxide, aluminum metals, oil, glasses and botanical samples, were used in the study [21-23]. The first part of this research (Chapter 2) is a continuation of this argon-oxygen mixed gas DSI-ICP study. The experiments were focused on the application of the method to environment related samples. These include NIST Standard Reference Materials, waste water and solid waste.

The DSI-ICP has a low sample intake, i. e. less than 20 mg of sample was used for each determination. It seems sensible to take replicate measurements in order to reduce the sample heterogeneity problem. By increasing the number of replicates the effect of inhomogeneity on the reproducibility may be minimized and increasing the number of replicates would be advantageous to the reproducibility of data obtained with solid sampling DSI-ICP. An automated solid sampling system is very helpful for this purpose. Such a system would permit the rapid analysis of a large number of samples. Therefore, development of an auto-sampler for the DSI-ICP is important. Over the last decade, a number of approaches were developed in this research group to accomplish this goal. However, all of the approaches involved an expensive and complicated set-up. The second part of this research is to utilize an inexpensive and simple motor drive from a power antenna for a car to develop, characterize and validate an automated DSI-ICP. In addition, all DSI-ICP set-ups eliminated the conventional pneumatic nebulization apparatus, therefore normal routine solution analysis could not be performed on the system without major change over. This could be one of the major reasons that DSI devices are not widely used in the laboratories. A dual mode torch was developed to accommodate both solid and liquid sample analysis on the same torch. The change over is simple and quick which facilitates the use of the DSI option on a conventional ICP. Chapter 3 describes the development of this new instrument. Characterization of the instrument is the main focus of Chapter 4 and the instrument validation though analyzing standard reference materials is presented in Chapter 5.

References

1. E. D. Salin and G. Horlick, *Anal. Chem.* **51**, 2284 (1979).
2. Y. B. Shao and G. Horlick, *Appl. Spectrosc.* **40**, 386 (1986).
3. V. Karanassios and G. Horlick, *Spectrochim. Acta* **44B**, 1361 (1989).
4. W. T. Chan and G. Horlick, *Appl. Spectrosc.* **44**, 525 (1990).
5. W. T. Chan, Ph.D. Thesis, University of Alberta (1989).
6. V. Karanassios, M. Abdullah and G. Horlick, *Spectrochim. Acta* **45B**, 119 (1990).
7. G. F. Kirkbright and Li-Xing Zhang, *Analyst* **107**, 617 (1982).
8. A. G. Page, S. V. Godbole, K. H. Madraswala, M. J. Kulkarni, V. S. Mallapurkar and B. D. Joshi, *Spectrochim. Acta* **39B**, 551 (1984).
9. M. Abdullah, K. Fuwa and H. Haraguchi, *Spectrochim. Acta* **39B**, 1129 (1984).
10. V. Karanassios and G. Horlick, *Spectrochim. Acta Rev.* **13(2)**, 88 (1990).
11. L. Blain and E. D. Salin, *Spectrochim. Acta* **47B**, 205 (1992).
12. L. Blain and E. D. Salin, *Spectrochim. Acta* **47B**, 399 (1992).
13. L. Blain and E. D. Salin, *Spectrochim. Acta* **47B**, 1471 (1992).
14. P. J. Purohit, S. K. Thulasidas, Goyal. N., and A. G. Page, *J. Anal. At. Spectrom.* **12**, 1317 (1997).
15. R. Rattray, J. Minoso, and E. Salin, *J. Anal. At. Spectrom.* **8**, 1033 (1993).
16. R. Rattray, and E. D. Salin, *J. Anal. At. Spectrom.* **10**, 829 (1995).
17. V. Karanassios, and G. Horlick, *Spectrochim. Acta* **44B**, 1345 (1989).
18. R. Rattray, and E. D. Salin, *J. Anal. At. Spectrom.* **10**, 1053 (1995).
19. V. Karanassios, K. P. Bateman and G. A. Spiers, *Spectrochim. Acta* **49B**, 847 (1994).
20. V. Karanassios, K. P. Bateman and G. A. Spiers, *Spectrochim. Acta* **49B**, 867 (1994).
21. X. R. Liu and G. Horlick, *J. Anal. At. Spectrom.* **9**, 833 (1994).
22. X. R. Liu, Ph.D. Thesis, University of Alberta (1994).
23. L. S. Ying, MS Thesis, University of Alberta (1992).

24. M. Umemoto and M. Kubota, *Spectrochim. Acta* **46B**, 1275 (1991).
25. C. D. Skinner and E. D. Salin, *J. Anal. At. Spectrom.* **12**, 1131 (1997).
26. K. D. Ohls, *Spectrochim. Acta* **51B**, 245 (1996).
27. J. M. Ren, and Salin, *Spectrochim. Acta* **49B**, 555 (1994).
28. J. M. Ren, and Salin, *Spectrochim. Acta* **49B**, 567 (1994).
29. J. M. Ren, and E. D. Salin, *J. Anal. At. Spectrom.* **2**, 59 (1993).
30. J. Alary, G. Hernandez, E. D. Salin, *Appl. Spectrosc.* **49**, 1796 (1995).
31. B. A. Bitterli, H. Cousin and B. Magyar, *J. Anal. At. Spectrom.* **12**, 957 (1997).
32. F. Vanhaecke, S. Boonen, L. Moens and R. Dams, *J. Anal. At. Spectrom.* **10**, 81 (1995).
33. L. Moens, P. Verrpt, S. Boonen, F. Vanhaecke and R. Dams, *Spectrochim. Acta* **50B**, 63 (1995).
34. X. R. Liu, and G. Horlick, *Spectrochim. Acta* **50B**, 537 (1995).
35. S. A. Baker, B. W. Smith and J. D. Winefordner, *Appl. Spectrosc.* **51**, 1918 (1997).
36. V. Kanicky, I. Novotny, J. Musil and J. Mermet, *Appl. Spectrosc.* **51**, 1042 (1997).
37. V. Kanicky and J. Mermet, *Appl. Spectrosc.* **51**, 332 (1997).
38. D. Figg and M. S. Kahr, *Appl. Spectrosc.* **51**, 1185 (1997).
39. W. T. Chan and H. H. C. Yip, *Anal. Chem.* **69**, 4871 (1997).
40. L. Moenke-Blankenburg, T. Schumann and J. Nolte, *J. Anal. At. Spectrom.* **9**, 1059 (1994).
41. D. S. Zamzow, D. P. Baldwin, S. J. Weeks, S. J. Bajic and A. P. D'Silva, *Enviro. Sci. Technol.* **28**, 352 (1994).
42. P. Goodall, M. E. Foulkes and L. Ebdon, *Spectrochim. Acta* **48B**, 1563 (1993).
43. C. Chen and T. W. McCreary, *Appl. Spectrosc.* **48**, 410 (1994).
44. A. A. Verbeek and I. B. Brenner, *J. Anal. At. Spectrom.* **4**, 23 (1989).
45. Y. Jiang, Z. Zeng, Y. Qing, and B. Hu, *J. Anal. At. Spectrom.* **10**, 455 (1995).
46. R. R. Greenberg, J. S. Kane and T. E. Gills, *Fresenius J. Anal. Chem.* **352**, 193 (1995).
47. M. S. Epstein, B. Diamondstone and T. E. Gills, *Talanta* **36**, 141 (1989).

48. Certificate of Analysis, SRM 2709, NIST, Gaithersburg, MD 20899, August 23 (1993).
49. Certificate of Analysis, SRM 2710, NIST, Gaithersburg, MD 20899, August 23 (1993).
50. Certificate of Analysis, SRM 2711, NIST, Gaithersburg, MD 20899, August 23 (1993).
51. X. Li, B. J. Coles, M. Ramsey and I. Thornton, *Analyst* **120**, 1415 (1995).
52. K. Vercootere, U. Fortunati, H. Muntau, B. Griepink and E. A. Maier *Fresenius J. Anal. Chem.* **352**, 197 (1995).
53. Donal A. Becker and Thomas E. Gills, *Fresenius J. Anal. Chem.* **352**, 163 (1995).
54. Certificate of Analysis, SRM 1515, NIST, Gaithersburg, MD 20899, January 22 (1993).
55. Certificate of Analysis, SRM 1547, NIST, Gaithersburg, MD 20899, January 22 (1992).
56. M. Ihnat and M. S. Wolynetz, *Fresenius J. Anal. Chem.* **345**, 185 (1993).
57. W. T. Buckley and M. Ihnat, *Fresenius J. Anal. Chem.* **345**, 217 (1993).
58. R. Zeisler, D. A. Becker and T. E. Gills, *Fresenius J. Anal. Chem.* **352**, 111 (1995).
59. Ph. Quevauviller, K. J. M. Kramer and T. Vinhas, *Fresenius J. Anal. Chem.* **354**, 397 (1996).
60. H. Schauenburg and P. Weigert, *Fresenius J. Anal. Chem.* **342**, 950 (1991).
61. U. Kurfurst, J. Pauwels, K. H. Grobecker, M. Stoeppler and H. Muntau, *Fresenius J. Anal. Chem.* **345**, 112 (1993).
62. E. Lucker, H. Konig, W. Gabriel and A. Rosopulo, *Fresenius J. Anal. Chem.* **342**, 941 (1992).
63. A. Wyttenbach, S. Bajo and L. Tobler, *Fresenius J. Anal. Chem.* **345**, 294 (1993).
64. H. Schauenburg and P. Weigert, *Fresenius J. Anal. Chem.* **342**, 950 (1991).
65. J. Pauwels, C. Hofmann and K. H. Grobecker, *Fresenius J. Anal. Chem.* **345**, 475 (1993).
66. J. Pauwels, U. Kurfurst, K. H. Grobecker and P. Quevauviller, *Fresenius J. Anal. Chem.* **345**, 478 (1993).

67. A. R. Byrne, *Fresenius J. Anal. Chem.* **345**, 144 (1993).
68. X. Mao and C. Chai, *Fresenius J. Anal. Chem.* **352**, 174 (1995).
69. J. Pauwels and C. Vandecasteele, *Fresenius J. Anal. Chem.* **345**, 121 (1993).
70. T.M. Sonntag and M. Roszbach, *Analyst* **122**, 27 (1997).

Chapter 2

Environmental Sample Analysis by Ar-O₂ Mixed Gas DSI-ICP

2.1 Brief Overview

The development of new instrumentation in the field of environmental air analysis tends to be governed to some extent by legislative requirements. If an existing technique is satisfactory for the determination of a specific element at a specific concentration then the technology stays static. When the legislative requirements change it is often necessary to determine elements at lower concentrations. New instrumental techniques or sample preparation techniques are then developed to meet the requirements.

Inductively Coupled Plasma Atomic Emission Spectrometry (ICP-AES) has enjoyed steady growth over the past two decades. It has become one of the standard techniques in almost all environmental analysis laboratories. The advantages of ICP-AES over the other techniques are its multi-element capability, wide linear calibration ranges and good precision and accuracy. However, it has its shortcomings such as modest detection limits (μgL^{-1}), matrix interferences, poor semiquantitative performance, no isotopic information, limited capabilities for non-metals, sample preparation (dissolution) and it is not well suited to micro-samples [1]. One recent study claimed that for every dollar spent on the analysis of a sample, 60 cents went towards sample preparation, 20 cents for the instrument and 20 cents for data output. Therefore, development of affordable and reliable new approaches to sample preparation is an urgent and challenging task for the analytical chemist.

Direct sample insertion coupled with the ICP has proven to be one of the means to reduce sample preparation and provide micro-sample analysis. With the recent success of oxygen - argon mixed gas DSI-ICP-AES, many samples with different sample matrices and elements that are difficult to volatile were analyzed by this method [2-4]. This chapter is a continuation of this argon-oxygen mixed gas DSI-ICP study. The experiments are focused on environment related samples. These include Standard Reference Materials, waste water and solid waste.

2.11 The DSI-ICP Instrument Setup

The schematic diagram of an Ar-O₂ mixed gas direct - reading spectrometer coupled with the direct sample insertion (DSI) apparatus is shown in Figure 2.1. It has a concave grating mounted in a Paschen-Runge configuration with a focal length of 1 m. In the system the entrance slit, grating, and focal plane lie on the circumference of the Rowland circle. An array of slits with mirrors projects and focuses the selected spectral lines onto the cathodes of the photomultiplier tubes (PMTs). The nebulizer/spray chamber found in the conventional ICP system has been replaced by the sample probe delivery mechanism of a DSI-ICP system. The ICP system and spectrometer are those described by Karanassios and Horlick [5]. A DSI device typically consists of a drive assembly, a computer for system control, a modified torch and a sample carrying probe.

2.12 The Drive Assembly

The sample insertion driving system is an important component of a DSI-ICP system. It requires fast insertion, and flexible and precise control in speed, timing, and positioning. A fast insertion speed produces sharp signals and better precision for volatile elements, thus improving analytical performance [6-8]. Precise control in timing, speed, and positioning is essential for reproducible analytical results. Flexible programming for timing and positions of drying, ashing, and atomization is very important for establishing optimum analytical conditions for different samples.

Compared to other driving systems, the computer controlled stepper motor sample insertion system provides the best fit to the above mentioned requirements, i.e., fast insertion, and flexible and precise control in speed, timing, and positioning. Therefore, such an insertion system was used in this study. The insertion distance from home (lowered) position to the final atomization position is 183 mm or 2170 steps that take about 2 seconds with an insertion speed of 1200 steps/s. The positioning accuracy is better than ± 0.1 mm.

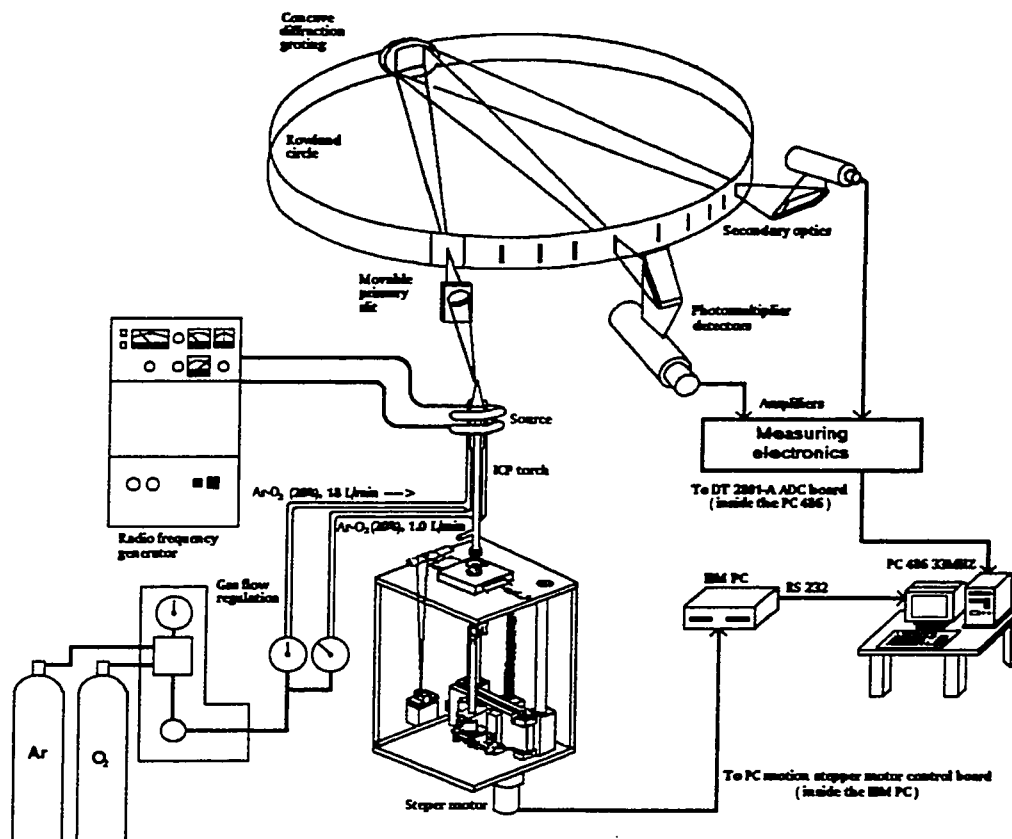


Figure 2.1 Schematic diagram of an Ar-O₂ (20%) mixed gas DSI-ICP-AES

2.13 Computer with Control Board

The readout electronics are those described by Horlick et. al. [7, 9, 10]. The system is further modified so that both the stepper motor and data acquisition can be controlled by an 8088 based IBM PC computer through a PCMotion* motor control board and a DT2801-A (Data Translation) data acquisition board that are plugged in the 8088 IBM PC expansion slot [2,3]. The signals from amplifiers are routed into the data acquisition board (DT2801-A). Up to 8 channels can be connected to the board's ADC differential input, although only 6 channels have been used. One of the disadvantages of the amplifiers is the inconvenience in changing gain. To change the gain, the resistance in the amplifier's feedback has to be manually changed. Because of the limited dynamic range of the ADC board (12 bit) the gain of these amplifiers had to be changed very often during the analysis of samples with a wide concentration range. Because of the transient nature of the DSI-ICP signal, it would be desirable to have fast amplifiers with programmable gain control. The amplifier's speed is especially important for *in situ* laser ablation ICP-AES as will be discussed later. There is a programmable gain amplifier on the ADC board but it only allows for limited ranges (2, 4, and 8 times). The specifications of hardware components and system operation parameters are listed in Table 2.1.

This system was further modified by Liu and Horlick, so that it could be controlled with an Intel 80486 based IBM compatible PC [2,3]. The data acquisition card, DT2801-A, is now plugged into the 486 computer. However, there was a problem with the stepper motor control card. When it was plugged into the 486 computer, the computer crashed when it tried to run the stepper motor. This very likely arose from a memory conflict with the motor driving routine program. Therefore the stepper motor driving card was left in the 8088 IBM PC and it was controlled by the 486 computer through the serial port (see Figure 2.1). An auto executive program was written for the old IBM PC. Once the computer (no keyboard and monitor are needed) is turned on the auto executive program loads the motor driver routine into its memory and waits for the 486 computer to send commands and parameters for running the stepper motor. The

ICP	Plasma Therm ICP 5000
ICP generator	HFS-5000D; 27.12 MHz; Max power, 5.5 kW
ICP typical operating conditions	Forward power 1.8 kW; reflected power < 30 w obs. height, 14 mm above load coil
Oxygen mix gas:	Outer gas, 18 L/min. with 20% O ₂ in Ar; intermediate gas, 1 L/min. with 20% O ₂ in Ar; central gas, 2 L/min. with water vapor.
Spectrometer	A 1-m, Pachen-Runge mount, 29-channel direct reader with a 1200 groove/mm concave grating.
DSI system	The DSI device has been described in detail in references 2 and 3. No major modifications were made except it is controlled by an IBM PC computer instead of Apple II+ .
DSI probe	Graphite electrodes with different size and shape were used (see text for discussion). SPEX Industries, Inc., Edison, NJ or Bay Carbon, Inc., Bay City, MI.
Stepper motor control board	PCMotion™ (Rogers Labs, 2727-E SO. Croddy Way, SANTA ANA, CA 92704) for IBM PC.
Data acquisition	DT2801-A (Data Translation, Inc., 100 Locke Drive, Marlborough, MA 01752-1192 USA) with a 12-bit ADC.
System computer	IBM compatible 486/33 MHz with 8 MB RAM, DOS 6.0 and Windows 3.1

Table 2.1. Hardware specification and typical operating conditions for the Ar-O₂ mix gas DSI-ICP system

DSI program runs from the 486 computer and when it needs to insert or withdraw the sample probes it sends the parameters for the stepper motor, such as ash time and position, atomization time and position, etc., to the old IBM computer. Once the old IBM computer receives these data, it runs the stepper motor according to the parameters.

2.14 The Torch and Gases

A modified Fassel torch with a big central tube that guides the sample probe into the plasma is used. It was found that the relatively large diameter of the central tube helps to keep the plasma stable because if the space between the central tube and sample probe is too small the plasma is extinguished upon rapid insertion of the probe into the plasma. A high outer gas flow rate is also effective in stabilizing the plasma while operating the DSI device.

A shutter is installed on the bottom of the torch to prevent the central and intermediate tubes of the torch from being damaged by the plasma while the sample probe is in the home position. However, it was found that the vibration caused by opening and closing the shutter can dislodge sample powder from the probe. The ICP torch was modified to introduce the sampling gas at an angle of about 45° through a restricted injection orifice. By choosing the sampling gas flow rate properly the plasma can be run safely without the use of the shutter. By using a small outlet orifice some air may be entrained into the plasma and thus keep the plasma away from the torch tube by a thermal pinch effect. If too much air is introduced into the plasma it may become unstable. The shutter still needs to be closed during plasma ignition.

About 20% O_2 (V/V) is added to the outer and intermediate gas flows. The central gas (Ar) was run through a plastic bottle containing distilled water. The water vapor carried by the Ar gas helped to quench the arc filament that tended to form in the central tube during insertion and retraction of the sample probe. To run a mixed gas plasma the capacitance in the ICP matching box must be changed to keep the reflected power low. By adding O_2 to the Ar, the plasma shrinks, thus altering the matching parameters. With the addition of 20% O_2 , the plasma's volume is reduced about 1/3 at

1.8 kW forward power. After this, more O₂ can be added with little change in the plasma's appearance. The O₂ content (~ 20%) was chosen such that the graphite cup is consumed in a reasonable time (~ 60 s). If the burning process is too slow the analysis time would be too long resulting in poor S/N ratios due to drawn out signals. On the other hand, if the burning process is too fast spattering of the sample tends to occur.

When the outer gas is switched from Ar to mixed gas the reflected power level increases to over 100 W. However, the adjustable range of the normal capacitance is too limited to allow lowering of the reflected power to its normal range which should be under 50 W. Additional capacitors of 150 pF total capacitance were added into the matching network to keep the reflected power level low [2,3]. After this change the reflected power could be kept under 20 W when running mixed gas DSI-ICPs. However as the additional capacitance is not adjustable, it is difficult to tune the reflected power to 0 W when running a pure Ar plasma.

2.15 The Probe

Graphite electrodes normally used for dc arc spectrometry have been adapted as sample cups for the direct insertion technique. Graphite is a favored material because of its thermal characteristics, ease of machining, and the relative simplicity of background spectra in the ICP. In terms of analytical performance, cup geometry has been shown to be quite critical. Intuitively, one would anticipate that sample cups of relatively small mass would undergo rapid heating of the DSI probe. This is analogous to step heating in the atomization stage of graphite furnace atomic absorption spectrometry and therefore should result in efficient vaporization of analyte and production of sharp transient signals. A smaller cup (4.5 mm outer diameter) is preferred over a larger one (6 mm) because it is less disruptive of the plasma and therefore may lead to better precision [9]. This was confirmed experimentally. It was also found that the smaller graphite electrode was less affected by a change of power and gas composition. The 4.57 mm undercut graphite electrodes (see Figure 2.2) were used in this study unless otherwise indicated.

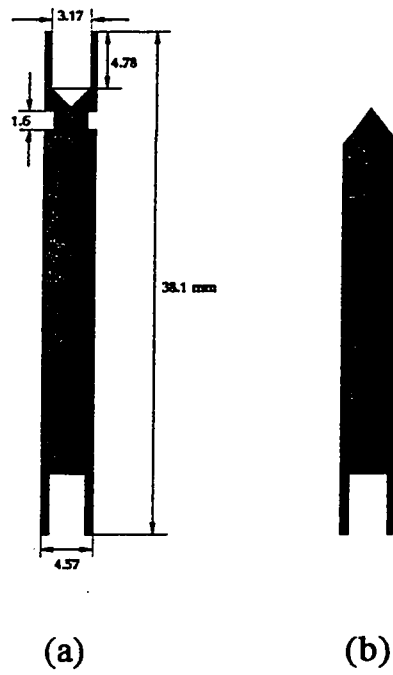


Figure 2.2 Graphite sample probes (a) before burning and (b) after burning

An arcing filament may form in the central tube when inserting and retracting the probe. Such a filament is even more serious when running mixed gas ICPs at higher power while using pure Ar in the central tube. Originally the foreign gas was introduced into the outer gas stream only and the filaments were found in both the intermediate gas stream and the central gas stream because these two streams were pure Ar. The filament may extend to the torch box through the Tygon tube of the intermediate gas and melt the Tygon tube. This is an important reason for introducing foreign gas into both the outer and intermediate gas streams in our system (see Figure 2.1). If this filament or arcing occurs in the central tube, it may spatter the sample before it reaches the plasma. It was found that a convenient and effective way to eliminate the arcing was to pass the central Ar gas through water vapor [2,3]. A very small amount of H₂O vapor can effectively quench the arcing. To this end, the central gas Ar is simply passed through a bottle containing distilled deionized water.

All graphite cups were pre-burned in the Ar-O₂ mixed gas plasma for about 30 seconds to remove impurities and contamination. This pre-burning step is also important in controlling the total analysis time as some of the graphite cup is burned off. This makes the cup wall thinner and it is thus easier to completely burn off the cup during an analysis run. During a run the pre-burned graphite cup is consumed within 80 seconds, resulting in the shape shown in Figure 2.2. For comparison, a new graphite cup used in this work is also shown in Figure 2.2. The burning speed is also dependent on the density of the graphite cup and lower density graphite consumed more rapidly.

2.16 Software

The data acquisition program is the main program for doing DSI analysis[2,3]. It contains some BASIC callable machine language subroutines for stepper motor control and data acquisition. The program is menu driven with a screen edit function providing for a convenient change of operating parameters, such as sample weight, ADC gain, probe position for ash and analyzing, etc. The profile displaying function allows the operator to have a quick view of the results. The data is saved to disk in binary code

format that saves time and disk space when large amounts of data are to be transferred. The data processing program is for post data processing and includes data loading, displaying, plotting, both peak height and peak area calculation, different background correction modes, detection limit calculations, etc. It also provides a data format converting function that converts binary code files into text files so that the data can be read and processed by other data processing programs.

There are four programmable gains that can be set for the ADC on the DT2801-A data acquisition board, and it is necessary to be able to adjust the gains for each channel and each sample to determine different concentrations. This means that the channel scan mode (in this mode the gain for all the channels must be same) cannot be used and instead the single channel convert mode must be used. However that sacrifices the total ADC speed, which is important in the case of sharp peak signals. To meet this consideration, the program was then compiled to form an executable program under the DOS system. The program can run fairly fast and is able to acquire 427 data points per second per channel. Eight consecutive data points are then added together on line to improve the S/N ratio and compress the data size without losing useful information. In practice this provided a good compromise between the measurement of sharp peak signals (from volatile elements) and wide peak signals (from nonvolatile elements) and the data size. The data acquisition speed is mainly limited by the computer's speed. Much higher ADC speed could be obtained with higher speed computers.

The MS Windows* based program for DSI-ICP analysis was developed using Borland* Turbo C++ for Windows. MS Windows* 3.1 provides a good GUI (graphic user interface).

2.17 DSI Sample Analysis

Samples, once loaded in the probes, were arranged in an aluminum holder placed in a plastic glass chamber with an IR lamp in the roof of the chamber for the purpose of drying. The chamber helps to effectively eliminate contamination from dust in the air. Samples could be dried inside the ICP torch by controlling the position of the probe.

However, it was found that the external drying process with the IR lamp in the chamber is more efficient and easier, especially when large numbers of samples are to be analyzed.

Sputtering can be a serious problem with an Ar-O₂ mixed gas DSI-ICP-AES, especially for those samples that will react with O₂ at high temperature, such as botanical samples. A boiler cap may help to prevent sample loss from sputtering [11]. However, the cap can fall off in the plasma during the burning process because the side walls of the graphite cup burn out first in the Ar-O₂(20 %) mixed gas plasma.

Using smaller amounts of sample and a deep cup are probably the easiest ways to eliminate sample sputtering. Also special attention may have to be paid to sample homogeneity when analyzing solid samples because the rather limited sample size of the DSI system can lead to significant sampling errors when dealing with inhomogeneous samples. If the average concentration of an inhomogeneous sample is required several replicate analyses should be performed.

For samples that have an organic matrix, an ashing step must be applied before the sample is inserted into the core of the plasma; otherwise the sample will be lost in the explosive release of vapors as the matrix is rapidly vaporized.

2.2 Sample Analysis by Conventional ICP

2.21 Conventional ICP Used in this study

The instrument used in this study was the Leeman Labs. ICP PS2000. The specifications of the ICP are listed in Table 2.2. The sample introduced into the ICP using a Hildebrand Grid nebulizer. In the Hildebrand Grid nebulizer the sample solution flows over two platinum screens to be sheared off by a high velocity flow of argon. This action generates a fine mist of sample solution which is contained within a spray chamber. The spray chamber is made of polypropylene with a Teflon baffle and, therefore, practically inert. The function of the spray chamber is to remove all but the smallest drops (<10 μm) from the nebulizer mist. The injector tube of the touch is made of alumina (ceramic), which is HF resistant.

Spectrometer:	Fixed echelle grating with quartz prism for order sorting. Exit slits on 2-dimensional aperture plate.
Slit widths:	Entrance: 60 μm . Exit: 30 μm .
RF generator:	40.68 MHz, free-running Flagg Oscillator. Power variable from 0.7 to 2.0 kw, in steps of 0.1 kw.
Wavelength:	190 - 800 nm.
Resolution:	200 nm: 0.0075 nm 400 nm: 0.012 nm 600 nm: 0.018 nm 800 nm: 0.024 nm
Torch:	Demountable torch (standard) One-piece quartz (optional) Alumina injector tube (optional)
Autosampler:	Two-44-place sample racks, plus one 14-place rack for standards
Computer:	IBM AT compatible, with 640 K RAM, 40 Mbyte hard disk. EGA color graphics monitor.
ICP operating conditions:	Coolant flow rate: 14 LPM Auxiliary flow rate: 0.4 LPM Nebulizer pressure: 45 psi Peristaltic pump: 1.5 ml/min

Table 2.2 Specifications of Leeman Labs ICP

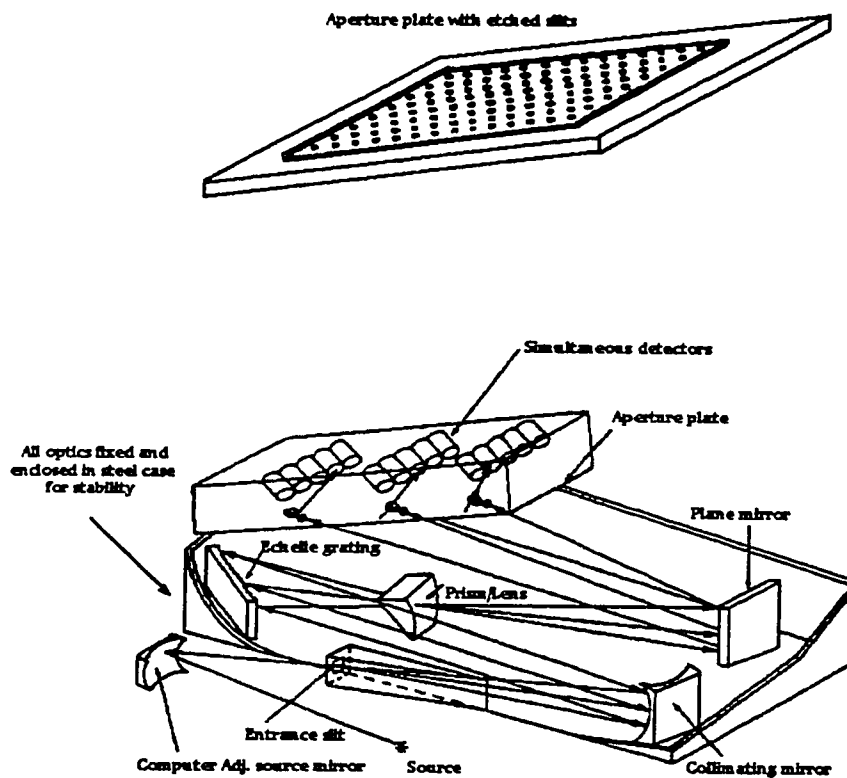


Figure 2.3 Leeman Labs. ICP Echelle optics

The PS series spectrometer uses a coarse-ruled echelle grating, teamed with a quartz prism. (Figure 2.3) An echelle grating provides such good resolution that larger slits can be used, so that detectors receive as much light from the emission line as possible (enhancing trace-level work). Light from the ICP source strikes the computer controlled mirror, which focuses an image of the plasma on the entrance slit. The mirror moves, under control of the computer, to scan the plasma image along x- and y-axes, for selecting the best viewing position for analysis.

Figure 2.3 shows an echelle grating spectrometer. After light passes through the entrance slit (60 μm wide and 1 mm high) into the light-sealed optics box, it is reflected by a collimating mirror onto the echelle grating. The echelle grating, like a conventional gratings, disperses the light horizontally by wavelength. It is blazed to concentrate light in high orders. The diffracted light then enters a prism/lens, which acts as an "order sorter", dispersing light according to wavelength perpendicular to the grating's dispersion. The result is a 2-dimensional "stacking" of orders, with all wavelengths well separated in space. The prism also acts as a lens, refocusing the light on the detectors at the exit slits. In order to keep the optics box compact, a plane mirror folds the light back and up, onto the aperture plate with hundreds of exit slits. Detectors either moving sequential or fixed simultaneous - measure light at positions corresponding to distinct wavelengths for analysis.

The aperture plate is a thin metal plate (with 90 μm by 1.5 mm slits etched at about 2 mm intervals) which sits at the top of the optics box, where the dispersed light comes to focus. It is a rigid frame, which can move in two dimensions to exactly position a slit over the desired wavelength. An aperture plate, containing preset aperture, is mounted at the focal plane. A mask plane, with slits and mirrors at appropriate positions, is located above the aperture plate. This assembly allows only the light from the wavelengths selected to reach the corresponding PMTs, mounted in the photomultiplier rack.

2.22 Microwave Digestion

Microwave sample digestion provides a number of advantages: fast decomposition, reduction in the amount of acid necessary for dissolution, reproducible thermal digestion conditions, and reduced likelihood of contamination and loss of volatile elements. It has become a standard operating procedure for environmental sample analysis [12-14].

The use of HF in conjunction with other acid mixtures for the digestion of solid samples containing silicon is a well established conventional approach. The microwave-assisted conventional HNO_3 -HF- H_2O_2 - H_3BO_3 digestion system was used for direct ICP-MS analysis of total metals in silicon-containing solid samples. The method proved to be suitable for routine analysis of at least 25 elements. The recoveries for most of these elements in standard reference materials including coal fly ash, urban particulate matter, sediment and soil were within 90-110%, and the relative standard deviations were within 5% [15].

The use of a microwave oven for the rapid digestion of dust samples has also been evaluated by Feng and Barratt [16]. Deposited dust collected for the study and reference samples representing municipal waste incineration ash, urban particulate matter and river sediments were the samples used in the study. A digestion procedure of 20-30 min for dust samples (0.1 - 1.0 g) allows recovery of Pb and Cd at over 80% with nitric acid or aqua regia and over 90% with a nitric/hydrofluoric mixture.

The CEM MDS-2000 (Microwave Sample Preparation System MDS-2000, CEM Corporation, Matthew, North Carolina 28106) was used for sample digestion in this study. The specifications of the microwave digestion oven and its vessel are listed in Table 2.3. It is equipped with an inboard pressure control system to monitor and control pressure conditions inside sample vessels as shown in the Figure 2.4. Tubing is attached to a sample vessel and routed outside the microwave cavity through one of the inlet/outlet ports. This tube is connected to a panel-mounted fitting leading to the pressure control components located in the base of the system. Pressure is sensed by a transducer and displayed graphically and digitally on the LCD display screen.

Power Range:	0 - 100 percent full power (630 w \pm 50 w), programmable in 1% increments.
Time Range:	Maximum of 59 minutes, 59 seconds in each of 5 successive stages, which can be combined in a sample preparation cycle, programmable from the front panel.
Readout Features:	An 8 line \times 40 character alphanumeric display and an audible tone (beeper) for operator feedback are used in each instrument.
Operator Control:	A keyboard with 22 keys is used to enter data and to control microwave heating cycles.
Safety Features:	Three independent door safety interlocks including an interlock monitoring system plus two independent thermal switches are used in each instrument. The instrument is equipped with a turntable interlock system which causes the turntable to rotate when microwave power is on.
Maximum Number of Vessel:	12
Vessel Volume:	100 ml
Maximum Operating Pressure:	200 psi
Maximum Organic Sample Size:	<0.5 gram
Material of Construction:	
Liner:	Teflon PFA [®]
Cover:	Teflon PFA [®]
Vessel Body:	Ultem [®] polyetherimide
Vessel Cap:	Ultem [®] polyetherimide
Vent Fitting:	Teflon PFA [®]

Table 2.3 Specification of MDS-2000 microwave oven

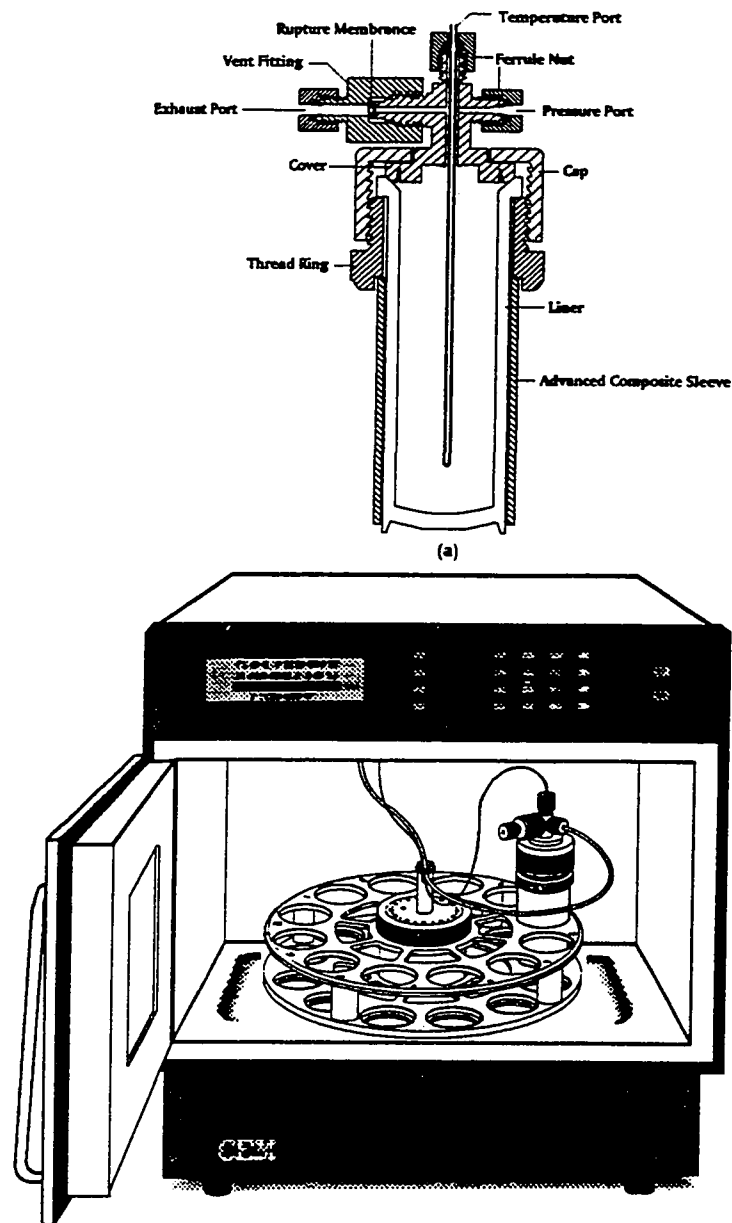


Figure 2.4 Microwave digestion system diagram with a control vessel diagram

Advanced composite vessels designed for use inside the CEM microwave sample preparation system were used. The vessel has a chemically resistant liner and cover to contain and isolate a sample solution as shown in Figure 2.4(a). The materials of the vessel are transparent to microwave energy so that liquid and sample inside can absorb the maximum amount of incident microwave energy.

The procedure of sample digestion was as follows: approximately 0.25 g of solid sample was weighed, to the nearest 0.1 mg, in the digestion vessel. For stack ash samples, 10 mL of concentrated HNO₃ were added to the sample for digestion. For bottom ash (slag) samples, an additional 2 mL of 48% HF and 2 mL of 30% H₂O₂ were added sequentially. After the strong initial reaction abated (approximately 5 min for most of the samples), the vessels were capped. The digestion program consisted of a ramp time of 20 min to reach 120 psi and a dwell time of 20 min at 160 psi both at the maximum power of 650 W and pressure limit of 200 psi. The digestion operation parameters are listed on Table 2.4. The vessel was cooled, vented and opened, and the solutions transferred into a 100 mL volumetric flask for the samples with nitric acid matrix and diluted to the volume or transferred into tared 100 mL HDPE bottles and diluted to 100 g by weighing for the samples with hydrofluoric acid matrix.

Digested blanks and pre-digested spikes were prepared in the same manner. Typically, nine samples, one blank, one NIST SRM 2704 Buffalo River Sediment and a duplicate and one sensor vessel control sample were prepared for simultaneous digestion.

2.23 Chemicals and Reagents

All stock standard solutions (10,000 mgL⁻¹) were purchased from SCP Science (Montreal, PQ, Canada) or from Leeman Labs (Lowell, MA, USA). The reagent blank always contained nitric, hydrofluoric and boric acids in corresponding amounts to the final solution of the sample. The following mixed stock standard solutions in 2 % HNO₃ were prepared from individual 10,000 mgL⁻¹ stock standard solutions. Stock standard solution contained 100 mgL⁻¹ each of As, Ba, Be, Ca, Cr, Cu, Fe, Mg, Ni, Pb, V, and Zn.

DDW was used directly from a NANOpure water purification (ion exchange) system (Barnstead, Fisher Scientific) fed with distilled water. High purity 45-51% HF, Fisher Scientific, certified 30% H₂O₂ (analytical reagent grade BDH) were used in the digestion procedure, and in the preparation of the reagent blanks and standard solutions for ICP measurement.

2.24 Standard Reference Materials

The following NIST standard reference Materials (SRMs) were used: SRM 1633b (Coal Fly Ash), SRM 2704 (Buffalo River Sediment), SRM 4355 (Peruvian Soil), SRM 679 (Brick Clay) [17-20]. Four reference soil samples were obtained from the Canadian Certified Reference Materials Project, Canada Centre for Mineral and Energy Technology, 555 Booth Street, Ottawa Ontario K1A 0G1. They were stored and handled as instructed.

Stage	(1)	(2)	(3)	(4)
Power (%)	60	80	100	100
Pressure (PSI)	40	80	120	160
Time (min)	10	10	20	20
Time at Pressure (min)	3	3	10	10
Fan Speed	100	100	100	100

Table 2.4 Operation parameters of microwave digestion oven

2.3 Source of sample - An Industrial Waste Treatment Plant

2.31 Introduction of Waste Process in a Hazardous Waste Plant

Samples were obtained from a fully-integrated waste management facility capable of handling all hazardous wastes with exception of pathological, explosive or radioactive materials. The facility consists of two high temperature rotary kilns, a physical/chemical treatment plant, a stabilization and solidification plant, several landfill cells and a deep well disposal facility. The treatment process diagram is shown in Figure 2.5. The organic wastes such as oil, solvents, and PCB's are treated by high temperature incineration. The inorganic waste, such as acids, alkalis and heavy-metal bearing materials are treated by physical/chemical processes such as neutralization and precipitation. Contaminants and bulk inorganic solids are treated through stabilization and solidification techniques.

2.32 Flyash and Slag (Bottom Ash)

The bigger rotary kiln has the option to incinerate wastes in either slagging or ashing modes. The slagging process allows for the immobilization of inorganic contaminants in a solidified molten matrix. Typical of wastes treated in this fashion are organic sludges with heavy metal content. The ashing mode enables certain non-leachable waste streams such as soils to be treated more cost effectively. A temperature of 1200 °C in the secondary combustion chamber is maintained to ensure complete destruction of all organics. The combustion gases pass through a high performance flue gas cleaning system which removes acid gases and solid particles before being discharged to the atmosphere. This emission control system includes: a spray drier, activated carbon injector, baghouse, saturator and high energy scrubber as they are described in Figure 2.6. Ash and slag are water quenched and then quarantined in an enclosed laydown building while leachate tests are conducted. Residues are stabilized as required to meet strict leachate standards prior to being sealed in secure Class 1 on-site landfill cells.

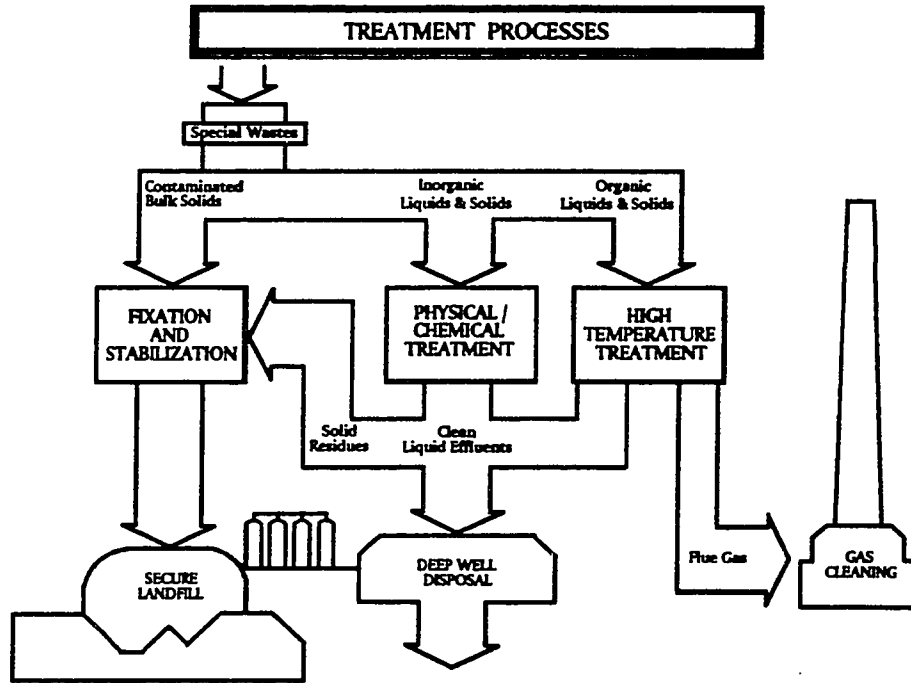


Figure 2.5 Hazardous waste plant process diagram

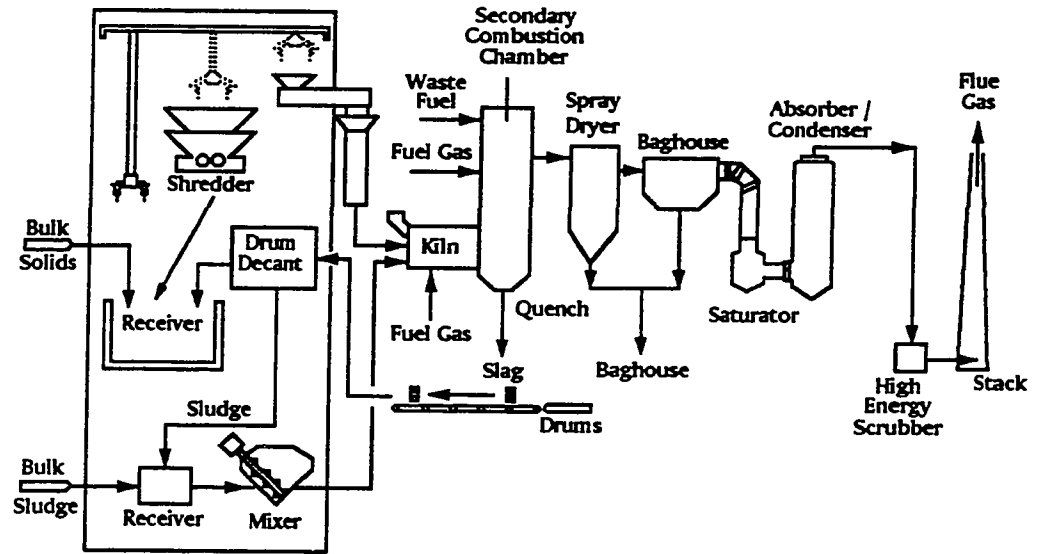


Figure 2.6 Slagging rotary kiln incineration system

Many people consider incineration as a complete alternative to landfilling. In fact, incineration reduces waste volumes considerably, but solid residues remain which have to be landfilled properly so as to prevent pollution transfer to air, soil or groundwater. Incinerating 1 ton of waste produces, on average, 300 kg of solid residue. Therefore, the amount of incineration residue is not negligible. In fact, three kinds of residues can be distinguished:

- Bottom ash or slag (about 300 kg/ton of waste incinerated). This is the material which remains on the grate after passing through the combustion zone.

- Baghouse ash, which comes from the scrubber system.

- In some cases, stack ash of gas cleaning systems from air pollution control equipment (depending on the system process).

The smaller kiln combines fly ash and bottom ash in a quench tank or similar container. The bottom ash consists predominantly of silicon oxide. Additional components include oxides of aluminum, iron, and calcium as well as sulfate and chloride ions.

2.33 Landfill Cell

A strategic component of the treatment and disposal process is the secure landfilling of treated waste residue for optimum security. Secure landfill cells are built into the thick impermeable clay layer native to the site. Each landfill cell has a multi-layer containment barrier which includes two high density polyethylene (HDPE) liners as well as protective geotextile and geogrid layers.

Above the HDPE liners is a leachate collection system consisting of a sump and piping system allowing for the extraction of liquid (called leachate) should it accumulate (Figure 2.7). All leachate is collected and treated before disposal to the deep well injection. As an additional safeguard, a leachate monitoring system is located between the

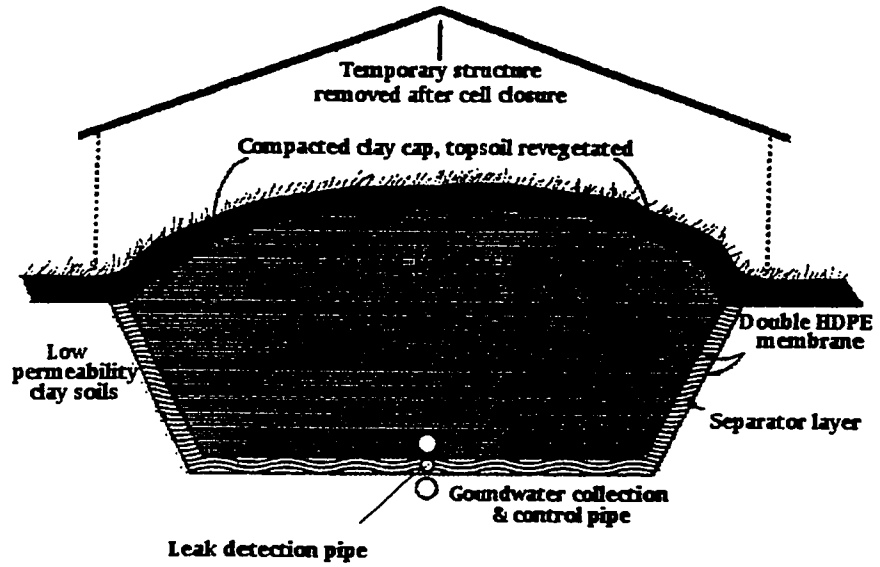


Figure 2.7 Landfill cell

two HDPE liners to check for leaks. Both systems are constantly monitored even though no free liquids are permitted to enter the cell. Further assurance is provided by a ground water collection system installed beneath the cell to minimize external forces on the cell liners and for the purpose of ground water monitoring. Although the landfill cell is licensed as Class 1 for hazardous wastes, the risk of potential environmental liability is further minimized by the pretreatment of all wastes. Before being landfilled, all generator wastes and residue must meet stringent requirements, i.e. U.S. EPA 1311 TCLP test [21].

2.4 Sample Analysis by O₂-Ar Mixed Gas DSI-ICP

2.41 Analysis Procedure

2.411 Calibration Curve

The calibration curves for DSI-ICP are generated by analyzing 10 µl of the 0.1 ppm to 400 ppm solution residue. They are shown in Figure 2.8. For Ca, V, Fe and Zn, the calibration curve started at 1 ppm. The 0.1 ppm solution residue did not generate a decent signal. Each data point is an average of at least 2 analysis results. The linearity and correlation coefficient for most of the elements tested were good. The slopes of the log-log plots are close to unity in most of the cases.

The intensity - time signals at 1 ppm and 10 ppm concentration levels for these elements are shown in Figures 2.9 and 2.10. With the Ar-O₂ mixed gas ICP, the base line gradually increases towards the end of a run. A probable explanation for this is that the plasma becomes brighter and brighter as the graphite electrode becomes smaller and smaller. This may result in problems for background correction and blank sample subtraction may be necessary. To do blank subtraction an empty graphite probe was run for every 15 sample runs. During data processing, both the sample signal and blank signals were normalized to the same gain and then the blank signal was subtracted from the sample signal. The data processing program can do the blank subtraction and base line adjustment automatically. However, such a subtraction may not be very accurate as the sample and blank are not analyzed at the same time and may not have identical burning

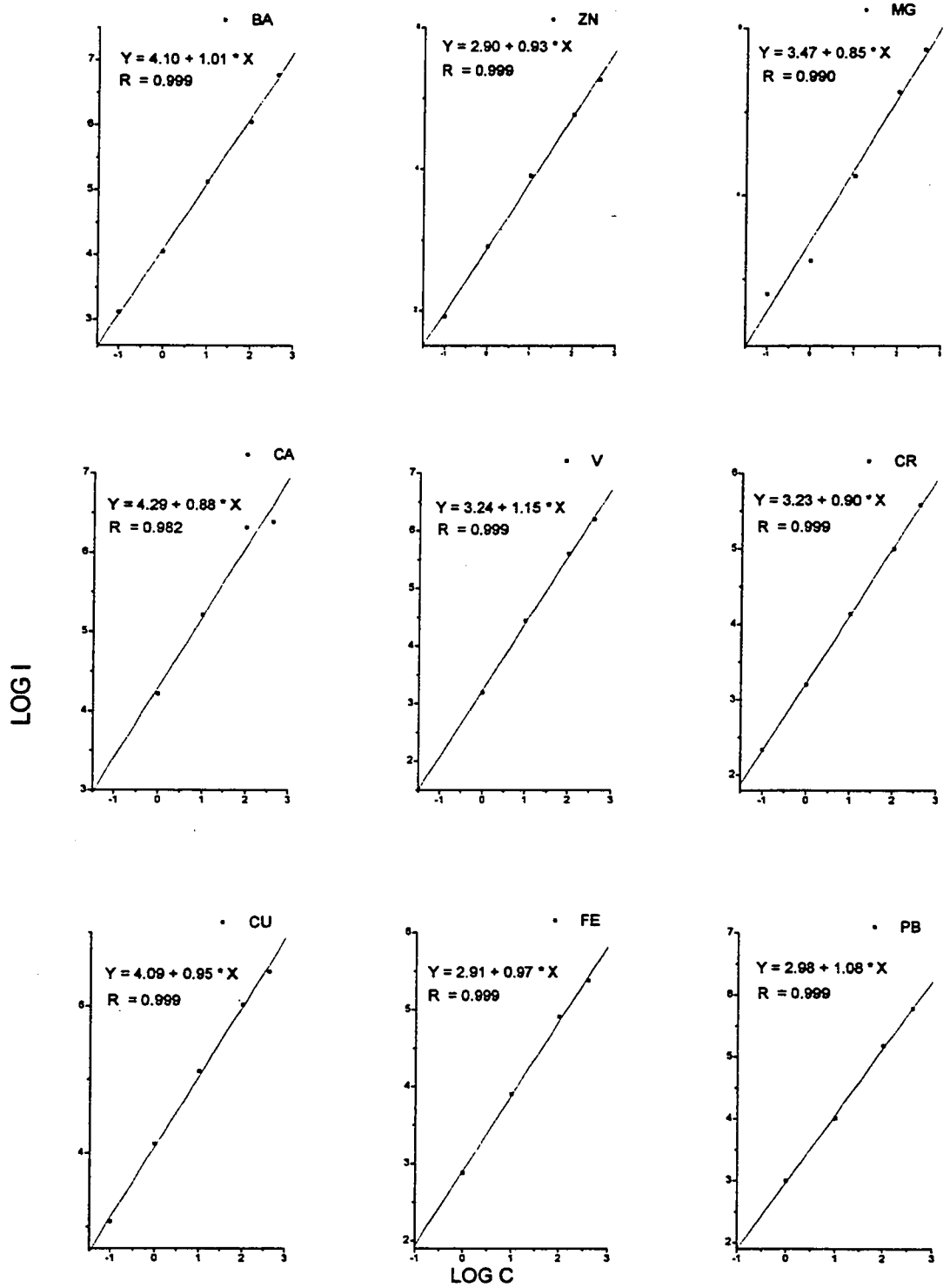


Figure 2.8 Nine element log-log calibration curves

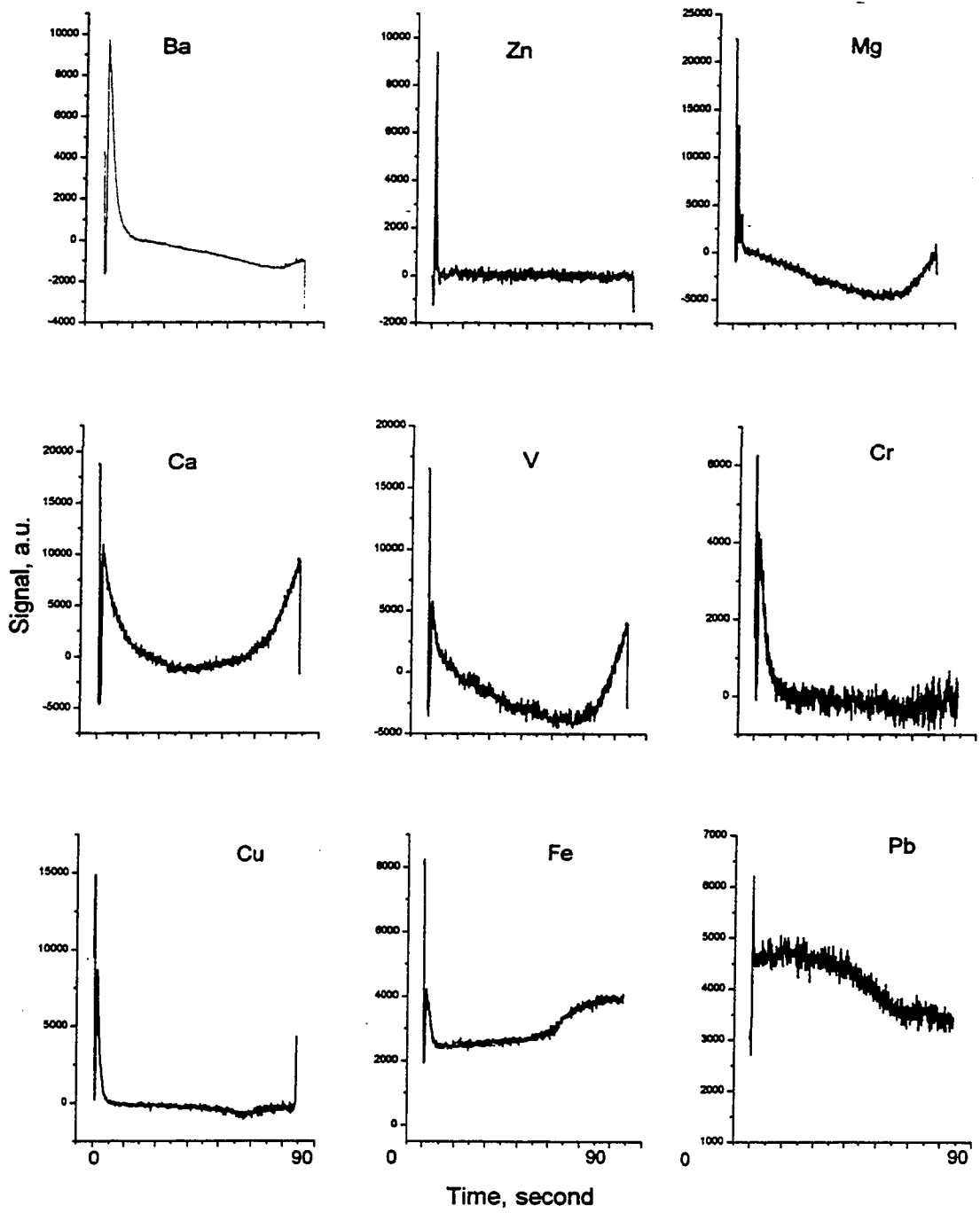


Figure 2.9 Signals at 1ppm concentration for nine elements

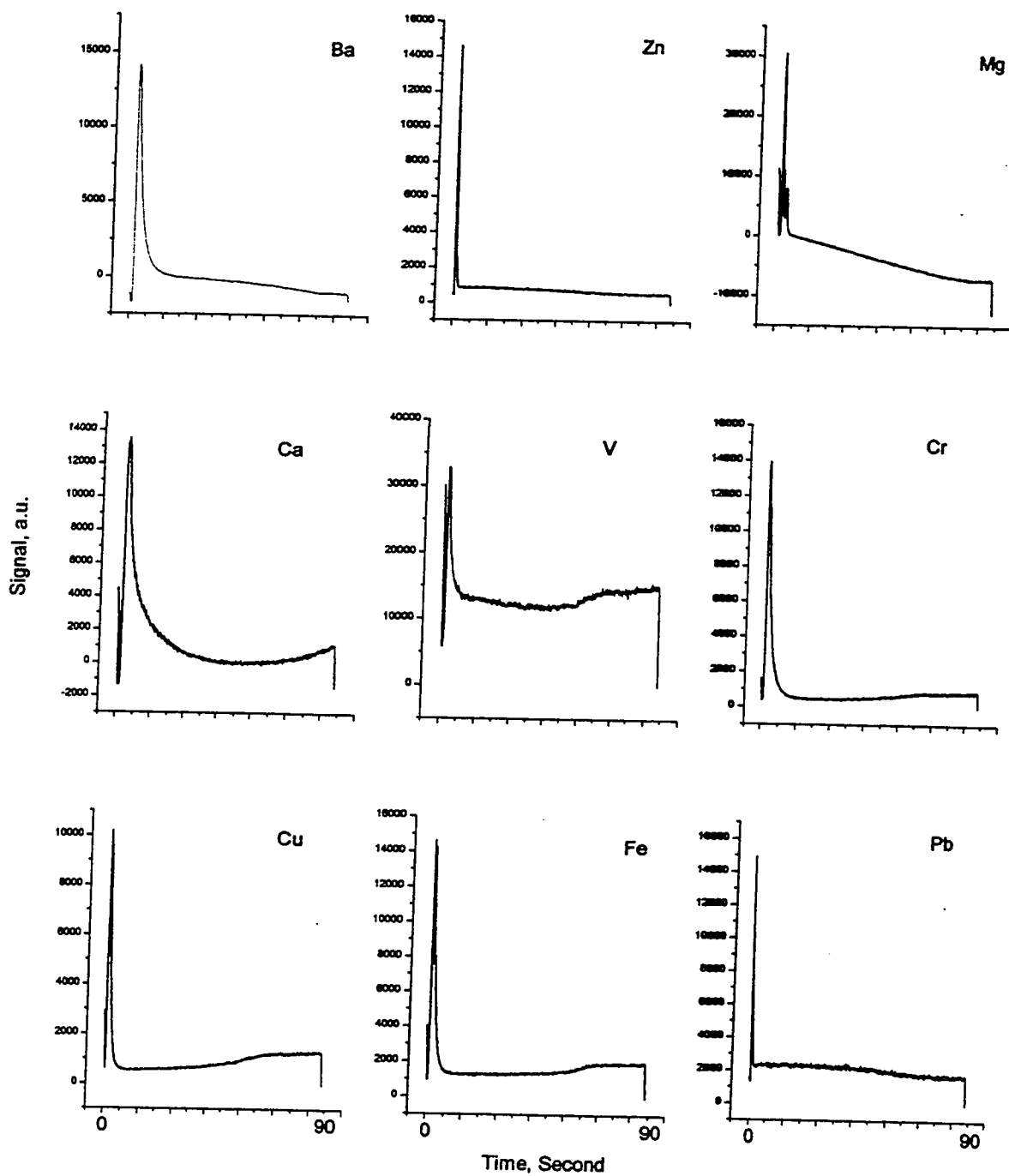


Figure 2.10 Signal at 10 ppm concentration for nine elements

processes. The ideal correction method would be to use simultaneous off-line background correction. In this case the analyte spectral line and the off-line background are monitored simultaneously. Real time changes on background signals can be corrected more accurately. However, this requires spectrometers incorporating array detectors such as PDAs.

2.412 Instrument Stability and Sample Homogeneity

Precision in DSI generally is inferior to that of solution nebulization techniques and typically ranges from 3 to 10% RSD for solution residues and 10 to 20% RSD for solid samples. Five different sample matrices were chosen for the study. The relative standard deviations for the resulting 9 analyses of five different matrices are listed in Table 2.5 . The RSD values for the five elements are around 15%. The overall RSD for the leachate is the lowest. These results are consistent with a previous study done on the same instrument. This level of precision is caused primarily by sample to sample heterogeneity, variability in sample size, irreproducibility in rate of vaporization, and imprecise sample insertion.

One of the major considerations in choosing the appropriate technique and operational conditions is the degree of sample heterogeneity. This consideration is significant when solids are introduced directly into the ICP. In the analysis of a solid that has been put into solution, the analyst has the benefit of selecting a large subsample of the solid sample to assured homogeneity for a valid representation of the bulk sample. This generally is assure when samples of the order of a gram or more are selected for preparing a solution. In contrast, DSI- ICP is restricted to much smaller samples, within the milligram range, which often can lead to poor sample-to-sample reproducibility.

The RSDs for solid samples are general higher than the RSD values from solution residues. This was also confirmed in this study. The RSD value of Cr in the NIST SRM 1633b is more than double the values from other matrices as shown in Figure 2.11. The Cr peak profiles of these matrices are illustrated in Figure 2.12. The flyash signal (SRM 1633b) has a secondary peak. This suggests that there may be different mineral forms with high Cr concentration present in the flyash.

		Cr	Cu	Pb	V	Zn
Buffalo River Sediment (SRM 2704)	RSD %	9.2	18	28	21	9.1
Fly Ash (SRM 1633)	RSD %	28	11	19	25	20
Stack Ash (6075)	RSD %	11	12	11	25	12
Bottom Ash (6917)	RSD %	8.5	10	16	12	13
Leachate (6157)	RSD %	5.0	9.2		14	16

Table 2.5 RSD summary of replicate analyses

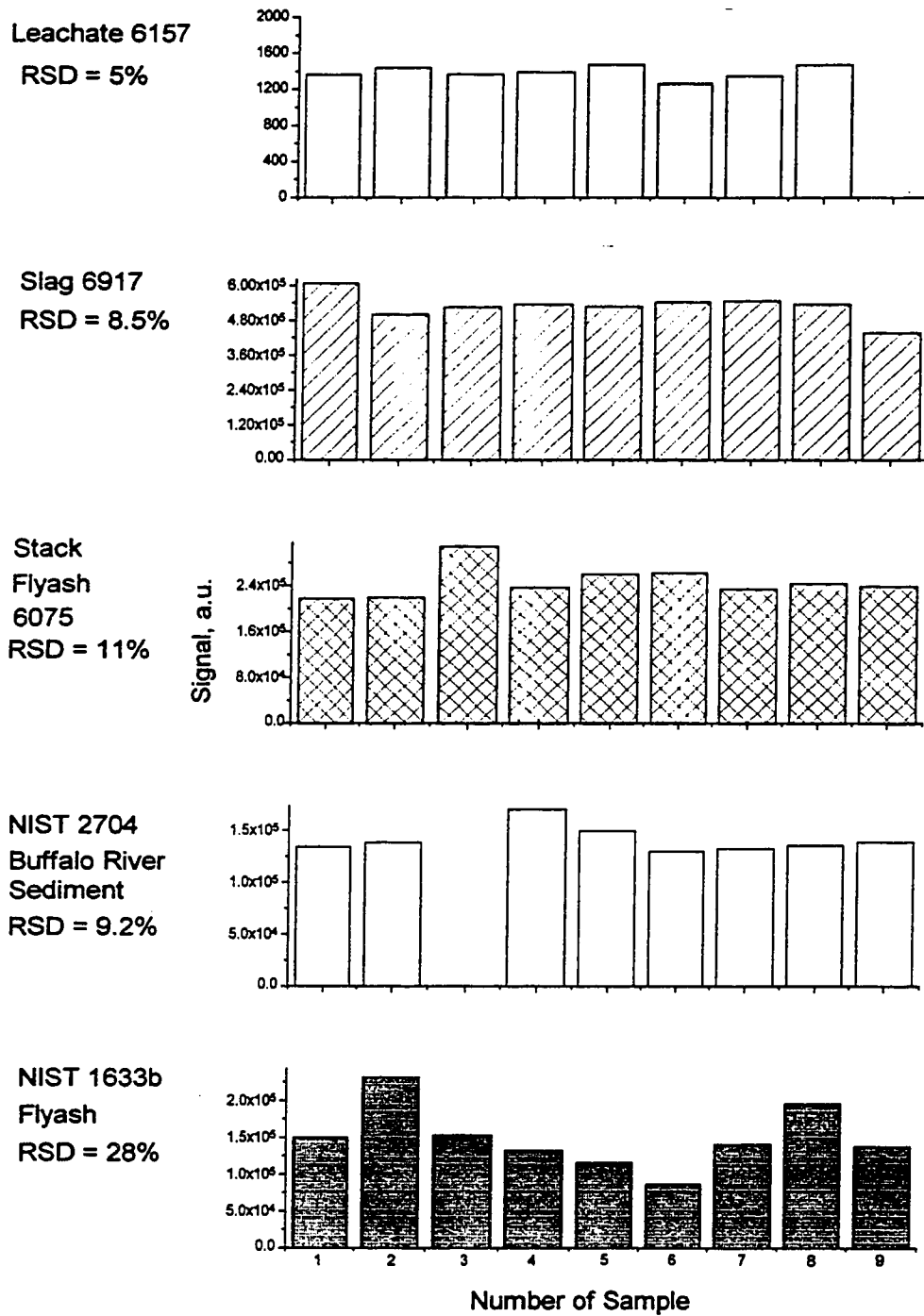


Figure 2.11 Sampling study of Cr in five different matrices

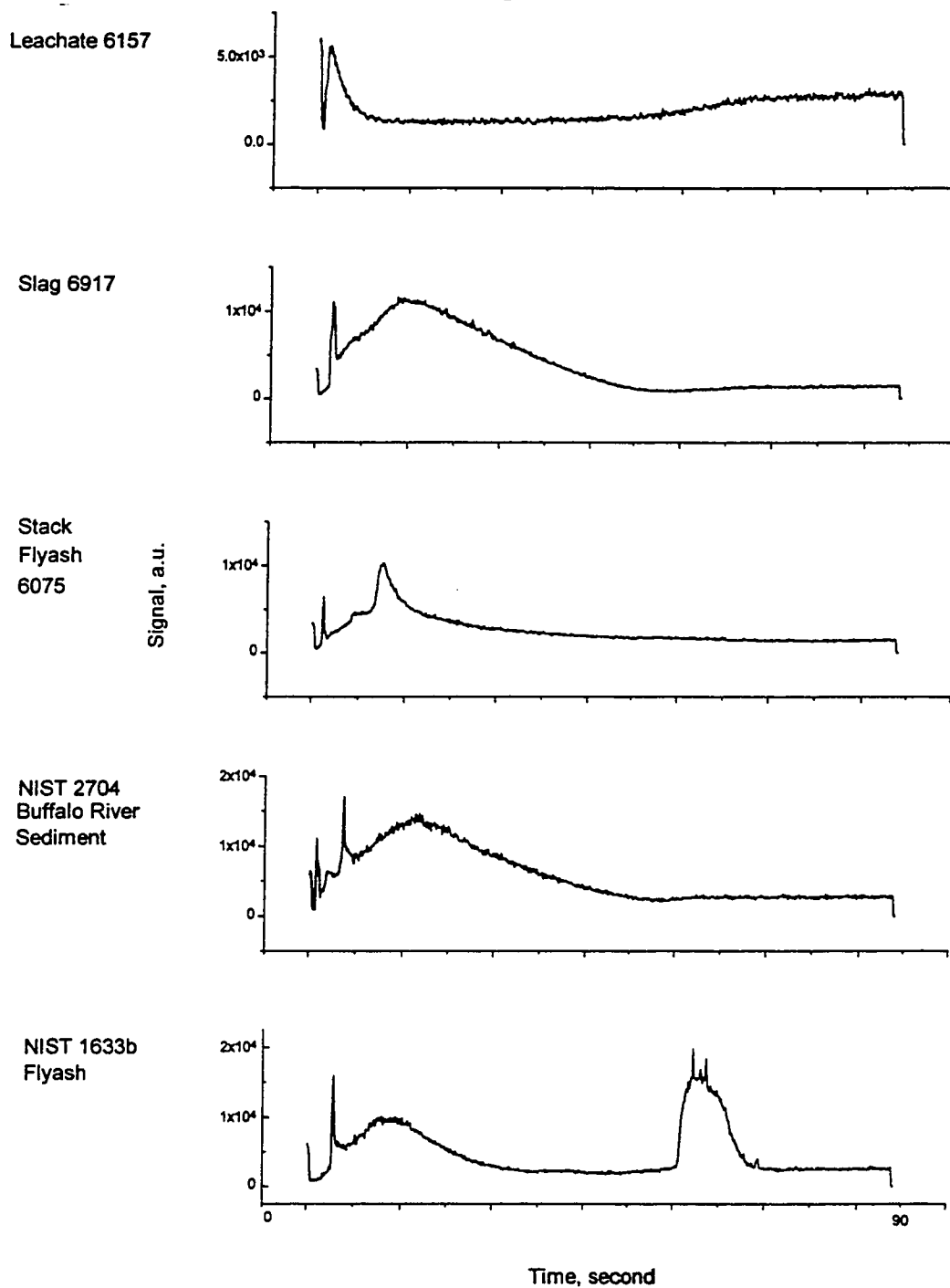


Figure 2.12 Cr peak profiles in five different matrices

		Cr	Cu	Pb	V	Zn
Buffalo River Sediment (SRM 2704)	NIST	135	98.6	161	95	438
(ppm)	DSI	128±11	110±20	153±43	105±22	460±41
Fly Ash (SRM 1633)	NIST	131	128	140	214	210
(ppm)	DSI	135±38	136±15	137±28	280±70	324±65
Stack Ash (6075)	NB	220	10900	12000	378	12800
(ppm)	DSI	223±24	2800±340	2700±300	313±78	11000±1500
Bottom Ash (6917)	NB	385	5500	844	2130	640
(ppm)	DSI	480±41	3800±385	776±126	2300±261	774±101
Leachate (6157)	NB	1.6	0.79		2.2	0.19
(ppm)	DSI	1.3±0.07	0.81±0.07		1.95±0.27	0.24±0.04

NIST: National Institute of Standards

DSI: Direct sample insertion

NB: Nebulization

Table 2.6 Sampling data summary

The concentration results of this sampling study are summarized in Table 2.6. Solution residue calibration plots were used for concentration determination. The DSI-ICP results are close to the NIST certified values or the values obtained through conventional nebulization ICP via microwave sample digestion. The poor results (Stack Ash 6075) for DSI compared to solution nebulization may be caused by the high concentration of the Cu (1.1%) and high concentration of the Pb (1.2%). The detector may have been saturated for the DSI measurements.

2.42 Leachate Analysis

2.421 Background

The US EPA Office of Solid Waste has specified that the following four tests be performed to determine if an unknown waste material may be hazardous:

- Ignitability - causes or exacerbates a fire[22, 23].
- Corrosive - pH limits exceeded or corrodes steel [24, 25].
- Reactivity - unstable[26].
- Toxicity - may leach from a landfill and contaminate groundwater [21].

A primary concern with the handling and disposal of incineration ash is whether contaminants will leach (become soluble) and migrate to groundwater supplies. The Toxicity characteristic is the most quantitative of the four tests and is performed using the toxicity characteristic leaching procedure (TCLP). The TCLP mimics the type of processes a waste might be exposed to under natural conditions in a landfill. If hazardous components migrate from the disposal site into a water source, drinking water supplies may be contaminated. The TCLP test consists of two parts: extraction of contaminants using an acetic acid buffer solution, followed by analysis of the resultant extract to determine the concentration of representative contaminants. If a TCLP determination indicates that these elements are present at concentrations that exceed the maximum contaminant levels, then the original waste is considered to be toxic and is subject to stringent disposal regulations.

A series of physical, chemical and microbiological processes can occur in landfills and the subsequent leachates can change in composition and concentration with time. Thus, the control of these effluents becomes essential not only to check the presence of possible toxic substances, but also to assess their behavior in order to select the most suitable procedure to clean up. Analytical determinations in this kind of matrix, due to its very complex composition (high amount of organics, chlorides, sulphides, bromides, complexing agent, etc.), are not an easy task. In the analysis of metals and trace elements, which are often present at ppb levels, accurate determinations can be conveniently carried out only if specific analytical procedures are followed. For many elements highly sensitive and specific methods of analysis, such as ETAAS and NAA, suffer from matrix effects and element or compound interferences: i.e. high chloride concentration can seriously affect the determination of cadmium and lead at trace level by GFAAS, while, in the case of NAA, the presence of high amounts of sodium and bromine simply prevents the quantitative analysis of many trace elements.

Gallorini etc. developed methods to separate and eliminate the matrix and interfering compounds or elements which reduce and in some cases impair the sensitivity of the technique [27]. For analyses by GFAAS a preliminary preconcentration and separation procedure, based on the ion exchange resin Chelex-100, has been developed to determine Pb, Cd, Co, Cu, Ni and Sn. In the case of NAA a specific radiochemical separation was developed for the analysis of Sn, V, W, Mn, Cr, As, Sb, Se, Th in the presence of high bromine and sodium concentrations. Furthermore, different mineralization procedures using both microwave digestion and a Teflon bomb were compared and evaluated. Four elements (Cr, Mn, Ni and Zn) could be directly determined by AAS in the leachate samples, while for all the others a chemical separation had to be applied. The results obtained after determining the same elements by different analytical techniques were in excellent agreement, as in the case of Co, Mn and Ni. Only in the case of Zn were the values scattered (S.D. ~ 15% of the medium values). The proposed procedures meet the principal requirements necessary for trace element analysis in samples of landfill leachate and allow the determination of several elements at the ppb level.

Ninety per cent of the 130 million tonnes of waste produced in the UK each year is directly disposed in landfills. This makes landfill one of the most important waste disposal options in the country, mainly because it is so economically favorable. The characteristics and composition of leachate have not been fully researched previously, especially with respect to the effect leachates may have on the stability of the clay barriers. Owen and Manning studied silica geochemistry of landfill leachates [28]. Two sites were chosen to provide sample characteristic of the composition of leachate. Exploratory work has been carried out to determine the chemical composition of landfill leachates. The samples were analyzed by using an ICP-AES for cations and an ion chromatograph for anions. pH, conductivity and suspended solids were also determined. A wide range of values were found, attributable to the non-uniformity of the chemical composition in the landfill sites. Samples were collected periodically to study the change in leachates over time and significant changes were noted over a period of two months.

Gludenis and co-workers employed a P-E Optima 3000 ICP-OES for the determination of metals in TCLP extracts using RCRA (Resource Conservation and Recovery Act) ICP method 6010 [29]. Excellent spike recoveries and close agreement with the established values for the laboratory control sample were demonstrated. The average recoveries for three samples studied were 94.9%. The EPA RCRA limits for recoveries specified in the method are 75-125%. The results were obtained quickly, with rapid confirmation by the use of a second wavelength for each element, and elements only of passing interest could also be determined without sacrificing analysis time because of the complete simultaneous coverage of the Optima 3000.

2.422 Results and Discussion

The leachate was filtered with glass fiber and membrane filters (0.2 μm) after collection to remove suspended soils and to rid the samples of microbes, which also helps to stabilize the composition of the liquids. The samples were analysed by using: an inductively coupled plasma atomic emission spectrometer for cations; an ion chromatograph for anions; and various wet chemical methods/meters for pH, conductivity

and suspended solids.

Three sets of leachate samples were chosen for the comparison between the DSI-ICP method and the conventional ICP method. The samples were acidified to 2% (v/v) by HNO_3 . Each set of samples consisted of one above liner sample and one below liner sample. The data is summarized in Table 2.7. The above liner sample usually contains some heavy metals leached out from the bottom ash or stabilized waste. All three above liner samples contain Cr in the sample. This is very normal for the waste landfill cell. The Cr (VI) does not form a hydroxide to precipitate. It has to be reduced to Cr (III) to be stabilized. The Cr and V are major components of many catalysts. Zinc and copper are major components of electrical wires. The below liner leachates show very little heavy metals which indicates no leaks in the cell.

Figure 2.13 presents six signals from sample 6157 (C1A). All peaks are very sharp except for Ca. This was consistent with earlier findings in our group [30]. Ca shows no signal suggesting that a refractory carbide is formed in the graphite cup during insertion. In addition, sodium chloride is not a good enhancement modifier. This was very true in this case as a high concentration of the chloride is present in the leachate and had no effect.

2.43 Slag and Flyash Analysis

2.431 Background

Heavy metal concentration levels in slags from an Italian medical waste incinerator were evaluated by Santarsiero and Ottaviani [31]. The legal status of the slag (hazardous or nonhazardous) was discussed according to the heavy metal content. Several elements (Cd, Cr, Cu, Ni, Pb and Zn) were analyzed by atomic absorption spectrometry from slag samples collected for a period of time. BCR 176 (Community Bureau of Reference) city waste incineration ash was used as a quality control check and showed a good degree of accuracy in the determination of all the elements investigated.

Cadmium and lead were detected in the combined ash (slag and flyash). These contaminants occur most frequently and in the highest concentrations in the fly ash

		6155	6156	6157	6158	6159	6160
		D3A	D3B	C1A	C1B	C3A	C3B
Ca	NB	365	263	9.06	404	150	235
(ppm)	DSI	334	239	10.2	411	144	237
Cr	NB	3.51		1.6		0.10	
(ppm)	DSI	3.28		1.3		0.14	
Cu	NB			0.79		0.2	
(ppm)	DSI			0.81		0.2	
Mg	NB	70.4	47.3	0.2	87.8	19.0	58.2
(ppm)	DSI	75.3	53.0	0.2	111	22.7	60.1
V	NB			2.2			
(ppm)	DSI			1.9			
Zn	NB	0.10		0.19	0.12	0.39	0.55
(ppm)	DSI	0.06		0.24	0.15	0.38	0.36
Cl ⁻	(ppm)	2490	25.2	4860	13	216	9.92
SO ₄ ⁼	(ppm)	189	184	1890	829	390	416
Na	(ppm)	1470	34	9280	56.9	241	34.6
K	(ppm)	48.9	6.1	6090	31.8	35.2	11.2
pH		7.8	6.9	12.6	7.1	7.2	7.2

NB: Nebulization
DSI: Direct sample insertion

Table 2.7 Summary of leachate results

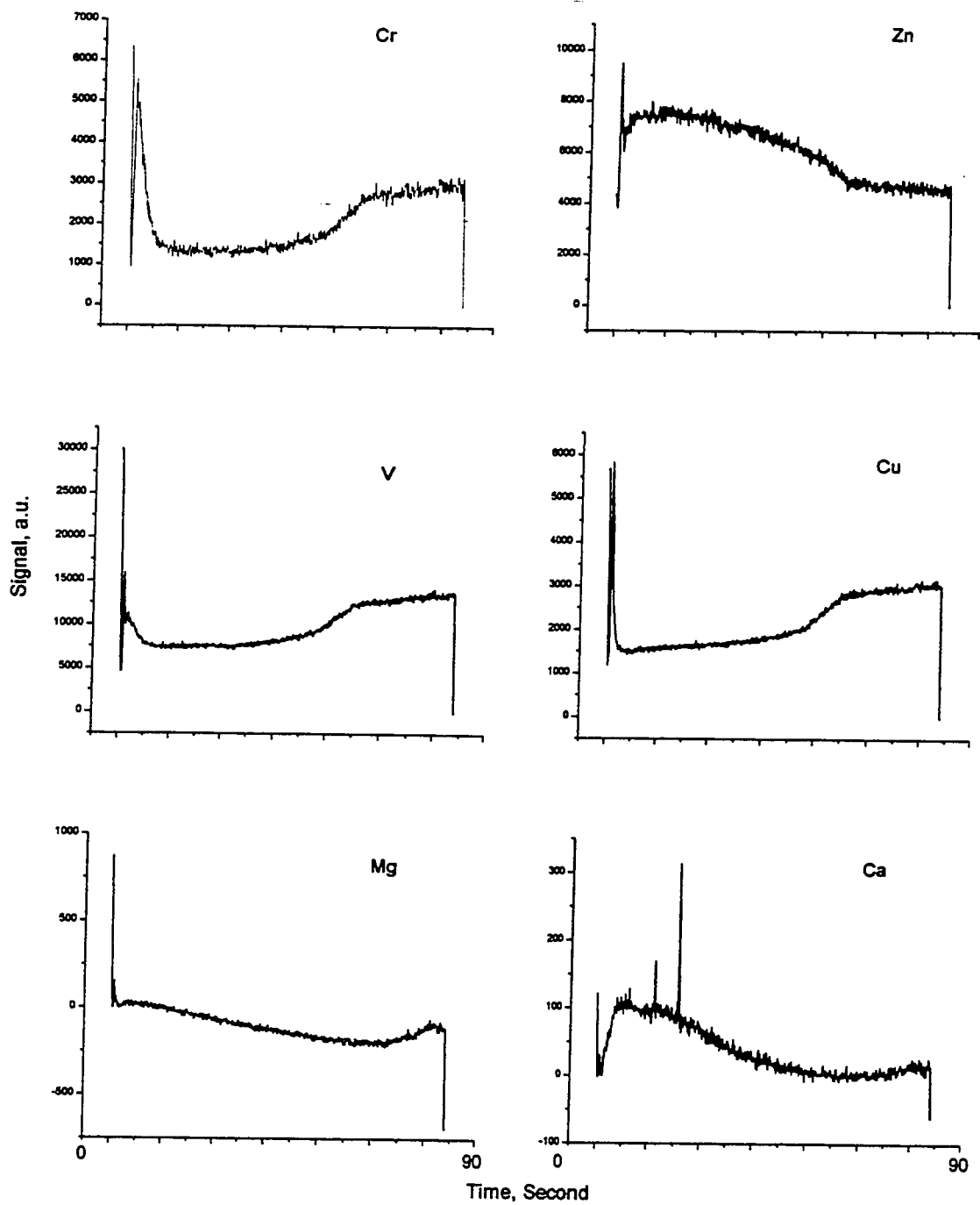


Figure 2.13 Six element peak profiles in leachates

fraction, a phenomenon related to the combustion process as well as to the physical and chemical properties of the contaminants. The results show that the absolute concentration of some metals in slags is not such as to classify them as toxic and harmful. According to these results it might be much better to separate bottom ash and smoke purification residues as soon as they are produced and to dispose of them separately. Bottom ash does not seem as dangerous as other kinds of incineration residues.

The proper disposal of solid residues from incineration depends on the absolute concentration of some metals and their concentration in the elutes obtained from elution tests. These concentrations are subjected to the same regulations regarding the discharge of the waste waters into surface water bodies. According to the Italian landfill guidelines, there are three risk categories. The first category represents the lowest risk and the third category the highest. For the second category there are three possible classifications depending on the type of pollutants the waste contains or on the treatment the waste has been previously subjected to. An overview of the characteristics of residues coming from an incineration plant suggests that landfills for slag have to be allocated to the second category onward. The reason for this choice is also the lack of guidelines regarding residue sampling and testing methods, as well as the control conditions on the combustion system being tested.

Trace metals (TM) released in the atmosphere from pollution sources may lead to serious problems for public health depending on their concentrations, oxidation state, chemical form, and interactions with the environment and biosystem. Along with some toxic elements such as As, Cd, Cr, Hg, and Pb, whose potential hazards are well established, the concentrations of many other trace elements are increasing in the air of urban and industrialized areas.

Gallorini used neutron activation analysis to monitor trace elements in atmospheric pollution processes during a monitoring campaign in Milan (Italy) [32]. Hundreds of samples, often of a few milligrams or a fraction of a milligram (i.e., dust on air filters), were collected for the determination of as many trace elements as possible. In particular, the following have been studied: i) the emission from different solid waste municipal incinerators, ii) the characterization of dry deposition particulates in urban and

industrialized areas, and iii) a preliminary series of results obtained in the analysis of air samples collected during a monitoring campaign in Milan (Italy).

Neutron activation analysis (NAA) offers the great advantage of combining high sensitivity and accuracy with multielement capacity. NAA was used mainly for the determination of all the elements investigated, except for lead, which was determined by AAS. Samples of solid materials such as flyash and suspended particulate and air filters were sealed in polyethylene vials and irradiated in the TRIGA nuclear reactor at the University of Pavia. Standards were both primary standard solutions and standard reference materials from NIST (SRM 1648 Urban Particulate, SRM 1633a Fly ash) as comparator standards. Finally, the multielement capability offers information on elements such as Eu, Sc, Rb, Cs, and rare earths which, at the present, may not be completely involved in the usual atmospheric pollution but can furnish additional information to the total pattern of the trace metals in the environment.

2.432 Results and Discussion

Four bottom ash samples were pulverized to less than 100 mesh powder for DSI-ICP analysis. The data is summarized in Table 2.8. In general, good agreement was obtained with nebulization ICP results. For samples 7204 and 7206, the Pb concentrations were too high for the DSI-ICP. The sample may have to be diluted by graphite powder to get within the analytical range. As expected, Fe is a major component in the bottom ash. The signals shown in Figure 2.14 are very uniform. This could be due to the high temperature incineration treatment where all elemental species are transformed to metal oxide.

Five stack ash samples were collected from stack filters. These samples consist of very fine particles and no size reduction was necessary. The data is summarized in Table 2.9. The Pb and Cu concentrations were too high to be determined by DSI-ICP. The DSI results are in very good agreement with the values obtained from the conventional methods. The elemental form is likely to be salt, as chloride and sulfate concentrations are very high. The signals shown in Figure 2.15 are fairly smooth as well.

Element	Sample	6915	6917	7204	7206
Cr	NB	347	385	240	218
(ppm)	DSI	305	310	268	206
Cu	NB	6550	5500	5240	3150
(ppm)	DSI	6780	4920	4440	2860
Fe	NB	96800	90000	98000	91000
(ppm)	DSI	97500	85000	85000	103000
Pb	NB	1090	844	22000	25300
(ppm)	DSI	1028	775	SA	SA
Zn	NB	722	640	1856	2362
(ppm)	DSI	803	790	1620	2070
Cl ⁻	(ppm)	2230	1560	<500	<500
SO ₄ ⁼	(ppm)	11600	14900	12100	16600
Na	(ppm)	8000	10600	10700	6780

NB: Nebulization
DSI: Direct sample insertion
SA: Saturation

Table 2.8 Bottom ash (slag) data summary

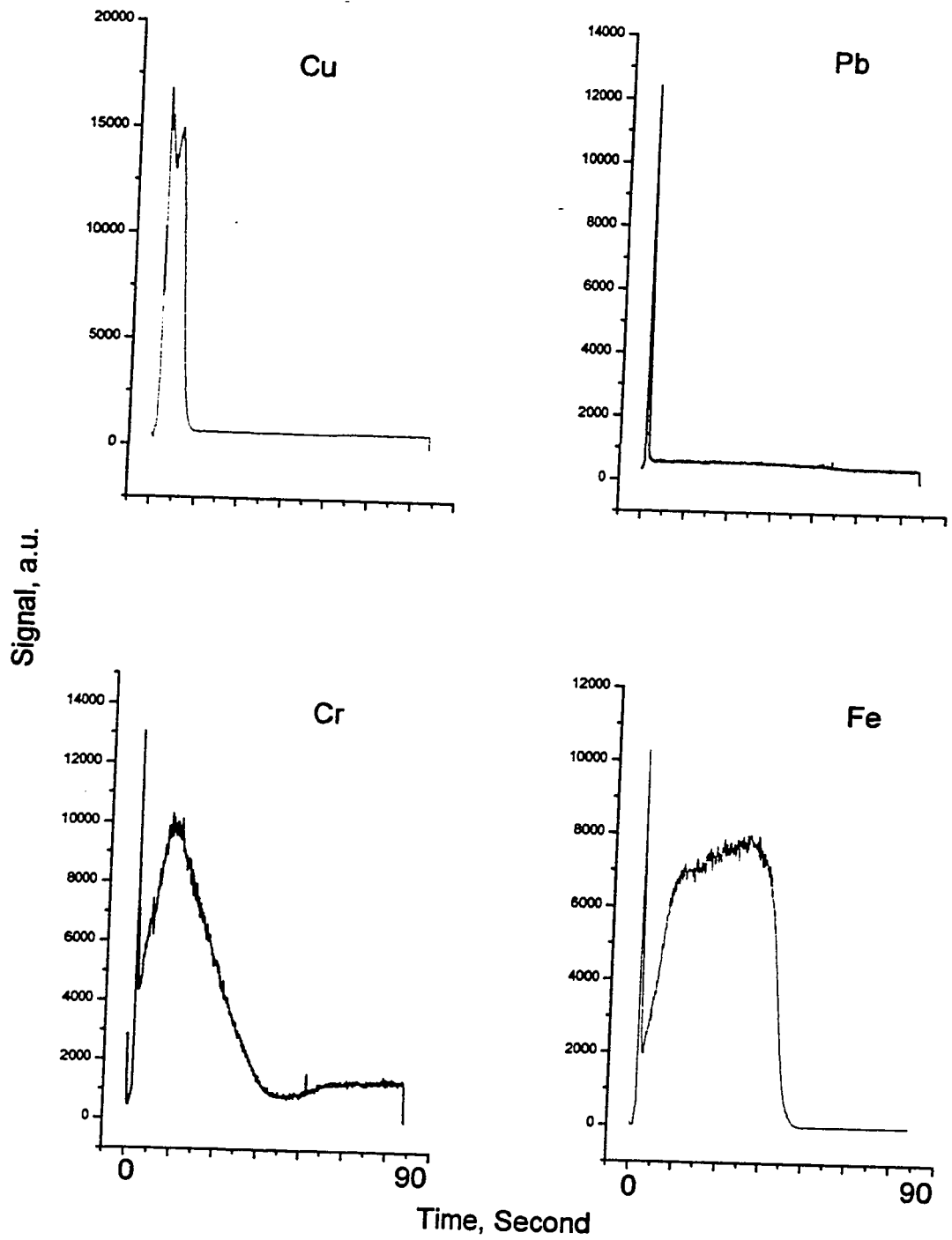


Figure 2.14 Four element peak profiles in slag

Element		6075	6089	6113	6138	6172
Cr	NB	220	250	203	1570	2480
(ppm)	DSI	223	236	175	1650	2741
Fe	NB	1130	1060	1050	1150	1370
(ppm)	DSI	1100	1110	1150	1340	1270
Zn	NB	12800	8480	5040	5300	9400
(ppm)	DSI	10500	8900	5111	6440	9150
Pb	(%)	1.20	1.97	6.01	5.67	4.81
Cu	(%)	11.0	4.71	3.74	3.55	13.7
Cl ⁻	(%)	5.20	3.70	2.87	2.80	4.72
SO ₄ ²⁻	(%)	<0.05	2.05	<0.05	0.55	2.58
Na	(%)	3.30	2.29	1.84	1.26	2.35

NB: Nebulization

DSI: Direct sample insertion

Table 2.9 Stack ash data summary

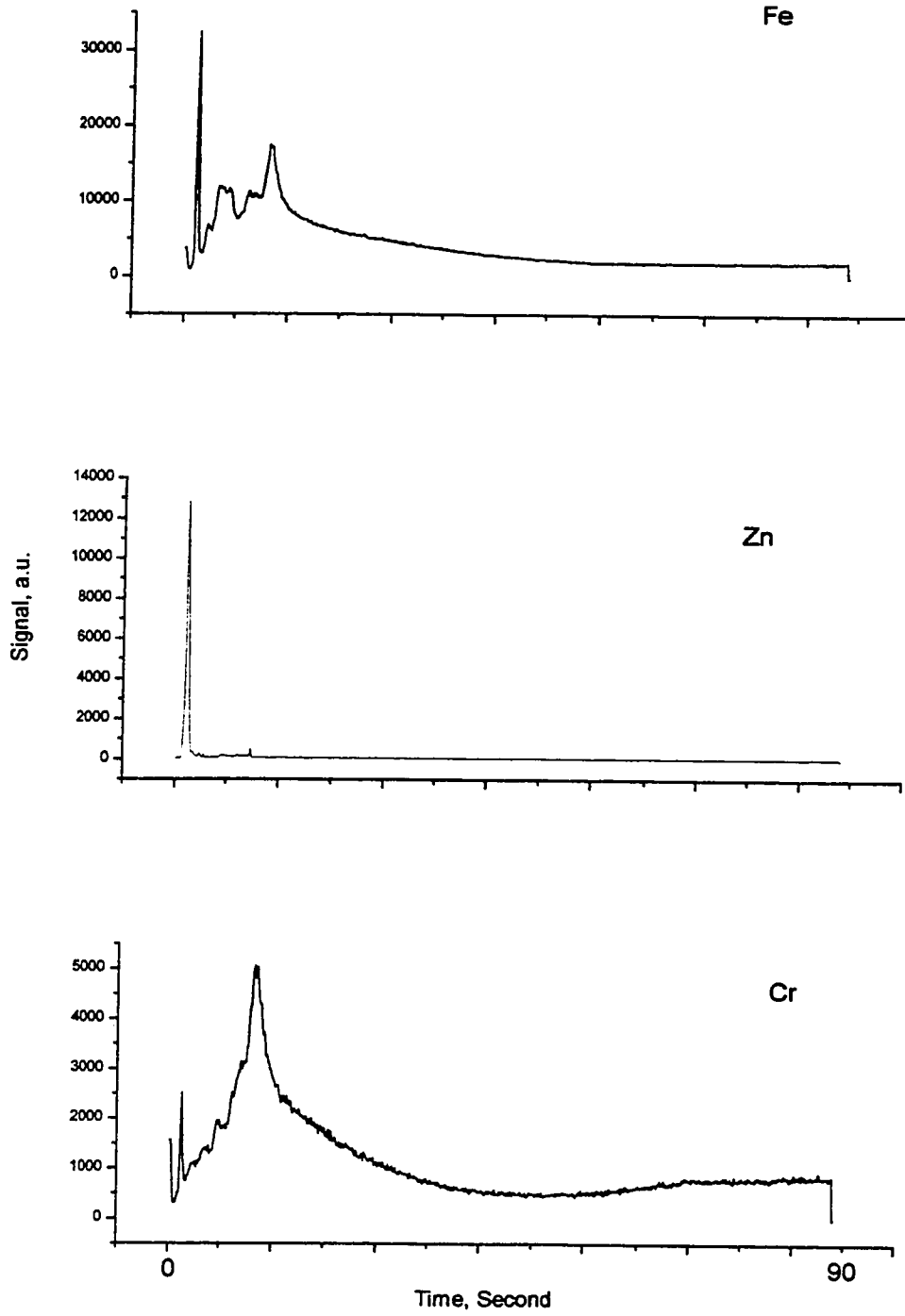


Figure 2.15 Three peak profiles in stack ash

The above results confirm the analytical capability offered by DSI-ICP analysis in issues related to the determination of trace elements in environmental-related samples. As can be observed, this analytical technique is suited to situations where a large number of small samples have to be analyzed for several elements at a trace level. As DSI-ICP does not require dissolving the samples, the analytical operations are considerably reduced and losses or contamination are minimized.

2.44 Standard Reference Materials Analysis

2.441 Background

An important characteristic of the DSI technique coupled with the ICP is the ability to use solid standards of substantially differing matrix compositions for calibration. Several studies have reported this feature and suggest a relative insensitivity of the technique to element origin [3, 4, 6, 8, 33]. Calibration curves may be constructed using solid samples of known elemental concentration. Standard reference materials (SRMs) have been used extensively and include NIST coal and botanical SRMs, BAS and NIST nickel alloy SRMs, U.S. Geological Survey (USGS) silicate materials, and SPEX G and SPEX TSAL solid standards (used in dc arc calibration, SPEX Industries, Edison, NJ). In general, calibrations are linear over at least three orders of magnitude. Linear calibration curves for Fe, Cu, Si, Ti and Mn in both high and low aluminum alloy were constructed using aluminum as the internal standard, when Ar-O₂ mixed plasma was used [3]. A linear calibration curve for Zn was also constructed among several different SRMs leaves, coal and flyash [34]. Furthermore, calibration based on dried solution residues has been shown to be valid for analysis of low-boiling-point elements in nickel alloys [35].

2.442 Results and Discussion

Seven Standard Reference Materials from NIST and Canadian Certified Reference Materials Project were used to construct calibration curves for Fe, Cu, Cr and Zn. The three NIST SRMs were SRM 2704 (Buffalo River Sediment), SRM 4355 (Peruvian Soil),

Element	NIST 4355 Peruvian Soil	NIST 2704 Buffalo River Sediment	NIST 679 Brick Clay	Reference Soil-1	Reference Soil-2	Reference Soil-3	Reference Soil-4
Fe (%)	4.45	4.11	9.05	6	5.56	1.51	2.37
Cr (mg/g)	28.9	135	109.7	160	16	26	61
Cu (mg/g)	77.1	98.6		61	7	17	22
Zn (mg/g)	368	438	150	146	124	52	94

Table 2.10 Certified Metal Concentrations in Several Standard Reference Materials

SRM 679 (Brick Clay). Four reference soil samples were obtained from Canadian Certified Reference Materials Project, Canada Centre for Mineral and Energy Technology, 555 Booth Street, Ottawa Ontario K1A 0G1. The certified metal concentrations of these materials are listed in Table 2.10.

The sample size for the DSI analysis was about 1 to 3 mg, which is only a hundredth of the recommended weight by NIST. This is the major uncertainty for the analysis. Usually, four replicates of each material were weighed, but the first one or two samples were used to adjust the gain size on the data acquisition board. Therefore, only two to three usable values were available for averaging. The calibration plots of Fe, Cu, Cr and Zn are shown in Figures 2.16 to 2.19. The correlation coefficients of these plots are reasonably good considering direct solid analysis and small sample size. The slopes of the log-log plots for Cu, Cr and Zn are close to unity.

The signals for Fe, Cu, Cr and Zn are shown in Figures 2.20 to 2.23. The form of the element may be different in the different samples and may also be changing with temperature during the vaporization process. In general, the peak width of Zn is the narrowest as it has the lowest melting and boiling point. The broad peak width of Fe is likely due to the high concentration of Fe present in the samples. Different matrices also play a major role in the vaporization pattern. Therefore, it is no surprise to see that the same element shows a very different vaporization pattern in different samples.

2.45 NIST Wear Metal Oil Analysis

2.451 Background

Cost associated with maintenance due to engine and machine wear can be significant. Therefore, diagnostic methods for determining the condition of engines and other machinery are very important. Mixing engine oil with xylenes or other solvents followed by direct aspiration into an ICP using a pneumatic nebulization system is a standard method in industry for the analysis of wear metals [36, 37]. However, the high viscosity and flammability of many oils and gasolines can cause difficulties. Carbon deposition on the sampling tube tip is a nagging problem when conventional nebulization

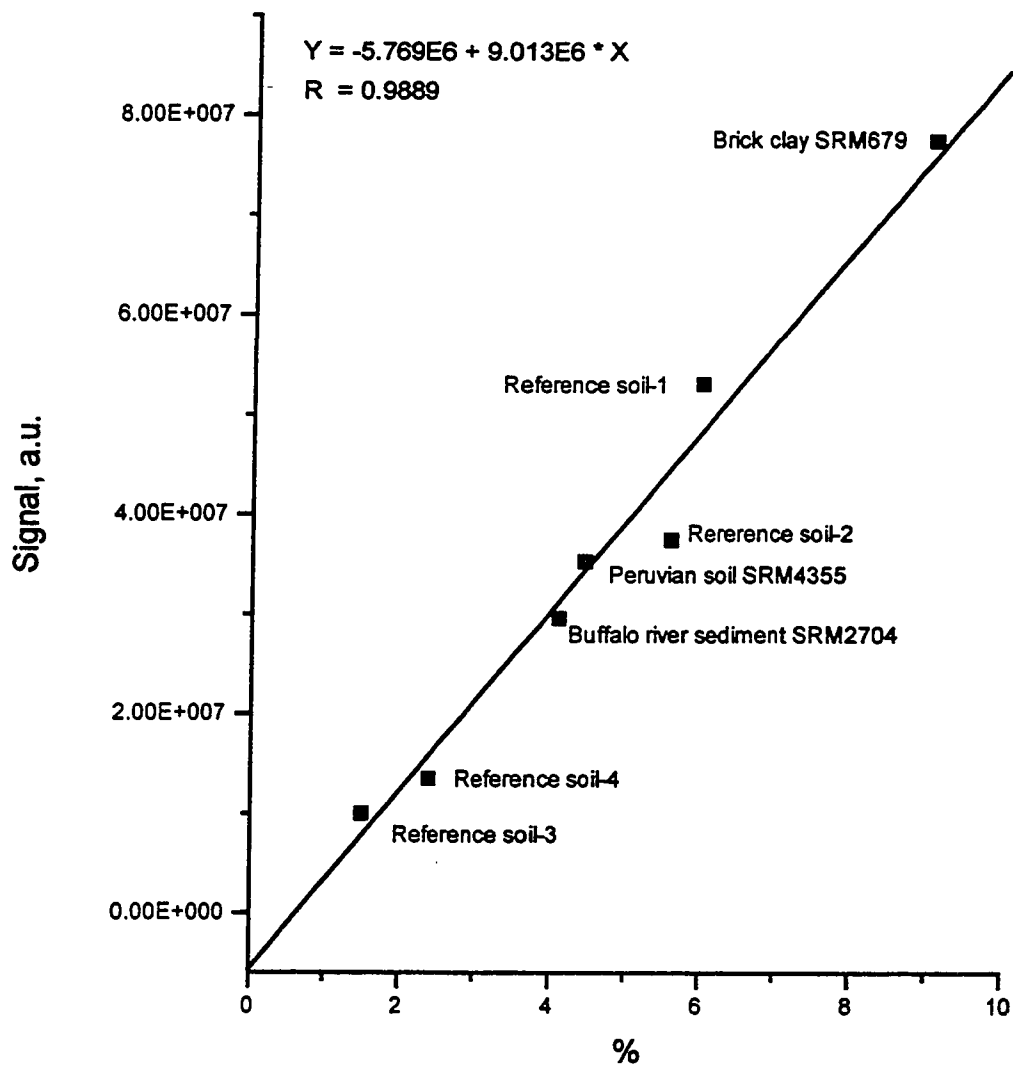


Figure 2.16 Fe calibration curves by standard reference materials

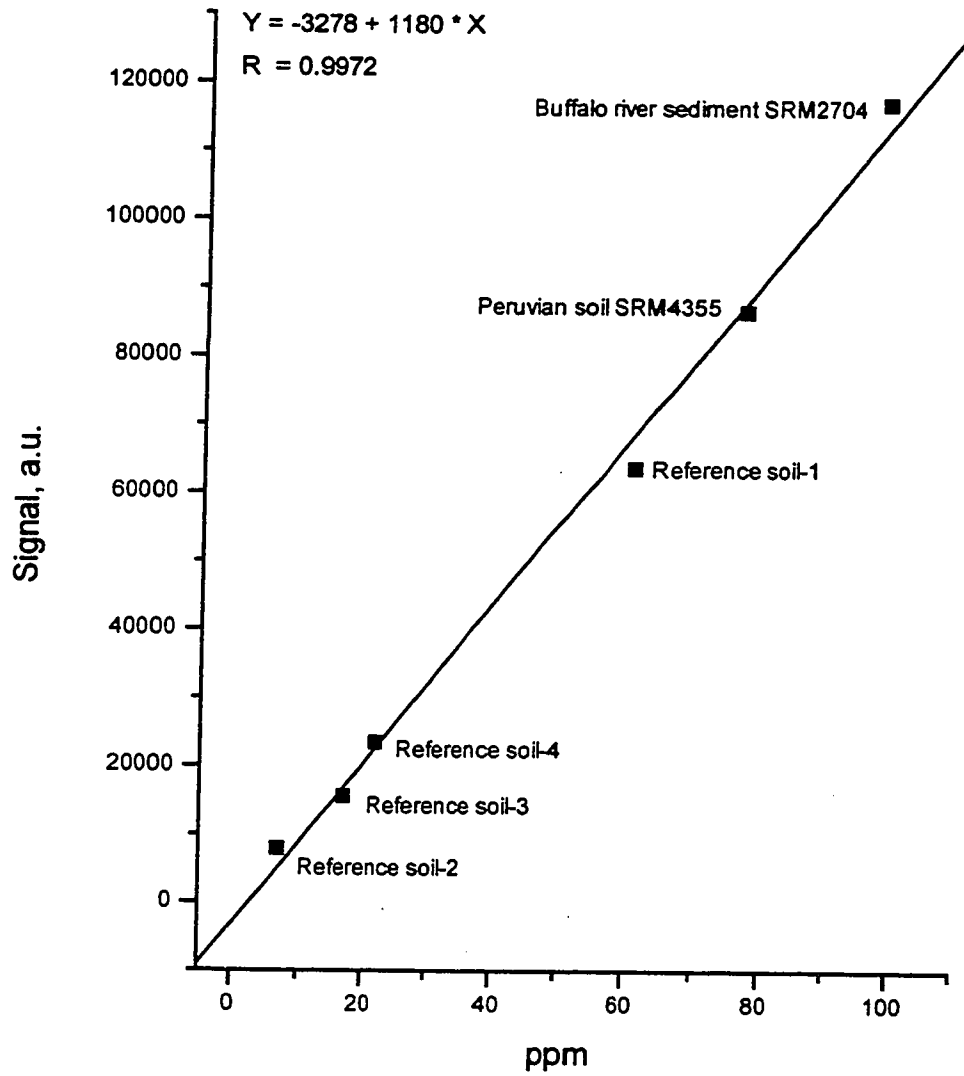


Figure 2.17 Cu calibration curves by standard reference materials

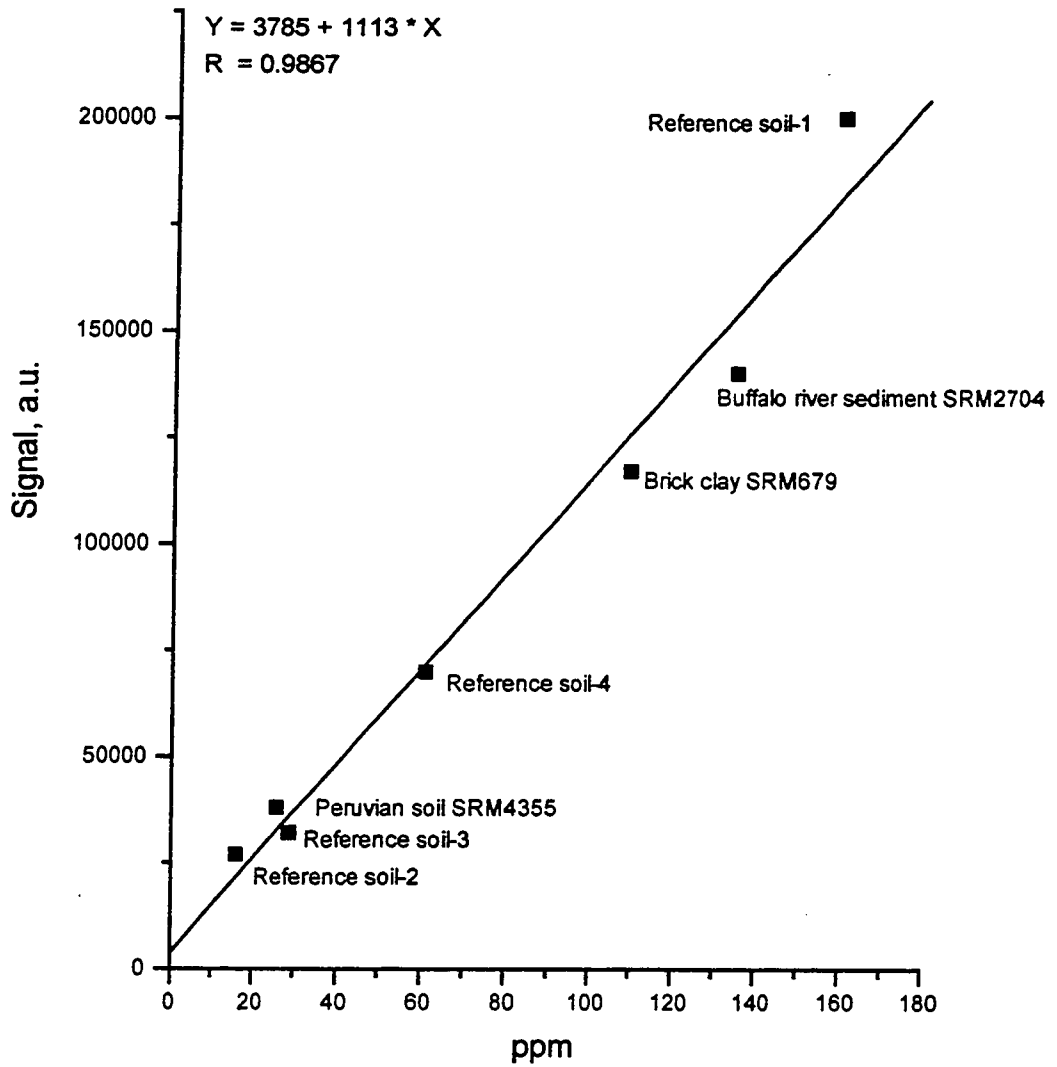


Figure 2.18 Cr calibration curves by standard reference materials

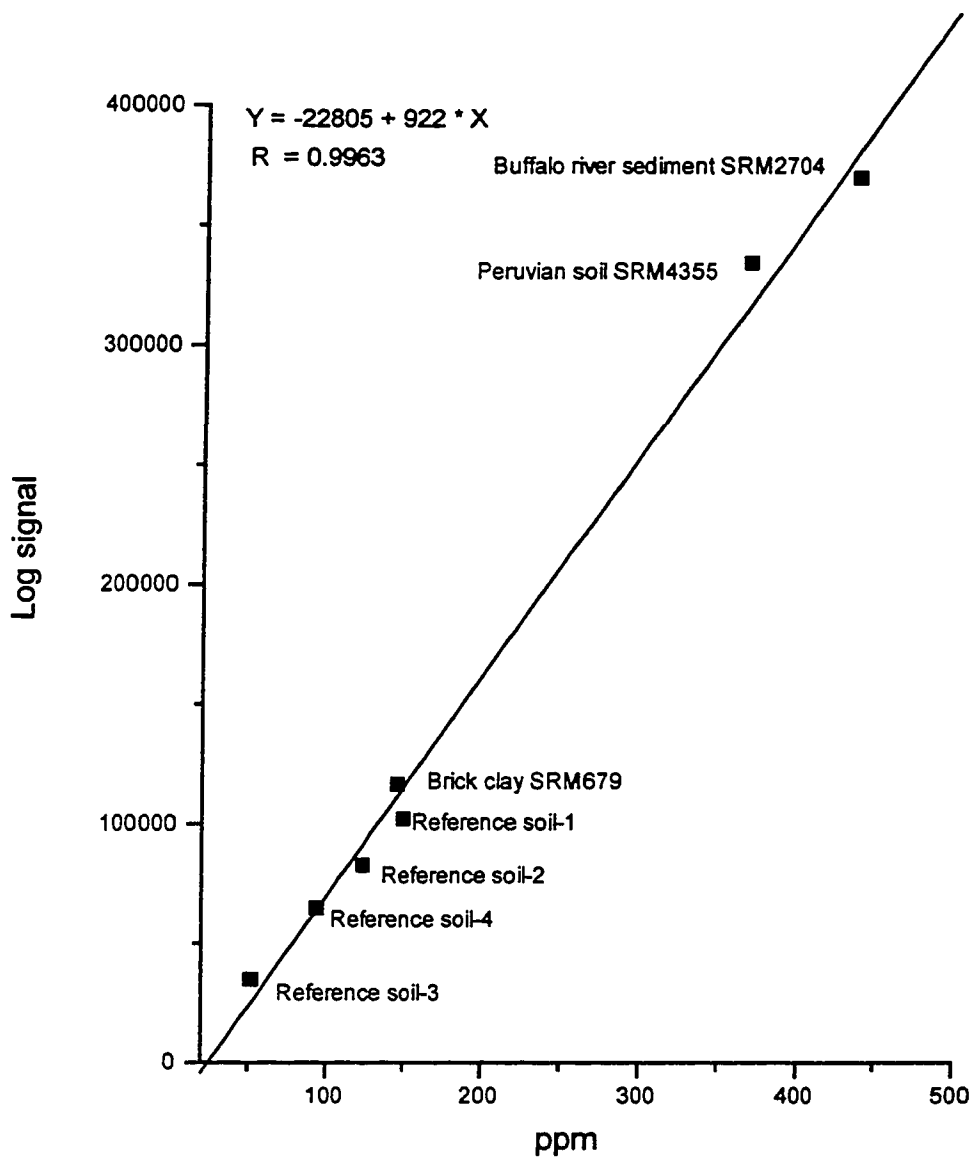


Figure 2.19 Zn calibration curves by standard reference materials

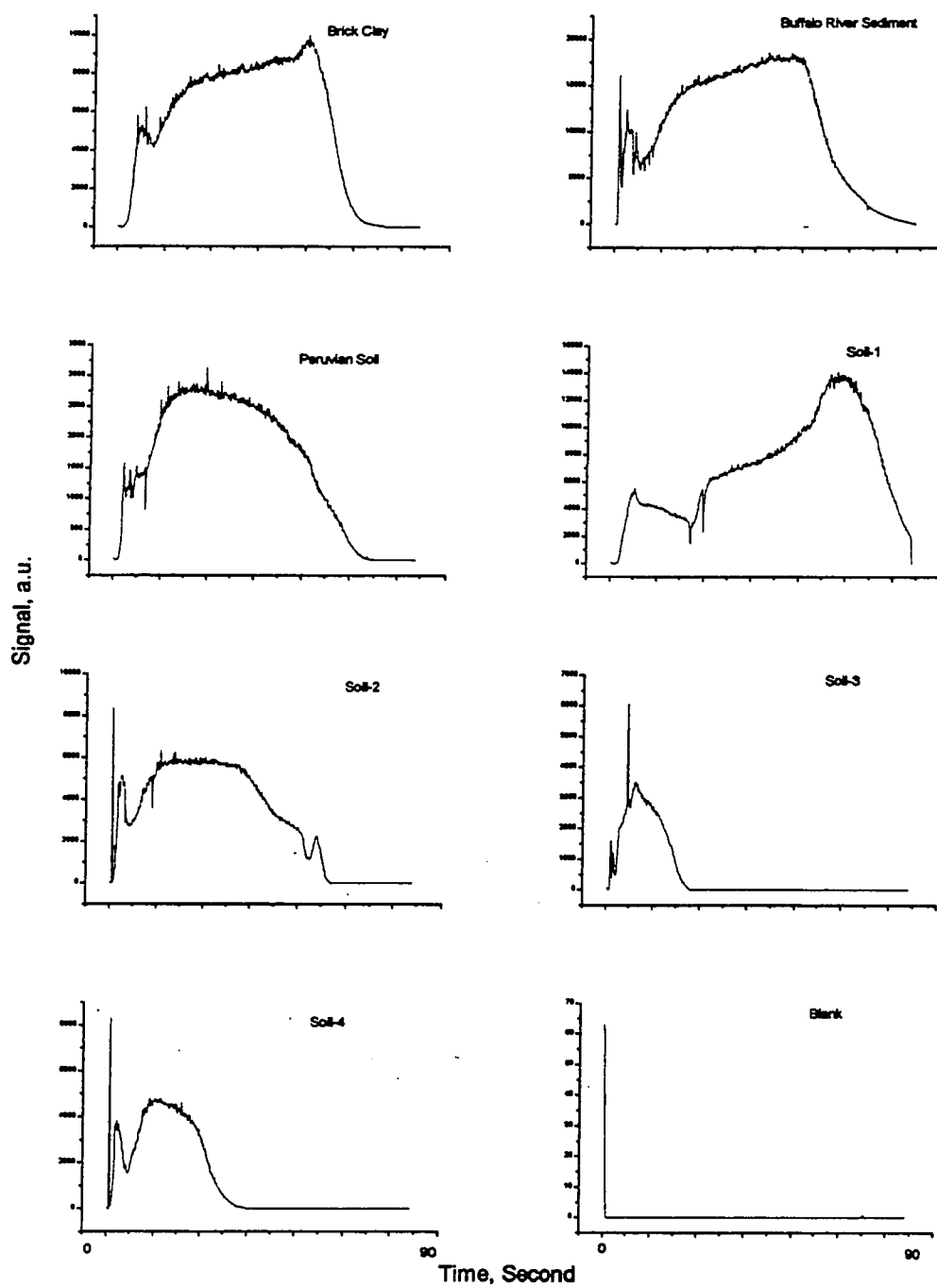


Figure 2.20 Fe signals in different SRM matrices

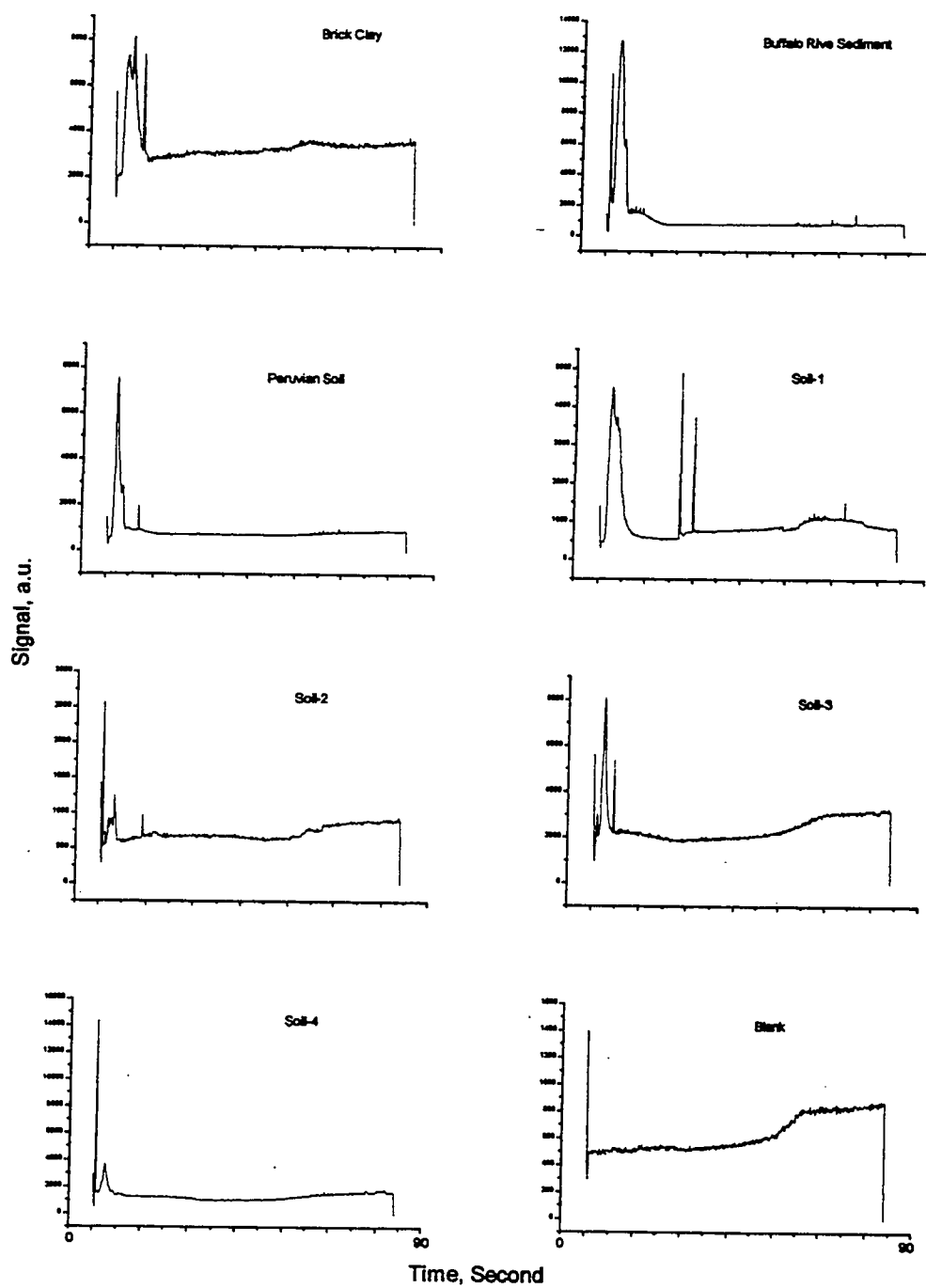


Figure 2.21 Cu signals in different SRM matrices

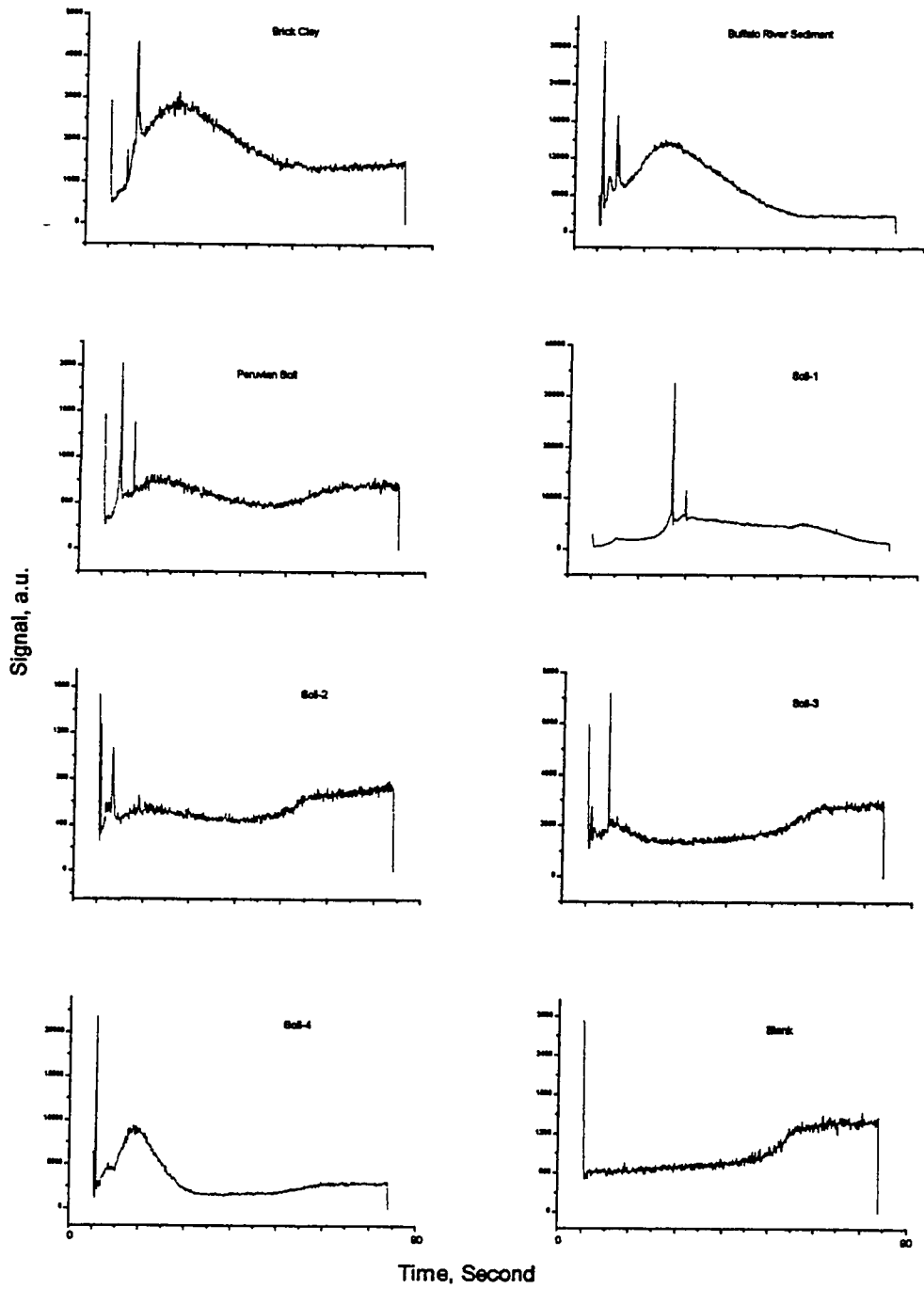


Figure 2.22 Cr signals in different SRM matrices

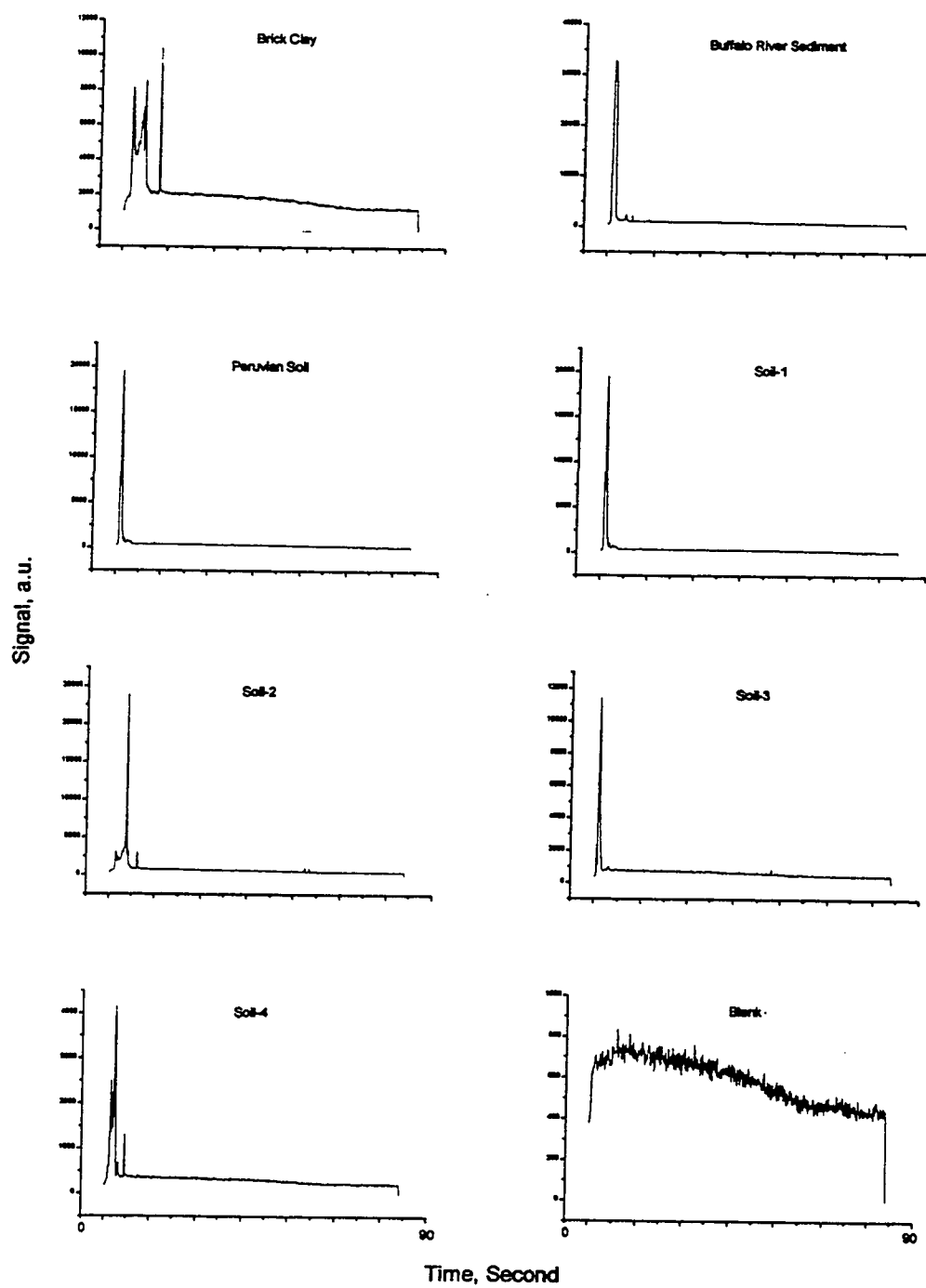


Figure 2.23 Zn signals in different SRM matrices

ICP is used with organic solvents. The DSI -ICP was tested for wear metal oil analysis by Liu and Horlick and proved to be a powerful tool [3]. Calibration curves, from 0.1 to 500 ppm, for Mn, Fe, Ni Cu and V in oil standards (CONOSTAN S21, CONOSTAN division, Conoco Inc., Ponca City, Oklahoma) were constructed. The linearity of the calibration curves was good with slopes close to unity for most of the elements.

2.452 Results and Discussion

In this study, two NIST SRM wear metal oil samples (SRM 1084a and SRM 1985a) were tested against a calibration curve obtained using aqueous standards [38, 39]. Four elements Cr, Cu, Pb and V were studied. An ashing time of 40 seconds was used for oil sample analysis. That is much longer than the ashing time used for other matrices. Using a long ashing time should avoid incomplete ashing and sample ejection from the electrode upon insertion. The results for these elements are listed in Table 2.11. The concentrations obtained by the DSI method are within 10% of NIST certified values at the 100 ppm level. The concentrations obtained from the DSI method are within 20% of NIST certified values at the 300 ppm level. Figure 2.24 presents signals for Pb, Cr, Cu and V in SRM 1084a wear metal oil at the 100 ppm concentration level. Peaks for Cr, Cu and Pb are very sharp. The peak shapes in the oil are similar to the shape in the aqueous standard as they were shown in Figure 2.11. However, the peak shape of V in oil is much broader. Vanadium is an involatile element and it forms a refractory carbide with a boiling point of 3900 °C. During the insertion, low boiling point components will be evaporated and yield emission signals while the refractory species will remain in the graphite cup. As the graphite cup is burned away the analyte may be carried into the plasma as a gas or in the form of fine particles. The form of the element may be different in different samples and may also be changed with temperature during the vaporization process. Different matrices will also affect the vaporization pattern.

	Cr	Cu	Pb	V
NIST Certified Value (ppm)	98.3	100.0	101.1	95.9
DSI Concentration (ppm)	90	99	99	90
NIST Certified Value (ppm)	296.3	295.1	297.4	292.4
DSI Concentration (ppm)	335	347	345	366

Table 2.11 DSI-ICP analysis results of NIST wear metal oil

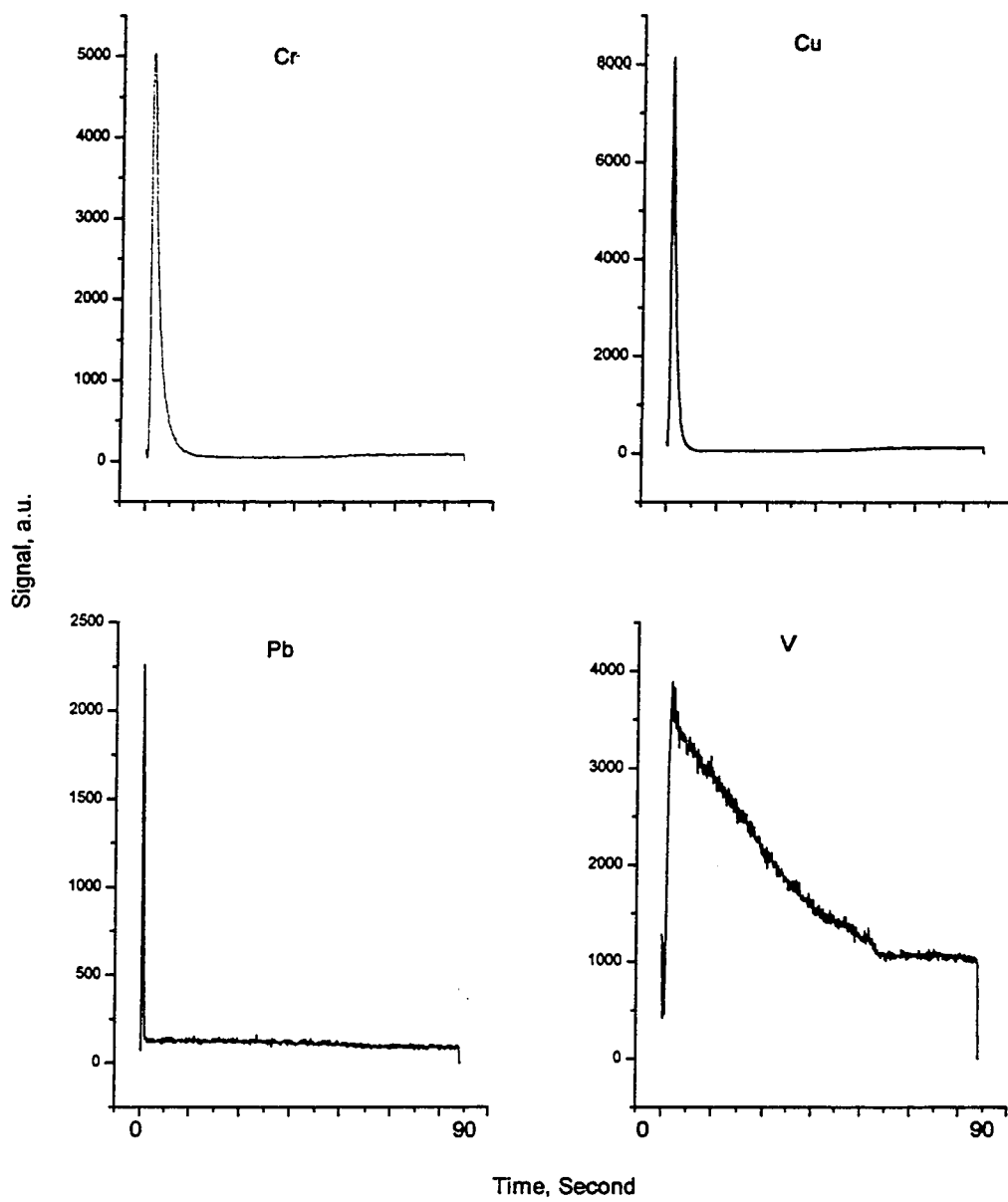


Figure 2.24 100 ppm Cr, Cu, Pb and V in NIST wear metal oil

2.5 Limitations and Future Work

DSI-ICP with an Ar-O₂ mixed gas plasma has shown good analytical potential for analyzing real world samples with different matrices. However, the current system suffers limited multielement capability, inflexible gain control, single sample manual operation and inconvenient operating software. Sensitive and fast solid state array detectors should be ideal for DSI-ICP analysis. An autosampler for delivering sample probes into the plasma would also be beneficial. Systematic characterization of the vaporization process of different elements, different species, and different samples is of great interest and remains a challenging field. This should be facilitated by new solid state multichannel spectrometers. The next sections of the thesis deal with construction and testing of an automated multichannel based system for DSI-ICP-AES.

References

1. G. M. Hieftje, *J. Anal. At. Spectrom.* **11**, 613 (1996).
2. X. R. Liu and G. Horlick, *J. Anal. At. Spectrom.* **9**, 833 (1994).
3. X. R. Liu, *Ph.D. Thesis*, University of Alberta, 1994.
4. L. S. Ying, *MS. Thesis*, University of Alberta, 1992.
5. V. Karanassios and G. Horlick, *Spectrochim. Acta* **45B**, 85 (1990).
6. W. T. Chan and G. Horlick, *Appl. Spectrosc.* **44**, 380 (1990).
7. V. Karanassios and G. Horlick, *Spectrochim. Acta* **44B**, 1345 (1989).
8. V. Karanassios, G. Horlick and M. Abdullah, *Spectrochim. Acta* **45B**, 105 (1990).
9. Y. B. Shao and G. Horlick, *Appl. Spectrosc.* **40**, 386 (1986).
10. W. T. Chan and G. Horlick, *Appl. Spectrosc.* **44**, 525 (1990).
11. T. B. Reed, *Journal of Applied Physics* **32**, 2534 (1961).
12. U.S. EPA Test Method 3051, Microwave Assisted Acid Digestion of Sediments, Sludges, Soils, and Oils.
13. U.S. EPA Test Method 3052, Microwave Assisted Acid Digestion of Siliceous and Organically Based Matrices.
14. U.S. EPA Test Method 3015, Microwave Assisted Acid Digestion of Aqueous Samples and Extracts.
15. W. Shao, X. Feng, Y. Zhao and A. Wittmeier, *J. Anal. At. Spectrom.* **11**, 287 (1996).
16. Y. Feng and R. S. Barratt, *The Science of the Total Environment* **143**, 157 (1994).
17. NIST Certificate of Analysis, SRM 2704
18. NIST Certificate of Analysis, SRM 4355
19. NIST Certificate of Analysis, SRM 679
20. NIST Certificate of Analysis, SRM 1633b.
21. U.S. EPA Test Method 1311, Toxicity Characteristic Leaching Procedure.
22. U.S. EPA Test Method 1010, Pinsky-Martens Closed-Cup Method for Determining Ignitability.
23. U.S. EPA Test Method 1020A, Setflash Closed-Cup Method for Determining Ignitability.

24. U.S. EPA Test Method 9040B, pH Electrometric Measurement.
25. U.S. EPA Test Method 1110, Corrosivity Toward Steel.
26. U.S. EPA Test Methods for Evaluating Solid Waste (SW-846), Chapter 8.3, Reactivity.
27. M. Gallorini, M. Pesavento, A. Profumo and C. Riolo, *The Science of the Total Environment* **133**, 285 (1993).
28. J. A. Owen and D. A. C. Manning, *Analytical proceedings including analytical communications*, September, **31**, 277 (1994).
29. T. J. Gluodenis, D. A., Yates and Z. A. Grosser, *Atomic Spectroscopy*, **7/8**, 164, (1994).
30. V. Karanassios, M. Abdullah and G. Horlick, *Spectrochim. Acta* **45B**, 119 (1990)
31. A. Santarsiero and M. Ottaviani, *Microchemical Journal* **51**, 166 (1995).
32. M. Gallorini, *Microchemical Journal* **51**, 127 (1995).
33. Inductively Coupled Plasmas in Analytical Atomic Spectrometry, edited by A. Montaser and D. W. Golightly, 1992 VCH Publishers, Inc., Chapter 16, Induction of Solids into Plasma, contributed by C. W. McLeod, M. W. Routh and M. W. Tikkanen.
34. W. E. Pettit, Ph.D. Thesis, University of Alberta (1991).
35. C. W. McLeod, P. A. Clarke and D. J. Mowthorpe, *Spectrochim Acta* **41B**, 63 (1986).
36. ASTM D5185-95, Standard Test Method for Determination of Additive Elements, Wear Metals, and Contaminants in Used Lubricating Oils and Determination of Selected Elements in Base Oils by Inductively Coupled Plasma Atomic Emission Spectrometry, Annual Book of ASTM Standards, Vol 5.03.
37. ASTM D4951-96, Standard Test Method for Determination of Additive Elements in Lubricating Oil by Inductively Coupled Plasma Atomic Emission Spectrometry, Annual Book of ASTM Standards, Vol 5.02.
38. NIST Certificate of Analysis, SRM 1084a.
39. NIST Certificate of Analysis, SRM 1085a.

Chapter 3

Development of an Automated Solid/Liquid Interchangeable DSI-ICP System

3.1 Introduction

Analytical instruments are a major financial investment to all laboratories, whether these instruments are located within large corporate research and development laboratories or are the major source of revenue for a smaller environmental contract laboratory. For this reason, a particular instrument's ability to be utilized for a broad range of sample analyses is considered a desirable feature, since this cuts down on the overall number of instruments potentially needed in the laboratory. When taken together, the ability to handle a wide range of sample matrices as well as determine major and trace element concentrations with a single instrument can at the same time reduce operating costs and improve laboratory productivity.

For over a decade, inductively coupled plasma spectrometry has been rapidly establishing itself as the analytical technique for trace element analysis. ICPs possess exceptional characteristics that make them excellent sources for vaporization, atomization, ionization and excitation. As a multielement technique, ICP-AES is superior to GFAAS in terms of productivity; however, it falls short in the area of detection limits. DSI systems provide graphite furnace-like capability for an ICP system. The first DSI-ICP system [1] was operated by manual insertion. Since then, different DSI systems have been developed. Except for one transverse insertion system [2,3], in which probes were inserted transversely into the plasma cross-section just above the torch, the parallel insertion model has been exclusively used in DSI-ICP insertion mechanisms in which probes are inserted into the core of the plasma along the central tube of ICP torch.

Main hardware differences among different DSI-ICP systems are associated with the drive mechanism and sample change over mechanism. The drive mechanisms include manual insertion systems [1-9], a car aerial [10], dc motor driven insertion systems [11-13], pneumatic insertion systems [14-17], and stepper motor driven insertion systems [18-

28]. The stepper motor driven system is readily computerized while dc motor driven systems are usually stop-start switch controlled. Sample change over is accomplished manually in most systems, but automatic carousels [15, 29] and robot control [18, 30] have been used.

Most DSI-ICP studies have been carried out with AES spectrometry. There are only a few studies using mass spectrometry with DSI-ICP [19-21, 26-27]. This is related to the difficulty of current ICP-MS instrumentation in handling transient signals for a wide mass range.

3.2 Objectives

The ideal detection system for ICP-AES should be able to accommodate simultaneous multielement analysis and offer a totally flexible choice of analytical lines. Multichannel spectrometers like the "direct reader" have simultaneous multielement capability but cannot be reprogrammed conveniently to view a new set of the analysis lines. Sequential scanning systems have excellent flexibility but can acquire information at only one wavelength at a time. Both of these types of systems are incapable of viewing an analytical line and the adjacent background radiation simultaneously because they employ single channel photomultiplier tube detectors. A Leco photodiode array ICP spectrometer in our laboratory could overcome some of these problems and was chosen for this study.

The prime objective was to develop an automated solid sampling system (DSI) with the ability to also readily accommodate both solid and liquid sample analysis. The overall diagram of the final system is shown in Figure 3.1.

3.3 Leco Spectrometer

3.31 Optics

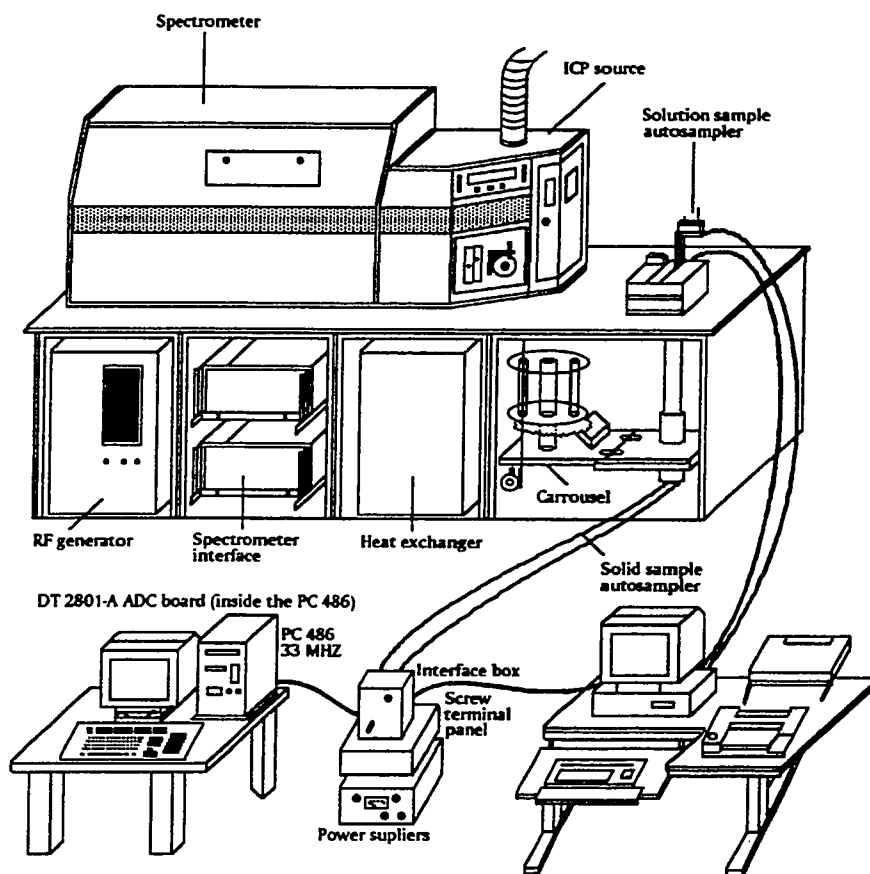


Figure 3.1 Schematic diagram of an automated direct sample insertion device for ICP-AES

The approach adopted for this instrument design was to separate the required function of the spectrometer into three optical systems: a pre-selection polychromator (PSP), a recombination system, and an echelle spectrometer. A schematic diagram of the optical system is shown in Figure 3.2. The technical specifications of the Leco ICP spectrometer are summarized in Table 3.1.

The pre-selection polychromator (PSP) is comprised of the entrance slit, the concave grating and the mask. Radiation from the source is imaged onto the entrance slit using a quartz lens 2.5 in. (64 mm) in diameter with a focal length of 10.9 in. (276 mm) at 250 nm. The lens is situated at a distance of 21.7 in. (551 mm) from the source and from the entrance slit to produce a 1:1 image of the plasma on the slit. The PSP is a 0.5-m optical system operating as a low-resolution multiple spectral bandpass filter. The mask and slit are situated on the Rowland circle of the concave grating, which has a radius of curvature of 0.5-m and a groove density of 590 g/mm, resulting in a reciprocal linear dispersion of 3.4 nm/mm. The entrance slit is laterally adjustable in 5 μm increments to facilitate alignment of the PSP spectrum with the slots in the mask.

The entrance slit width was 50 μm , the mask slot widths were 150 μm , and both were about 1 cm high. Although the slots in the mask have slit-like dimensions, it is important to bear in mind that a small wavelength window (0.5 nm) is actually transmitted by each slot and not just a single spectral line.

The function of the mask is to allow only the radiation from the regions of the analytical lines of interest to pass to the remaining optical systems of the spectrometer. Since both line radiation and associated background are preselected, simultaneous background correction can be performed in a single measurement. The slot positions used in manufacturing the masks are determined by a computer program which requires the user to input the element symbols and the wavelength of the line of interest. The ability to implement any number of customized masks provides the analyst with a flexible choice of analytical wavelengths.

The function of the recombination system is to recombine the preselected, dispersed radiation, for further processing by the echelle-based spectrometer section. This function is performed by the corrective mirror and a second grating. The mirror

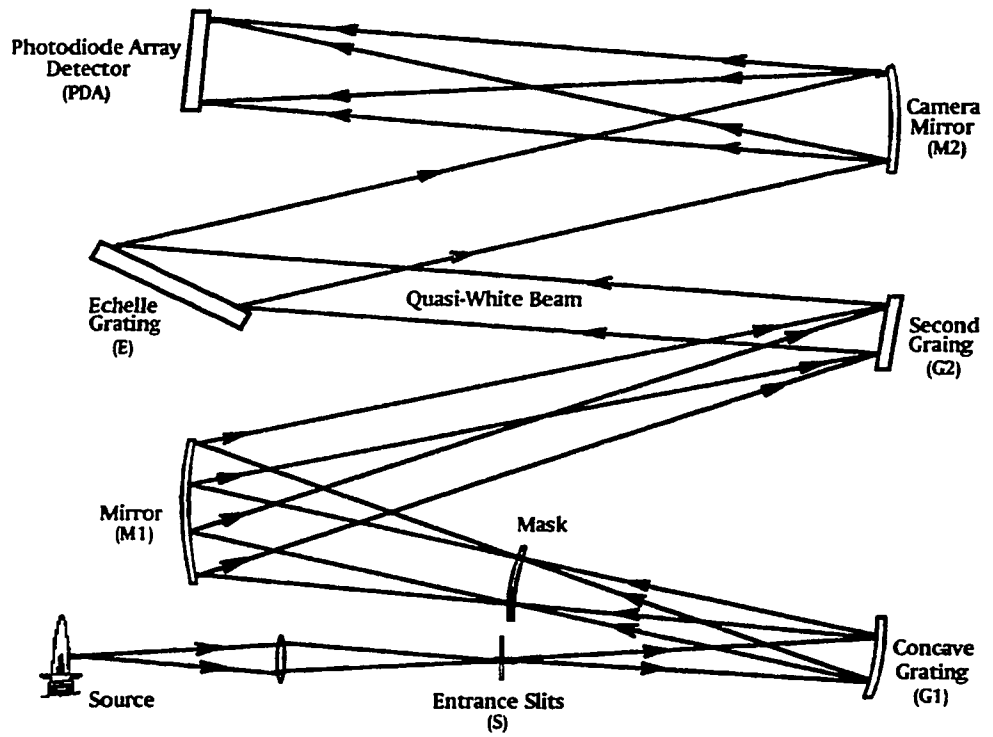


Figure 3.2 Leco optical diagram

ICP generator	Frequency: 40.680 MHz or 27.120 MHz RF Output Power: 2 kw
Gas control:	Coolant gas: 8 - 20 lpm Auxiliary gas: 0 - 2 lpm Nebulizer gas: 0 - 2 lpm
Forward power regulation:	1% for load changes from 1:1 VSWR to 30:1 within foldback limits
Output power stability:	0.05% (after 10 minute warm up in 23 °C room)
Protection:	Forward power limited at 300 watts reflected (625 watts reflected during ignition). PA current determined by junction temperature. All critical components thermally protected.
Sample Introduction:	Torch: 18 mm fixed torch Nebulizer: concentric glass Sample uptake: 10-roller peristaltic pump, about 1 l/min
Spectral Range:	190 - 420 nm
Spectral resolution:	200 nm: 0.0055 300 nm: 0.0082 400 nm: 0.011
Optics:	Preselection Polychromator: Rowland circle mount with 0.5 m focal length and concave grating with 590 lines/mm. High resolution echelle spectrograph: Echelle spectrograph without order cross-dispersion with 1 m focal length, and echelle grating with 31.6 lines/mm
Detection system:	1024 channel linear self-scanning photodiode array
Computer:	386 PC with 387 math co-processor, 4 Mb RAM and 80 Mb hard drive

Table 3.1 Leco ICP Technical Specifications

accepts the radiation passing through the mask and collimates it while reflecting it toward the second grating. The second grating is a plane grating with exactly the same groove density as the first one. Therefore, it recombines the collimated, dispersed radiation into "quasi-white" light. The term quasi-white is used because most of the original radiation has been removed by the PSP. The quasi-white beam is directed toward the echelle grating (31.6 g/mm). Then the light is focused by a 1-m focal length camera mirror. The change in focal length from 0.5 m to 1-m results in a magnification of the slit images by a factor of 2. The echelle is mounted close to the Littrow angle (63.5 ° blaze) and produces characteristic multiple orders and high angular dispersion. The camera mirror focuses the high resolution spectrum onto a photodiode array (PDA) detector, while a short focal length cylindrical lens situated just prior to the detector reduces the beam height to match the 2.5 mm diode height. This feature enables the use of the entrance slits up to 12 mm in height.

This echelle-based system does not employ a cross-dispersing element to separate the multiple orders. The spectrum presented at the PDA therefore consists of multiple overlapped orders. Within each order a nearly linear relationship exists between wavelength and a detector pixel may receive radiation from several different wavelengths.

The system works despite this overlap because the PSP removes most of the unwanted radiation and thus eliminates most cross-order spectral interference. Within a single order, spectral interference is minimized as a result of the high dispersion. When cross-order interference does occur, i.e. when a line from another order falls at nearly the same pixel as a sought analytical line, the analyst has to select an alternate line or modify the mask configuration to block the interfering line. Alternatively, the mask slot transmitting the interfering line can be blocked temporarily to permit the measurement.

3.32 Mask

The mask consists of a piece of 0.004 in. (0.01 mm) thick stainless steel which has slots cut vertically at the positions where the sought analytical lines will pass through the focal plane. These slots are 0.005 in. (130 μm) wide and are cut with an accuracy of

0.0001 in. (2.5 μm) by use of an electrical discharge machining (EDM) method. This corresponds to a selection accuracy of 0.009 nm for a bandpass region of 0.44 nm. The mask is mounted on a mask holder which matches the Rowland circle and can be inserted in <1 minute.

The mask is simply a curved thin metal plate that is positioned in the exit focal plane of this predispersion polychromator. Slots are cut (machined) in the mask at appropriate positions to allow light from preselected narrow-wavelength regions to pass through the mask to a concave mirror. The slot positions are normally centered on spectral lines of interest and two masks were used in this work, one set up for six lines (MEM6) and one for twenty four lines (MEM24). The wavelengths and correspond diode numbers are presented in Figure 3.3 and Figure 3.4. MEM6 is for Al, Cd, Cu, Mg, Mn and Zn. These elements are present in a so call "super standard solution" that is used for optimizing the system. MEM 24 is a multi-element general purpose mask for Al, Ar, As, Ca, Cd, CdAs, Co, Cr, Cu, Fe, Hg, In, Mg, Mn, Na, Ni, Pb, Sc, Si, Sn, Y, and Zn.

The maximum number of slots that can be cut into a single mask without producing interferences depends on the particular sample matrix and set of elements to be analyzed. Sometimes, even when only one mask-slot is open, due to the relatively large bandpass of the slots (typically about 0.44 nm/slot), more than one spectral line of the same element may appear on the detector. This phenomenon can be seen in Figure 3.3 and Figure 3.4. The solid lines are the sought for lines and dotted lines are the leaks. Alternately, lines arising from other elements present in a sample from the matrix may leak through the same slot and appear on the final spectrum, thus giving rise to potential spectral interference.

3.33 RF Generator

The Leco solid-state ICP source is a 2 kw generator which can be operated at 27.1 or 40.6 Mhz. A dedicated microprocessor controls and monitors all pertinent ICP operating conditions. Forward power is limited at 300 watts reflected (625 watts reflected during ignition). All critical components are thermally protected.

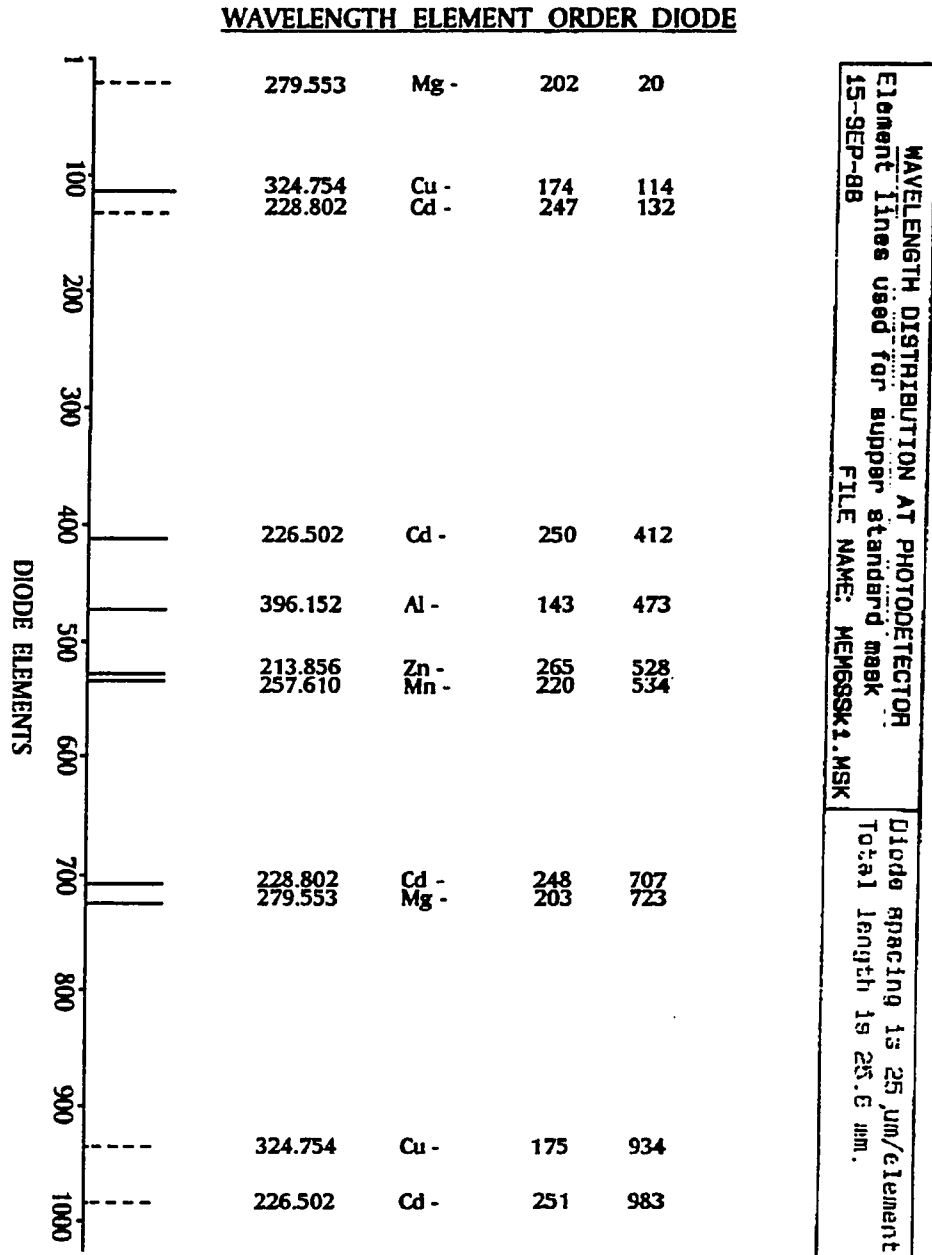


Figure 3.3 Six element mask

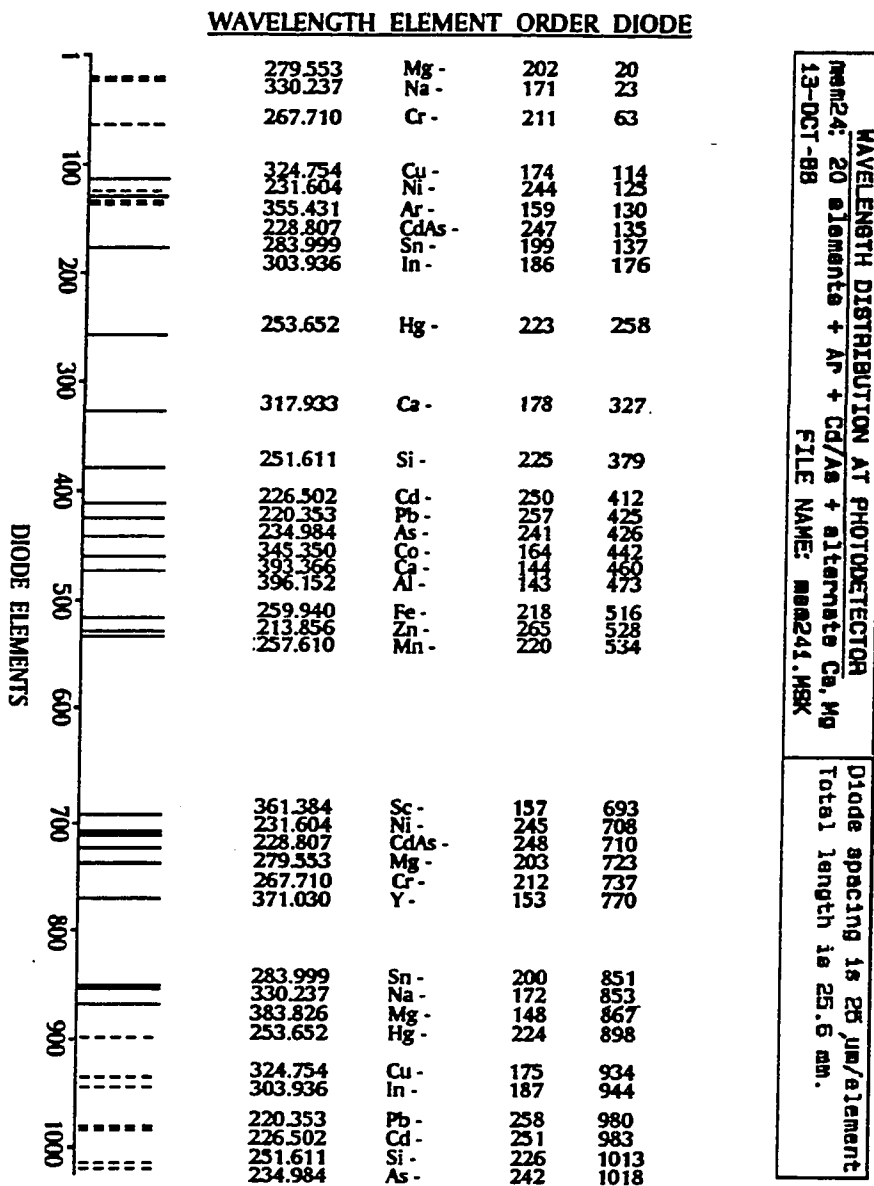


Figure 3.4 Twenty element mask

3.34 Plasma

The position of the plasma can be adjusted both vertically and horizontally to optimize the plasma viewing region for each application. The plasma is able to use either Ar or a mixed gas. The reflected power is subject to change as the plasma condition changes, especially when the sample probe enters the mixed gas plasma. The fine tuning capacitance on the matching network box is monitored by a computer. No modification of the ICP matching network was done to enhance the tolerance of the system to reflected power due to the complexity of the ICP electronic system. Therefore, the capability of using a mixed gas plasma on this instrument was somewhat (i.e. only small amount of the foreign gas could be added to the Ar) limited.

3.35 Detector

The PDA sensor was maintained at a temperature of $-25\text{ }^{\circ}\text{C}$ using a Peltier thermoelectric cooling system. The quartz faceplate of the PDA and the electronics within the camera head were kept free of condensation by purging with a low flow of dry nitrogen. The readout rate of the camera was set to 40 kHz which corresponds to a 1024 pixel spectrum acquisition time of 25.6 ms. The integration period was controlled from the PC computer, and integration periods $> 100\text{ s}$ were possible. However, integration periods of $< 100\text{ s}$ were employed to avoid dark current saturation. The entire spectrum was acquired for all readouts; however, the presentation of the data could be limited to any region of the PDA, and the intensity axis could be set to a fixed full scale or automatically scale to maintain the largest possible vertical amplification without exceeding the dimensions of the computer screen.

The intensity data correspond to background-corrected peak areas using the five most intense pixels. The background was calculated using 16 pixels on the low-pixel side of the measured peak and extrapolating under the peak.

3.36 Detection System

The information furnished by a PDA detector requires that a dedicated computer be an integral part of the detection system. The PDA camera is connected to a controller/data acquisition interface which incorporates a dedicated microprocessor and a 14-bit analog-to-digital converter (ADC). The interface is connected to an PC computer.

The software written for the Plasmarray can be divided into diagnostic, methods development, and applications programs. The diagnostic programs enable the analyst to confirm that the spectrometer is functioning properly. Method development software provides the tools necessary to develop analytical parameters for a new analysis, and applications programs.

Part of the method development software is a program which enables the analyst to design a custom mask. The analyst inputs the wavelengths of the analytical lines, and the program furnishes the slot positions for the mask and predicts where the lines will fall on the detector. The analyst is informed of any slot spacings which are physically too close together. Emission lines that may interfere with one another at the detector are identified based on a user selectable separation criterion. The same program also can be used to predict where lines other than the sought analytical line will fall on the detector. The line prediction accuracy is within a few pixels and is sufficient in most cases for wavelength identification. In cases where two or more lines may be present in the same pixel region, an unambiguous identification can usually be made by blocking all slots except the slot of interest.

3.4 Autosampler for DSI

3.41 Background

While a number of researchers have reported automated introduction of a single sample probe into the ICP, our group has developed two computer-controlled systems

with full software support capable of introducing multiple sample cups in an unattended fashion. In one approach, a 24-position autosampler carousel was modified to accommodate sample probe assemblies. The system is described in a great detail in reference [15]. The sample probe is transported by a pneumatic system. The carousel is rotated to bring the next probe below the injection point, whereupon the injector gas is activated and the assembly is driven into the torch at a rate dependent on gas pressure. The injector line contains a ballast tank to ensure a smooth insertion and retraction. During retraction, a snuffer gas also is activated to eliminate discharge filaments. System design allows for precise positioning of the probe at locations near and within the plasma. The sample probe can be either inserted rapidly into the plasma in one continuous movement or mechanically driven to a position just below the load coil and then slowly raised into the ICP. As demonstrated by several groups, the thermal gradient that exists below the plasma can be used for sample drying and ashing steps in an approach analogous to that used during electrothermal atomization.

An alternative approach to automated direct sample insertion involves the use of a robot arm for exchange of sample cups [18]. Up to 20 sample cups accommodated in a robot work station were introduced, in programmed sequence, into the ICP using a stepper motor driven insertion device. The system was reported to be simpler and more convenient to operate than the pneumatic-mechanical insertion device, and also to yield an improved analytical performance.

This study employs some of the design ideas of both the above systems. The system includes a number of the critical parts. The following will describe each part and its function in detail.

3.42 Torch

The torch used on the DSI system is typically modified from the normal Fassel torch by replacing the conventional injector tube (e. g. central tube) with an open quartz tube. The size of the central tube depends on sample probe size. The central tube partially acts as a guide for the sample carrying probe into the torch and partially helps in

cooling the probe upon retraction at the end of the analysis. Upon retraction, the formation of a discharge filament between the plasma and the probe has been reported for some systems [13, 15].

The use of a central tube gas flow is essential. A flow rate of 0.1 l/min has been found to be necessary if a dry/ash cycle is to be utilized and continuous plasma operation is to be sustained [15]. In addition, the use of a central tube gas flow counteracts filament formation upon probe retraction [13]. Also, for a mixed gas plasma, a water vapor saturated Ar central gas flow is effective in quenching any filaments that tend to form [32, 33].

A unique design of the torch used in this study is the ability to switch back and forth between DSI and liquid analysis. This dual mode torch could be converted to accommodate the conventional pneumatic nebulization for normal routine solution analysis by just dropping a cap in the center tube. The cap is made of a quartz rod with a 0.5 mm opening in the middle. Figure 3.5(c) shows a magnified diagram of the cap. The outside diameter of the cap just fits into the center tube as shown in Figure 3.5 (b). The bottom of the rod is tapered to collect the aerosol generated from the nebulizer. The top of the rod is flatted to cover the center tube outside diameter. By removing the cap, the torch can be used for DSI analysis immediately.

The spray chamber is attached on the side of the center tube as shown in Figure 3.5 (b). The angle between the center tube and the connector of the spray chamber is about 45°. The connector itself is a standard ground ball joint. A metal clamp holds the connector and spray chamber together. The center gas tube is below the spray chamber connector and is about 90° off from the spray chamber connector. Therefore, this additional attachment does not hinder any DSI operation as shown in Figure 3.6. The spray chamber used in this study was a standard Scott spray chamber with a concentric nebulizer. This dual mode torch really speeded up the change over between solid and liquid analysis.

Figure 3.7 gives an overall diagram of the DSI system. It includes a dual mode torch, a shutter, a carousel with a turn table, an electric car antenna for vertical drive, a Hall effect sensor for positioning the antenna, a magnetic shield screen and a sample plug

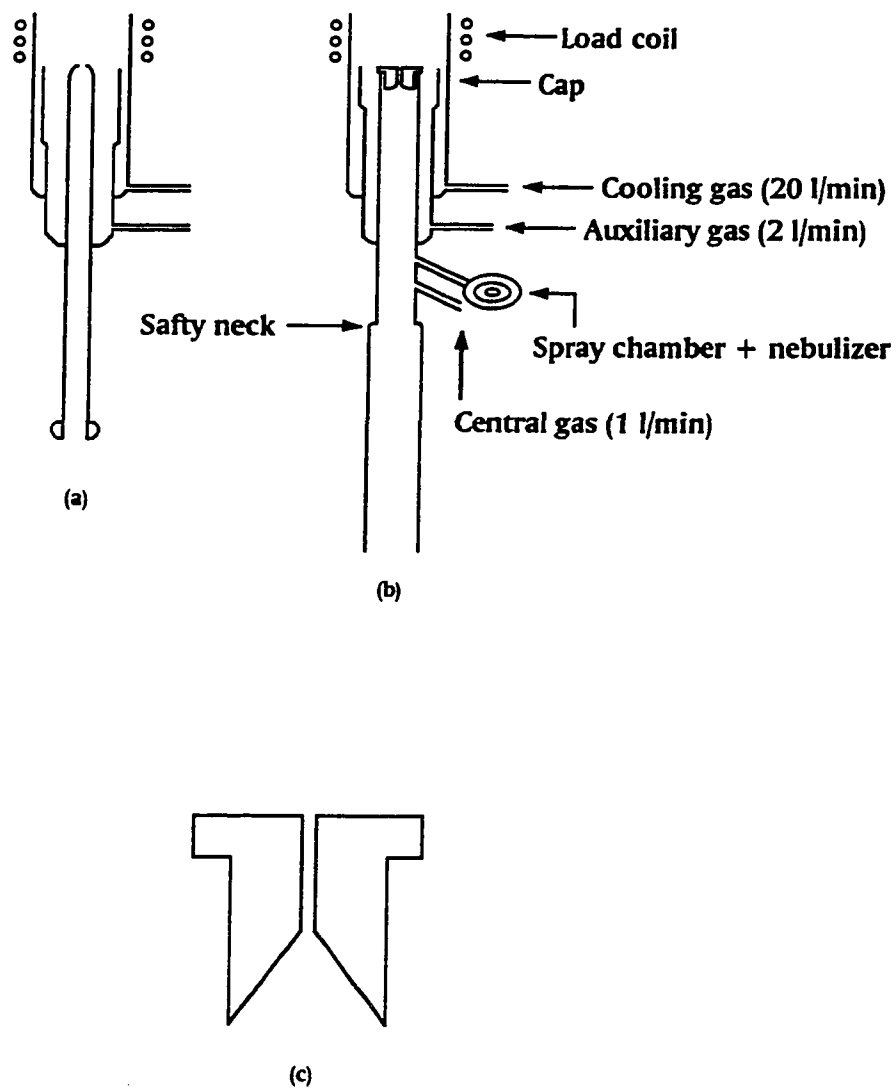


Figure 3.5 A typical Fassel type torch (a), dual-mode torch (b), and a cap (c)

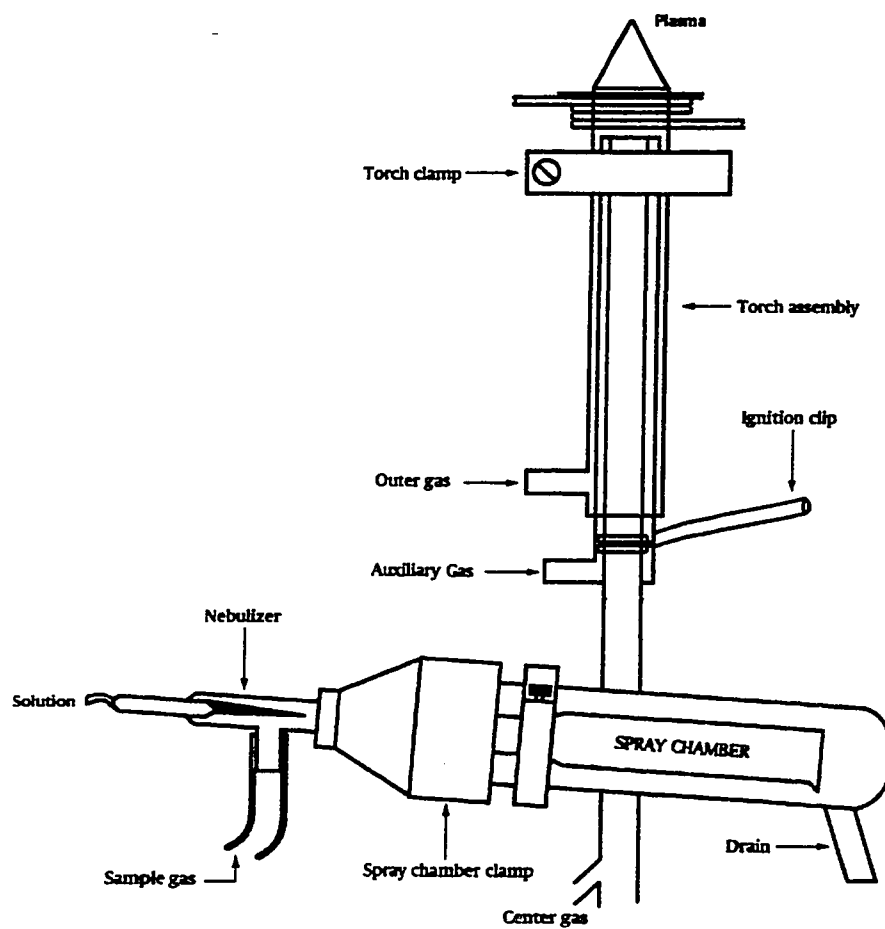


Figure 3.6 Diagram of the torch set-up with a spray chamber

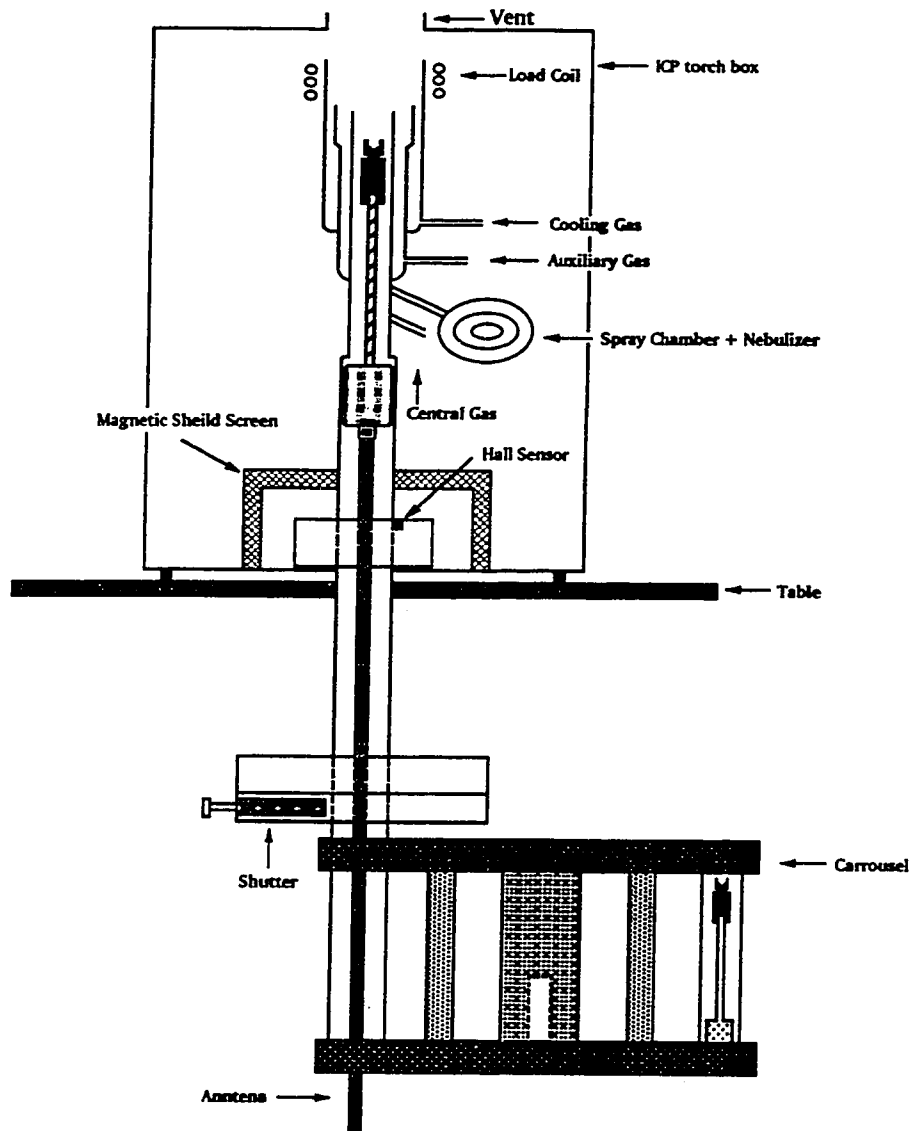


Figure 3.7 Automated direct sample insertion system

for holding a graphite cup. The bottom of the ICP torch was cut a open square. A hole was drilled on the table in order to accommodate the torch central tube. The central gas had to be controlled by an external flow meter as the existing gas plumbing were used for cooling gas, auxiliary gas and nebulizer. The existing torch holder was also modified to accommodate the extra long dual mode torch.

3.43 Antenna

The use of an electrically operated car aerial for sample insertion was reported in the middle 80's [8], but no detailed information of the operation and control of the device appeared in the literature. However, a car antenna is a attractive device due to its simplicity and low cost.

The car antenna chosen for sample transport in the direct insertion system of this study was a semi automatic power antenna (model MX-1) which was built for AM-FM radios on common cars. It was purchased from a local Canadian Tire store. It was made by Harada Antennas Ltd., Pickering, Ontario, L1W 3H2. The antenna weighs 1 lb. 8oz, and is 10.5 inches long when retracted. It has 5 extension sections, and is 31" long extended. The detailed diagram is shown in Figure 3.8. The up and down switch was replaced with a single pole double throw switch and controlled by the computer. A high current 12 V power supply was built for the antenna. The red and green lines on the upper right side of the electronic control box are for the antenna. The red (pin 1) and orange (pin 5) wires on the upper left side of the electronic control box (Figure 3.9) are from the digital I/O DT707 screw terminal panel (Figure 3.10) port 0 bit 0 and bit 1. They control the up and down movement of the antenna.

The antenna is mounted on the end of the carousel support arm. A magnified diagram of the antenna top is shown in Figure 3.11. The mounting nut is screwed tightly on the aluminum plate. The head of the antenna is made of steel. A hole was made in the middle of the head to hold two magnets. The magnets are used for triggering a position sensor. This technique is widely used on GC autosamplers for syringe needle injection. The difference in this application is that the sensor is on the outside of the glass tube and

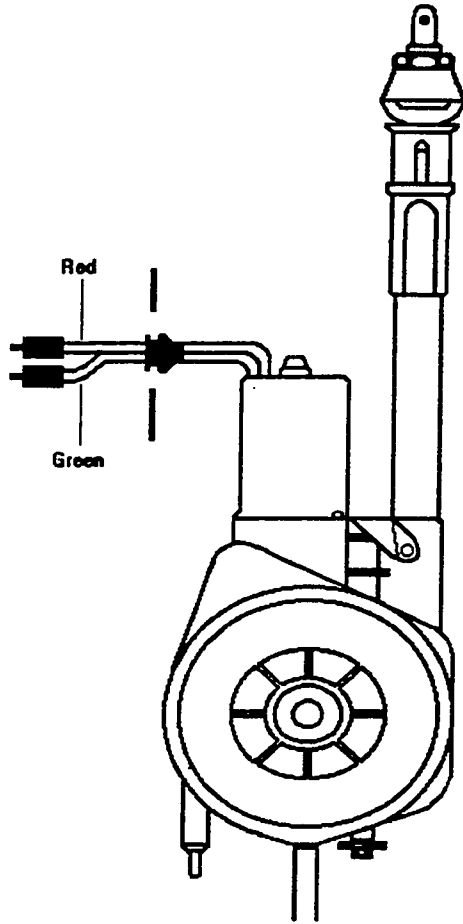


Figure 3.8 Schematic diagram of car antenna

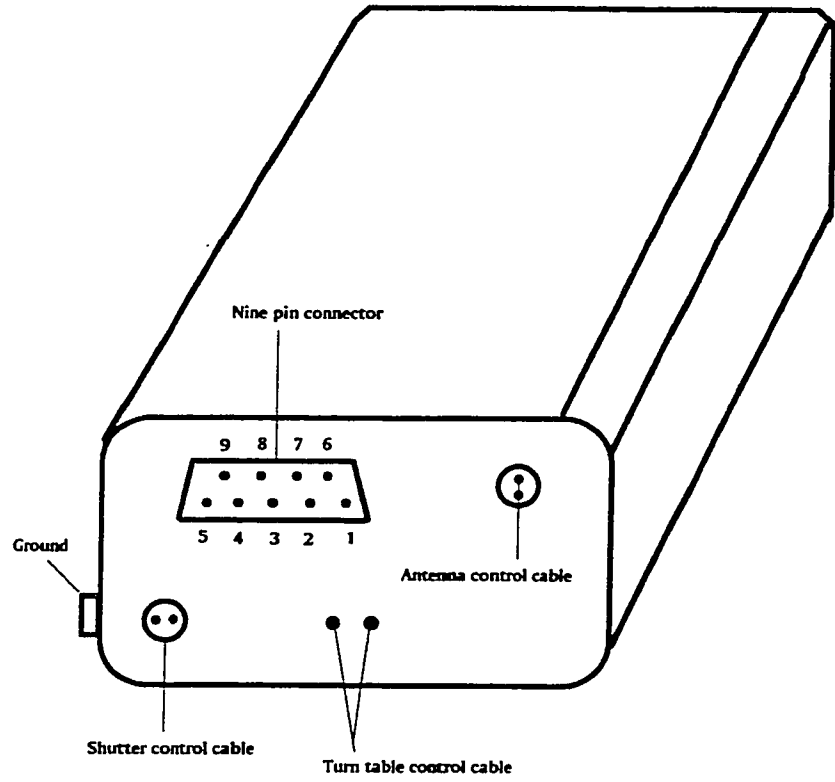


Figure 3.9 Interface box

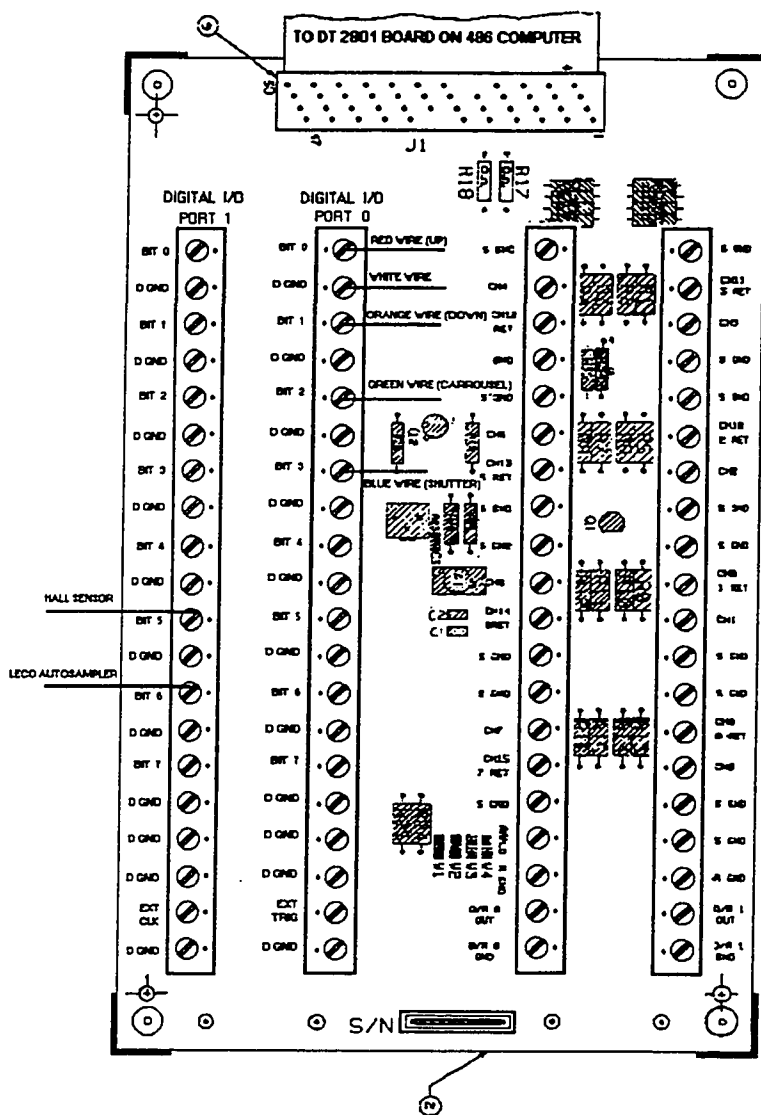


Figure 3.10 DT707 screw terminal panel

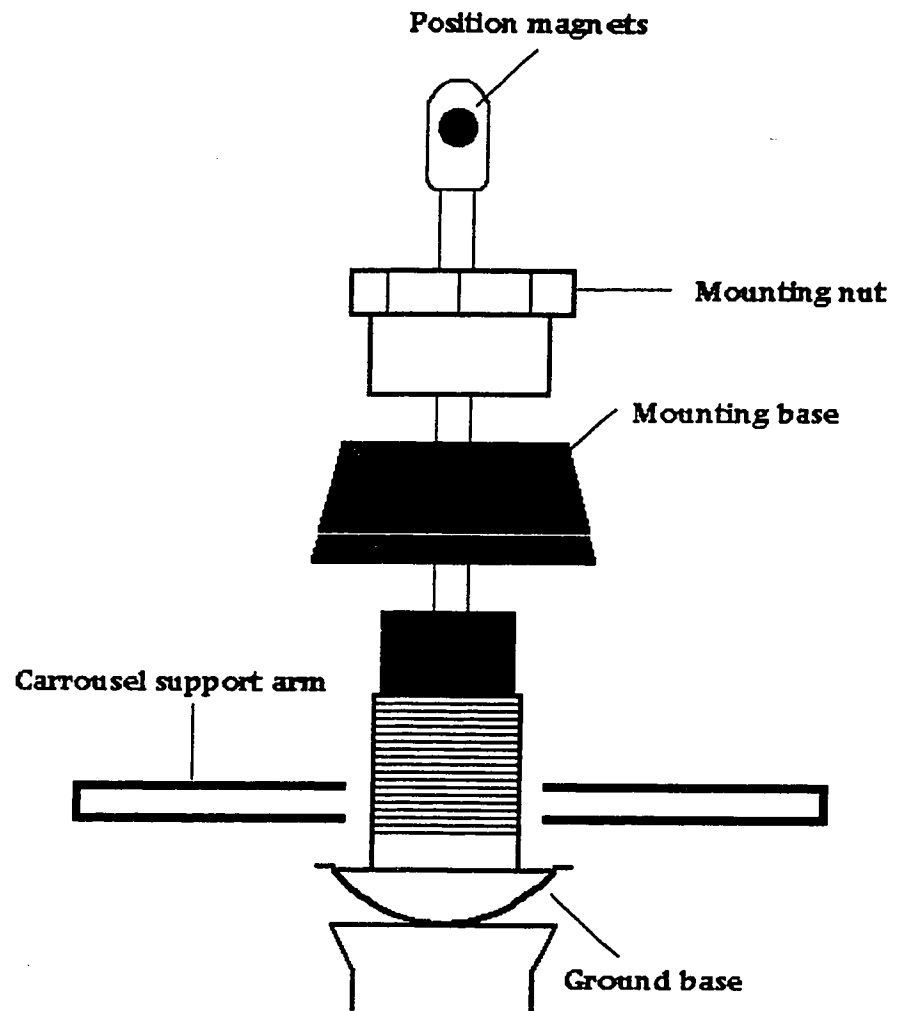


Figure 3.11 Diagram of antenna head part

the magnet is in the middle of the glass tube. The larger air gap between the sensor and the magnet requires precise alignment.

The rate of insertion and retraction is very fast. However, the rate is not controllable. After repeated tests, the antenna has been proven to be mechanically simple and reliable. It fits the DSI system very well.

3.44 Position Sensor

Precise positioning of the sample probe, as required for reproducible vaporization and excitation, is achieved in a number of ways. The simplest implementation is a mechanical stop, attached to the insertion assembly, which positions the sample electrode in a fixed location relative to the ICP. This approach limits the final position to a single location. Stepper motors could provide easy control of multiple stop positions, but are usually more complicated and expensive. The antenna is able to provide multiple stop positions, but the positions are not highly reproducible when no other control device is in place. A Hall effect digital switch was chosen for the purpose of position control in this system.

The Hall effect is the production of a transverse voltage in a current-carrying conductor (usually a semiconductor) in a magnetic field. Type 3020 Hall effect digital switches offer highly responsive magnetic characteristics and fast, trouble-free switching. The unit used in this system (Figure 3.12) was manufactured by Sprague Electric Company, 70 Pembroke Road, Concord, N. H. 03301, USA [34]. Technical information on the sensor is listed in Table 3.2.

Figure 3.13 (upper diagram) presents a Hall effect circuit that includes a voltage regulator, Hall voltage generator, signal amplifier, Schmitt trigger and open-collector output on a single silicon chip. The on-board regulator permits operation over the supply-voltage range of 4.5 to 24 V. The switches' open-collector outputs can sink 20 mA at a conservatively rated repetition rate of 100 kHz. The bottom diagram is the test circuit used in this experiment.

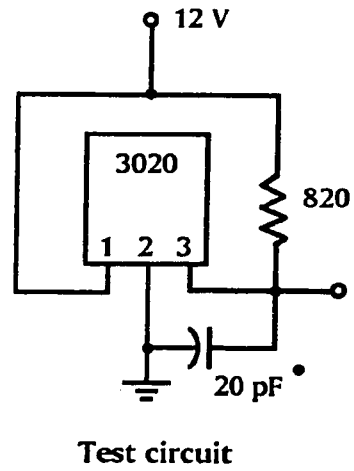
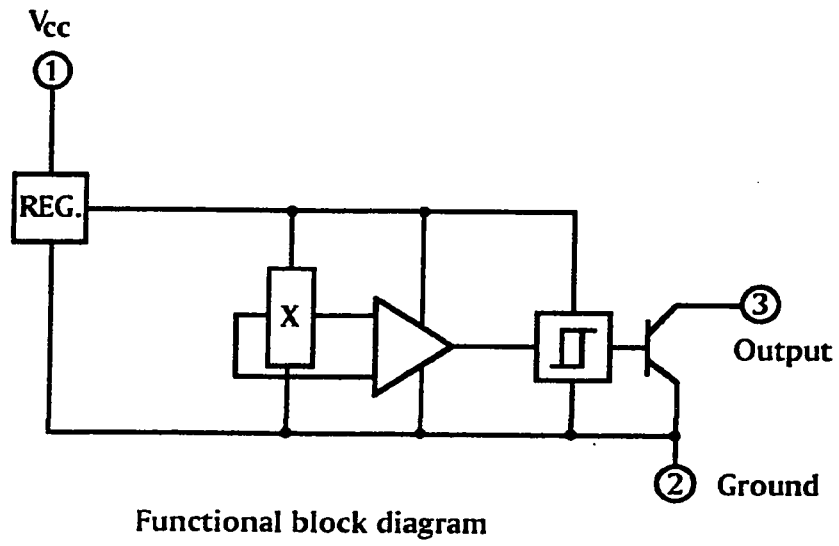


Figure 3.13 Sensor electronic diagram

Supply Voltage V_{cc}	25 V
Magnetic Flux Density, B	Unlimited
Output OFF Voltage	25 V
Output ON Current, I_{SINK}	25 mA
Operating Temperature Range, T_A	-20 °C to + 85 °C
Storage Temperature Range, T_s	-65 °C to + 150 °C

Table 3.2 Hall Effect Digital Switch Maximum Ratings

The most common modes of operation are head-on and slide-by. As shown in Figure 3.12, the magnet's polar axis is the centerline of the Hall Effect package. Change of operating states in the slide-by mode is accomplished by up and down movement the magnet.

The device is turned ON by presenting the south pole of the magnet to the branded face of the package, which is opposite the side with the ejector pin indentation. With the branded side facing front and the pins pointing down, pinouts are, from left to right: (1) Vcc, (2) GND, (3) Vout. This is shown in Figure 3.12.

The output transistor is OFF when the flux density of the magnetic field perpendicular to the surface of the chip is below threshold (operate point). When flux density reaches the operate point, the output transistor switches ON and is capable of sinking up to 25 mA of current.

The total effective air gap is the sum of active area depth and the distance between the package's surface and the magnet's surface. Type 3020 Hall Effect switches are offered in two packages. The U package is about 0.05 mm thinner than the T package. The difference is found in the distance from the surface of the Hall cell to the branded face of the package. The T pack's active area depth is 0.9 mm; the U pack's is 0.4 mm. The total effective air gap for T pack is 3.55 mm, and for U pack is 3.05 mm.

The sensor is mounted on a Teflon clamp (Figure 3.14 (a)). There is a small indentation for housing the Hall sensor on one half of the clamp. The clamp is held tightly on the center tube of the torch by two screws and sits on the bottom of the torch box as shown in Figure 3.14 (b). Once the head of the antenna triggers the sensor, it will stop immediately (within 0.1 mm as estimated). It is found that the antenna could provide a reproducible insertion after it stops at the pre-set position. Then ashing position and atomization position are controlled by the on and off time on the switch.

The sensor and its electronic circuit were found to be prone to interference from the ICP. Once the plasma was turned on, the sensor would malfunction. Therefore, a magnetic shield is installed to enclose the sensor and its circuit to prevent the interference. The shield was made of aluminum net and grounded on the torch box as shown in Figure 3.7, and proved to eliminate the interference and provide reliable operation.

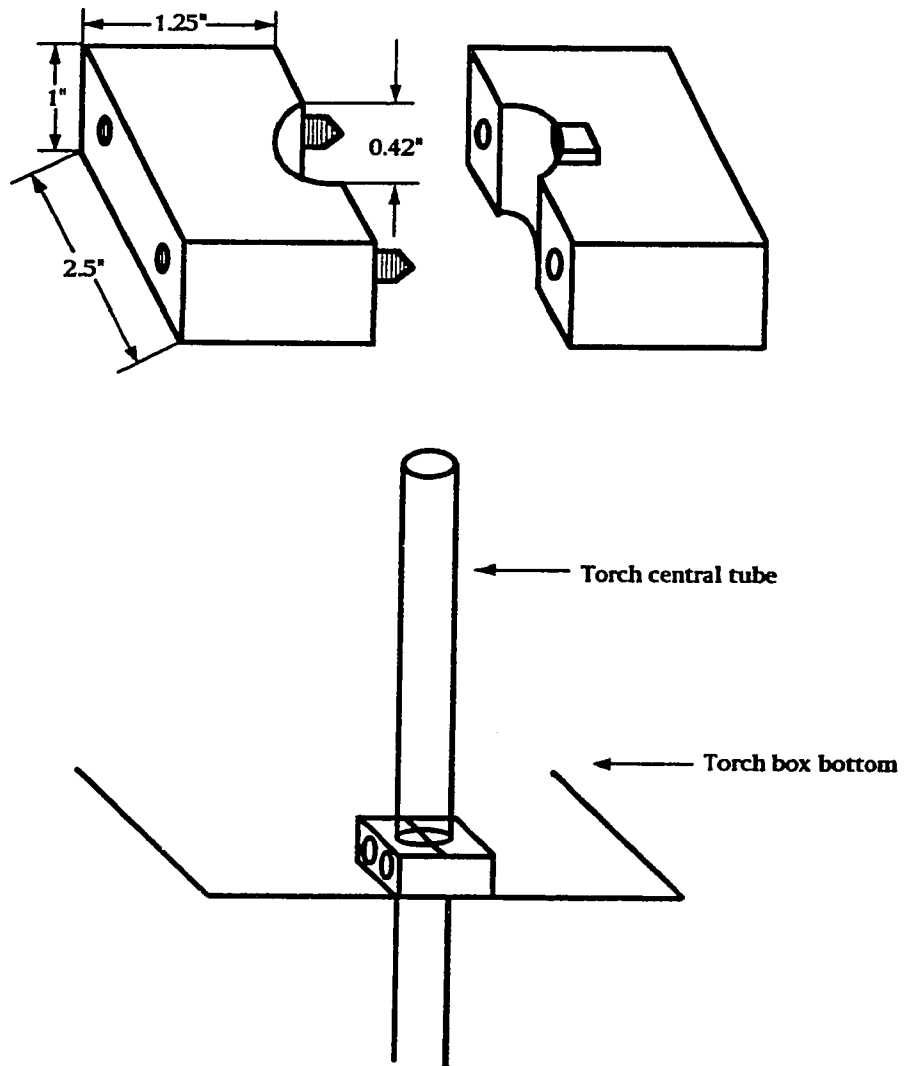


Figure 3.14 Hall effect sensor holder

3.45 Shutter

A shutter was used in this set-up to close the bottom of the torch when the sample probe was in the tray. Otherwise, the plasma would push downwards and damage the central and intermediate tubes of the torch. The shutter was made from two pieces of the Teflon as shown in Figure 3.15. The torch assembly is inserted in the top. The internal diameter of the hole in the bottom part has the same diameter as the central tube. This ensures smooth transition from the torch to the shutter, then to the tray. The shutter has its own 110 V power line, and open and close is controlled through an electronic relay that is operated by the computer. The computer signal through the digital I/O port 0 and bit 3 (figure 3.10) to the pin 4 of the nine pin connector on the interface box (Figure 3.9) for shutter control. The left bottom outlet in the electronic box is for controlling the relay on the shutter. The shutter opens two seconds before the antenna starts and closes after the antenna goes back to the home position.

3.46 Carousel

The carousel tray holds 24 samples, and trays can be exchanged without disturbing plasma operation. Details of the sample carousel tray are shown in Figure 3.16 and presented in Table 3.3. The tray was constructed by sandwiching 24 glass tubes between an aluminum upper plate and a plexiglass lower plate. Hole size on the upper aluminum plate has the same diameter as the glass tube internal diameter. Smaller diameter holes passed through to the bottom surface in order to leave support for the sample plugs. Three steel standoffs and a central plexiglass standoff provided rigidity.

This tray design proved to be very functional as the glass tubes withstood repeated exposures to hot sample cups without degradation and the tray was easy to handle during laboratory operations such as sample loading and removal.

Sample plugs (Figure 3.17) were machined to close tolerance to insure reproducible injection velocities between samples. A minimal clearance between plug and guide tube wall also permitted the use of a low central gas flow. These close tolerances in

Top Plate

Parameter	Specification
Material	Aluminum
Diameter	202 mm
Thickness	6 mm
Sample tube holes	Twenty four 10.6 mm diameter holes, centered 12.3 mm from plate edge and 16.3 mm from one another
Outer standoff holes	Three 9 mm diameter holes taped to accept 3.5 mm diameter screws, centered 38 mm from plate edge and 110 mm from one another
Center standoff recess	9.5 mm diameter center hole, 6 mm deep

Sample Tubes

Parameter	Specification
Material	Glass
O. D.	13.0 mm
I. D.	10.6 mm
Length	204 mm

Outer Standoffs

Parameter	Specification
Material	Aluminum
Outer Diameter	8 mm with flat on each end and a hole to accept 3.5 mm diameter screw
Length	195 mm

Table 3.3 Carrousel tray specifications

Center Standoff

Parameter	Specification
Material	Plexiglass
Center Diameter	25.6 mm
Length	204 mm with top end 9.5 mm diameter at depth of 6 mm, and bottom end 18 mm diameter at depth of 3 mm
Carousel drive shaft receptacle	9.5 mm diameter and 68 mm depth hole in bottom of standoff

Bottom Plate

Parameter	Specification
Material	Plexiglass
Diameter	202 mm
Thickness	6 mm
Sample tube holes	Twenty four 13 mm diameter at 1.5 mm deep recesses with 9 mm diameter holes centered in each recess and extending remaining distance through plate for antenna entry
Outer standoff holes	Holes same as for the top plate
Center standoff recess	18 mm diameter with 3.0 mm deep recess for the center standoff with a 9.5 mm hole continuing through the plate for the drive shaft
Driveshaft locating key	7.3 mm hole centered 71 mm from the plate edge

Table 3.3 Carrousel tray specifications (Continued)

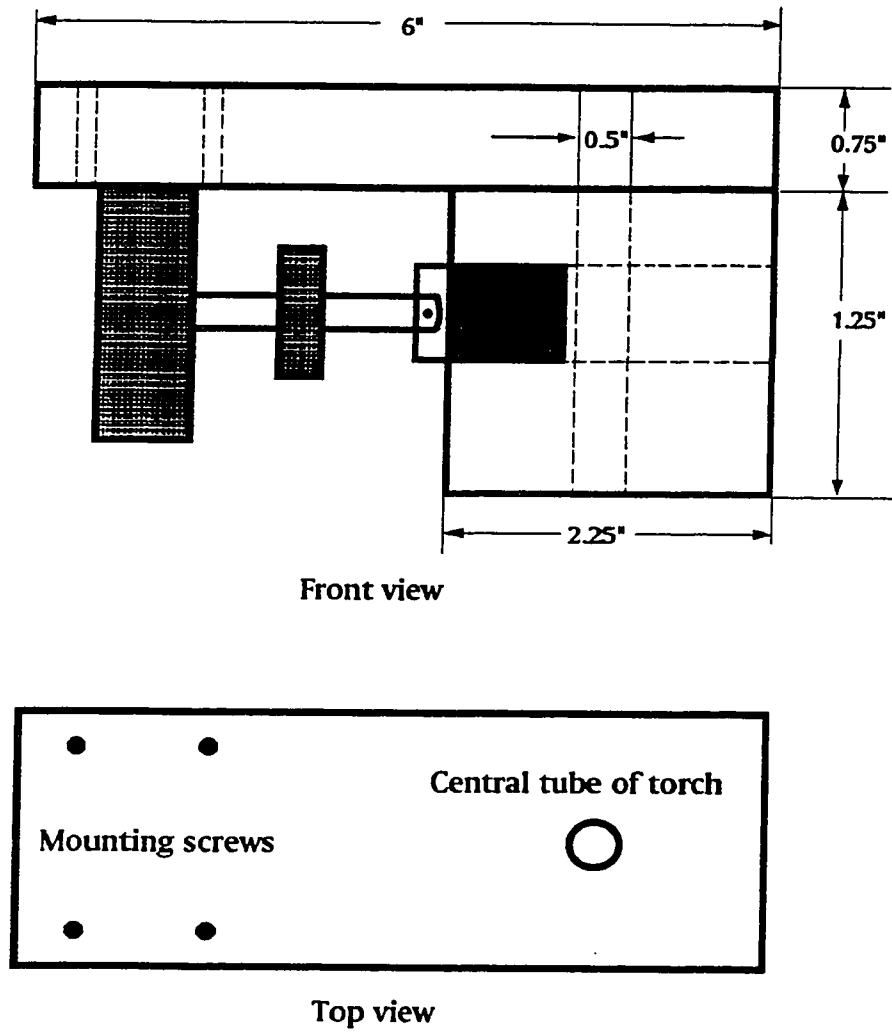


Figure 3.15 Diagram of shutter

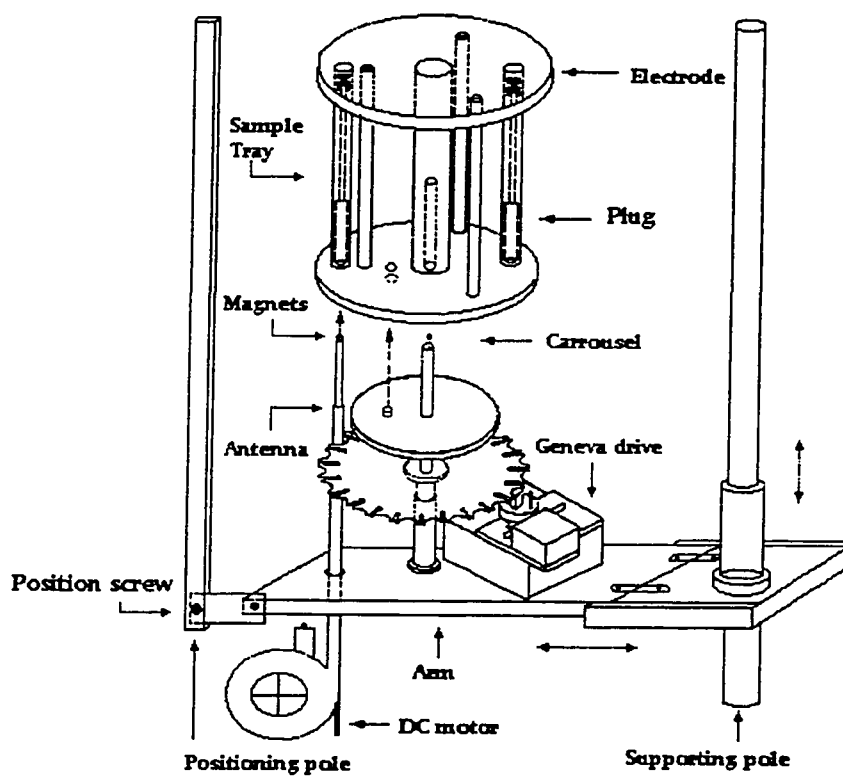


Figure 3.16 Diagram of the solid sample autosampler

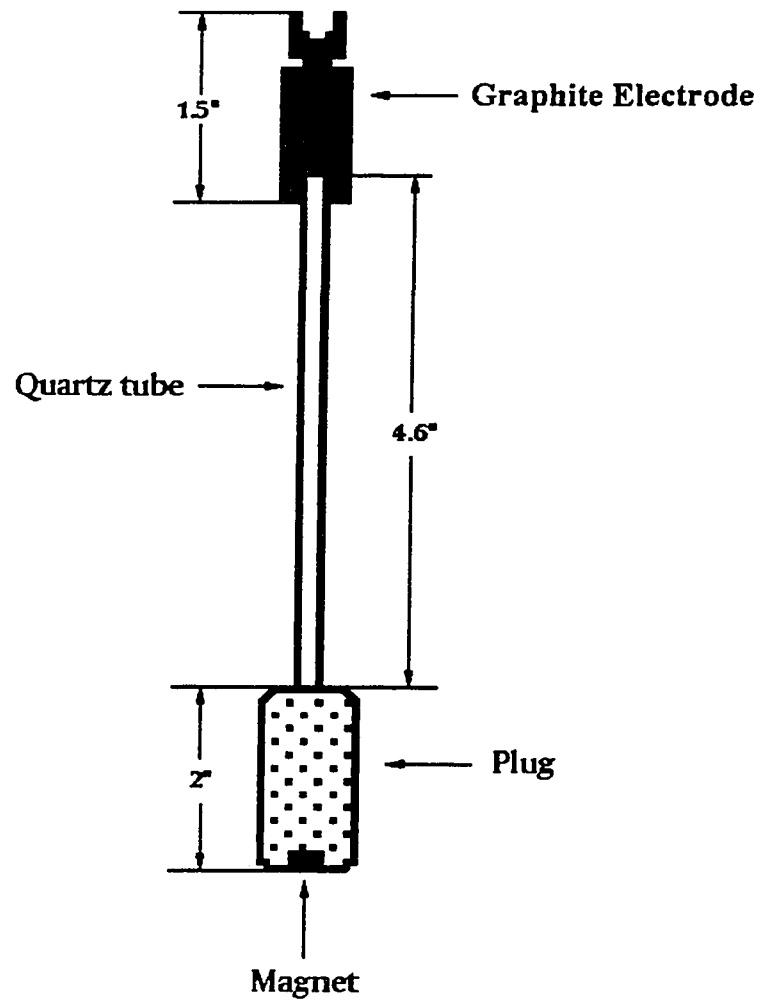


Figure 3.17 Sample plug with electrode

turn dictated a precise indexing between the carousel tray and touch central tube. A precise drive and stable mount were therefore required for the carousel.

Samples were prepared as a group before analysis. A carousel organizer was built to make sample loading more convenient. The organizer was made of a sheet metal and twenty four screws as shown in Figure 3.18. The screw pushes out the sample plug when the carousel sits on the top of the organizer. Once the sample is weighed, the electrode can be easily put on the quartz tube as it stands out of the carousel.

3.47 Turn Table

A refurbished commercial sample changer provided the requisite precision in the carousel drive. Details of the sample carousel tray and its drive are given in Figure 3.16. This motor's output was governed by a mechanism ("Geneva mechanism") which accommodated imprecision in primary shaft position to give precise rotary displacement of the driver shaft.

The original driver shaft was replaced with an extended version fit with a circular plate on which the carousel tray could rest. The length of shaft above this plate then fit into a hole drilled into this lower end of the tray's central standoff. A small key on this plate also fit an indentation in the bottom surface of the tray to insure reproducible positions. The drive is bolted on the carousel support arm.

3.48 Mounting

The Leco spectrometer sits on a big table top that is bolted on several heavy rectangular aluminum riders. These riders sit on the top of a rail bed that is sturdily mount on floor. Two additional riders are used for hanging the autosampler. First, a cross bar is bolted on these two slide bars in order to balance the weight of the autosampler. Then a support pole is bolted to one end of the cross bar. A non-bearing sleeve is tightly inserted in the support pole. The sleeve can move up and down to provide vertical adjustment. The support arm is bolted on the sleeve. It can turn 360°.

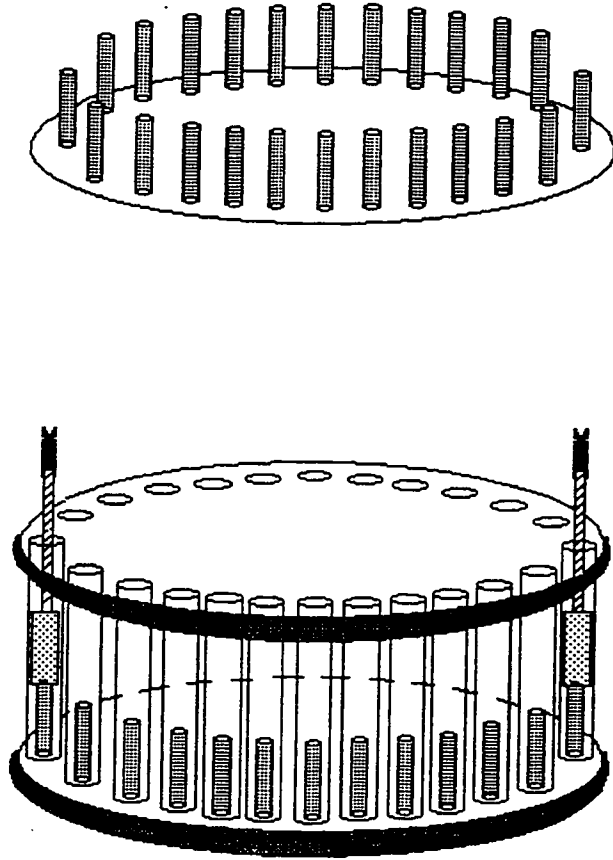


Figure 3.18 Carousel organizer

The arm consists two sections. The outer section has room of several centimeters of horizontal adjustment. Stability of the carousel is guaranteed by a rigid support pole and the supporting arm as shown in Figure 3.16. The position pole is bolted on the other end of the cross bar. The position pole is used for fixing the carousel in one position. The final position of the carousel is fine tuned by adjusting the screw on the bottom of the position pole. This ensures the carousel position does not change when the sample tray is reloaded.

3.49 Sample Plug Insertion and Retraction

Smooth sample insertion and retraction is very critical to the ICP operation. The plasma could experience major fluctuation or even extinguish due to the large volume of air or Ar gushing upward or downward when a sample plug moves up and down. The problem of air was taken care of by using a central Ar gas flow. The upward pressure problem was solved by implementing a two step insertion procedure. The sample stops twice before reaching the ashing position. This ensures that no large volume of gas is pushed rapidly upward to disturb the plasma. The distance from ashing position to the final atomization position is very short. Therefore, there is not enough gas movement to destabilize the plasma at this step.

Sample retraction usually is not a problem for the plasma and using a cooling step (delay stop on the way down) essentially eliminated any plasma fluctuation. However, there was a major problem for consistent sample plug retraction into the tray. The weight of the plug is simply not heavy enough to drop itself into the carousel. This is especially true when the alignment between the carousel and torch is not perfect. Unreliable sample plug retraction could result in major problem. When the plug jammed in the center tube of the torch or in the shutter, one had to stop the turn table and the plasma. Sometimes, the stem of the plug was broken by the shutter in the case of a jam. On other occasions, the carousel would not be able to turn when the plug stopped between the tray and the shutter.

A solution was found to address this problem. A hole was machined in the bottom of the plug and a magnet pellet was glued to the bottom of the plug (Figure 3.17). The pellet surface had to be perfectly aligned with the bottom of the plug to ensure that the height of every plug is the same. The attraction between the magnet and steel head of the antenna provided enough force to pull the plug down to the tray. This mechanism provided a very reliable sample retraction even when the carousel and the shutter was not perfectly aligned.

3.410 Data Acquisition Board

The antenna motor, the turn table, Hall sensor, the shutter and autosampler synchronizer signals are all controlled by and fed to a data acquisition board. The DT2801-A card is employed for this purpose. It is a high performance analog and digital I/O board which is compatible with the IBM personal computer. The board can be programmed from the IBM personal computer's interpreted or compiled BASIC language to perform analog to digital (A/D) conversions; digital to analog (D/A) conversions; and digital input and digital output (I/O) transfers. The specifications of the board are listed in Table 3.4. PCLAB is a real-time software package designed for use with data translation's DT2801 series of IBM PC compatible analog and digital I/O boards. The board is plugged into an Intel 80486 based IBM compatible PC running at 33 MHz.

The DT2801 series boards feature two 8-line digital I/O ports which can be used separately to read or write 8-bit transfers, or simultaneously for a 16-bit transfer. The DT 707 is a companion screw terminal panel for the DT 2801. The diagram of the terminal panel was shown earlier in Figure 3.10. The DT707 supports all the analog and digital I/O functions of the DT2801 and, with an integral interconnection cable, provides for easy connection of user signals.

Four bits on the digital I/O port 0 were used for writing data out of the board. Bit 0 is for antenna up, bit 1 is for antenna down, bit 2 is for carousel forward, and bit 3 is for shutter open.

Digital Inputs:	
Input Type	Level sensitive
Logic Family	TTL
Logic Load	Presents 1 TTL load
Logic High Input Voltage	2.0 V minimum
Logic Low Input Voltage	0.8 V maximum
Logic High Input Current	1.0 mA @ 5.5 V maximum 0.07 mA @ 2.7 V
Logic Low Input Current	0.250 mA maximum
Digital Output:	
Logic Family	TTL
Logic High Output Voltage	2.4 V minimum
Logic Low Output Voltage	0.5 V maximum
Logic High Output Current	24 mA maximum 6.5 mA @ 2.4 V
Logic Low Output Current	24 mA maximum

Table 3.4 Specifications of DT2801-A Digital I/O Subsystem

Two bits on the digital I/O port 1 were used for reading data into the board. Bit 0 to bit 4 are malfunction. Bit 5 is for reading the signal from the Hall sensor circuit in order to stop the antenna. Bit 6 is for reading a signal from the Leco computer to synchronize the DSI system.

3.411 Synchronizing

The computer on the Leco system has a 15 pin Sub 'D' interface connector to connect to its solution autosampler. The function of the connector can be seen in Figure 3.19. If the sampler is used without the wash station, it can be controlled by only two external signals; the lower signal (pin 4), which will lower the pipet into the sample tube, and the advance signal (pin 2) which will first raise the pipet from the sample tube, and then advance the racks to the next sample.

For example, the single pole double throw switch of an injection valve can be connected with pin 1 of the sampler going to the common terminal of the switch, lower (pin 4) to the load sample position of the switch, and advance (pin 2) to the inject sample position of the switch. The sampler will lower the pipet into the sampler whenever the inject valve goes from the inject position to the load sample position, and raise the pipet and advance to the next sample during the injection of the sample just loaded.

These input control lines are activated by a contact closure between the specific input control lines and common (pin 1) or by TTL logic low voltage (0 to 0.8 V) with respect to common (pin 1). Inactive inputs will have a voltage of approximately +5 V. Output lines will have a voltage of 2.5 to 5 volts when active and less than 0.8 volts when inactive.

In the case of our study, pin 1 and pin 2 were used for sending the signal to the DSI autosampler. The pin 1 wire is connected to the ground of the digital I/O port 1. Pin 2 is connected to bit 6 on port 1, as shown in Figure 3.10. Once the DSI autosampler receives the start signal, it will function according to the program parameters. Table 3.5 lists these parameters as an example for synchronized analysis.

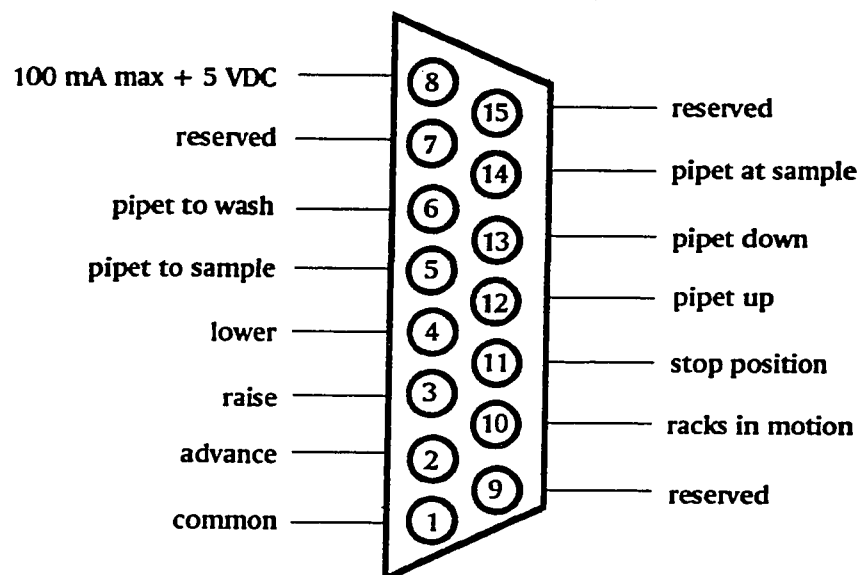


Figure 3.19 Autosampler fifteen pin connector

Leco Run-Time Parameters	DSI Autosampler Analysis Parameters
Clearing Time: 30 seconds	Ashing Time: 17 seconds
Integration Period: 25 seconds	Atomization Time: 30 seconds
Washing Time: 25 seconds	Cooling Time: 12 seconds
	Home Time: 12 Seconds

Table 3.5 Synchronized operation parameters for DSI operation

3.5 Software

3.51 Background

Several in house software systems have been developed for control and data processing of DSI systems in our group [3-8]. Some of the systems were developed for the Apple and Macintosh computers in the late 80's and early 90's. Karanassios and Horlick developed a system for DSI-ICP-MS which supports high speed transfers and implements the virtual reality concept. The latest system was developed for Windows based Intel PC's.

Windows extends DOS so that programs can have a consistent, mouse-oriented graphical user interface, complete with pop-up menus, windows, controls and dialog boxes, which, in addition to the visual interaction between user and computer, make the program easy to use. In addition, Windows makes it possible to run multiple programs simultaneously and to take advantage of all the memory available on today's PCs. A common user interface is an interface that is similar regardless of the program being executed. The basic operational concepts in Windows always remain the same so the user can use new programs productively with little training. Certain elements of the environment are defined by Microsoft to make communication between programs easy. Many complex graphics routines are part of Windows. Microsoft defines many core graphics features, which enables one to develop complex graphical displays with minimum effort.

3.52 DSID Program Windows Application

Turbo C++ for Windows was chosen as a programming language. The tools in the Turbo C++ for Windows include : 1) A full Integrated Development Environment (IDE). This enables one to edit, compile, and link programs while running Windows. 2)

Turbo Debugger for Windows (TDW). This is for tracking the messages critical to Windows operation. 3) The Resource Workshop. This is a visual tool kit that enables one to quickly design and manage custom resources, including icons, cursors, bitmaps, menus, dialog boxes, menu accelerator keys, and string resources. 4) The ObjectWindows Library (OWL). It is a framework for rapid development of Windows applications without having to rewrite similar code. However, sometimes C++ for Windows programming can be a bit overwhelming for the beginner. Therefore, the logic of the program is described by the flow charts in Figures 3.20 (a), (b) and (c). Figure 3.20 (a) gives an overview of the functions performed by the program. Figures 3.20 (b) and (c) explain how the carousel and antenna portions perform each task. These flow charts provide information for program modification and trouble shooting.

Figure 3.21 (a) shows the appearance of the DC Motor program for Windows. The carousel control functions are under the DSID pull down menu. Several dialog boxes are in this sub-menu. Dialog box "positions" is for entering the sample probe position. The current position is the position that sample holder is on the top of the antenna. The initial position is the position where a set of run starts. The carousel will advance to the initial position when the initial position is not equal to the current position. The final position is the position where the run ends. The final position cannot exceed 24. The program will not let a user enter any number larger than 24. Dialog box "motor" is for manual control of the carousel. The carousel can start and stop at any time when either button is clicked. This is a convenient feature for trouble shooting and initial setting. Dialog box "method" gives three ways to start a run. First, the manual method will only allow the antenna to move though one up/down cycle. Then it waits for the next instruction. Second, the automatic method will follow the pre-programmed run. This is a useful method to pre-burn electrodes. Last, the synchronized method is almost the same as the automatic method except the start signal is from the Leco computer. The default button sets the current position and initial position to 1 and final position to 10, and method to manual. Once the number is entered, one can chose either cancel or OK. The run button is "clicked" to start.

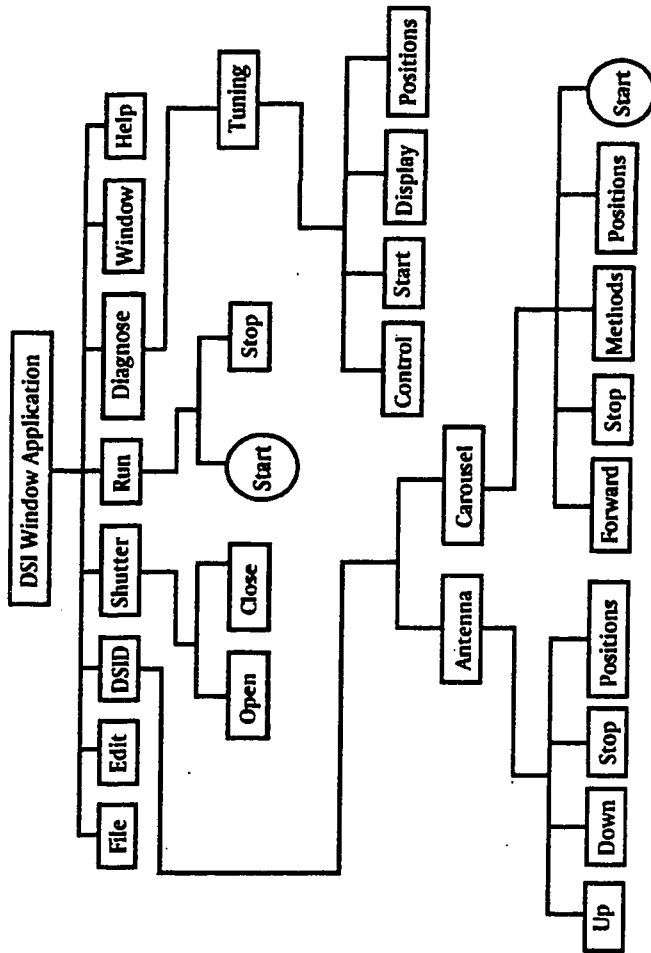


Figure 3.20 (a) The flow chart of DSI Windows application - main menu

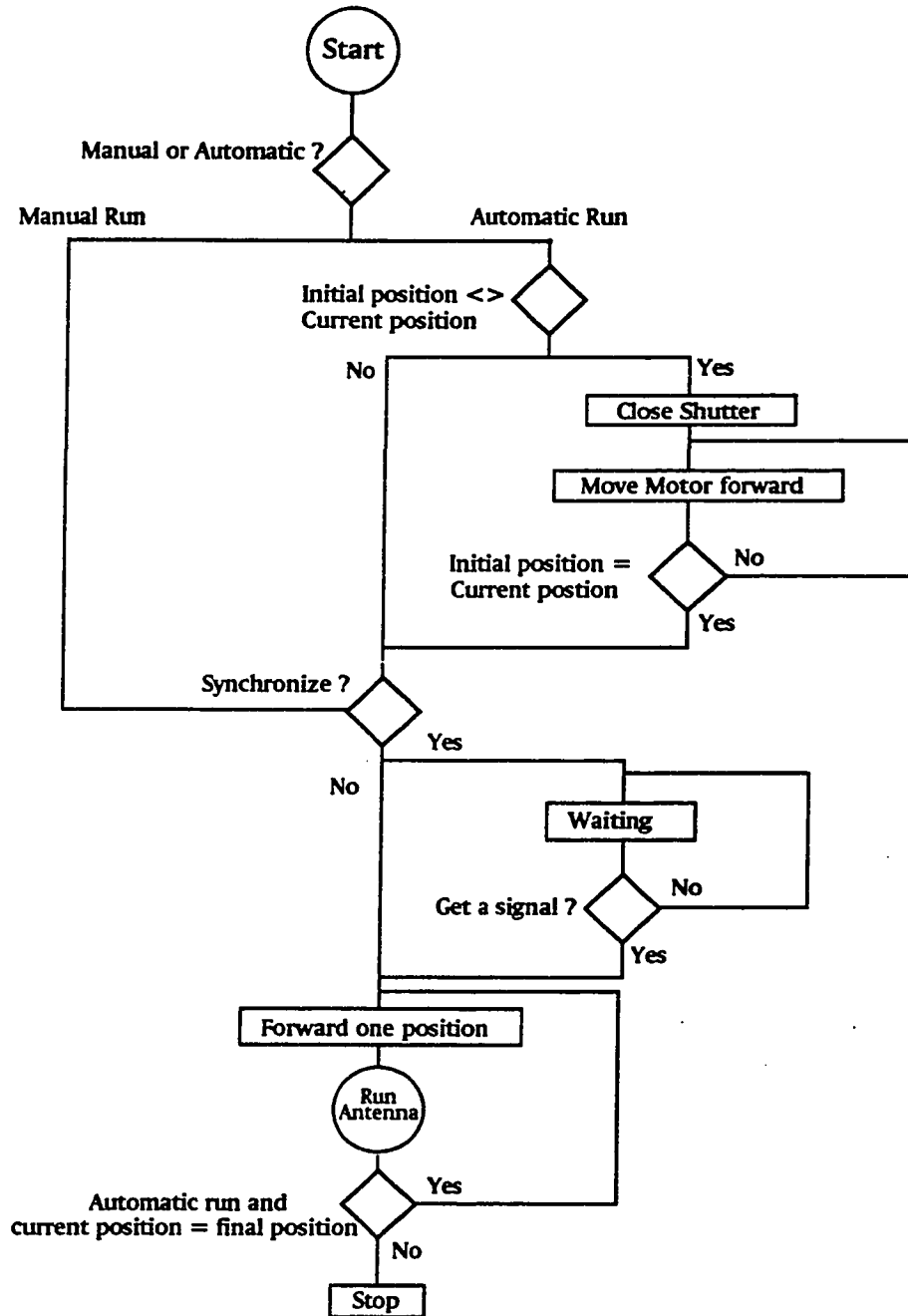


Figure 3.20 (b)

The flow chart of DSI Window application - Carousel

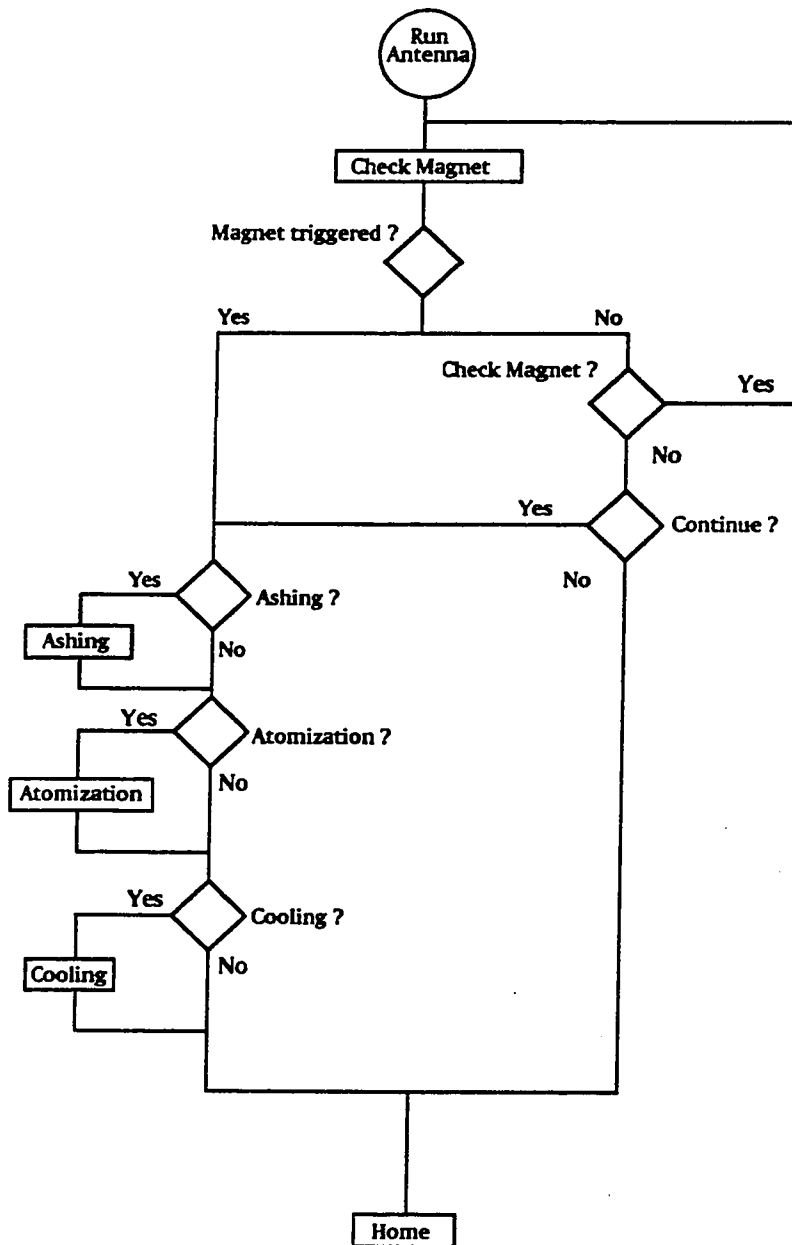


Figure 3.20 (c) The flow chart of DSI Window application - antenna

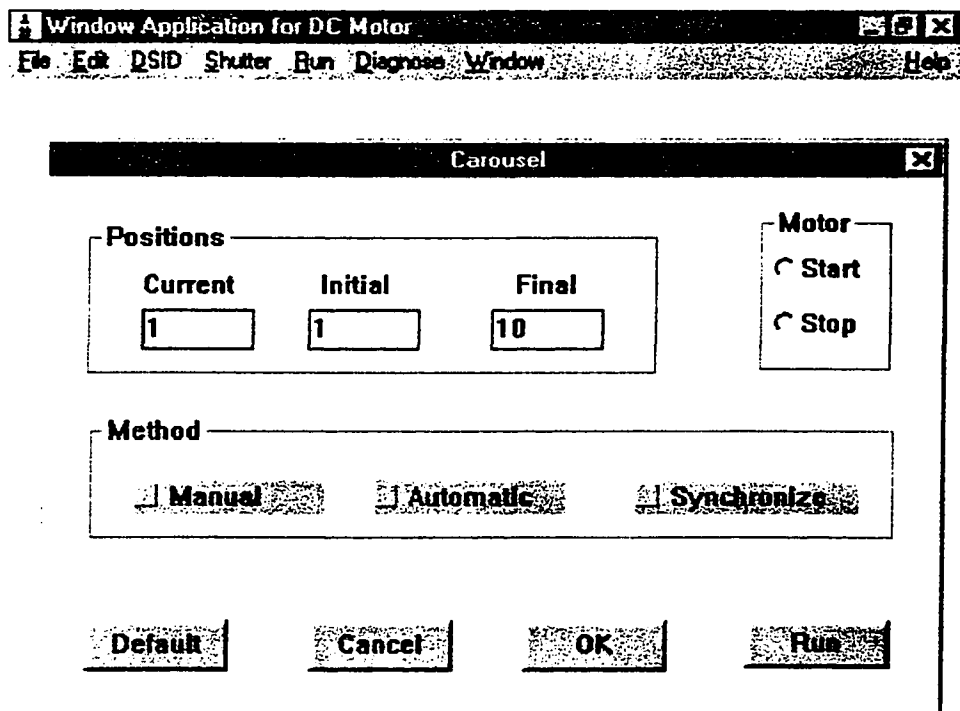


Figure 3.21 (a) Screen copy of DC Motor program for MS Windows
This is a Carousel Control dialog box

Figure 3.21(b) is sub-menu “Cup Position” under the DSID menu. The user can specify parameters for the sample probe such as ash position/time, atomization position/time, cooling position/time. The home position is mandatory and set by default, the other three positions are chosen by the user. Default is all position checked and time 5 seconds. Like the carousel motor, the antenna motor can be operated though manual control as well.

After the antenna and carousel parameters are entered, the user should pull down the run status sub-menu under the “Run” as shown in Figure 3.21 (c). The black dot indicates where a sample cup is in the carousel. Once the start button is pushed, the program will execute the run according to the parameters. The time shown in the Antenna box will count down the time spent on each position.

As mentioned before, it is very important for the antenna to trigger the Hall sensor and stop. Then any programmed position above that point will be reproducible. If the sensor is not triggered, the analysis results will be impaired. The program will send a warning message to the user if the sensor was not triggered as it is shown in Figure 3.21 (d). The user has three choices. First, let it continue. This is likely the case for a pre-burn electrode sequence. The final antenna position is not as critical. Second, stop the run. Sometimes, this is the only choice. Third, adjust the antenna head position and try it again. If this is the choice, the antenna will come down to the home position for adjustment and another pop-up window will appear.

Figure 3.21 (e) shows the adjustment window. Once the direction of the magnets is adjusted, the user can click the OK button to continue the run. Sometimes, one adjustment is not enough, and this can be a tedious procedure.

Another convenient feature of the program is to set up a diagnostic menu. By pulling down the tuneup sub-menu, the user can move the antenna to test if the sensor is being triggered before any analysis begins. This is shown in Figure 3.21 (f). The user can push the start button to move the antenna to a certain height. The start point can be changed manually. By clicking the Mag up or down button, the antenna will move accordingly. The speed of the antenna can also be adjusted. One is the slowest speed, three is medium and 10 is fast. If the magnet is at the right direction, the Hall sensor will

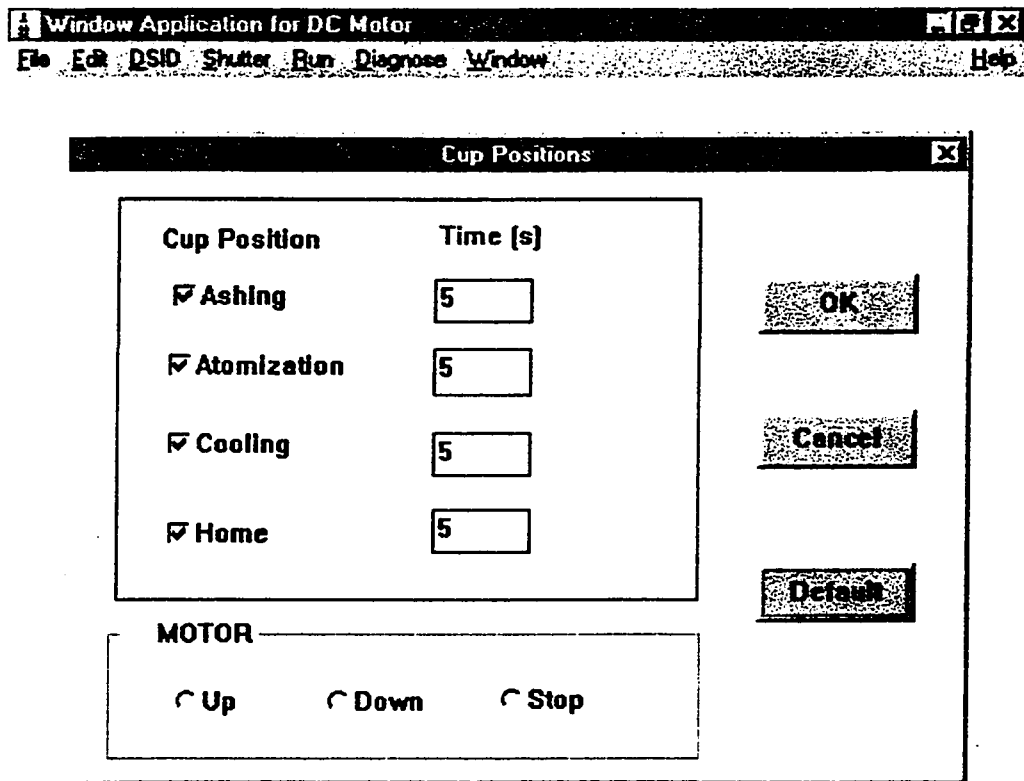


Figure 3.21(b) Screen copy of DC Motor program for MS Windows

This is a Cup Position Control dialog box

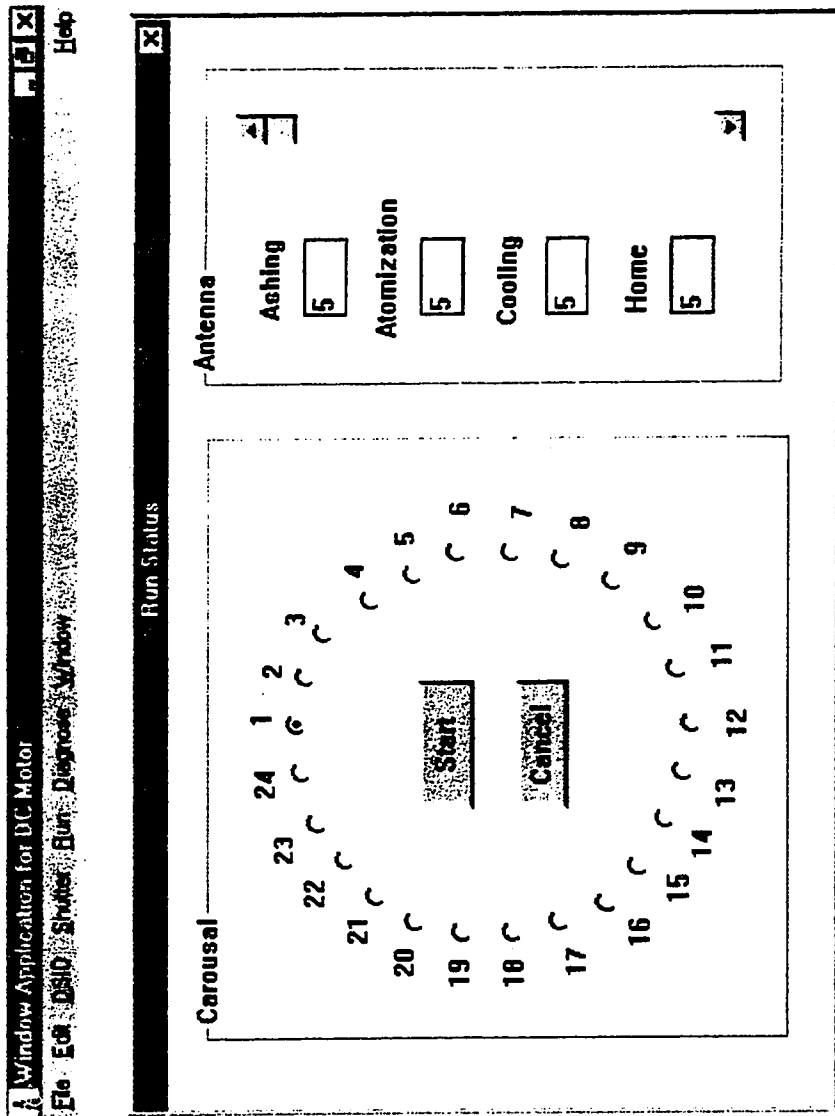


Figure 3.21 (c) Screen copy of DC Motor program for MS Windows

This is a Run Status dialog box

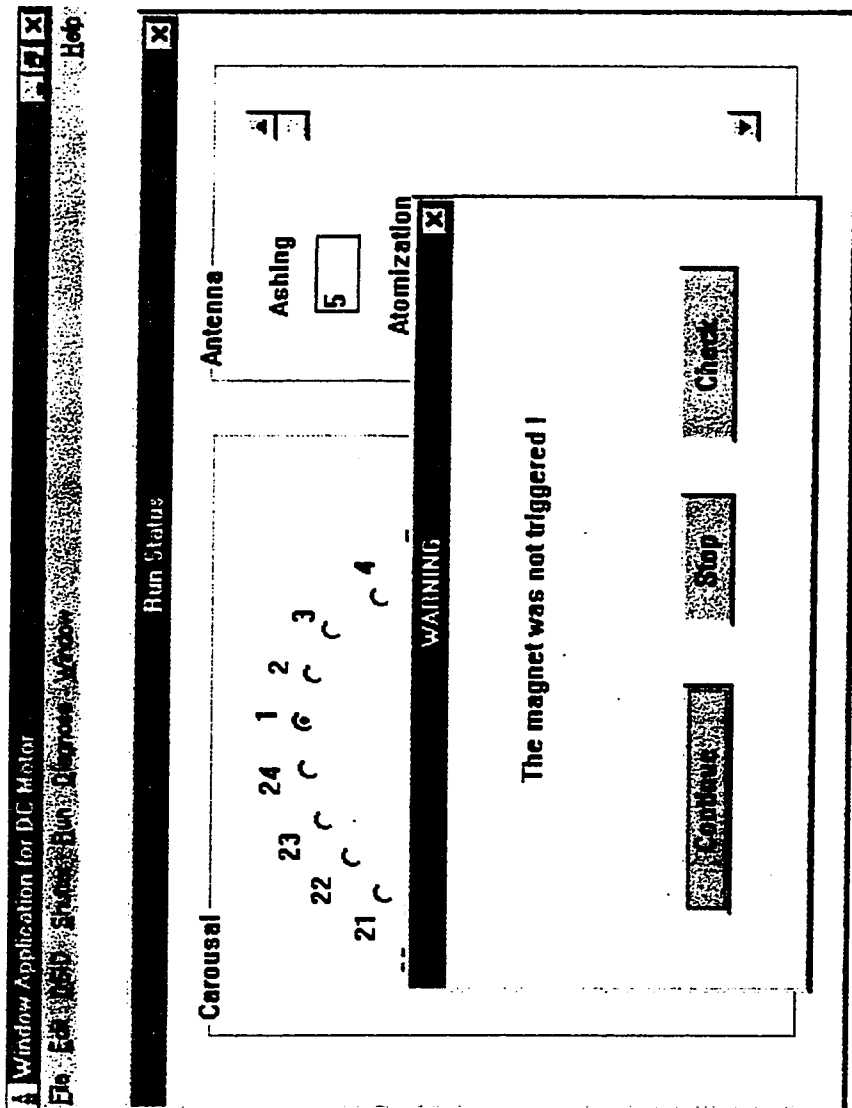


Figure 3.21(d) Screen copy of DC Motor program for MS Windows
This is a Warning dialog box

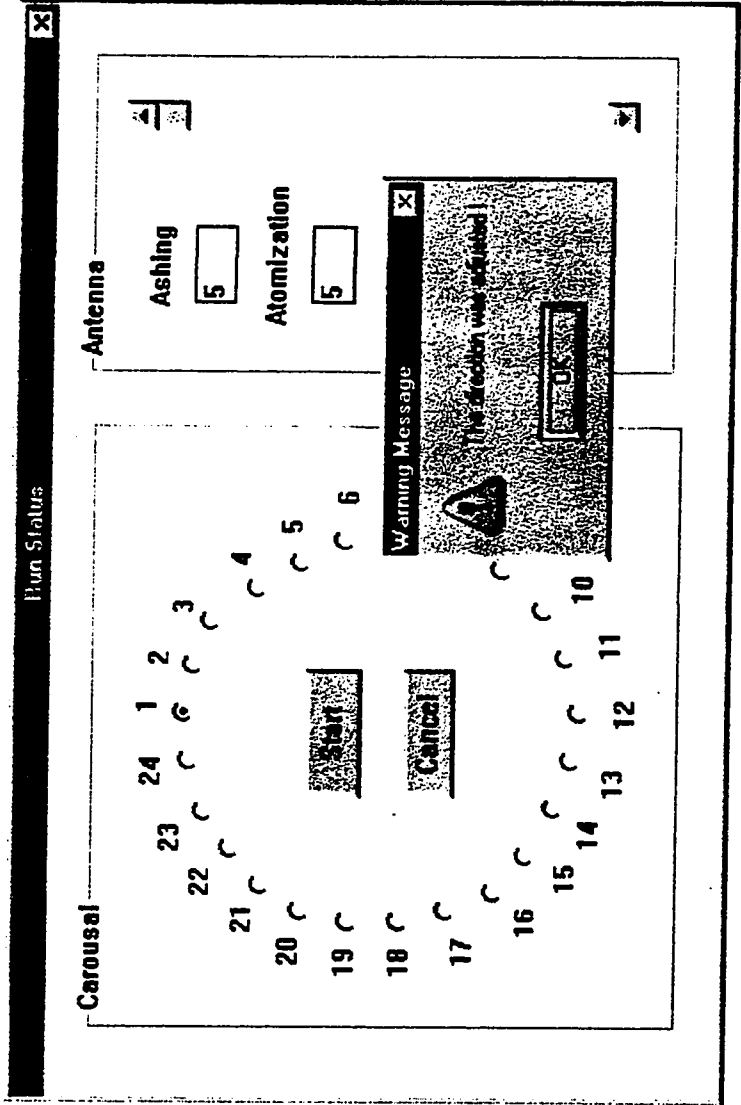


Figure 3.21(e) Screen copy of DC Motor program for MS Windows

This is a Warning Message box

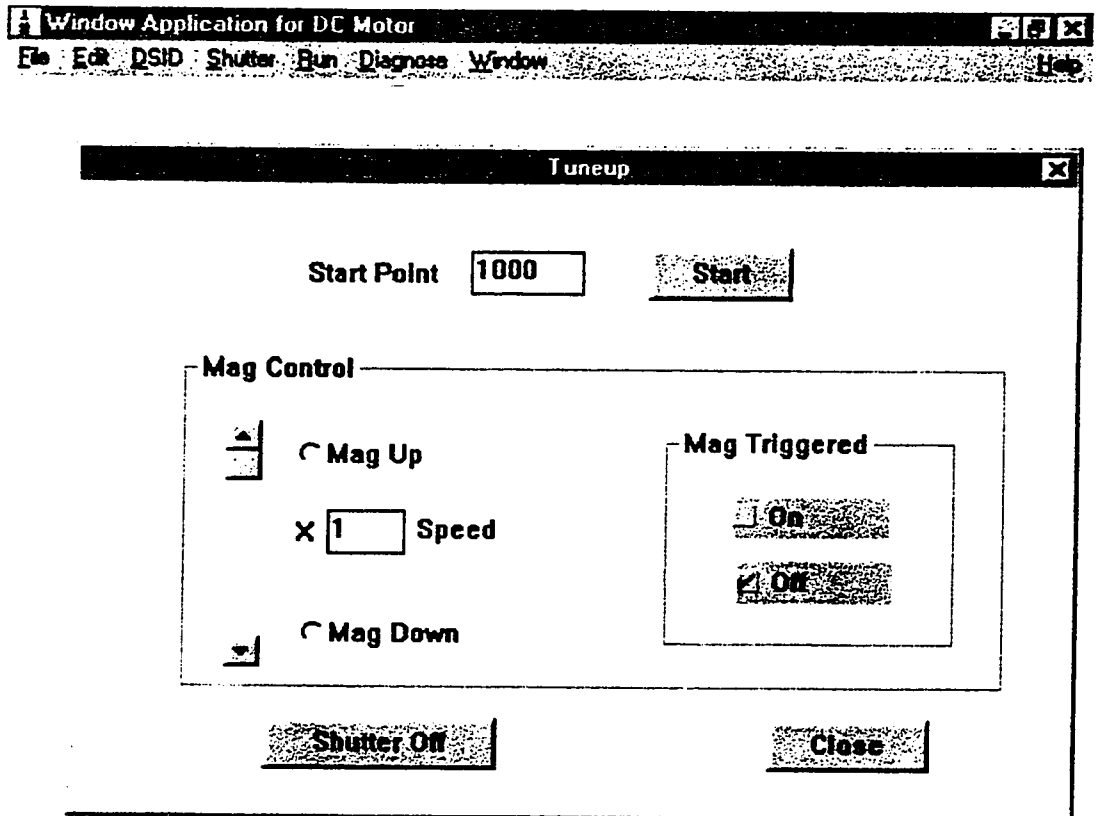


Figure 3.21 (f) Screen copy of DC Motor program for MS Windows

This is a Tuneup dialog box

be triggered and the check mark will move up the "ON" box. This is a very useful tool for initial instrument set-up.

3.6 Summary

The direct sample insertion device with a dual mode torch has been successfully developed for automatically analyzing samples. First of all, continuous plasma operation and automatic sample insertion resulted in a significant improvement in analytical performance relative to the pneumatic transport system. The system could be retrofitted to most commercial ICP spectrometers. The DSI could be envisioned as a modular subunit of a larger analytical system. The mechanical problems have been overcome and the system is reliably operated under computer control. It is necessary only to load a carousel and input operating parameters at the computer terminal; the system runs automatically from that point.

3.7 References:

1. E. D. Salin and G. Horlick, *Anal. Chem.* **51**, 2284 (1979).
2. A. Lorbe and Z. Goldbart, *Analyst* **110**, 155 (1985).
3. I. B. Brenner, A. Lorber and Z. Goldbart, *Spectrochim. Acta* **42B**, 219 (1987).
4. G. F. Kirkbright and L. X. Zhang, *Analyst* **107**, 617 (1982).
5. G. F. Kirkbright and S. J. Walton, *Analyst* **107**, 276 (1982).
6. A. G. Page, S. V. Godbole, K. H. Madraswala, M. J. Kulkarni, V. S. Mallapurkar and B. D. Joshi, *Spectrochim. Acta* **39B**, 551 (1984).
7. M. Abdullah, K. Fuwa and H. Haraguchi, *Spectrochim. Acta* **39B**, 1129 (1984).
8. C. V. Monasterios, A. M. Jones and E. D. Salin, *Anal. Chem.* **58** (4), 780 (1986).
9. M. M. Habib and E. D. Salin, *Anal. Chem.* **57** (11), 2055 (1985).
10. C. W. McLeod, P. A. Clarke, and D. J. Morthorpe, *Spectrochim. Acta* **41B**, 63(1986).
11. Gy. Zaray, J. A. C. Broekaert and F. Leis, *Spectrochim. Acta* **43B**, 241 (1988).
12. Gy. Zaray, P. Puba, J. A. C. Broekaert and F. Leis, *Spectrochim. Acta* **43B**, 255(1988).
13. Y. B. Shao and G. Horlick, *Appl. Spectrosc.* **40**, 386 (1986).
14. D. Sommer and K. Ohls, *Fresenius Z. Anal. Chem.* **304**, 97 (1980).
15. W. E. Pettit and G. Horlick, *Spectrochim. Acta* **41B**, 699 (1986).
16. E. D. Salin and R. L. A. Sing, *Anal. Chem.* **56**, 2596 (1984).
17. D. W. Boomer, M. Powell, R. L. A. Sing and E. D. Salin, *Anal. Chem.* **58** (4), 975(1986).
18. W. T. Chan and G. Horlick, *Appl. Spectrosc.* **44**, 380 (1990).
19. V. Karanassios and G. Horlick, *Spectrochim. Acta* **44B**, 1345 (1989).
20. V. Karanassios and G. Horlick, *Spectrochim. Acta* **44B**, 1361 (1989).
21. V. Karanassios and G. Horlick, *Spectrochim. Acta* **44B**, 1387 (1989).
22. M. Abdullah and H. Haraguchi, *Anal. Chem.* **57**, 2059 (1985).

23. M. Abdullah, K. Fuwa and H. Haraguchi, *Appl. Spectrosc.* **41**, 715 (1987).
24. L. X. Zhang, G. F. Kirkbright, M. J. Cope and J. M. Watson, *Appl. Spectrosc.* **37**, 250 (1983).
25. N. W. Barnett, M. J. Cope, G. F. Kirkbright and A. A. H. Taobi, *Spectrochim. Acta* **39B**, 343(1984).
26. L. Blain, E. D. Salin and D. W. Boomer, *J. Anal. At. Spectrom.* **4**, 721 (1989).
27. G. E. M. Hall, J. C. Pelchat, D. W. Boomer, and M. Powell, *J. Anal. At. Spectrom.* **3** (6), 791(1988).
28. R. L. A. Sing and E. D. Salin, *Anal. Chem.* **61** (2), 163 (1989).
29. V. Karanassios and G. Horlick, *Spectrochim. Acta* **45B**, 85 (1990).
30. W. T. Chan and G. Horlick, *Appl. Spectrosc.* **44**, 525 (1990).
31. G. M. Levy, A. Quaglia, R. E. Lazure and S. W. McGeorge, *Spectrochimica Acta* **42B**, 341 (1987).
32. X. R. Liu and G. Horlick, *J. Anal. At. Spectrom.* **9**, 833 (1994).
33. X. R. Liu, Ph.D. Thesis, University of Alberta , 1994.
34. Hall Effect and Optoelectronic Sensor Data Book, Sprague Electronic Company, Semiconductor Group, 70 Pembroke Road, Concord, N.H. 03301, USA.

Chapter 4

Basic Performance of An Automated DSI-ICP with a Dual-mode Torch

4.1 Introduction

The system described in Chapter 3 is unique in terms of the dual-mode torch, the echelle spectrometer and the autosampler. In order to discuss the analytical characteristics of the system, it is important to understand how the non-cross dispersive echelle spectrometer works.

4.2 Principle of Non Cross-Dispersive Echelle Spectrometer

The Leco Plasmarray spectrometer combines several optical sub-systems in a unique arrangement enabling the acquisition of multielement spectra using a linear photodiode array[1]. The preselection polychromator provides a flexible choice of analytical wavelengths and removes most of the radiation not required for the analysis. The acquisition of wavelength information surrounding the analytical wavelength provides two advantages over systems which employ single channel detectors. First, background subtraction can be performed without acquiring a blank spectrum. Secondly, the analyst can view simultaneously the spectral region in the vicinity of the analytical wavelength to determine future action. Another advantage of this system results from the two focal planes which can be addressed independently. If two or more lines are present in the same pixel region on the detector, the mask can be modified temporarily by blocking slots to solve the ambiguity.

Conceptually, this instrument is a high-resolution echelle spectrometer with a random access predisperser. A set of small wavelength regions can be chosen, essentially at random, with an appropriate mask. The spectral information in these selected regions can then be measured under high resolution while still being packed into a short focal plane format. This process is illustrated schematically in Figure 4.1 [2]. The predisperser

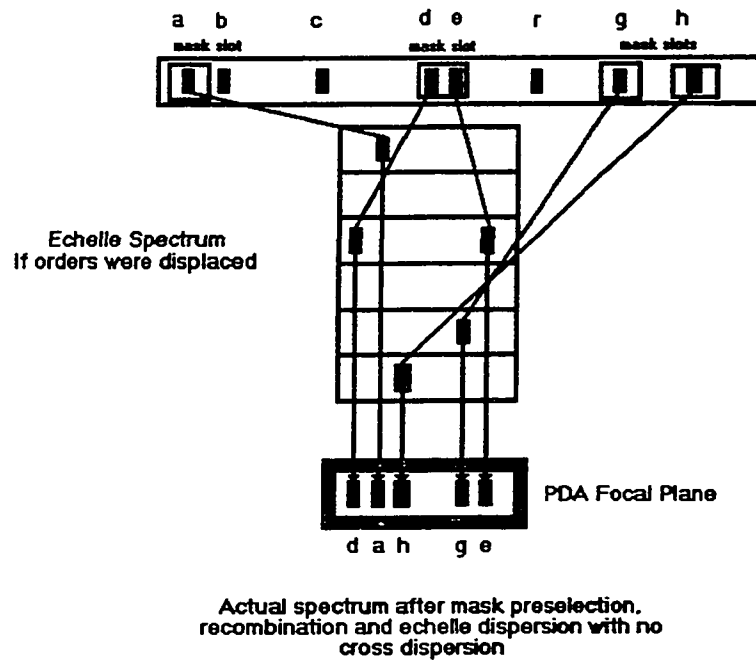


Figure 4.1 Diagram of a mask

focal plane and mask are depicted in Figure 4.1. In this example, eight spectral lines are present in the predisperser focal plane. To simplify matters, the mask has only four slots, which are positioned to select lines a, d, e, g, and h. Line a can be thought of being at the 200-nm end. In this example, then, lines a, d, e, g, and h, and spectral background adjacent to these lines, are all transmitted through to the recombination optics and the echelle-PDA spectrometer that was illustrated in Chapter 3. The remaining lines (b,c, and f) and spectral background get blocked off by the mask.

Although no cross-dispersion is involved in the echelle spectrometer, it is useful, at this stage, to think of the echelle spectrometer as if the orders were displaced. This is schematically represented in the central part of the figure, with 200-nm orders at the top and 400-nm orders at the bottom. Note that even though a mask slot may pass more than one spectral line, as depicted for the middle line (d and e), the lines will often be well resolved by the echelle spectrometer.

Since there is no cross-dispersion, the orders are not displaced and the “spectrum” as measured by the PDA in the echelle spectrometer focal plane appears as shown at the bottom of the figure. The PDA spectral axis cannot easily be defined in terms of wavelength because the lines are scrambled with respect to their true wavelength order. The PDA axis is best thought of as an element axis with certain elements falling at certain pixels, not unlike channels of a direct-reading spectrometer. The direct reader analogy can be carried even further: line selection is provided by the mask, and well-resolved element channels are formed on the PDA. But more importantly, this direct reader is easily reprogrammable. A new set of lines and /or elements can be put in the spectrometer simply by replacing the mask.

4.3 Characterization of Dual-Mode Torch for Solution Analysis

A “super solution” specified by Leco was used to verify the instrument performance. It includes Zn, Cd, Al Cu and Mg and the concentration of each element is listed in the Table 4.1. The mask used for the super solution analysis is MEM6. The

Element	Original	1:5 Dilution	1:25 Dilution	1:50 Dilution
Zn	100	20	4	2
Cd	50	10	2	1
Al	50	10	2	1
Cu	5	1	0.2	0.1
Mg	0.5	0.1	0.02	0.01

Table 4.1 Metal concentrations in super solution and its series dilution

spectral information for the mask is listed in the Table 4.2. Note that a Mn line (257.610 nm) is listed in the table, but the Zn line (213.856 nm, Pixel 528) and Mn line (Pixel 534) are too close to each other. There is spectral overlap based on the criteria of 20 pixels. Therefore, Mn is not included in the super solution. The buddy line is a spectral leak of the same wavelength but an adjacent order.

A detailed diagram of the dual-mode torch was presented in Figure 3.5 of Chapter 3. This torch provides a convenient feature for solution analysis on the DSI-ICP set-up. The Leco torch box provides two sets of the adjustment to set observation height. One is a lateral adjustment and the other is a vertical adjustment. Both adjustments are done manually with a dial box. These functions are designed for selecting the best observation height. Many of the modern instruments employ a motorized mirror to scan the plasma automatically in order to get the best observation height. The lateral scan of the plasma done here is different than the scan on the original Leco torch set-up. Figure 3.7 in Chapter 3 gives an overall diagram of the DSI set-up. The torch holder can be adjusted laterally. However, the entire torch does not move parallel as the bottom of the torch (central tube) is fixed on the shutter. Therefore, a lateral scan was more like an arc scan. The function of the cap in the central tube is to narrow the central channel. The open tube in the middle is about 2 mm in diameter. This is a bit larger than the size of the orifice on a normal Fassel torch injection tube. Therefore, the lateral scan of the plasma on this torch is wide as shown in Figure 4.2. The maximum intensity was in the middle of the torch.

A vertical scan is not possible in this DSI set up as the bottom of the torch is fixed on the shutter. Therefore, the viewing height is fixed depending on the length of the torch. Three different lengths of torches were tried in order to get a signal sensitivity similar to the normal Leco set-up. A spectrum of the super solution with the normal Leco torch is shown in Figure 4.3 (a). A spectrum with the dual-mode torch is shown in Figure 4.3 (b). The response of each line and the peak ratios were identical. The dual-mode torch provides the same response as the original torch. The observation height in the plasma with this torch was 12 mm above the top load coil. The same torch was also used for the DSI work.

Line	Wavelength	Label	Position	RLD	Pixel	Conflicting Line
1	213.856	Zn	13.208	1.498	528	6
2	226.502	Cd	10.290	1.588	412	
3	226.502	buddy	24.564	1.582	983	
4	228.802	Cd	17.683	1.601	707	7
5	228.802	buddy	3.293	1.607	132	9
6	257.610	Mn	13.357	1.804	534	1
7	279.553	Mg	18.083	1.956	723	4
8	279.553	buddy	0.504	1.965	20	
9	324.754	Cu	2.839	2.281	114	5
10	324.754	buddy	23.348	2.168	934	
11	396.152	Al	11.816	2.776	473	

Table 4.2 MEM 6 Wavelength positions on camera

Comments: Element lines used for super standard mask
Wavelength(nm), Position (nm), RLD (pm/pixel)

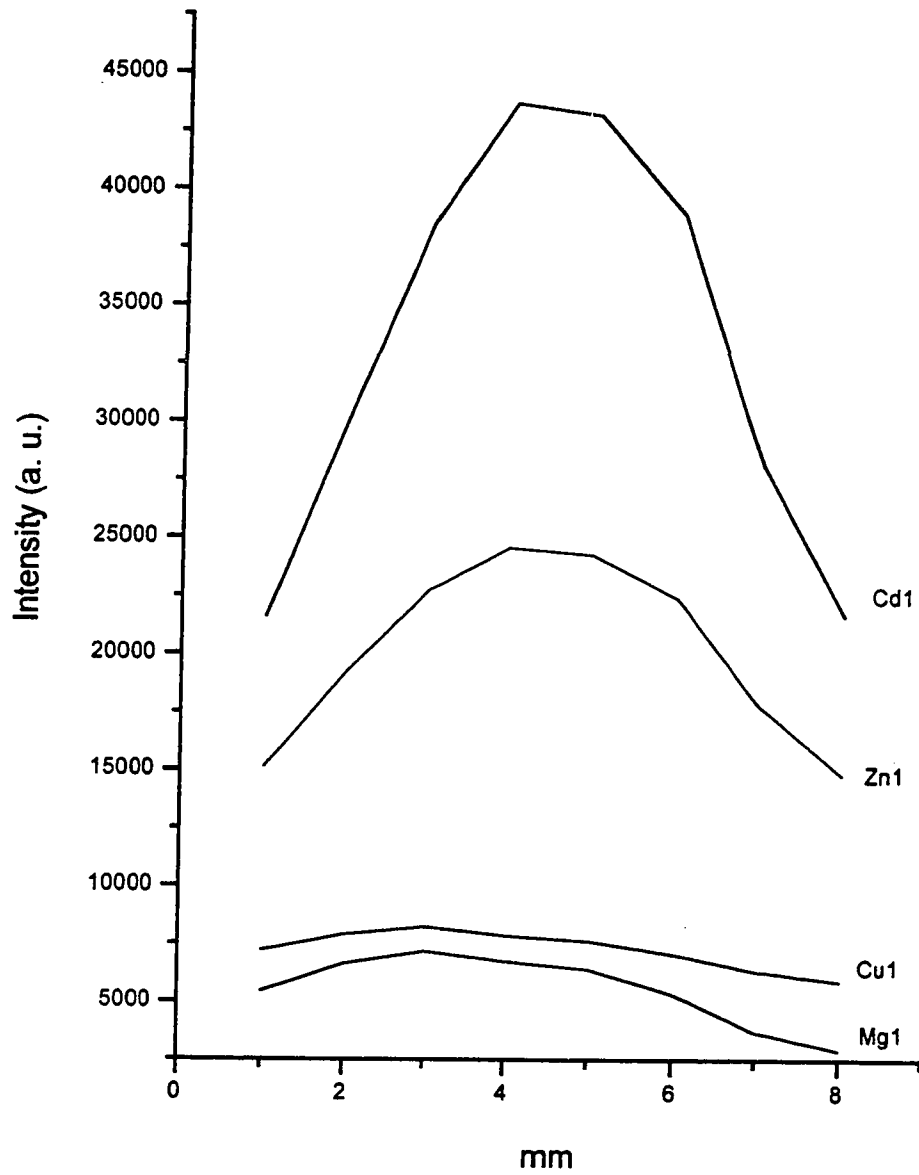


Figure 4.2 Lateral scan of ICP torch

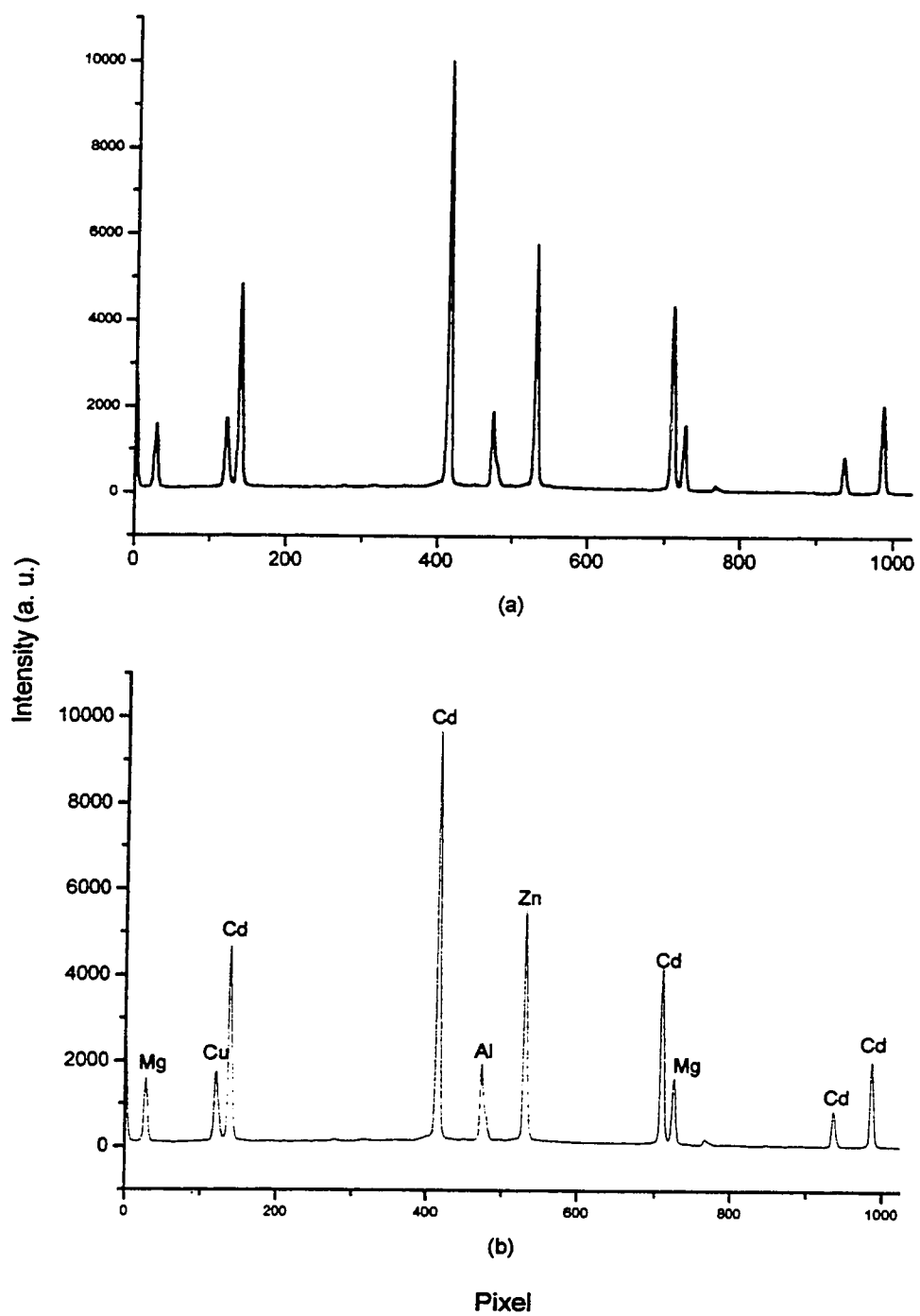


Figure 4.3 (a) Spectrum of super solution: original LECO ICP torch
(b) Spectrum of super solution: dual-mode torch

The inconvenience of the vertical and lateral adjustment in this set-up could be overcome by using a computer controlled entrance mirror for selecting the best viewing position in the plasma. Such a set-up for the Leeman instrument was described in Figure 2.3 of Chapter 2. The torch position is fixed. The entrance mirror scans the plasma image along x-y axes to search for the strongest intensity of an analytical line. This would make the initial characterization work much easier.

Another test was done to find if the cap on the dual-mode torch causes any memory effect. The time required for the signal from the plasma to rise to a steady state and then return to background level after completion of the aspiration of a sample is very dependent on features of the spray chamber and the cap on the central tube in this case. The rise time, known as the wash-in time, is defined as the period to achieve 97% of the steady-state signal from the background signal. The fall time, known as the washout time, is defined as the time interval required to reduce the steady-state signal to 0.1%. The experiment result is shown in the Figure 4.4. The sample wash-in time is about 60 seconds. This was longer than usual 30 seconds take up time on the normal torch. The 1 cm long narrow tube in the cap might delay the aerosol. This suggested that the length of the cap could be cut short to improve the take up time. The washout time was about 90 seconds that was also longer than the 40 seconds on the normal torch. A reason for this could be the side mounted spray chamber. The shape and position of the baffles and aerosol exit tube were not optimized for the side mounting.

Precision is a critical parameter of any analytical determination. It is a measure of repeatability and its magnitude depends on the time scale of measurement. If repeated integrations are made over the shortest possible time scale, with unbroken nebulization of the solution, the highest precision is obtained. If repeated integrations are made over the normally much longer time interval between calibration adjustments, then a more realistic value of precision is obtained. An RSD of 1-2 % is obtained for most analytes measured with modern ICP-AES instrument. An instrument stability test was also done here for a period of 30 minutes. The RSDs of all five elements were within 1.02%. This is shown in Figure 4.5. Ten repeated measurements were performed during this period. This clearly indicated that the dual-mode torch with the side mounted spray chamber was

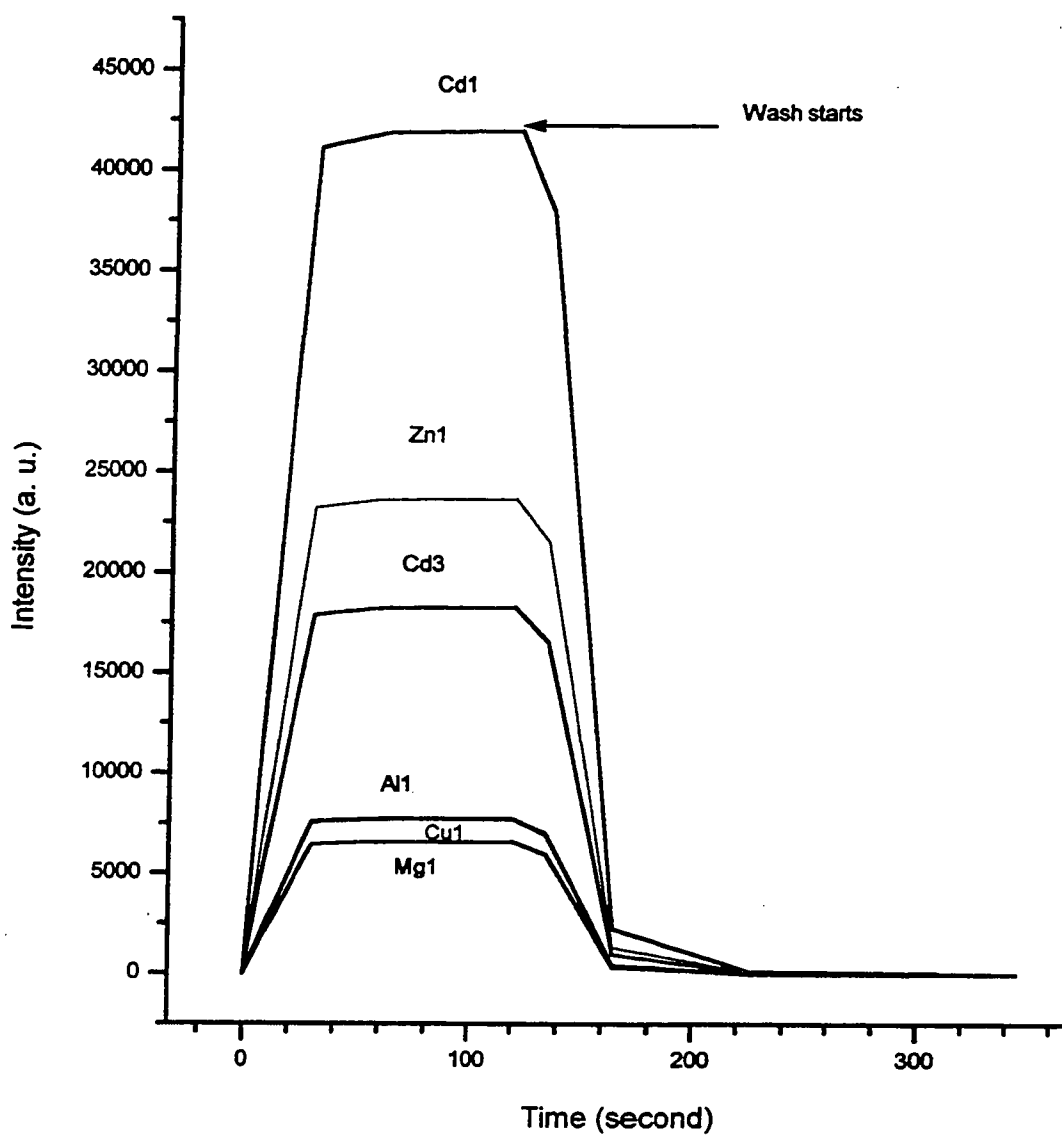


Figure 4.4 Sample take up time and wash time for solution nebulization

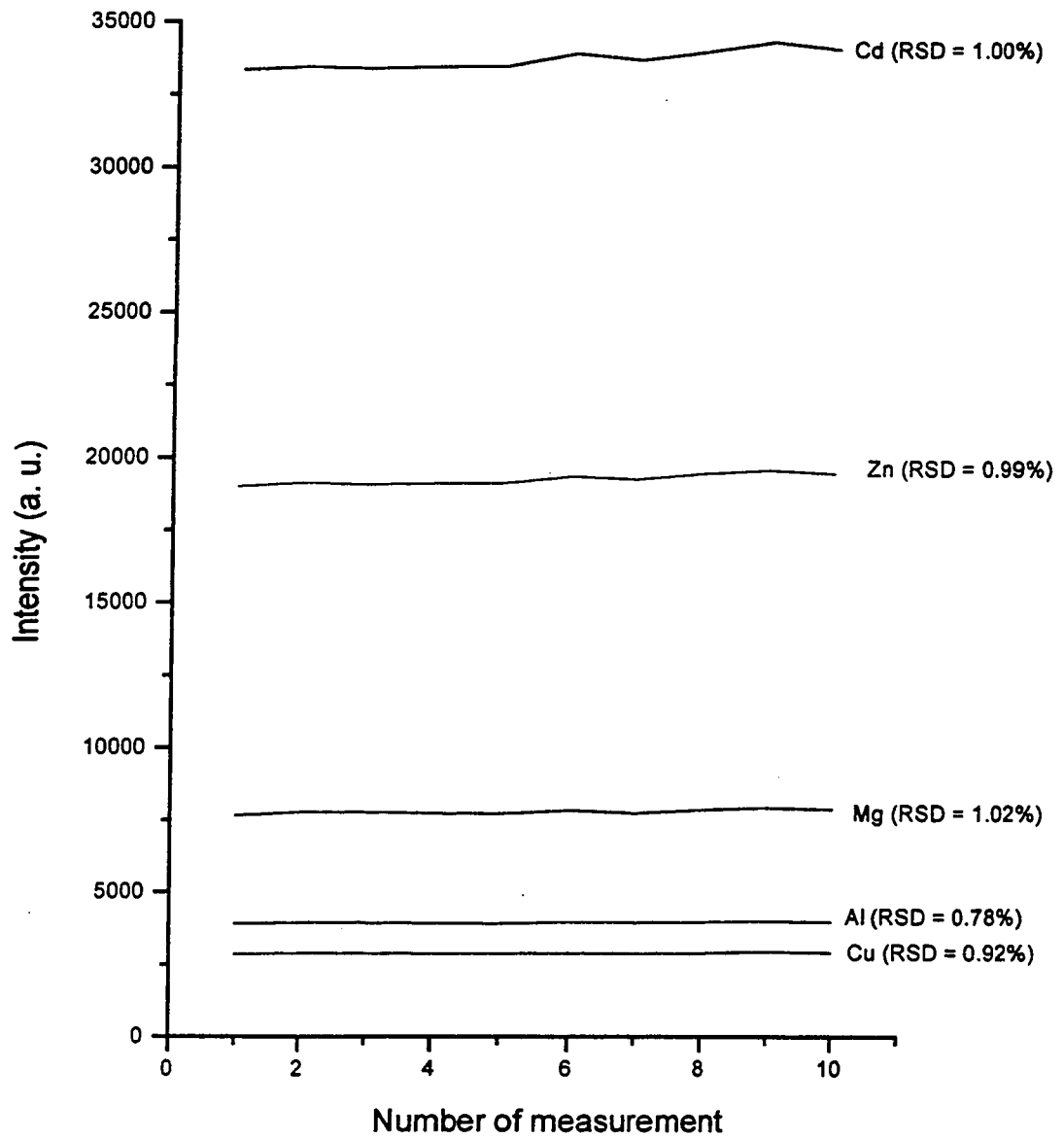


Figure 4.5 Signal stability of Leco ICP with a dual-mode torch

applicable to routine usage.

4.4 Characterization of Dual-Mode Torch for DSI

4.41 DSI Ar -O₂ Mixed Gas Plasma

As mentioned in the first chapter, this study started out as a continuation of the O₂-Ar mixed gas plasma study [3,4]. A key limitation of graphite cup DSI devices for ICP-AES is carbide formation. Because a broad range of elements form carbides, the analytical figures-of-merit of the device are impaired, its applicability is limited to volatile elements and the multi-element capability of the ICP is nullified. This may be solved with the addition of oxygen to the coolant gas of the ICP.

However, it was soon found out that the LECO torch box (i.e. electronics) could not handle much addition of O₂ to the Ar stream. It could tolerate only up to 5% O₂. More than 5% O₂ would extinguish the plasma due to an in-balance of the matching system. It was worse for DSI where the maximum amount of O₂ that could be added to the plasma was 1.5% without extinguishing the plasma during the insertion. Many attempts were tried to solve the problem, but none of them were successful. One of the attempts was to consume the graphite cup wall during the pre-burn period to make it very thin so that it could be consumed during the final sample analysis. However, 1.5% O₂ only made holes in the cup, and the process was not consistent.

Another approach was to use multiple insertions. The results for flyash are shown in the Figure 4.6. After three 90 second insertions in the 1.5 % O₂ plasma, some Ni and Cr still remained in the probe. Combining the peak areas from multiple insertions did not provide useful results.

4.42 Chemical Modifier

With a graphite cup based direct sample insertion device poor results were obtained for refractory and carbide forming elements such as Al, Ca, Cr and Ni. Chemical modifiers (i.e. halides) have been used to enhance volatilization. The concept of chemical

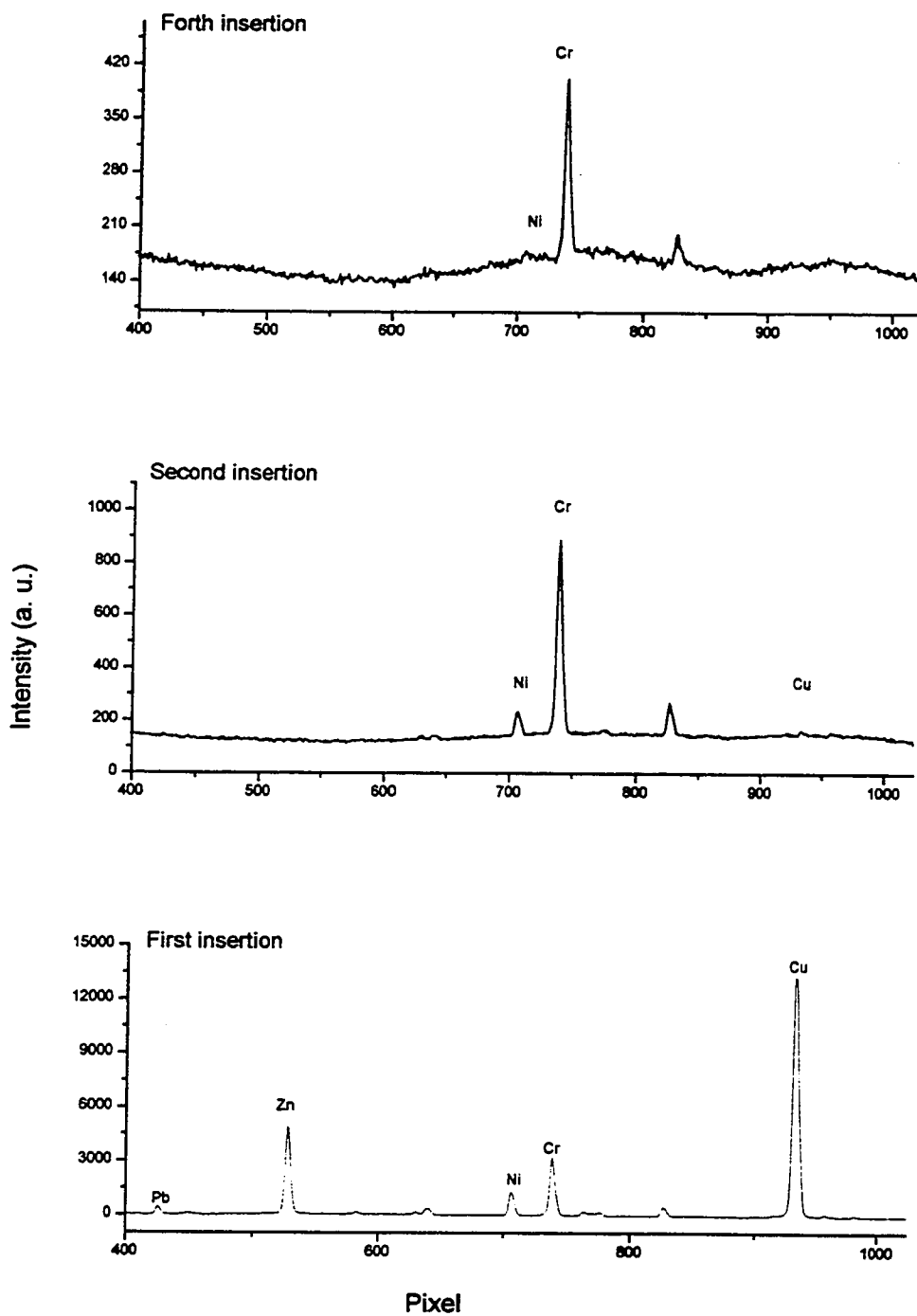


Figure 4.6 Pb, Zn, Ni Cr, and Cu spectrum of flyash in Ar-O₂ mix gas plasma

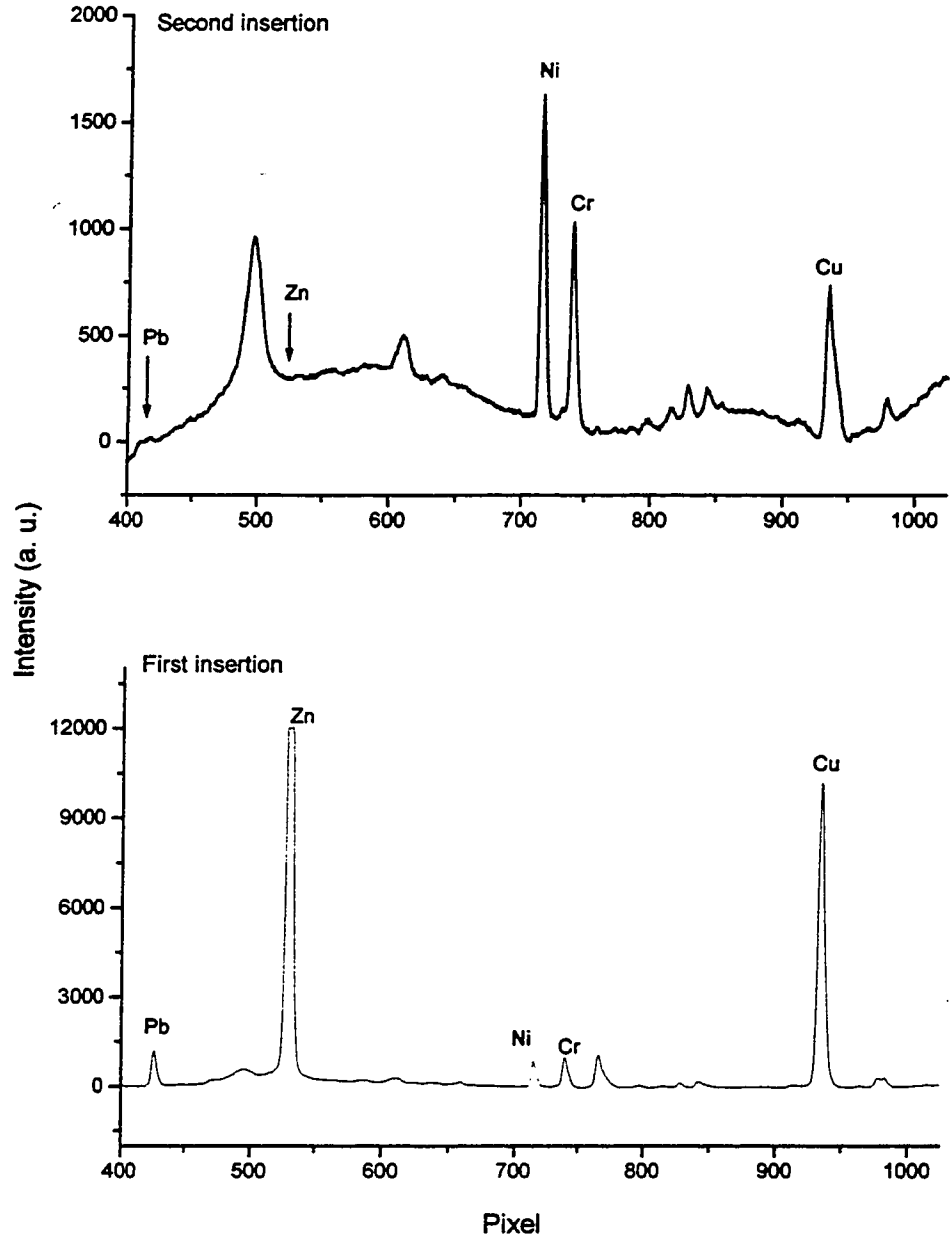


Figure 4.7 NaF effect on SRM 2704 Buffalo River Sediment in Ar plasma

modification is not new, it has been used for a number of years in both ETV techniques and in d.c. arc spectrometry and the approaches are easily transferable to DSI devices [5].

This was also tried on the SRM Buffalo River Sediment sample. A 20 μL aliquot of 1% NaF was added to the sample. Then it was dried under the IR lamp. The spectrum of the first and second insertions are shown in Figure 4.7. The effect was not as good as expected. Ni, Cr and Cu were certainly left after the first insertion even with the addition of NaF modifier.

4.43 DSI Ar Plasma

After the failure of the O_2 -Ar mixed gas plasma and the chemical modifier, the focus of the study was turned to volatile element determinations. Several improvements were made in this experiment after reviewing the information on DSI-ICP operation parameters and sample matrices in the literature [6-11]. First, the calibration range used in these experiments is smaller than most work in the literature. The emphasis is on linearity and accuracy rather than a large calibration range for covering unknowns. Second, a deep and smaller sample probe was used. A small probe disturbs the plasma the least and the probe heats faster. A deep cup prevents sample loss due to sputtering and overflowing during ashing. Third, partially matched sample matrices were used for calibration solutions. Matching each and every sample type is not feasible, but adding three hundred ppm of sodium and potassium to the multi element calibration solution provided a close simulation to the actual sample composition. Fourth, samples were externally dried and ashing time was relatively short (less than 30 seconds) which minimized analyte loss. The ashing position was 22 mm below the top of the load coil which positioned the cup 3 mm below the bottom of the plasma. The atomization position was slightly higher than the top of the load coil, about 1 mm. Lastly, smaller sample weights (1-5 mg) were used thorough out the study.

Figure 4.8 shows the spectra of first and second insertions of a 10 ppm multi-element standard solution. Pb, Zn and Cu have acceptable vaporization behavior, Cr and Ni do not. The mask used for this analysis was MEM 24. The technical information for

MEM24 is listed in Table 4.3. There are over twenty slots cut on the mask. Five of them were left open for the analysis and the rest of them were covered to avoid interferences. The ICP operating conditions are listed in the Table 4.4.

Figure 4.9 shows the spectra for first and second insertions of a flyash sample. Copper was almost, but not complete by vaporized in this case. Clearly, vaporization process should be checked for each sample.

A lateral scan of the DSI-ICP plasma was done by using the super solution (10 μ L of 1/5 original concentration). The plots are shown in Figure 4.10. The maximum intensities were not in the middle, but 1 to 2 mm off center. The electrode usually leans to the side of the central tube wall during insertion. Therefore, the observation position was fixed off center 1 mm to get the maximum signal.

The effect of power on the DSI signal is shown in Figure 4.11. The Maximum power specified by Leco was 2.0 kw. However, power starts to fluctuate above 1.9 kw. The power was set at 1.5 kw for this study. The plasma coil would over heat if the power was set above 1.5 kw after operated for several hours. It could be that the size of the radiator for the water coolant is too small and not efficient enough.

Calibration curves for, Cu, Cd and Zn are shown in Figure 4.12. The spectra for these calibration solutions are shown in Figure 4.13. The Mg peak in the spectrum of the 1/50 dilution was higher than it should be. This could be caused by contamination in the solution, as the Mg concentration was 0.01 ppm. The correlation coefficients for these plots (Figure 4.12) were excellent.

Calibration curves for As, Mn and Pb are shown in Figure 4.14. They were obtained from a multi element standard solution with 300 ppm Na and K.

Figures 4.15 and 4.16 show stability results of replicate measurement of solution residues. The RSD values were very typical for the DSI.

Line	Wavelength (nm)	Label	Position (mm)	RLD (pm/pixel)	Pixel	Conflicting Line
1	213.856	Zn	13.208	1.498	528	16, 17
2	220.353	Pb	10.619	1.545	425	4, 10, 31
3	220.353	buddy	24.504	1.539	980	5
4	226.502	Cd	10.290	1.588	412	2, 10
5	226.502	buddy	24.564	1.582	983	3
6	228.807	CdAs	17.761	1.601	710	8, 20, 33
7	228.807	buddy	3.371	1.607	135	9, 23, 32
8	231.604	Ni	17.688	1.620	708	6, 20, 33
9	231.604	buddy	3.122	1.627	125	7, 23, 27, 32
10	234.984	As	10.645	1.647	426	2, 4, 31
11	234.984	buddy	25.452	1.640	1018	13
12	251.611	Si	9.469	1.764	379	
13	251.611	buddy	25.330	1.757	1013	11
14	253.652	Hg	6.441	1.780	258	
15	253.652	buddy	22.444	1.772	898	
16	257.610	Mn	13.357	1.804	534	1, 17
17	259.940	Fe	12.898	1.821	516	1, 16
18	267.710	Cr	18.415	1.873	737	20
19	267.710	buddy	1.582	1.881	63	
20	279.553	Mg	18.083	1.956	723	6, 8, 18
21	279.553	buddy	0.504	1.965	20	30
22	283.999	Sn	21.266	1.985	851	29, 35
23	283.999	buddy	3.423	1.995	137	7, 9, 32
24	303.936	In	4.407	2.134	176	
25	303.936	buddy	23.593	2.123	944	28
26	317.933	Ca	8.184	2.230	327	
27	324.754	Cu	2.839	2.281	114	9, 32
28	324.754	buddy	23.348	2.268	934	25
29	330.237	Na	21.327	2.308	853	22, 35
30	330.237	buddy	0.579	2.322	23	21
31	345.350	Co	11.039	2.421	442	2, 10, 36
32	355.431	Ar	3.238	2.497	130	7, 9, 23, 27
33	361.384	Sc	17.329	2.529	693	6, 8
34	371.030	Y	19.238	2.595	770	
35	383.826	Mg	21.672	2.682	867	22, 29
36	393.366	Ca	11.499	2.757	460	31, 37
37	396.152	Al	11.816	2.776	473	36

Table 4.3 MEM 24 Wavelength positions on camera

Solution Nebulization:	Forward power: 1.5 kw, reflect power: < 1 w Coolant gas: 14 lpm Auxiliary gas: 1.2 lpm Nebulizer pressure: 28 psi Pump speed: 20 RPM, 0.8 ml/min.
Direct Sample Insertion with Ar Plasma:	Forward power: 1.5 kw, reflect power: < 2 w Coolant gas: 18 lpm Auxiliary gas: 1.4 lpm Center gas: 2 lpm
Direct Sample Insertion with Ar -O ₂ Plasma:	Forward power: 1.5 kw, reflect power: < 2 w Coolant gas: 20 lpm, with 1% O ₂ in Ar Auxiliary gas: 1.8 lpm, with 1% O ₂ in Ar Center gas: 2 lpm

Table 4.4 Typical operating conditions of ICP in the experiment

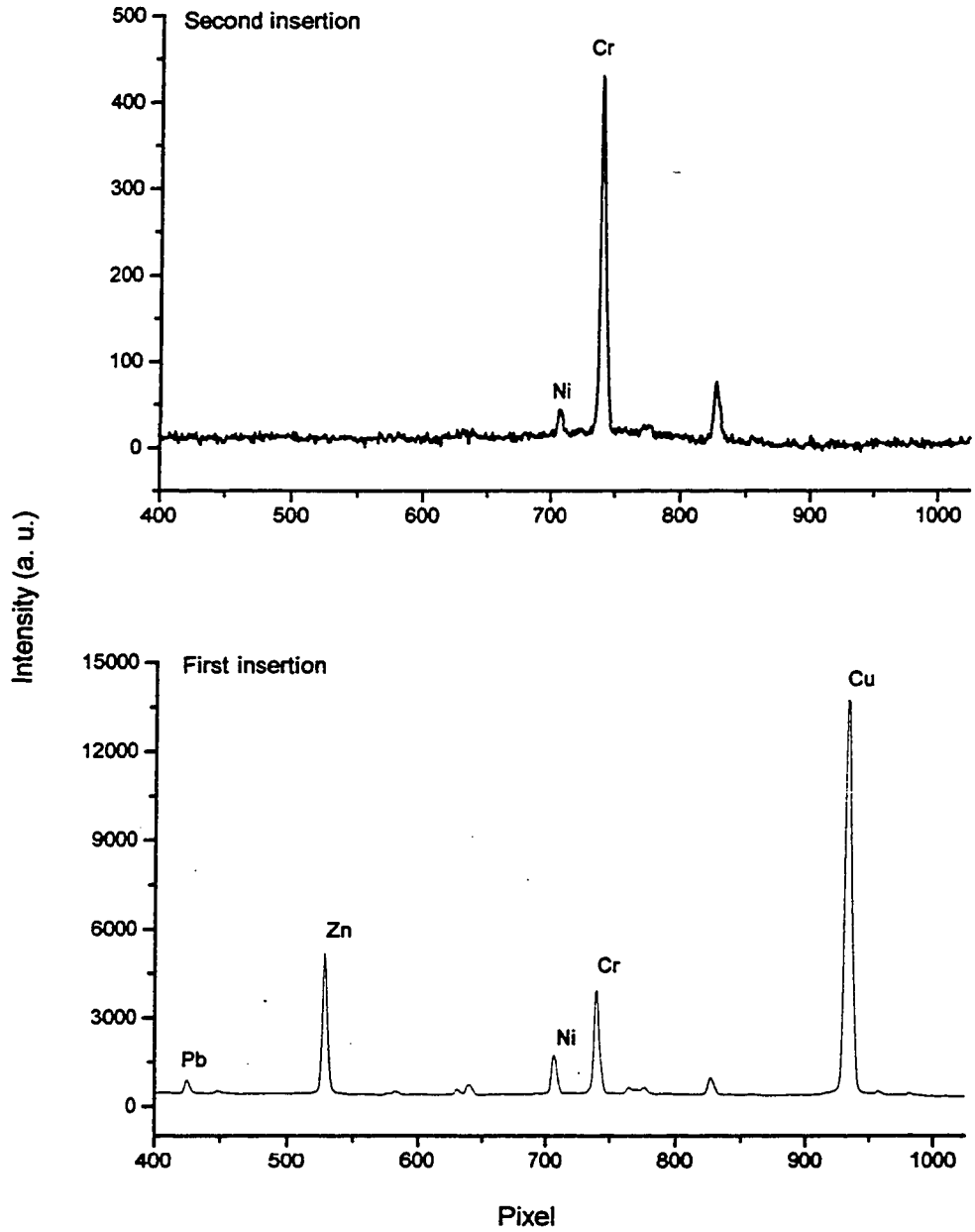


Figure 4.8 Pb, Zn Ni, Cr and Cu spectrum of 10 ppm solution residue in Ar plasma

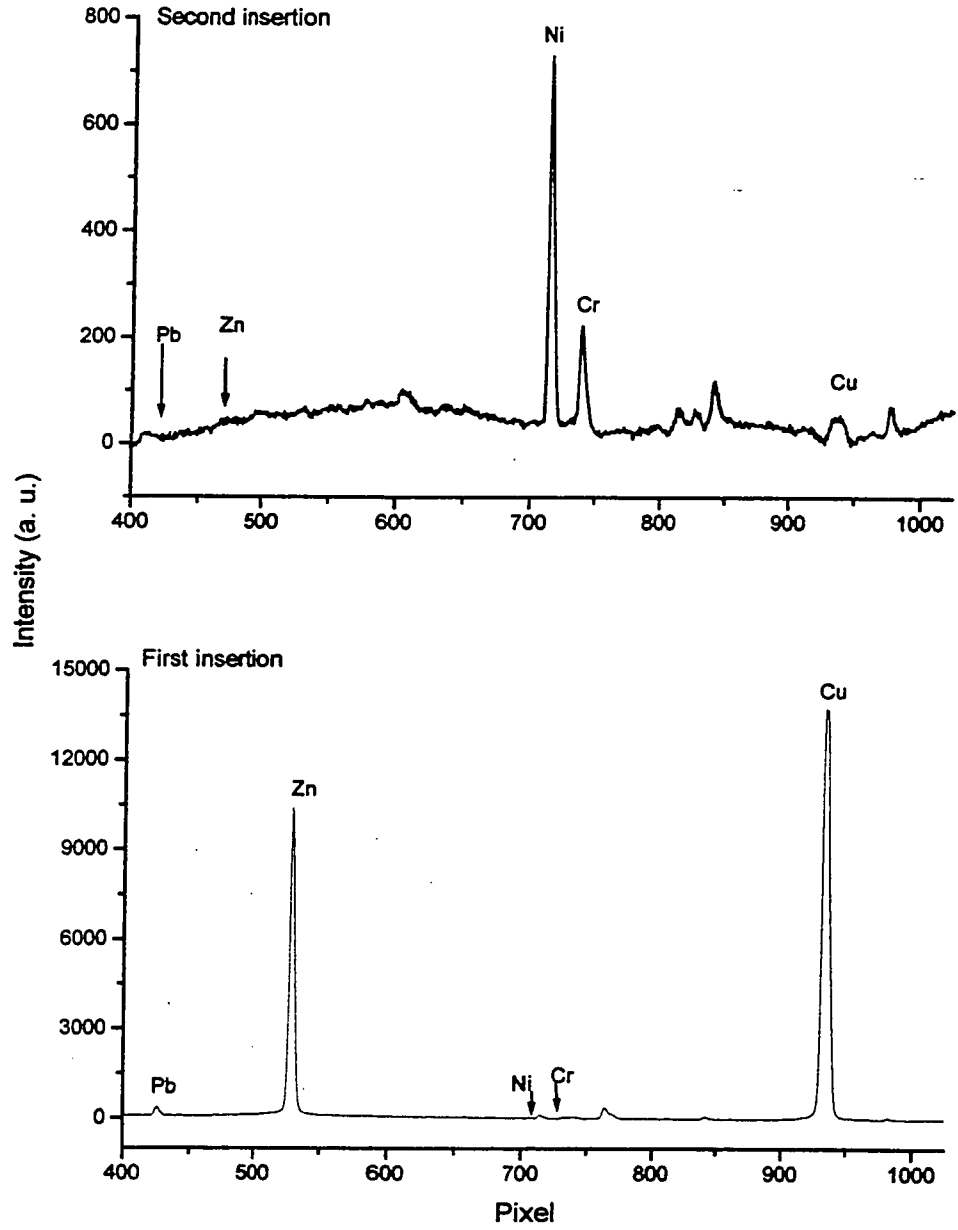


Figure 4.9 Pb, Zn, Ni Cr and Cu spectrum of flyash in Ar plasma

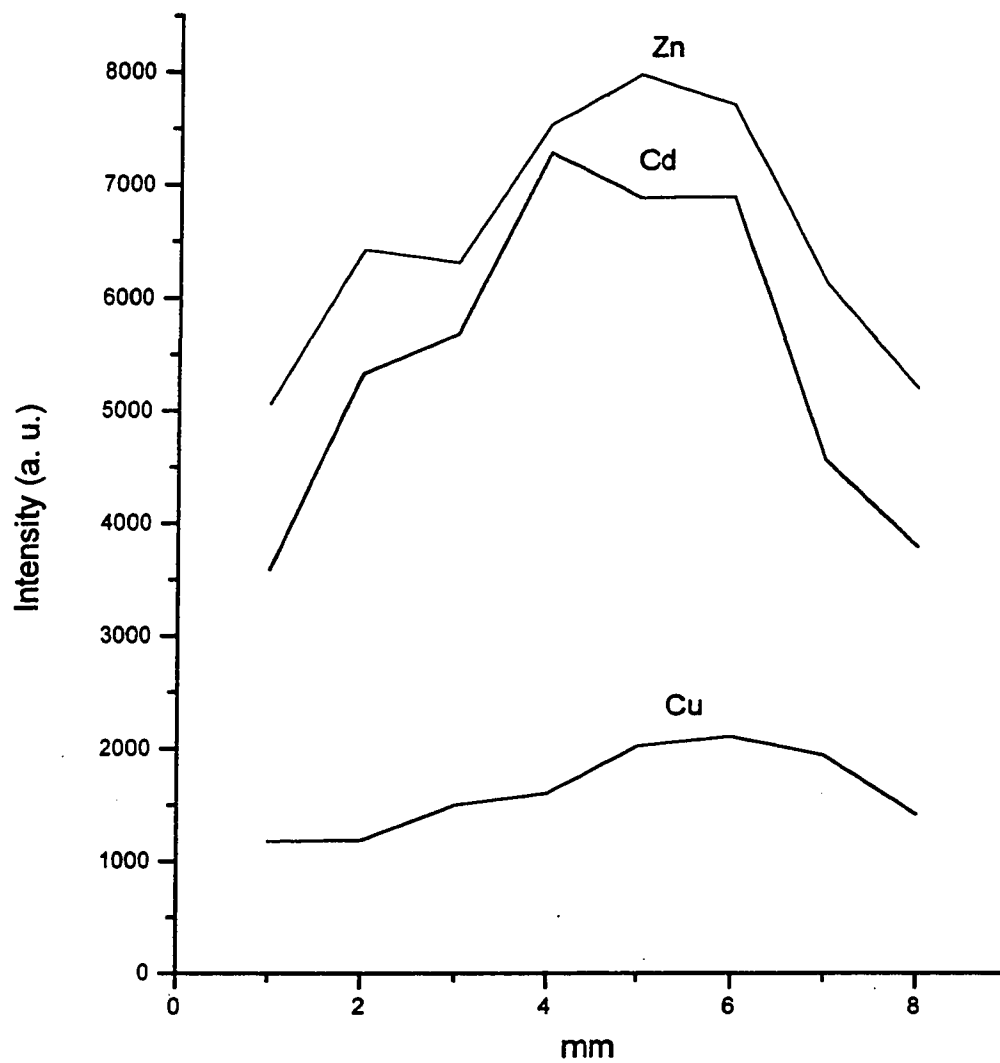


Figure 4.10 Lateral scan of DSI-ICP torch

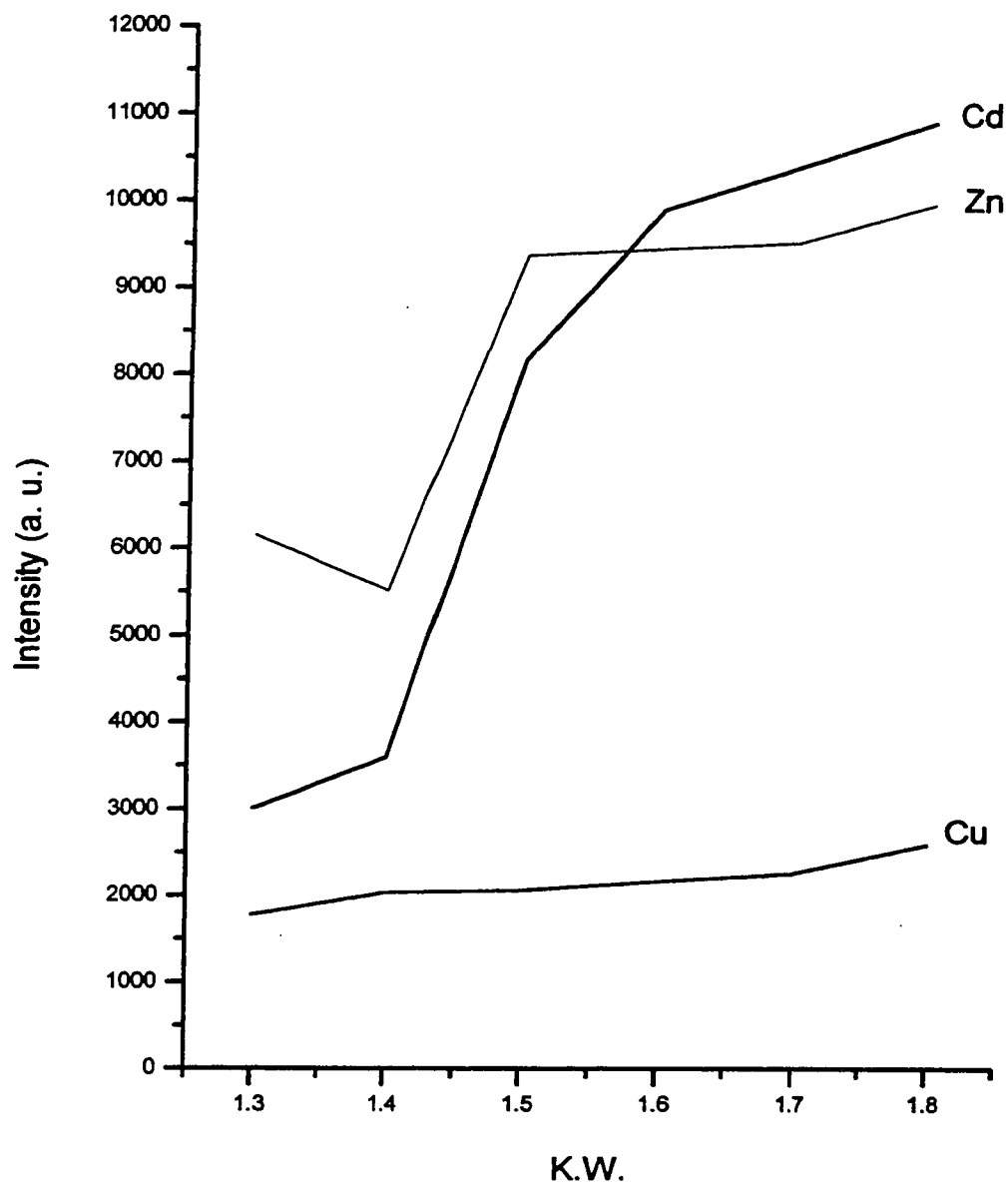


Figure 4.11 Power effect on DSI signal

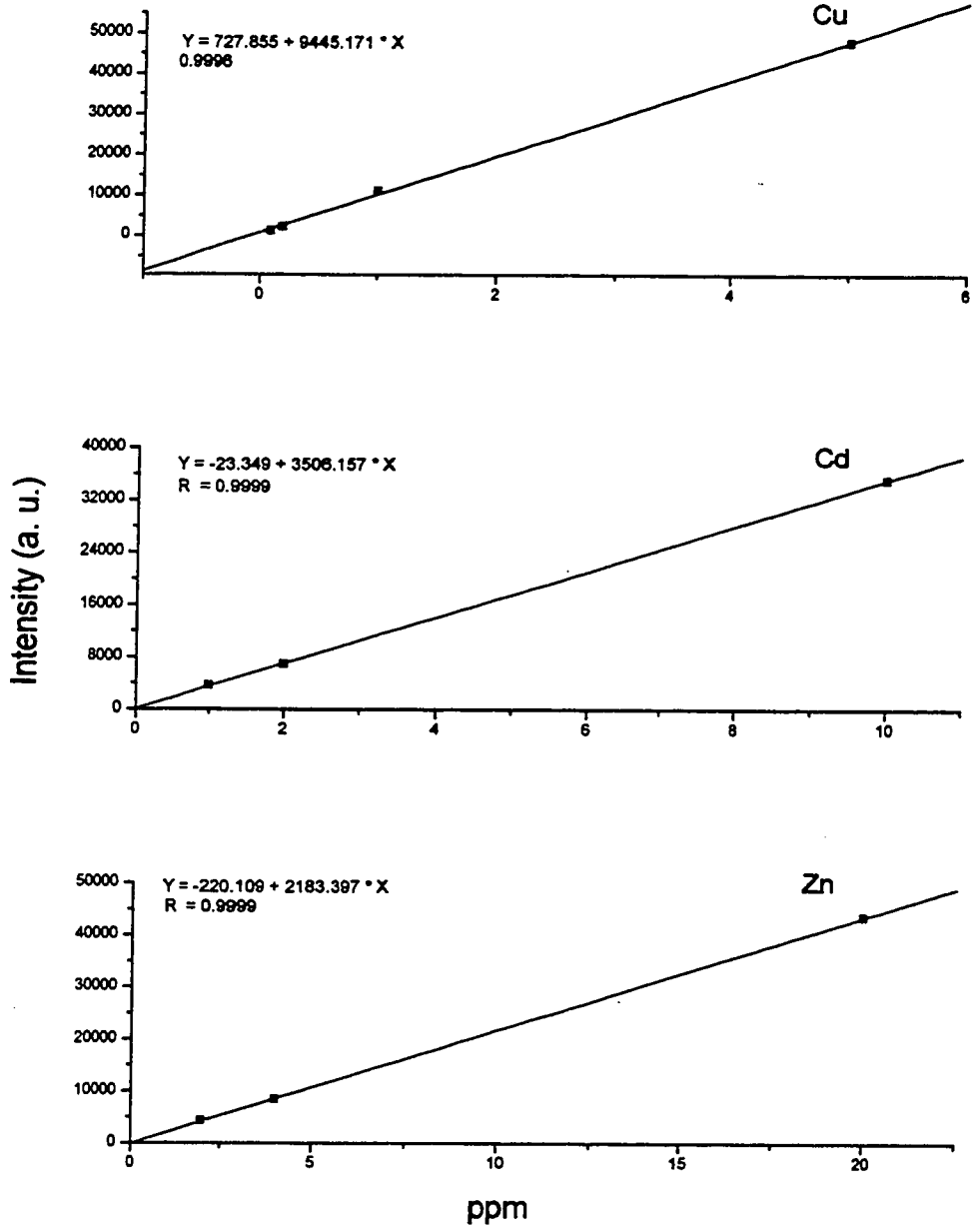


Figure 4.12 Calibration curves for super solution

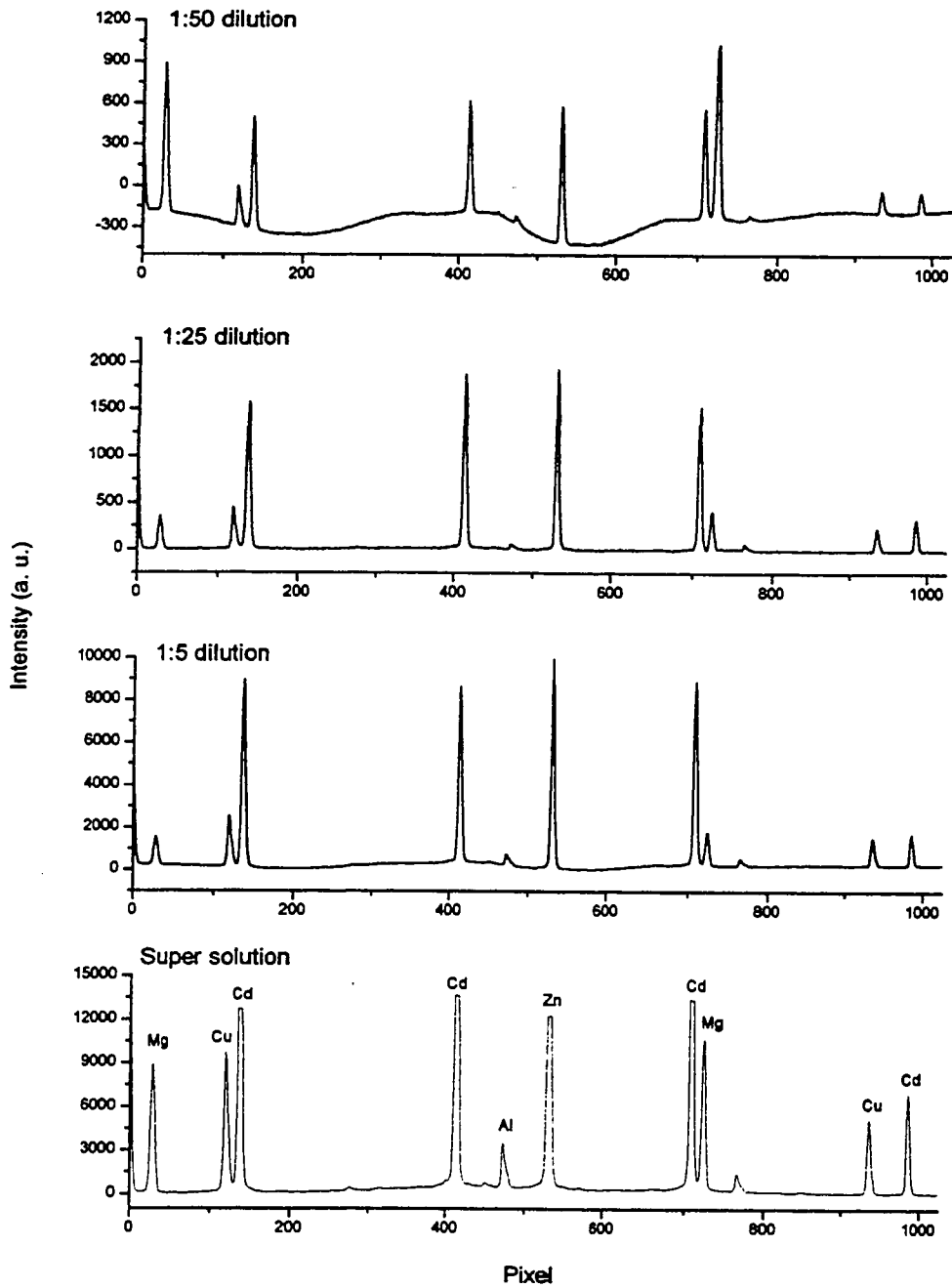


Figure 4.13 Al, Cd, Cu, Mg and Zn spectrum of solution residue at different calibration concentrations

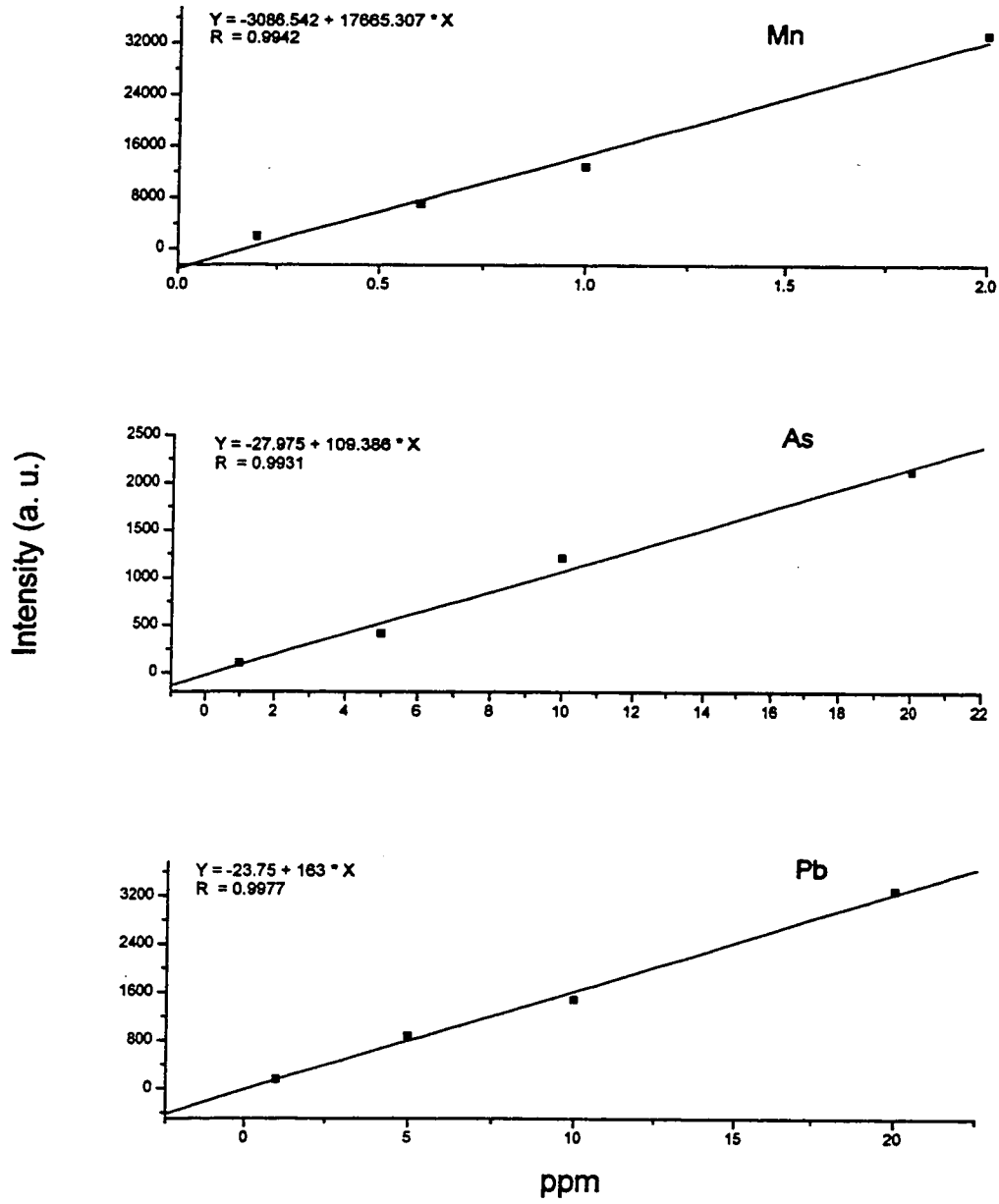


Figure 4.14 Calibration curves for As, Mn and Pb

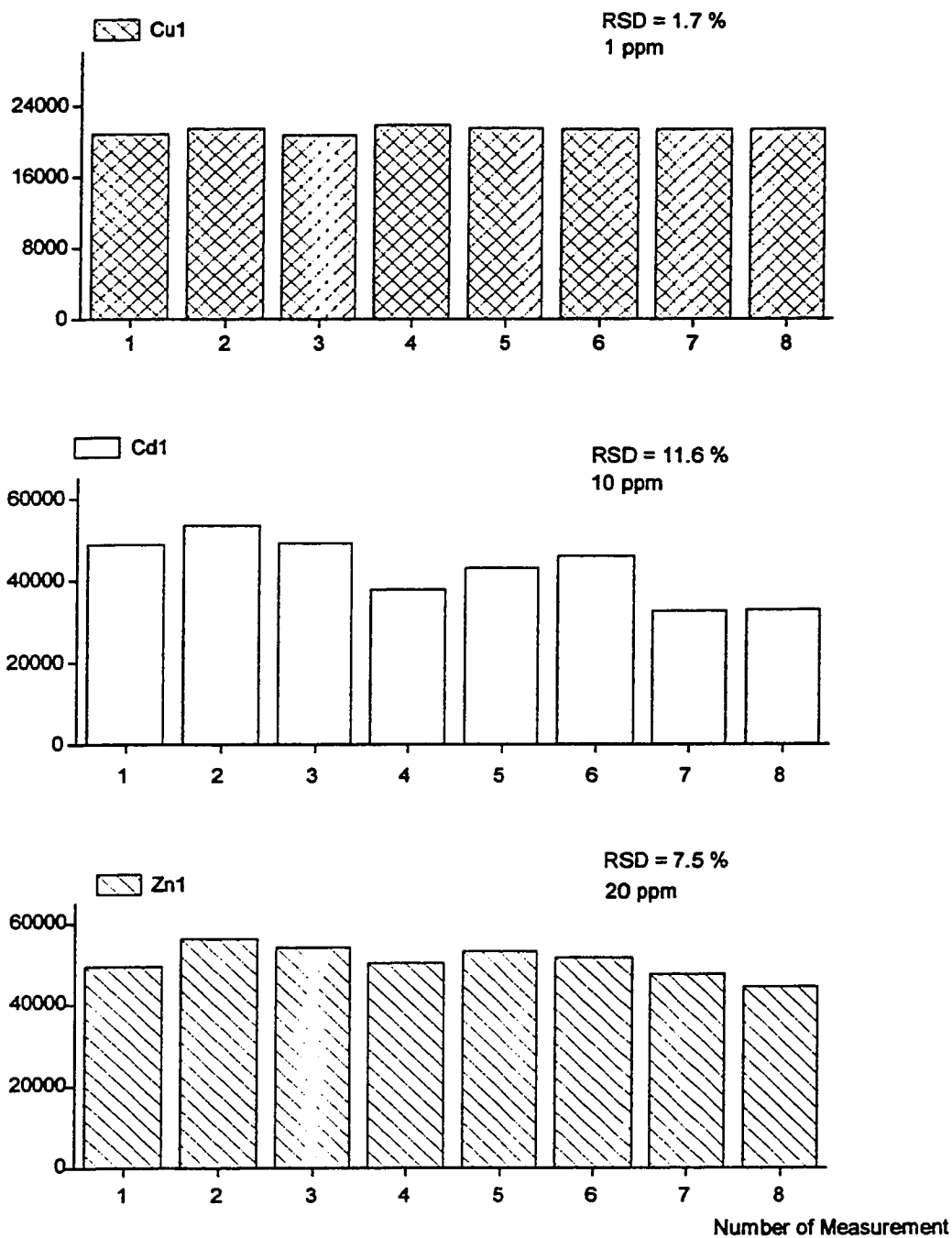


Figure 4.15 Replicate measurement of 1/5 Leco super solution in Ar plasma

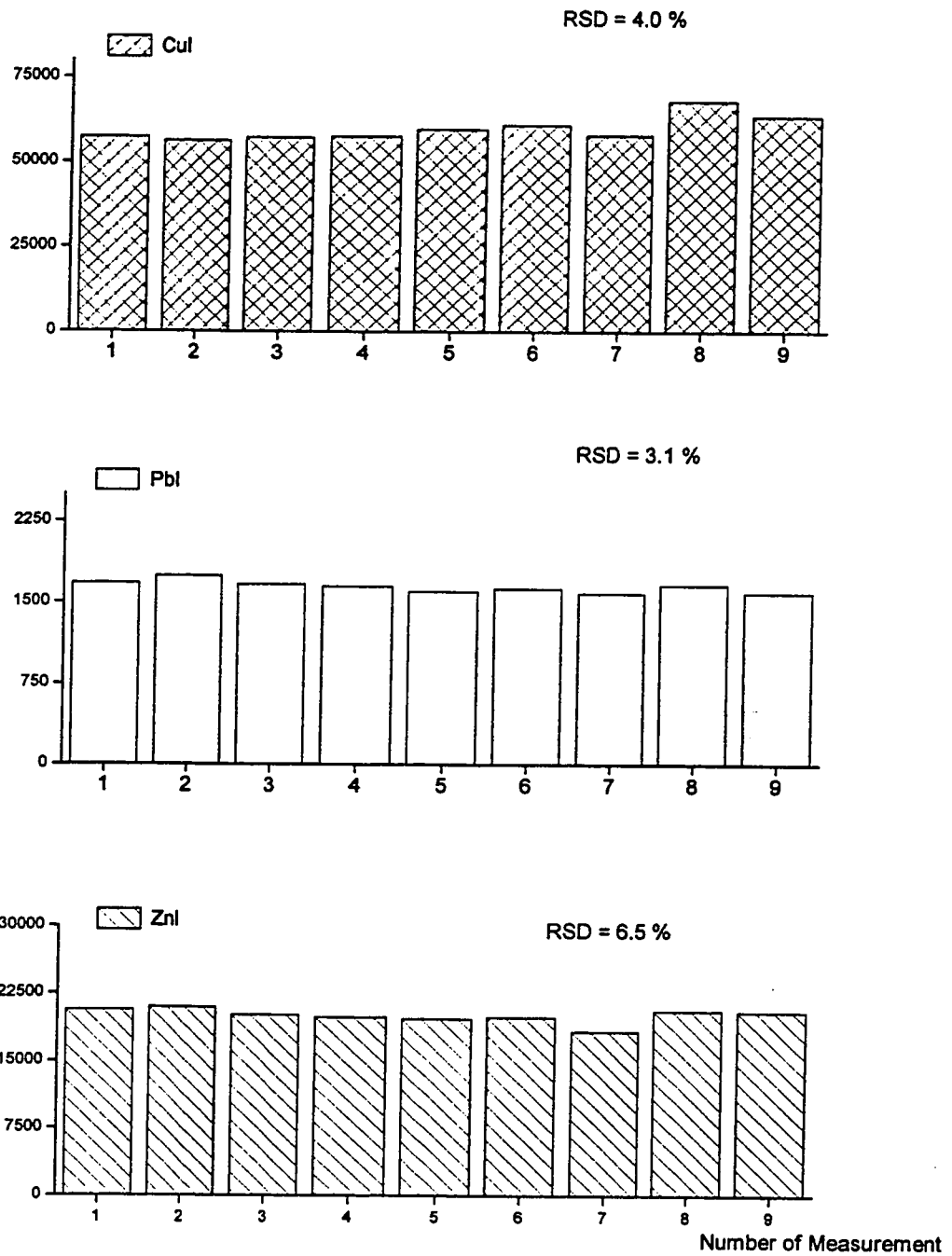


Figure 4.16 Replicate measurement of 10 ppm standard solution in Ar plasma

4.5 Conclusion

The dual mode torch showed excellent performance in terms of analytical stability and sensitivity. It certainly extended the DSI set up to aqueous sample analysis without major instrument modification. Meanwhile, the torch remained applicable to solid sample analysis (DSI). The LECO torch box was not able to handle mixed gas plasmas for the determination of non-volatile or refractory elements. Determination of volatile elements in solution residues showed satisfactory results.

References:

1. G. M. Levy, A. Quaglia, R. E. Lazure and S. W. McGeorge, *Spectrochim. Acta* **42B**, 341(1987).
2. V. Karanassios and G. Horlick, *Appl. Spectrosc.* **40**, 813 (1986).
3. X. R. Liu and G. Horlick, *J. Anal. At. Spectrom.* **9**, 833 (1994).
4. L. S. Ying, MS. Thesis, University of Alberta (1992).
5. V. Karanassios, M. Abdullah and G. Horlick, *Spectrochim. Acta* **45B**, 119 (1990).
6. V. Karanassios and G. Horlick, *Spectrochim. Acta Rev.* **13(2)**, 88 (1990).
7. Y. B. Shao and G. Horlick, *Appl. Spectrosc.* **40**, 386 (1986).
8. V. Karanassios and G. Horlick, *Spectrochim. Acta* **44B**, 1361 (1989).
9. W. T. Chan and G. Horlick, *Appl. Spectrosc.* **44**, 525 (1990).
10. W. E. Pettit and G. Horlick, *Spectrochim. Acta* **41B**, 699 (1986).
11. C. D. Skinner and E. D. Salin, *J. Anal. At. Spectrom.* **12**, 1131 (1997).

Chapter 5

Direct Analysis of NIST Standard Reference Materials by an Automated DSI-ICP

5.1 Introduction

An important characteristic of the DSI technique coupled with the ICP is the ability to use solid standards of substantially differing matrix compositions for calibration. Several studies have reported this feature and suggest a relative insensitivity of the technique to element origin. Calibration curves may be constructed using solid samples of known elemental concentration. Standard reference materials (SRMs) have been used extensively and include NIST coal and botanical SRMs, BAS and NIST nickel alloy SRMs, U.S. Geological Survey (USGS) silicate materials, and SPEX G and SPEX TSAL solid standards (used in dc arc calibration, SPEX Industries, Edison, NJ). In general, calibrations are linear over at least three orders of magnitude

McCleod et al [1] determined volatile elements in Ni base alloys based on calibration with dried solution residues. Abdullah and Haraguchi [2-3] determined volatile elements in coals and botanicals, and Horlick et al. [4-7] did a number of experiments on volatile elements in different sample matrices. Broekaert et al [8] determined volatile elements in aluminum oxide. In every case, it was found that volatile elements could be determined at levels down to a few parts per million ($\mu\text{g/g}$), and that matrix effects were not a serious problem. The refractory elements were found to be a problem for an Ar plasma, but were successfully determined using O_2 mixed gas plasmas [9,10].

As mentioned in Chapter 4, the current system is not able to handle a high percentage O_2 - Ar mixed gas for the ICP. As for the preliminary studies in the last chapter, the calibration range used in these experiments is smaller than most work done in the literature. The emphasis is on the linearity and accuracy rather than a large calibration range for covering unknowns. Second, a deep and smaller sample probe was used. A small probe disturbs the plasma the least and the probe heats faster. A deep cup prevents sample loss due to sputtering during ashing. Third, partially matched sample matrices

were used for calibration solutions. Matching each and every sample type is not feasible. But adding several hundred ppm of sodium and potassium to the multi element calibration solution provided a simulation of the actual sample composition. Fourth, samples were dried externally and ashing time was relatively short (less than 30 seconds). Finally, a small sample weight (1-5 mg) was used throughout the study. This is only applicable to samples which are adequately homogeneous.

Standard Reference Materials play an important role in Analytical Chemistry. They are used to evaluate the accuracy of new analytical methods and to maintain the quality of established measurement procedures. Thus they were used here to validate the volatile element determinations by this automated DSI-ICP system. Reference materials are well-characterized, stable, homogeneous materials having one or more physical or chemical properties determined within stated measurement uncertainty. These properties are sufficiently well-established to be used for the calibration of an apparatus or the assessment of a measurement method at specified quantity. Four types of the sample matrices were used in this study. They are soil, ash, food and leaves.

In recent years, many new standard reference materials have been certified at NIST. Combined with some existing SRMs in our laboratory, there are quite a number of materials that can be used in this study. The concentration range of elements for these materials is wider than a few years ago, which is also an advantage for the study.

Spectrum collection and data processing were already described in Chapter 4. The absence of a cross-dispersing element means that many orders are incident on the detector simultaneously. Thus, a straight forward wavelength axis cannot be defined. As a consequence, the ordinate of all spectra shown in this work is labeled as diode number (pixel). Due to the inherently integrating nature of the PDA detector, optical emission spectral intensity is integrated directly on the detector. With the measurement electronic sub-system used in this work, information about analyte emission temporal behavior is lost. This integrated signal (i.e. peak area) is proportional to spectral intensity at the spectral line of interest and, as a consequence, to concentration.

The integrated spectral intensities, initially stored in the controlling microcomputer using the manufacturer's file format, were processed off-line. Spectra

were transferred to an IBM PC-compatible system where they were converted to tab-delimited ASCII using Microsoft Excel.

5.2 Soil and Ash

5.21 Background

There were ten NIST SRMs used in this part of the study. Eight of them were certified within last five years. Two of them are already exhausted and are no longer available from NIST. These SRMs cover a wide range of concentrations. They are ideal samples for validation of DSI-ICP. The following paragraphs provide some basic information on these materials.

Environmental pollution from coal-burning can occur through direct stack emissions, as well as from the leaching of toxic metals from ash which is disposed of in landfills. NIST SRM 1633b is a well characterized, certified reference material[11]. It represents the fly ash generated by burning bituminous Pennsylvania and West Virginia (Appalachian Range) coals, and is a composite, rather than the ash which would result from burning any one specific coal. Prior to bottling, the material was sieved through a normal sieve opening of 90 μm (170 mesh) and then blended to assure homogeneity. Homogeneity testing was accomplished using instrumental neutron activation analysis and X-ray fluorescence.

This material is intended for quality assurance purposes in evaluating the analytical methods used for the determination of constituent elements in coal fly ash or in materials with similar matrices. It has been certified for 23 major, minor and trace elements using ten different analytical techniques. For an element to be certified in a NIST SRM, its concentration is usually determined by at least two independent analytical techniques. The concentrations of an additional 24 elements are provided for "information only" purposes in the new fly ash.

SRMs 2689, 2690, and 2691 [12] are intended for use in the evaluation of analytical methods and techniques used for the classification of coal fly ash and for the

determination of constituent elements in coal fly ash or materials with a similar matrix. Each SRM consists of 3 hermetically sealed glass vials of fly ash pulverized to less than 145 μm particle size and blended to a high degree of homogeneity. Each vial contains 10 g of fly ash.

The fly ashes were obtained from three different coal-fired power plants and are products of western Kentucky, Colorado, and Wyoming coals. The three different fly ash SRMs were on an “as received” basis chosen to cover a wide range of chemical and mineralogical compositions. Each fly ash was size classified using a Vortex C-13 air classifier and particles greater than 45 μm were removed for grinding. The coarse material consisted mostly of quartz and partially burned fragments. Once ground to pass a 145 μm (No. 100) sieve, this material was blended back into the rest of the fly ash, and the entire lot of material was homogenized in a ribbon blender, hermetically sealed in glass vials, and packaged. The packaging operations were performed in a temperature and humidity controlled atmosphere to minimize moisture differences between samples.

Homogeneity Testing: Stratified random selections of vials from each SRM were made and analyzed using X-ray fluorescence. Each vial was opened and two aliquots of 0.5 g were taken and fused into discs for XRF analyses. The duplicates of individual vials made a total of 50 g discs for each fly ash. For the elements measured (Al, Ca, Fe, and Si), no evidence of sample heterogeneity was observed.

The three new soil SRMs (2709, 2710, 2711) are intended primarily for use in the analysis of soil, sediments, or other similar materials [13-15]. The US Geological Survey (USGS), under contract to the NIST, collected and processed all three materials. The material was spread on 30.5cm \times 61 cm polyethylene-lined drying trays in an air drying oven and dried for three days at room temperature. The material was then passed over a vibrating 2 mm screen to remove plant material, rocks, and large chunks of aggregated soil. Material remaining on the screen was deaggregated and rescreened. The combined material passing the screen was ground in a ball mill to pass a 74 μm screen and blended for 24 h. Twenty grab samples were taken and measured for the major oxides using x-ray fluorescence spectrometry and for several trace elements using inductively coupled plasma atomic emission analysis to provide preliminary assessment of the homogeneity of

the material prior to bottling. The material was bottled into 50 g units and randomly selected bottles were taken for the final homogeneity testing. A minimum sample weight of 250 mg should be used for analytical results to be related to the certified values on this Certificate Analysis.

SRM 2709 is an agricultural soil from a ploughed field in the San Joaquin Valley in central California which has baseline trace element concentrations.

SRM 2710 is a highly contaminated soil from pasture land along Silver Bow Creek in the Butte, Montana area. The sampling site periodically floods depositing sediment with high concentrations of Cu, Mn, Pb and Zn from the settling ponds of a local industrial plant.

SRM 2711 is a moderately contaminated agricultural soil collected in the till layer of a wheat field. Addenda to these three SRMs provide additional leachable concentration information. For a number of environmental monitoring purposes, the concentrations of labile or extractable fractions of elements are more useful than total concentrations. Concentrations of labile or extractable fractions are generally determined using relatively mild leach conditions which are unlikely to totally decompose the sample. Therefore, reported concentrations of labile or extractable fractions of elements are generally lower than total concentrations; although recovery can be total if an element in a given sample is completely labile. Results are often presented as measured concentration in the leachate in comparison to the total or certified concentration. The recovery of an element as a percent of total concentration is a function of several factors such as the mode of occurrence in the sample, leach medium, leach time and temperature conditions, and pH of the sample-leach medium mixture.

Instructions for drying for soil and ash depend on the nature of the elements to be determined: When nonvolatile elements are to be determined, samples should be dried for 2 h at 110 °C. Volatile elements (i.e., Hg, As, Se) should be determined on samples as received; separate samples should be dried as previously described to obtain a correction factor for moisture. Correction for moisture is to be made to the data for volatile elements before comparing to the certified values. This procedure ensures that these elements are not lost during drying. The weight loss on drying has been found to be in

the range of 1.7 to 2.3 %.

5.22 Results and Discussion

All samples were weighed between 0.5 mg to 5 mg and accurate to 0.01 mg. Calibration curves were constructed based on 10 μL of standard solution residue. The multi-element standard solutions with 300 ppm Na and 300 ppm K were made in 2% HNO_3 medium. Solution standards were dried externally under an IR lamp for 10 minutes. A blank electrode and a three point calibration were used for every 20 samples. Thirty seconds was used for atomization for all samples. Ashing time varied from 5 seconds for ash and soil samples, to 30 seconds for leaves. Signals were collected by the LECO computer. LECO built-in software was used for all peak area integration. As ICP intensity varied slightly from day to day, calibration for each analysis was necessary. Since most of the data presented here were not done on the same day, an average of found results vs. certified values were plotted in this chapter. Error bars represents one standard deviation based on three data points.

The Pb and Zn results determined by DSI-ICP-AES for these NIST SRMs (Ash and Soil) are listed in Table 5.1. The results obtained from DSI-ICP are in good agreement with the certified values. The plots of found concentrations against the NIST certified concentrations are presented in Figures 5.1 and 5.2. Figure 5.1 presents four flyash samples and one coal sample. The correlation coefficient of the plot is very good and the slope is close to unity. However, this is not the case for the results shown in figure 5.2. The slope (0.884) deviates from unity and intercept value is high. This curve cannot be used for sample analysis. The main reason for the poor slope is the SRM 2710 Montana Soil Highly Elevated Traces. The Pb concentration is too high, and the Pb peak may be saturated. Also the large error bar may be caused by using a small sample size. Weights of all three replicates are around 0.5 mg, thus weighing error contributes more percentage error at such a low weight. By deleting this point (SRM 2710), the slope of the curve become close to unity (1.03) and the intercept value (Y) was reduced from 50 to 6.3.

	Pb Concentration ($\mu\text{g/g}$)		Zn Concentration ($\mu\text{g/g}$)	
	NIST	Found	NIST	Found
Coal (Bituminous) (SRM 1632b)	3.67	4.79 \pm 1.34	11.89	11.98 \pm 0.38
Coal Fly Ash (SRM 1633b)	68.2	66.9 \pm 3.6	210	229.3 \pm 21.7
Estuarine Sediment (SRM 1646a)	11.7	18.0 \pm 5.1	135	123.0 \pm 20.5
Buffalo River Sediment (SRM 2704)	161	182.6 \pm 10.8	438	265.1 \pm 31.8
San Joaquin Soil Baseline (SRM 2709)	18.9 \pm 0.5	18.1 \pm 4.1	106 \pm 3	130.8 \pm 22.3
Montana Soil High Traces (SRM 2710)	5532 \pm 80	4916 \pm 565	6952 \pm 91	415.3 \pm 71.5
Montana Soil Mod Traces (SRM 2711)	1162 \pm 31	1207 \pm 113	350.4 \pm 4.8	355.0 \pm 16.8
Coal Fly Ash Low Lime (SRM 2689)	(52)	52.3 \pm 13.2	(240)	157.6 \pm 0.6
Coal Fly Ash Med. Lime (SRM 2690)	(39)	33.6 \pm 3.8	(120)	97.7 \pm 10.8
Coal Fly Ash High Lime (SRM 2691)	(29)	24.5 \pm 2.1	(120)	104.7 \pm 10.3

Table 5.1 Pb and Zn in NIST Standard Reference Material Ash and Soil

- Value in parentheses are not certified, but are given by NIST for information only
- Uncertainties of NIST values represent 95% confidence interval
- Uncertainties of found values represent ± 1 standard deviation ($n=3$)

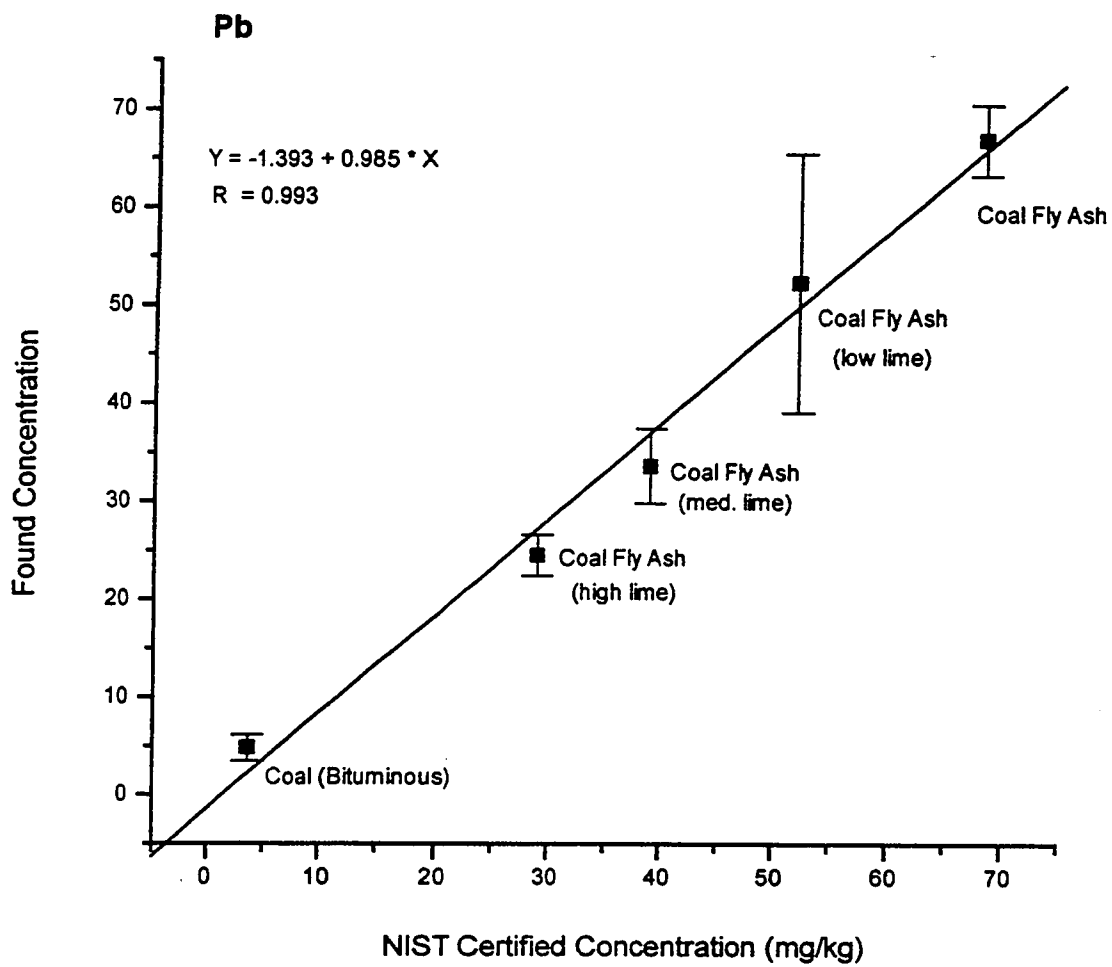


Figure 5.1 Pb concentrations in NIST Coal Ash SRMs

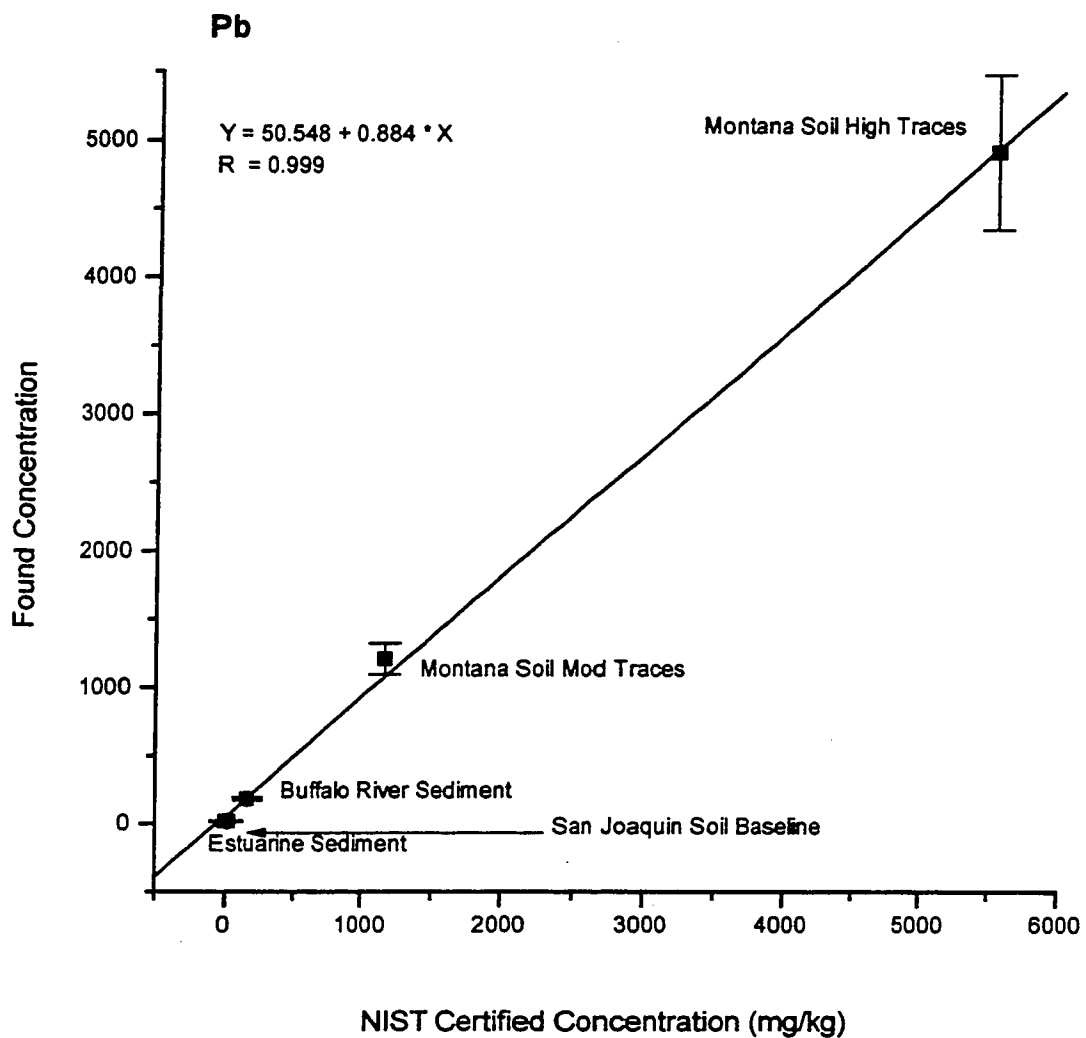


Figure 5.2 Pb concentrations in NIST Soil SRMs

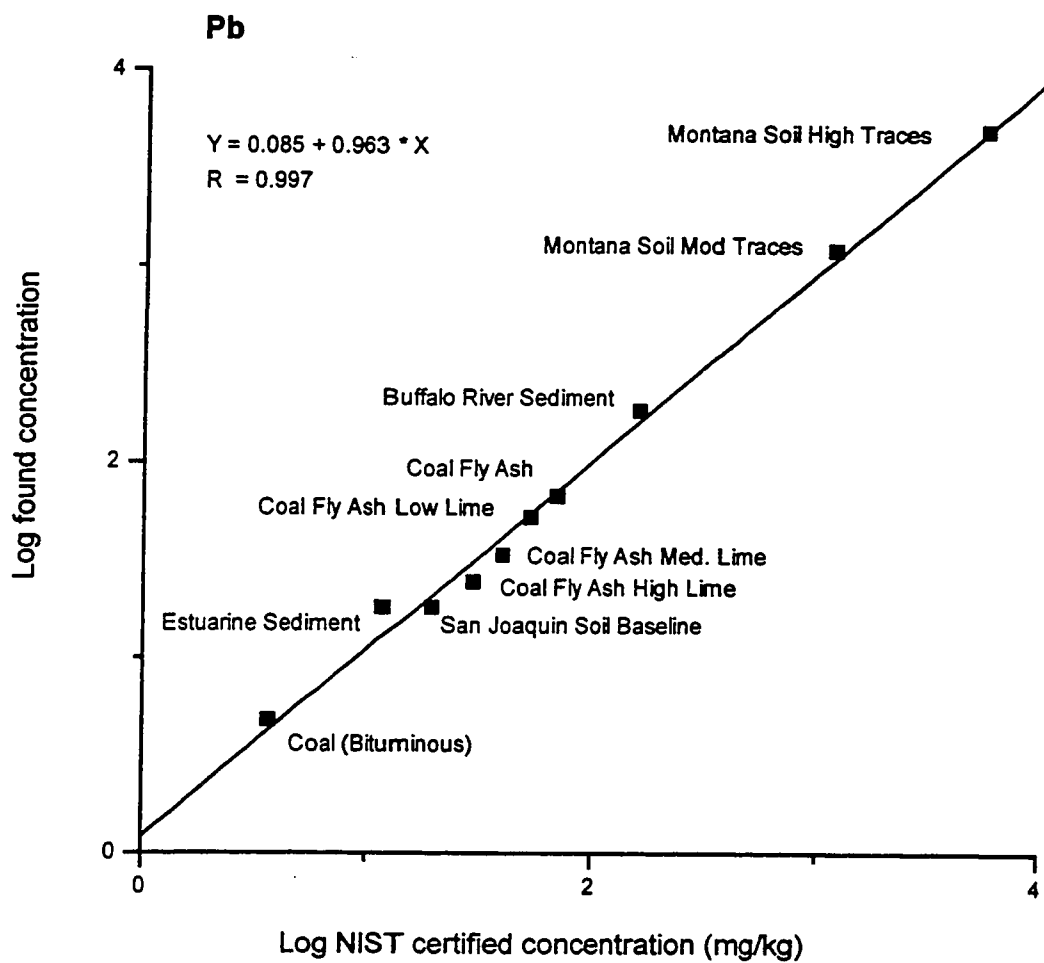


Figure 5.3 Pb concentrations in NIST Ash and Soil SRMs

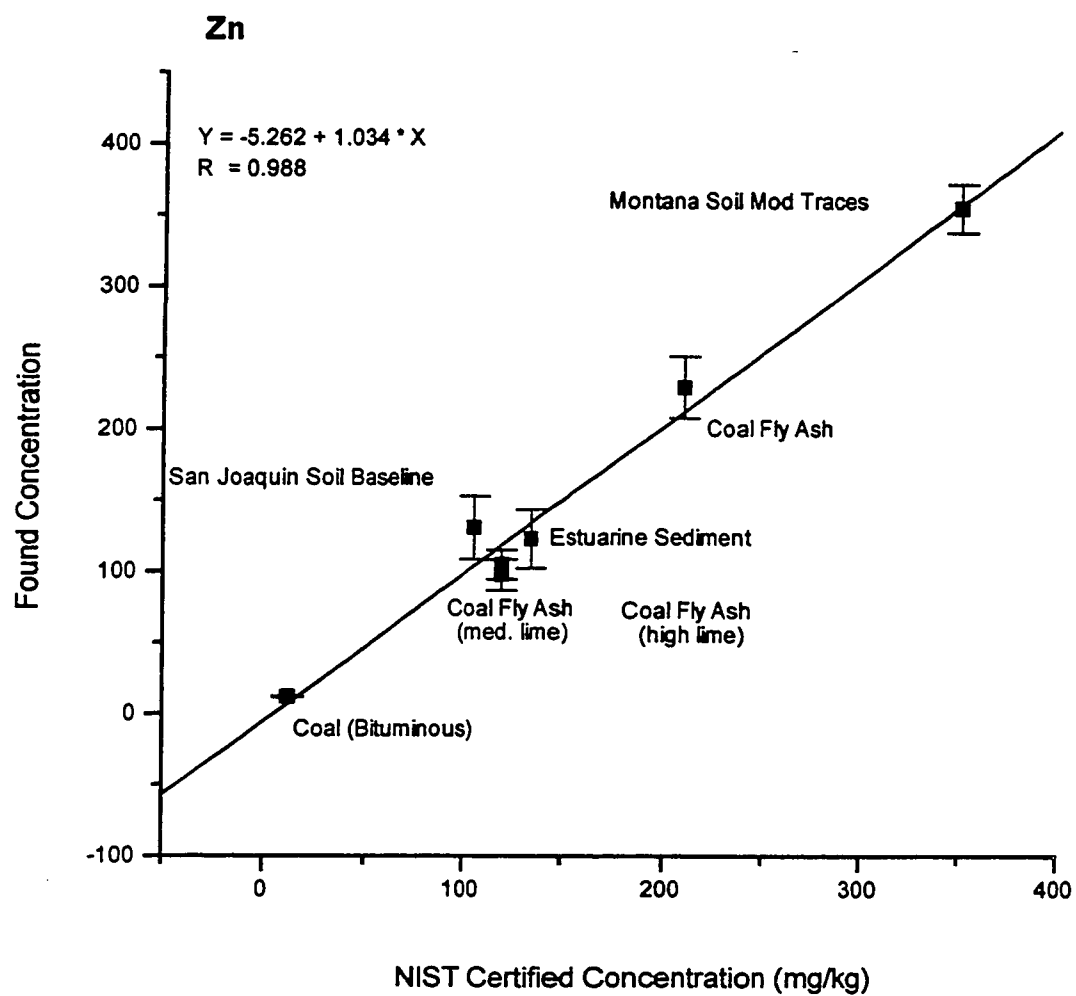


Figure 5.4 Zn concentrations in NIST Ash and Soil SRMs

The data presented in Figure 5.3 is a combination of that from Figure 5.1 and Figure 5.2. The X and Y axes are converted to log values in order to accommodate the wide concentration range. The curve demonstrates four orders of magnitude linearity for the determination of Pb by DSI-ICP-AES.

The results for the determination of Zn in these SRMs are also listed in Table 5.1. The results for seven out of the ten SRMs are plotted in Figure 5.4. It shows close to unity slope and good linearity. The Zn concentration in the other two SRMs (2704 and 2710) are very high and caused the detector to saturate. This is clear in the spectrum shown in Figure 5.5 where the Zn peak at pixel 528 is flat topped. There is no alternative line (less sensitive) for Zn on either mask MEM6 or MEM24, therefore it is impossible to determine Zn in these SRMs by simply reducing the sample weight. The Zn result found for SRM 2689 is lower than the information value provided by NIST. No visible detector saturation of the Zn peak was found in the spectrum. Lowering sample weight may provide information on whether the detector is saturated. However, this was not done in the study. In addition, the minimum weight requirement for SRM 2689 is 0.5g which is higher than the weight (0.25 g) normally required by most other SRMs.

The As and Cd results are listed in Table 5.2. Only six SRMs were included in this study. The coal fly ash SRMs were not purchased at the time of the experiment, therefore they were not analyzed. In general, the experiment results are in good agreement with the certified values except SRM 1646a Estuarine Sediment. Figure 5.6 and Figure 5.7 present the plots of found results vs. certified values. The slopes of the As and Cd plots are very close to unity, and the intercepts are also close to zero. These curves demonstrate the possibility of using the solution residues to calibrate the DSI system for unknown sample analysis.

Figure 5.8 shows the spectral differences by opening one more slot on the MEM24 mask. The baseline of the left side of the As peak is more complicated in the bottom spectrum (Ni slot open). The MEM24 mask is designed for multi element determinations, but in reality it may only be used for a maximum of half dozen elements at one time. This is especially true for solid sample analysis as the spectral background may

	As Concentration ($\mu\text{g/g}$)		Cd Concentration ($\mu\text{g/g}$)	
	NIST	Found	NIST	Found
Coal Fly Ash (SRM 1633b)	136.2	129.5 \pm 8.9	0.784	0.91 \pm 0.11
Estuarine Sediment (SRM 1646a)	6.23	12.0 \pm 1.7	0.148	0.21 \pm 0.04
Buffalo River Sediment (SRM 2704)	23.4	26.1 \pm 8.3	3.45	3.9 \pm 0.5
San Joaquin Soil Baseline (SRM 2709)	17.7	18.3 \pm 6.1	0.38	0.34 \pm 0.05
Montana Soil High Traces (SRM 2710)	626	637 \pm 15	21.8	18.9 \pm 2.4
Montana Soil Mod Traces (SRM 2711)	105	105.4 \pm 18.4	41.7	44.5 \pm 3.3

Table 5.2 As and Cd in NIST Standard Reference Material Ash and Soil

- Value in parentheses are not certified, but are given by NIST for information only
- Uncertainties of NIST values represent 95% confidence interval
- Uncertainties of found values represent ± 1 standard deviation ($n = 3$)

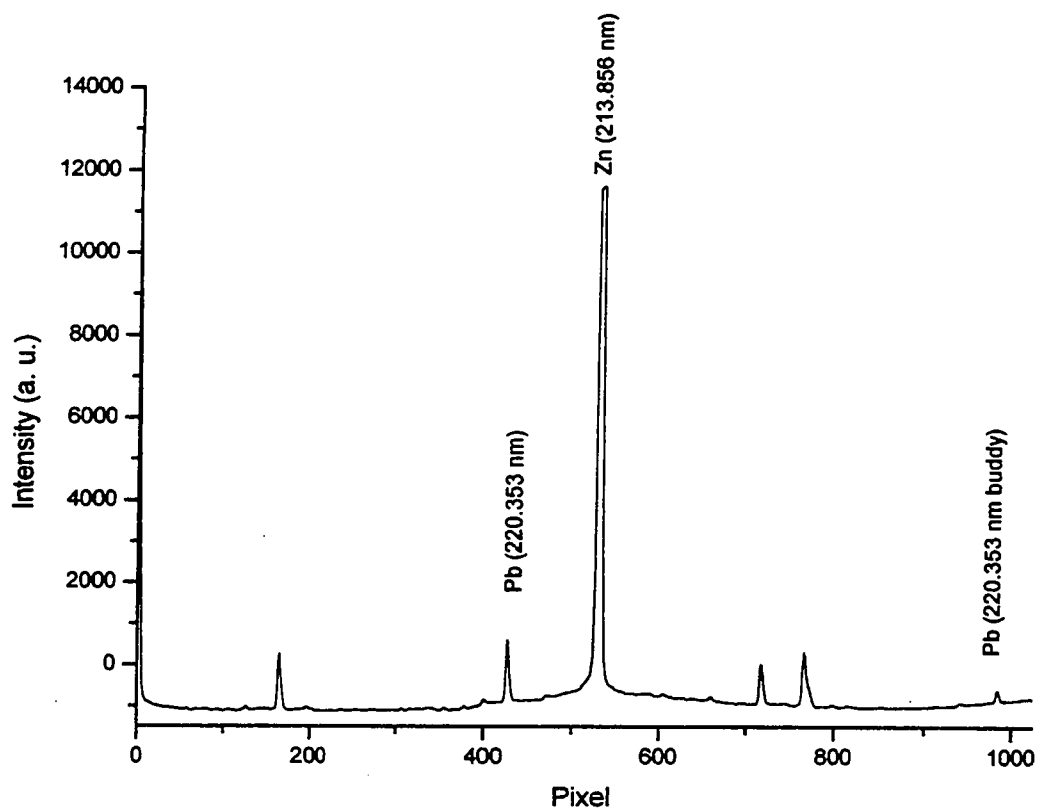


Figure 5.5 Pb and Zn spectrum of SRM 2704 Buffalo River Sediment

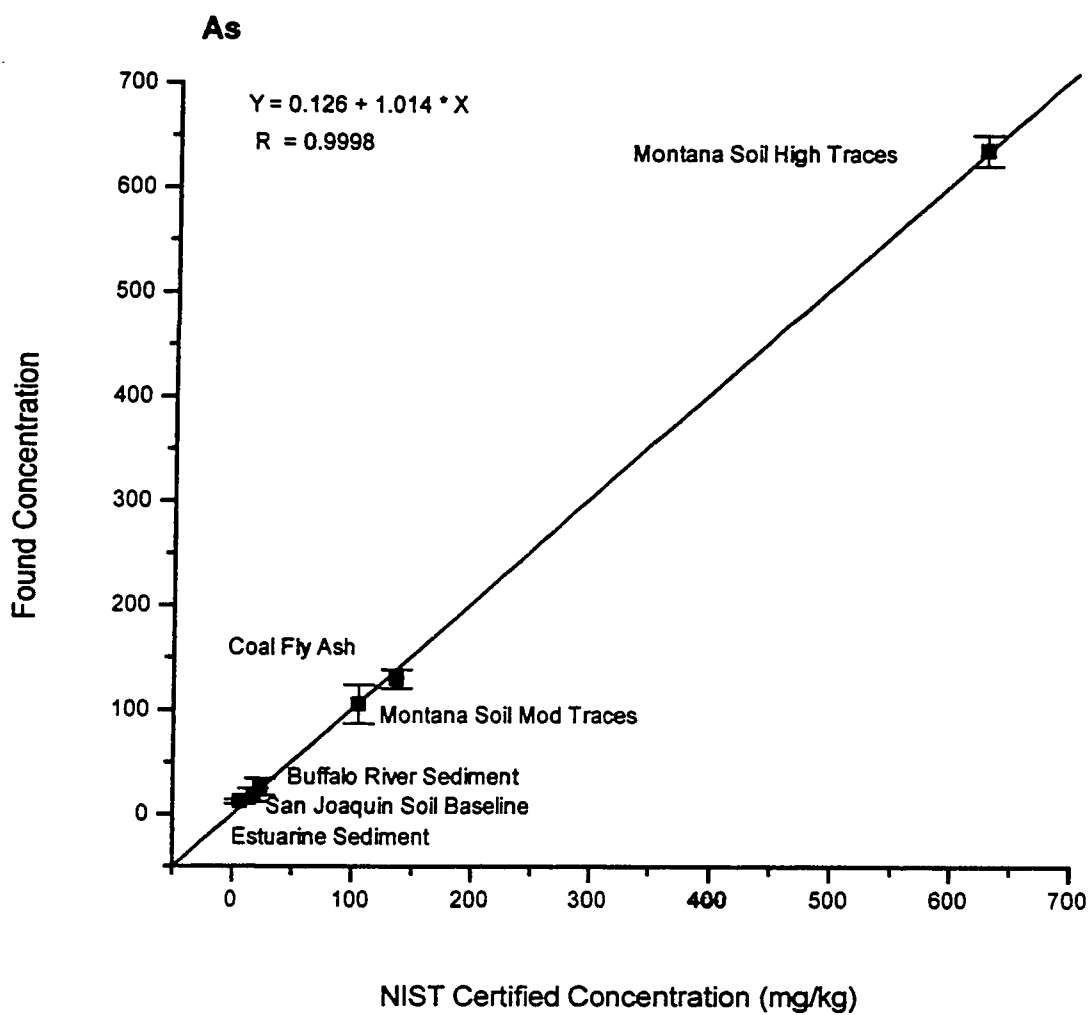


Figure 5.6 As concentrations in NIST ash and soil samples

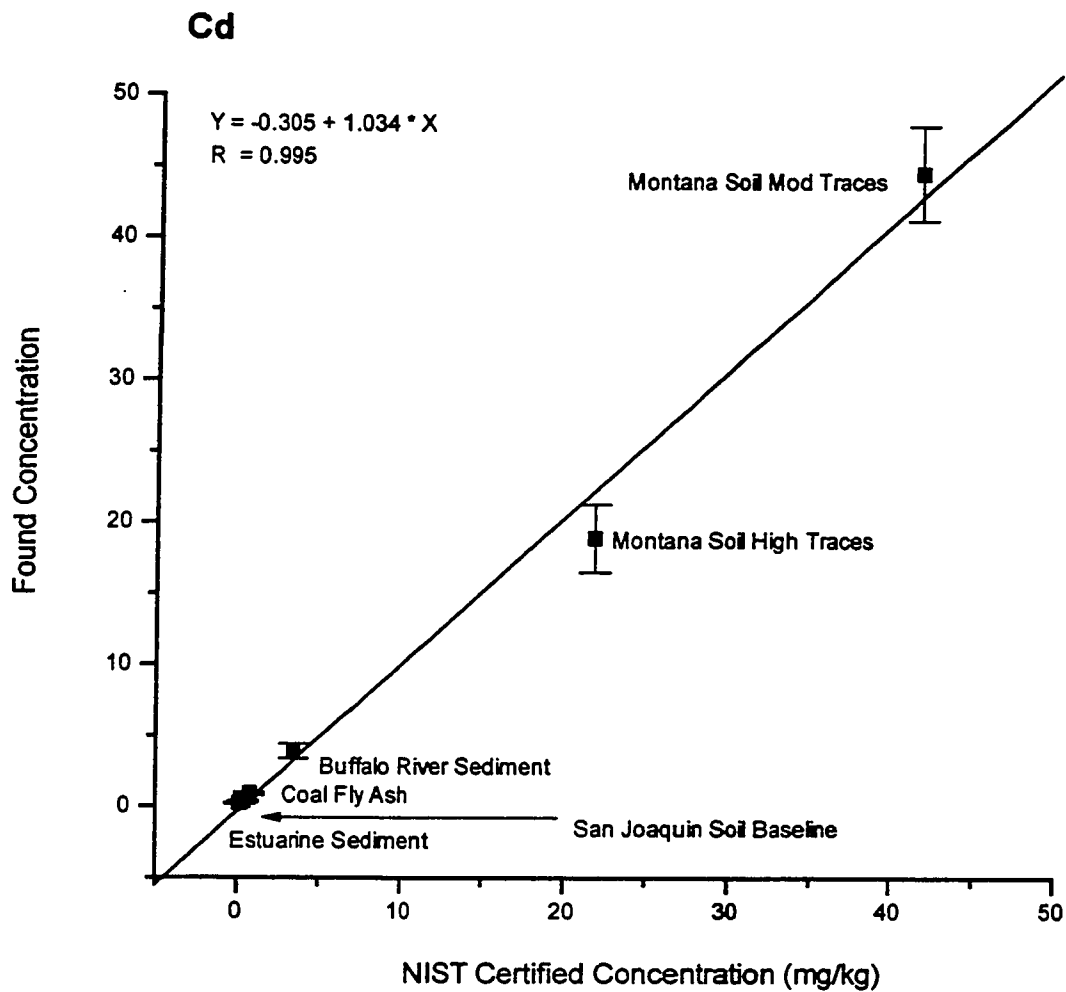


Figure 5.7 Cd concentrations in NIST ash and soil samples

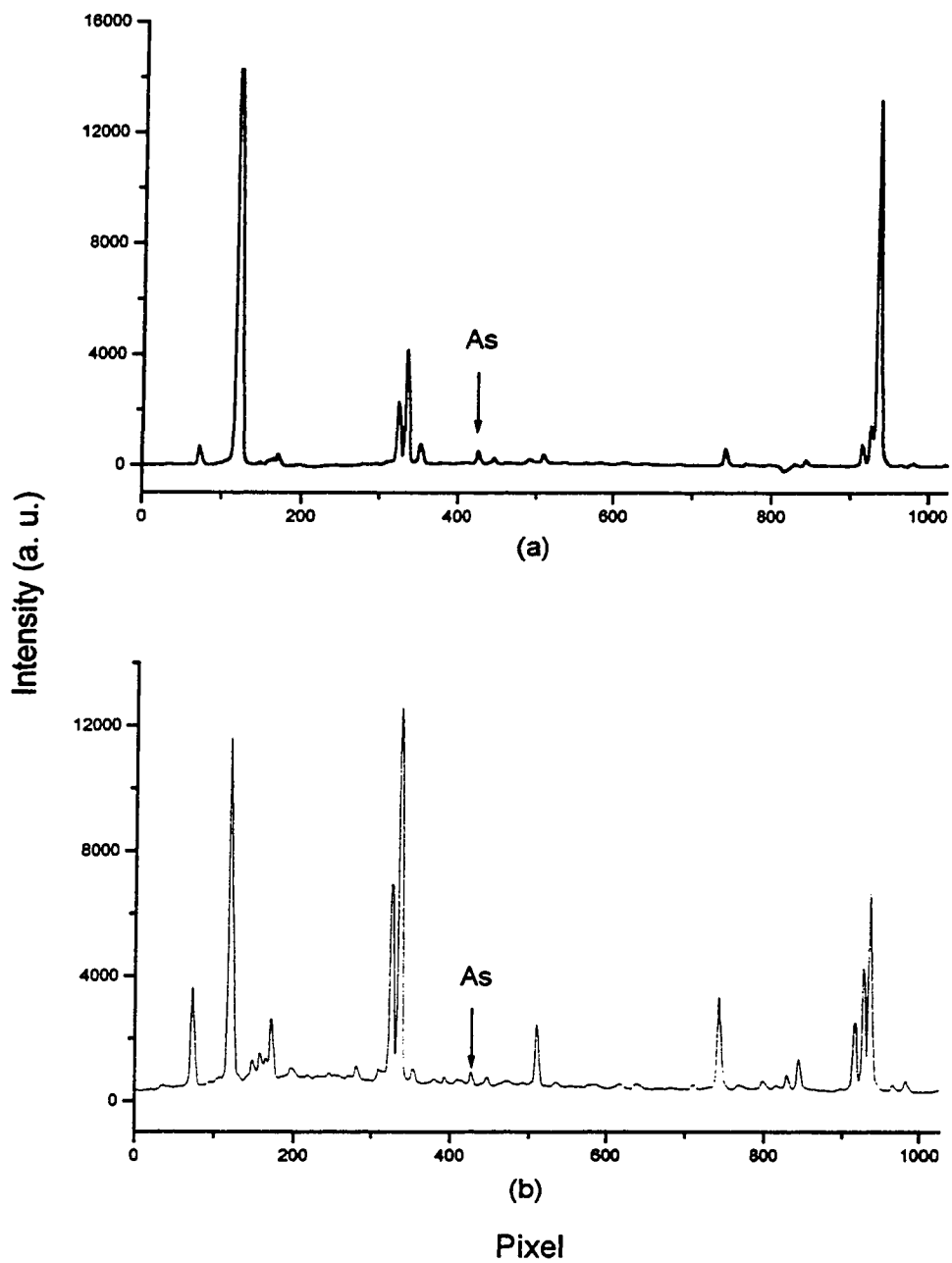


Figure 5.8 As spectrum of SRM 1633b Coal Flyash

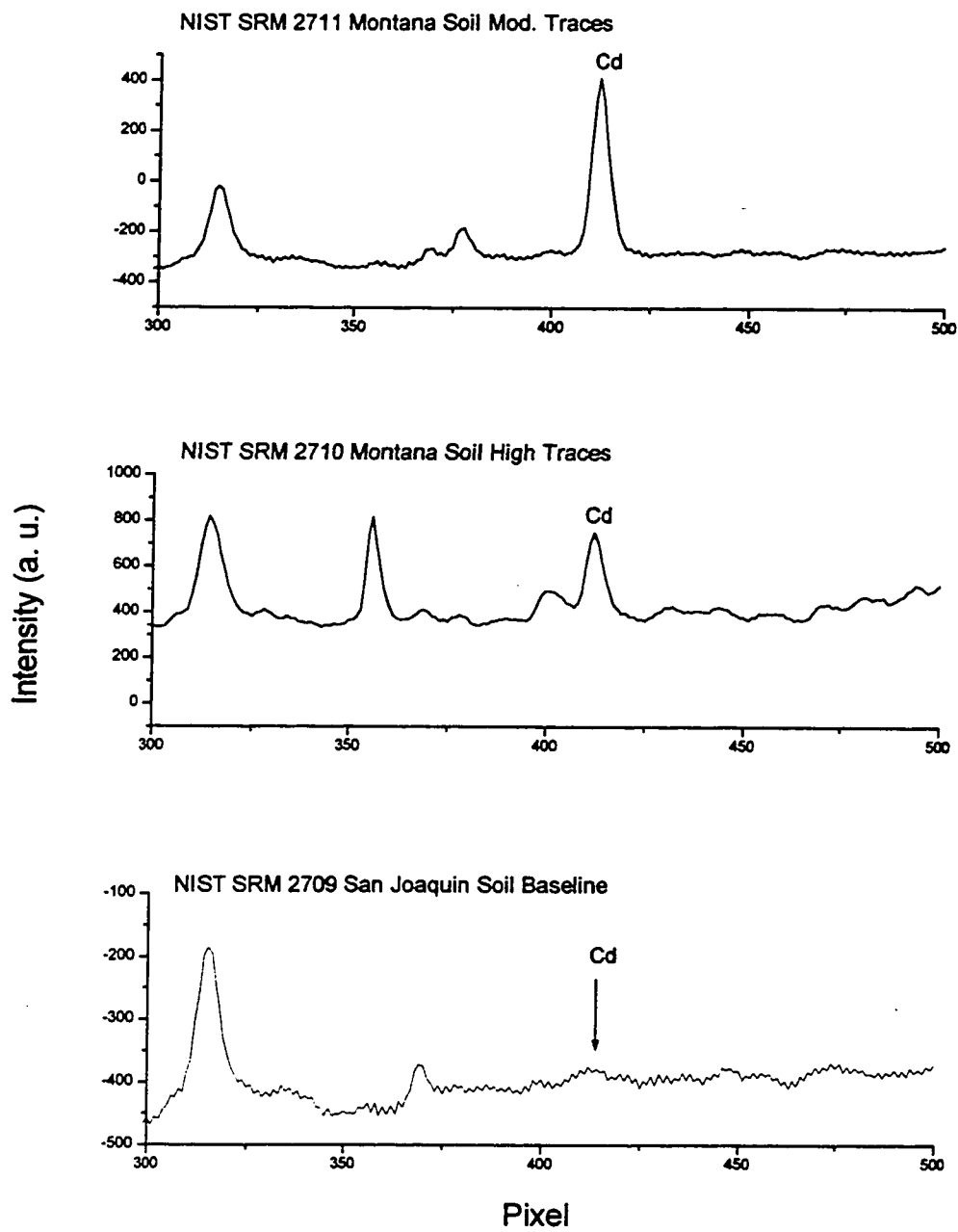


Figure 5.9 Cd spectrum of NIST Soils

be quite complex.

Figure 5.9 presents Cd spectra in three different soil samples. The Cd spectrum of SRM 2709 San Joaquin Soil Baseline shows almost no-visible peak for Cd at 0.38 ppm. But the built-in software integrated the peak area correctly and gave results close to the NIST certified results.

An ideal situation for quantitative analysis would be if a calibration curve of an analyte could be applied to the analysis of all types of samples. This is almost achieved for aqueous sample analysis. For solid sample analysis, matrix effects are still a major hurdle to overcome. Techniques like matrix matching, internal standardization and standard addition are used for many solid analyses. However, these approaches are tedious and complicated. Using solution residues to calibrate for solid sample analysis is certainly an attractive option. But it does not work for every element in all sample types. Using partial matched calibration standards for the determination of several volatile elements in solid matrices does give satisfactory results as demonstrated in this experiment. These results also confirm several other studies [1-5, 9-10] verifying that the DSI technique is relatively insensitive to element origin. And finally, it is certainly a simple method for direct solid analysis if complete volatilization of analytes is achieved.

5.3 Food

5.31 Background

Although the number of biological SRMs characterized for trace elements has been increasing in recent years, there is still a need for a greater range of elemental concentrations and a greater variety of matrix types. The level of accuracy of trace element analysis depends on interference from sample matrix components and on the concentration of the analyte itself. Analytical confidence is substantially increased by matching both elemental concentration and sample matrix between unknown samples and reference materials (SRMs).

In order to augment the ranges of elemental concentrations and matrix types available to the analytical community, 12 candidate agricultural/food SRMs were prepared by Agriculture Canada [16]. These materials were characterized for an extensive range of elements by a variety of analytical techniques in selected laboratories.

BCR CRM-422 Cod Muscle [17] was prepared at Commission of the European Communities, Joint Research Center, Central Bureau for Nuclear Measurements (CBNM) by cryogrinding and subsequent freeze-drying, mixing and bottling under controlled conditions. After completion of the production process, the material was examined for microhomogeneity by solid sampling Zeeman atomic absorption spectrometry (SS-ZAAS) on 85 to 138 microsamples for five elements: Pb, Cd, Hg, Fe and Zn. The minimum representative sample size of CRM-422 was determined experimentally for these elements. The minimum mass for Fe was 68.7 mg, for Zn was 20.8 mg, for Pb was 11.6 mg, for Cd was 24 mg and for Hg was 416 mg.

5.32 Results and Discussion

A variety of food samples were analyzed for Zn, Cu and Mn. The results are listed in Table 5.3. The experiment results vs. certified values are plotted in Figures 5.10 to 5.12. Concentrations of Cu in Corn Kernel, Rice Flour and Wheat Flour were very close to each other. Therefore, a log-log plot is also presented for Cu in Figure 5.11. Again, the results are in good agreement with the certified results in most cases. It should be noted that as the Zn peak (pixel 528) appears within 20 pixels of the Mn peak (pixel 534), Zn and Mn determinations had to be performed on separate runs. Zn and Cu were determined on the same sample. Typical spectra of Zn and Cu in the food matrices are shown in Figure 5.13. The concentration of Zn in these samples ranges from 19.4 $\mu\text{g/g}$ to 160 $\mu\text{g/g}$ and the concentration of Cu in these samples ranges from 0.7 $\mu\text{g/g}$ to 127 $\mu\text{g/g}$.

There were a few cases where experiment results were significantly lower than the certified values. This includes Zn in Oyster Tissue (SRM 1566a) and Mn in Rice Flour (SRM 1568a). Detector saturation was found in both cases. Figure 5.14 shows the saturated Zn peak at pixel 528 and the Cu peak at pixel 116. For Cu, there was an

	Zn Concentration		Cu Concentration		Mn Concentration	
	NIST	Found	NIST	Found	NIST	Found
Non-fat Milk Power (SRM 1549)	46.1	42.3±4.7	0.7	0.66±0.03	0.26	0.27±0.01
Oyster Tissue (SRM 1566a)	830.0	269±82	66.3	64.4±9.6	12.3	13.3±2.3
Wheat Flour (SRM 1567a)	11.6	13.4±2.2	2.1	2.16±0.13	9.4	8.72±0.98
Rice Flour (SRM 1568a)	19.4	22.3±3.5	2.4	2.72±0.24	20.0	10.11±1.25
Bovine Liver (SRM 1577b)	160.0	167±34.5	127	119.5±8.0	10.5	9.99±1.23
Corn Stalk (SRM RM 8412)	(32.0)	32.5±5.2	(8.0)	10.5±1.4	(15.0)	18.9±2.5
Corn Kernel (SRM RM 8413)	(15.7)	20.8±1.0	(3.0)	2.83±0.24	(4.0)	4.38±0.59

Table 5.3 Zn, Cu and Mn in NIST Standard Reference Material Food

- Value in parentheses are not certified, but are given by NIST for information only
- Uncertainties of found values represent ± 1 standard deviation ($n = 3$)

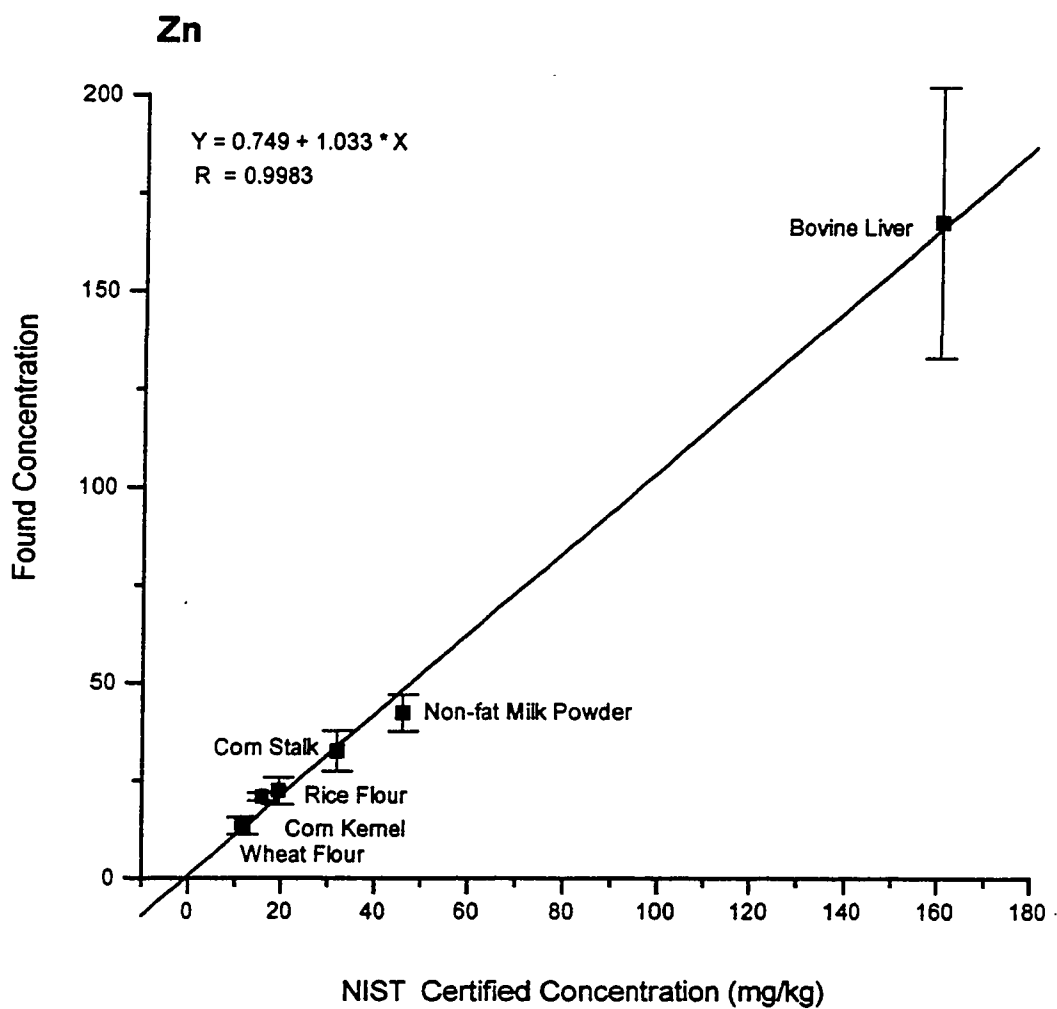


Figure 5.10 Zn concentrations in NIST Food SRMs

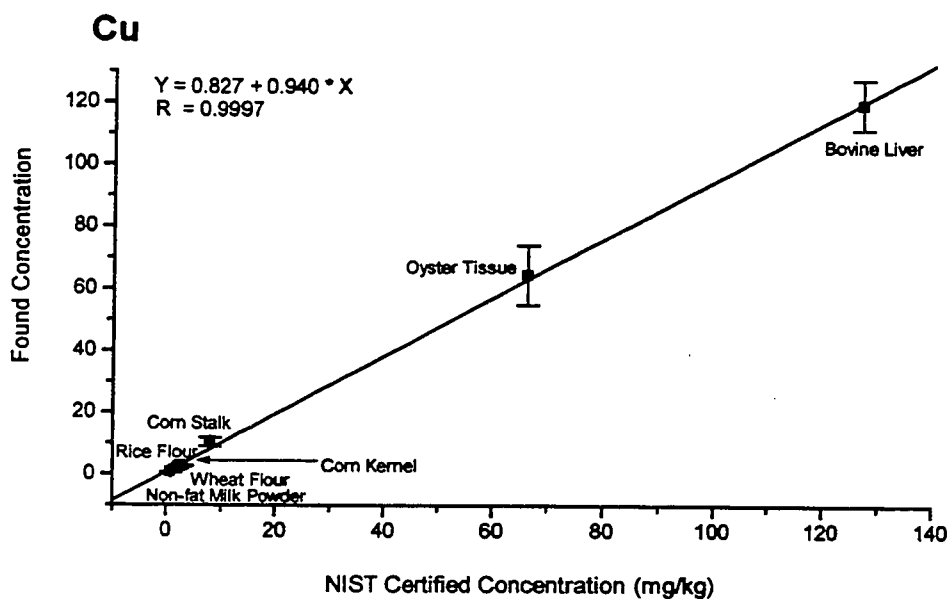
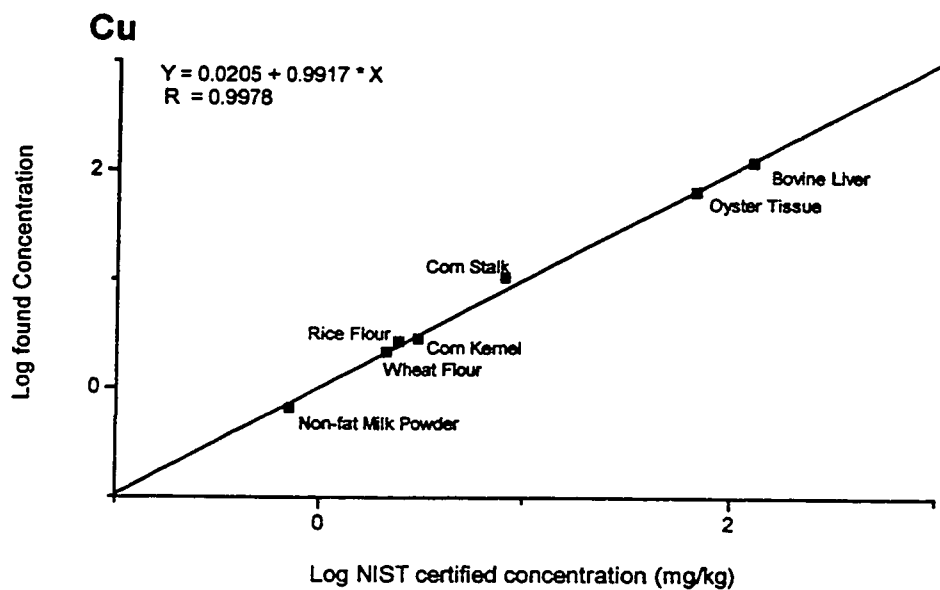


Figure 5.11 Cu concentrations in NIST Food SRMs

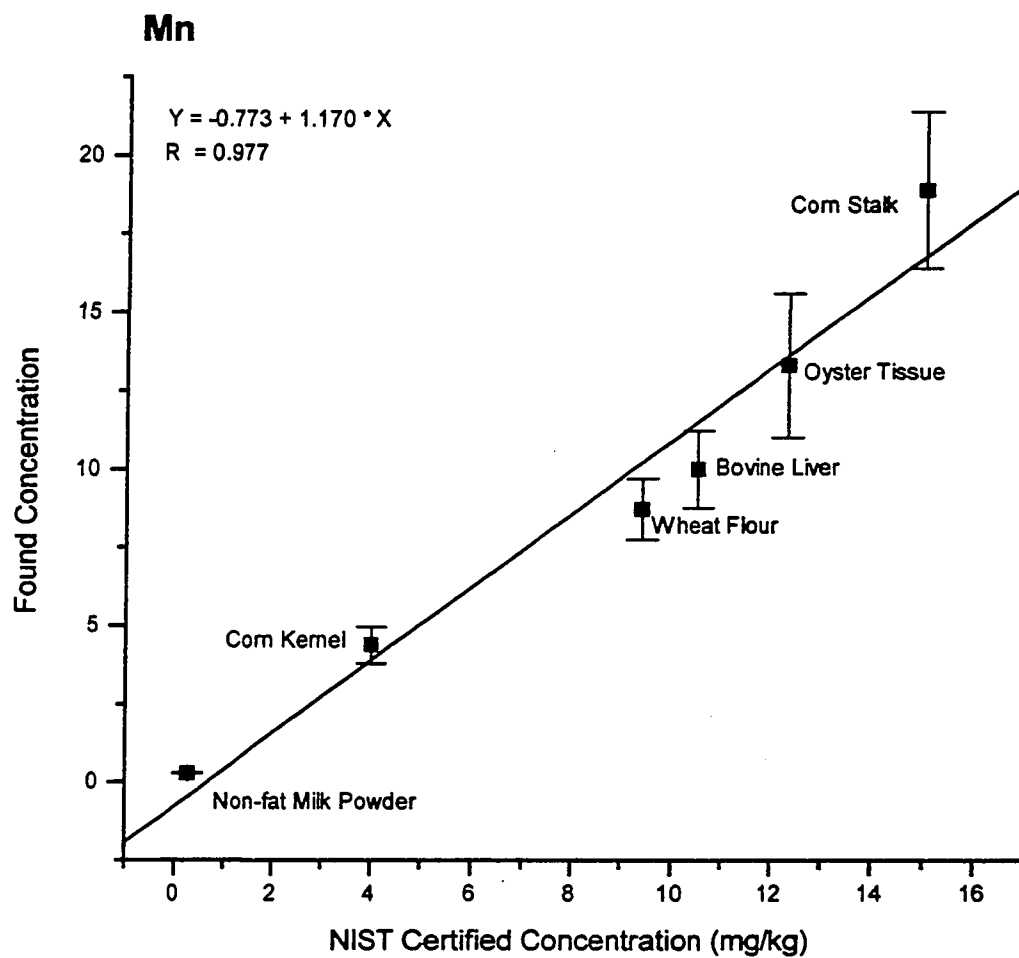


Figure 5.12 Mn concentrations in NIST Food SRMs

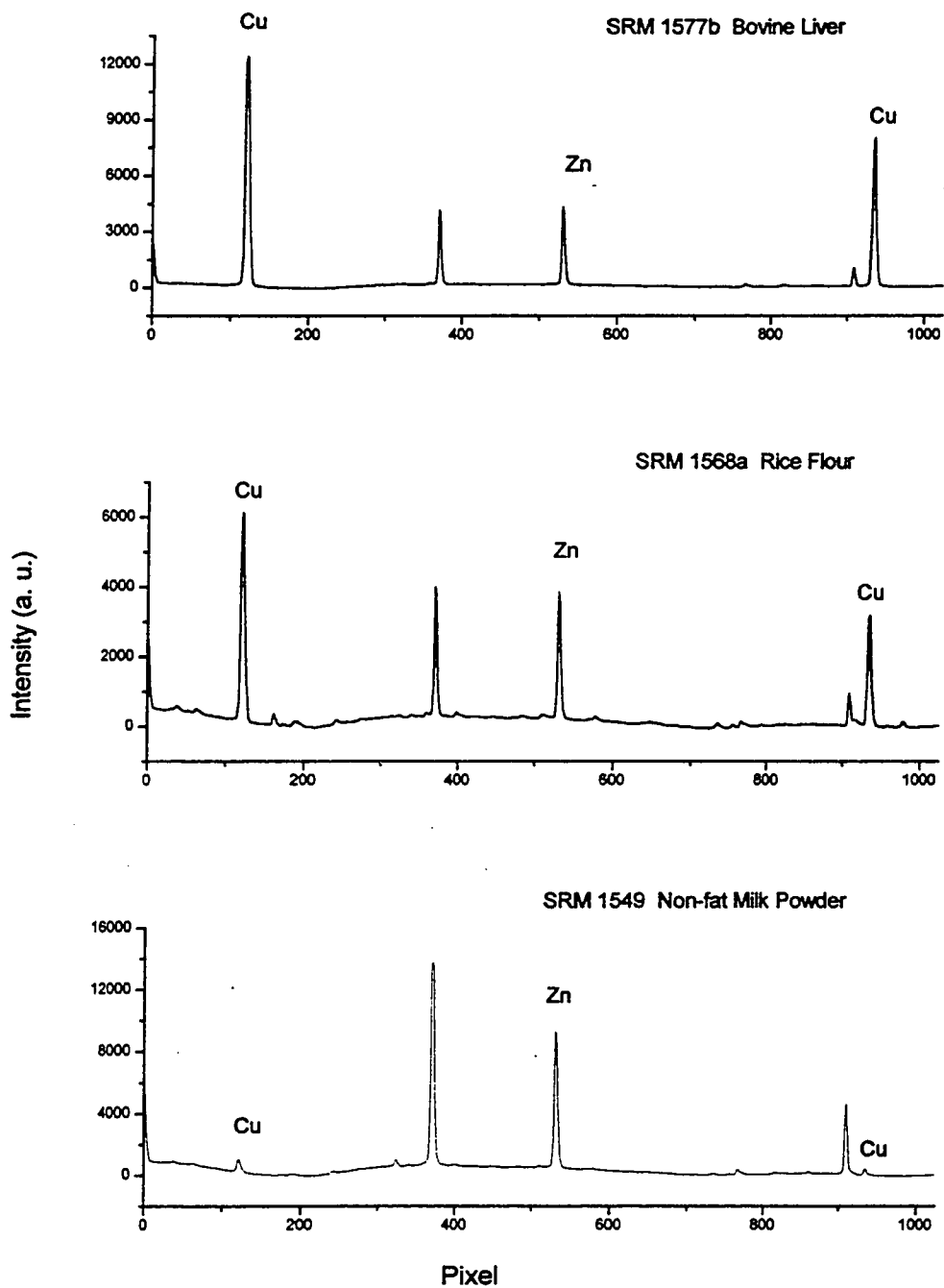


Figure 5.13 Zn and Cu spectra for Food SRMs

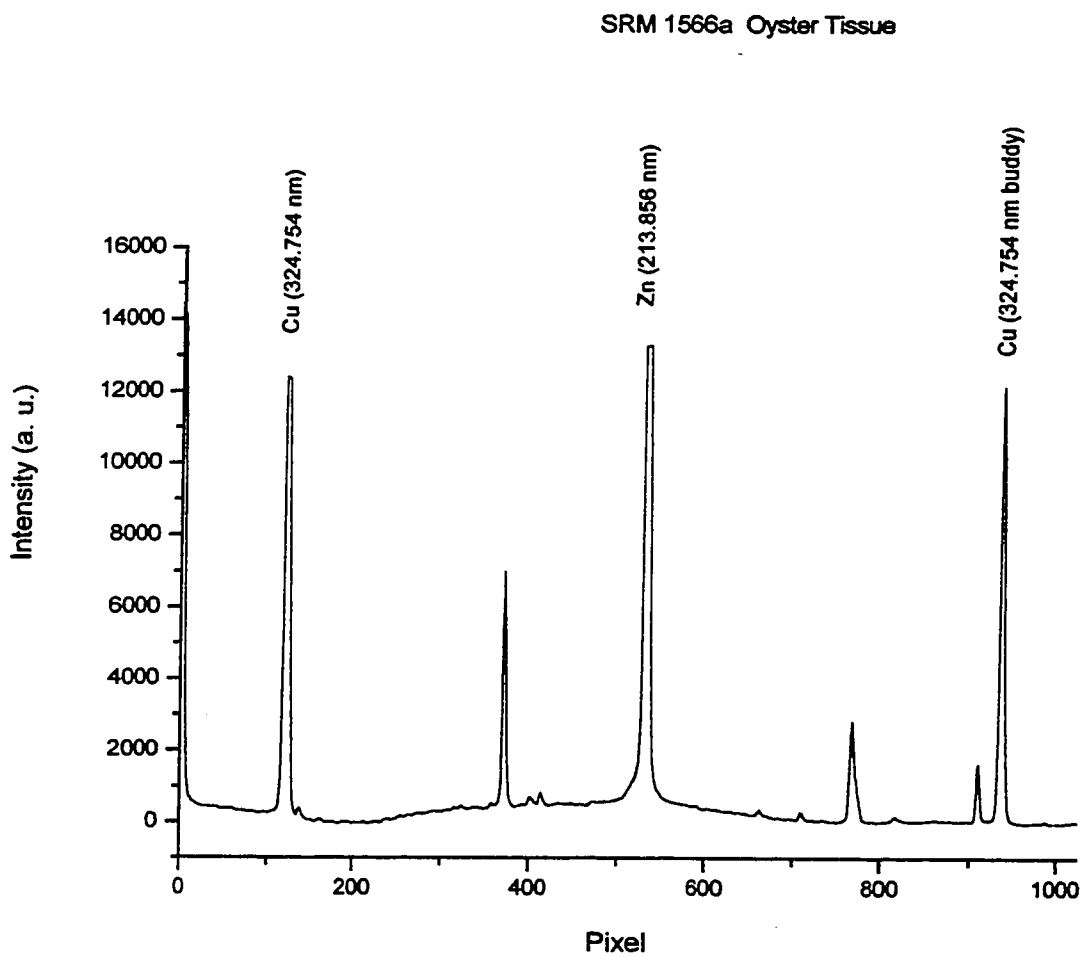


Figure 5.14 Zn and Cu spectrum of SRM Oyster Tissues

alternative "line" (a buddy line) that is less sensitive at pixel 934. A separate calibration for the less sensitive Cu buddy line can be used in this case. For Zn, there was only one peak available on the masks available in the laboratory. The weight for the oyster issue sample was already reduced to about 0.5 mg, and it was impossible to continue to reduce the sample weight to avoid detector saturation. Another mask with a less sensitive Zn line should be cut and ordered to fulfill the need.

This is the same situation for Mn in rice, which is shown in Figure 5.15. However, there was room to reduce the sample weight to avoid the detector saturation as the sample weight was around 3 mg. This was not recognized at the time, but could be remedied in the future.

5.4 Leaves

5.41 Background

Botanical SRMs issued since 1991 are improved over previous materials in a number of ways [18]. Probably the most significant change is the use of a jetmilling process to grind them to extremely fine particles. This has resulted in botanical SRMs with significantly improved homogeneity.

Natural botanical materials used for the production of reference materials generally contain a small amount of siliceous or calcareous mineral matter (hereafter called "grit"), even though a washing step may have been used. This grit may cause one or both of following problems:(1) elements present in the grit phase may not be dissolved by the methods used to decompose the bulk matrix; (2) if one or more elements are present mainly in a small number of high concentration grains, the statistics of sampling may lead to an observed heterogeneity. These problems were examined for NIST botanical SRMs in two recent studies. For the older SRMs, the amount of the element in the grit can often exceed 30% for elements such as Cr, As, and Al. With the jetmilled SRMs, however, the grit content is substantially reduced as the air classification system discriminates against the higher density grit particles, therefore eliminating them from the

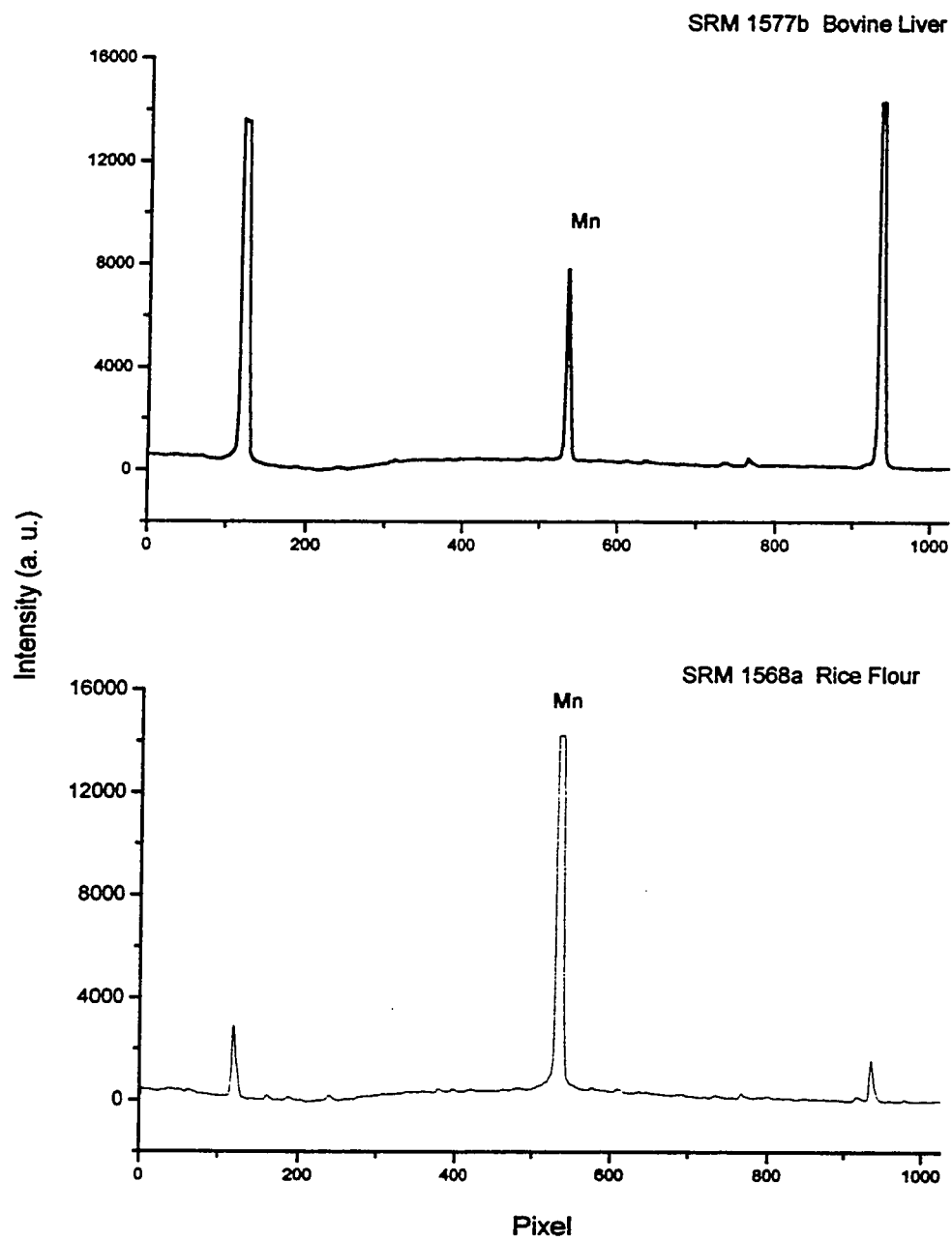


Figure 5.15 Mn spectra for two NIST Food SRMs

reference material. While this lower grit content produces a reference material with substantially improved homogeneity, it may not challenge the analytical system in the same way as a natural matrix botanical sample, thus partially defeating the purpose of a certified control sample.

SRM 1570a, Spinach Leaves [19]: The material, (approximately 2270 kg) for this SRM was obtained from a commercial supplier by Oregon Freeze-Drying Corp., Albany, OR. It consisted of a U.S. Grade A chopped frozen spinach. The material was thawed, placed in a ribbon mixer, thoroughly mixed, and blended. After mixing, the spinach was freeze-dried. The freeze-dried material was then ground in a stainless steel grinder and shipped to NIST. At NIST, the freeze-dried material was sieved through a polypropylene sieve having openings of 0.25 mm (equivalent to a US Series 60 standard sieve). The sieved material was then jet milled and air classified to a particle size of approximately 75 μm (200 mesh). After mixing in a large blender, the spinach was irradiated with cobalt-60 radiation to a minimum absorbed dose of approximately 27.8 kGy for microbiological control and bottled.

SRM 1547, Peach Leaves [20]: The plant material for this SRM was collected and prepared under the direction of R. A. Isaac. Soil Testing & Plant Analysis Laboratory, The University of Georgia College of Agriculture. Leaves, representative of healthy Georgia peach trees, variety "Coronet", were picked from a field in Peach County, Georgia approximately 150 miles south of Athens, Georgia. Fungicide and insecticide sprays were controlled to minimize heavy metal contamination. The leaves were dried and ground in a stainless steel mill to pass a 1 mm screen. The sieved material was then jet milled and air classified to a particle size of approximately 75 μm (200 mesh). After mixing in a large blender, the spinach was irradiated with cobalt-60 radiation to a minimum absorbed dose of approximately 27.8 kGy for microbiological control and bottled.

SRM 1515, Apple Leaves [21]: The plant material for this SRM was collected and prepared under the direction of C.B. Smith, College of Agriculture, The Pennsylvania State University, University Park, PA. Midshoot leaves were collected from orchards

adjacent to the Fruit Research Laboratory at Bigleville, PA and from orchards at the Horticultural Research Farm at Rock Spring, PA. Approximately equal amounts of leaves from Golden Delicious and Rome varieties were used. Fungicide and insecticide sprays were controlled to minimize heavy metal contamination. The leaves were dipped into a non-ionic detergent solution, rinsed in distilled water, dried in ovens at 60 °C, and ground to pass a 425 μm (40 mesh) screen in a stainless steel mill. The sieved material was then jet milled and air classified to a particle size of approximately 75 μm (200 mesh). After mixing in a large blender, the spinach was irradiated with cobalt-60 radiation to a minimum absorbed dose of approximately 27.8 kGy for microbiological control and bottled.

For these jet-milled materials, it was expected that a high degree of homogeneity would be obtained. Prior to this, all botanical SRMs were certified only for sample sizes of 250 mg or larger. Since the Apple leaves (SRM1515) and Peach Leaves (SRM 1547) were the first jet-milled botanical SRMs developed by NIST, these materials were studied to determine whether acceptable homogeneity could be established for 100 mg samples of these two materials [18]. This study employed instrumental neutron activation analysis to determine concentrations of 12 different elements (Al, Ca, Cl, Cr, Co, Fe, K, La, Mn, Na, Sc, Sm) in 15 samples of each SRM. The results showed remarkable homogeneity for such small samples of a natural matrix material, with seven elements showing less than 1.5% variability (1σ) for the Apple Leaves and six elements for the Peach Leaves. Only one element in one of the materials showed greater than three times the expected variability due to statistical counting uncertainty; this was scandium in the Peach Leaves, with a total analytical precision of 2.62% (1σ).

Recent improvements in production techniques have made the newer botanical SRMs even more useful. It may also be interesting to note that average uncertainties for the certified values have continued to decrease with time, with the Tomato Leaves renewal SRM 1573a (1993) having the lowest uncertainties of all the botanical SRMs issued to date (all 15 elements above 1 mg/kg average $\pm 2.65\%$ relative uncertainty; all six elements below 1 mg/kg average $\pm 5.85\%$ relative uncertainty (both 1σ)).

Pettit and Horlick employed an automated DSI-ICP to determine Zn in powdered samples without any pretreatment other than weighing out the 30 mg sample[5]. The NIST SRM's included sub-bituminous coal (#1635), coal (#1632), orchard leaves(#1571), spinach (#1570), tomato leaves (#1573) and coal flyash (#1633). Drying and ashing of the botanical samples and the raw coals was carried out *in situ* just below the plasma discharge by programming the sample positioner. Typically the drying step took about 30 s and ashing 60 s. Results of the experiment indicated that quantitative results can be obtained for the analysis of powdered material for relatively volatile elements. The direct sample insertion technique can facilitate the analysis of many types of powdered sample forms with minimal pretreatment. With the automated sample presentation provided with the carousel-pneumatic delivery system, survey analytical data can be rapidly obtained for powdered samples.

Drying of powder in a desiccator at room temperature (approximately 22 °C) for 120 h over fresh anhydrous magnesium perchlorate was used here. The sample depth should not exceed 1 cm. Vacuum drying at room temperature and oven drying at elevated temperatures have resulted in excessive weight losses and therefore are not recommended.

5.42 Results and Discussion

NIST issued the first botanical reference material certified for elemental content in January 1971, as standard reference material 1571, orchard leaves. In the following years a total of nine additional botanical certified reference materials have been issued by NIST. Seven of these materials were used in this study. SRM 1572 Citrus Leaves was no longer available at NIST, and SRM 1573a Tomato Leaves was not purchased for this study.

The results for the determination of Zn, Cu in NIST SRM leaves are listed in Table 5.4. The calibration curves were constructed so that the concentration range of standard solutions covered the Zn and Cu concentrations in the samples. The experiment results were in good agreement with the certified values in most cases.

	Zn Concentration		Cu Concentration	
	NIST	Found	NIST	Found
Apple Leaves (SRM 1515)	12.5±0.3	12.6±1.8	5.64±0.24	5.22±0.43
Peach Leaves (SRM 1547)	17.9±0.4	19.8±4.3	3.7±0.4	3.1±0.5
Tomato Leaves (SRM 1573)	62±6	52.9±3.0	11±1	10.8±0.4
Pine Needles (SRM 1575)	67(*)	51.3±4.7	3.0±0.3	4.8±1.7
Spinach Leaves (SRM 1570)	50±2	49.2±2.1	12±2	13.2±0.8
Spinach Leaves (SRM 1570a)	82±3	70.8±5.9	12.2±0.6	14.2±1.0
Orchard Leaves (SRM 1571)	25±3	27.1±2.2	12±1	11.5±1.2

Table 5.4 Zn and Cu in NIST Standard Reference Material Leaves

(*) - Literature value

- Uncertainties of NIST values represent 95% confidence interval
- Uncertainties of found values represent ±1 standard deviation (n =3)

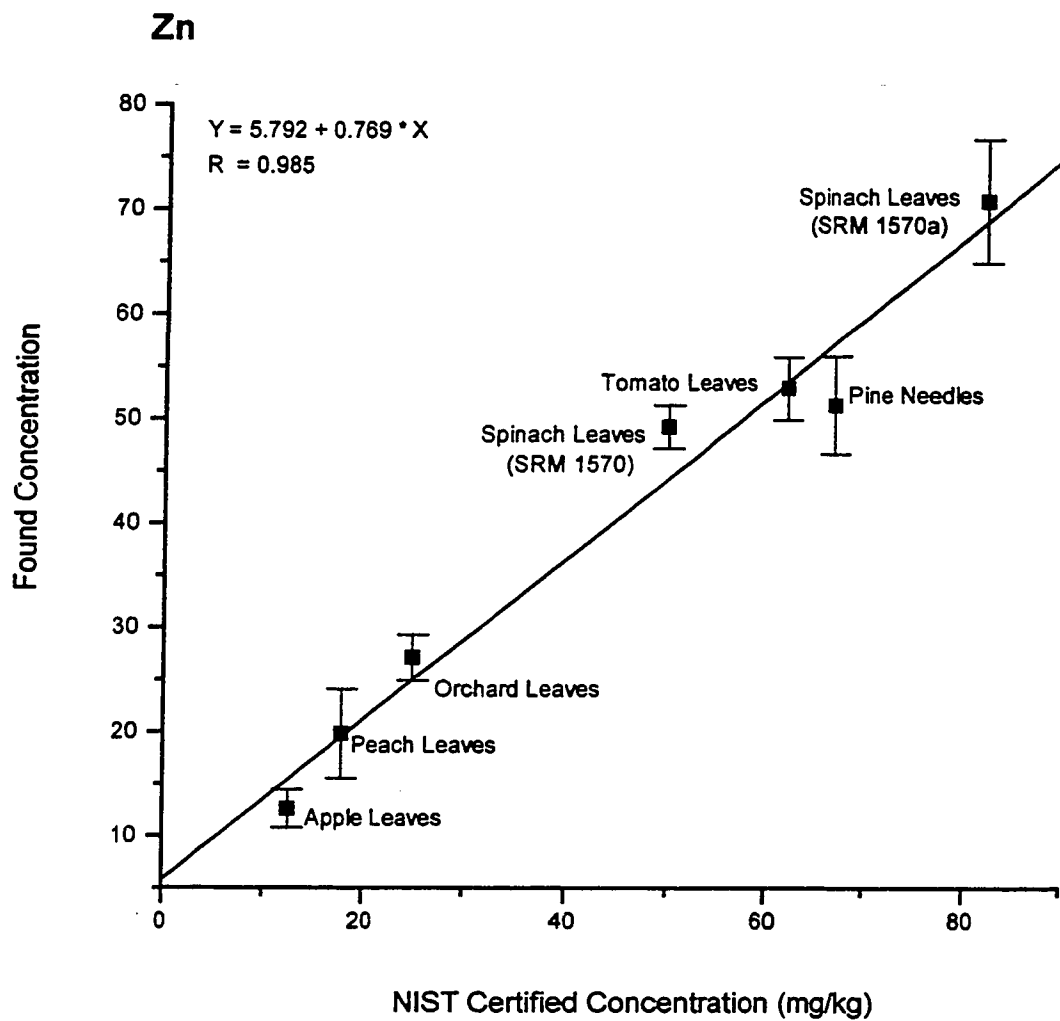


Figure 5.16 Zn concentrations in NIST Leaf SRMs

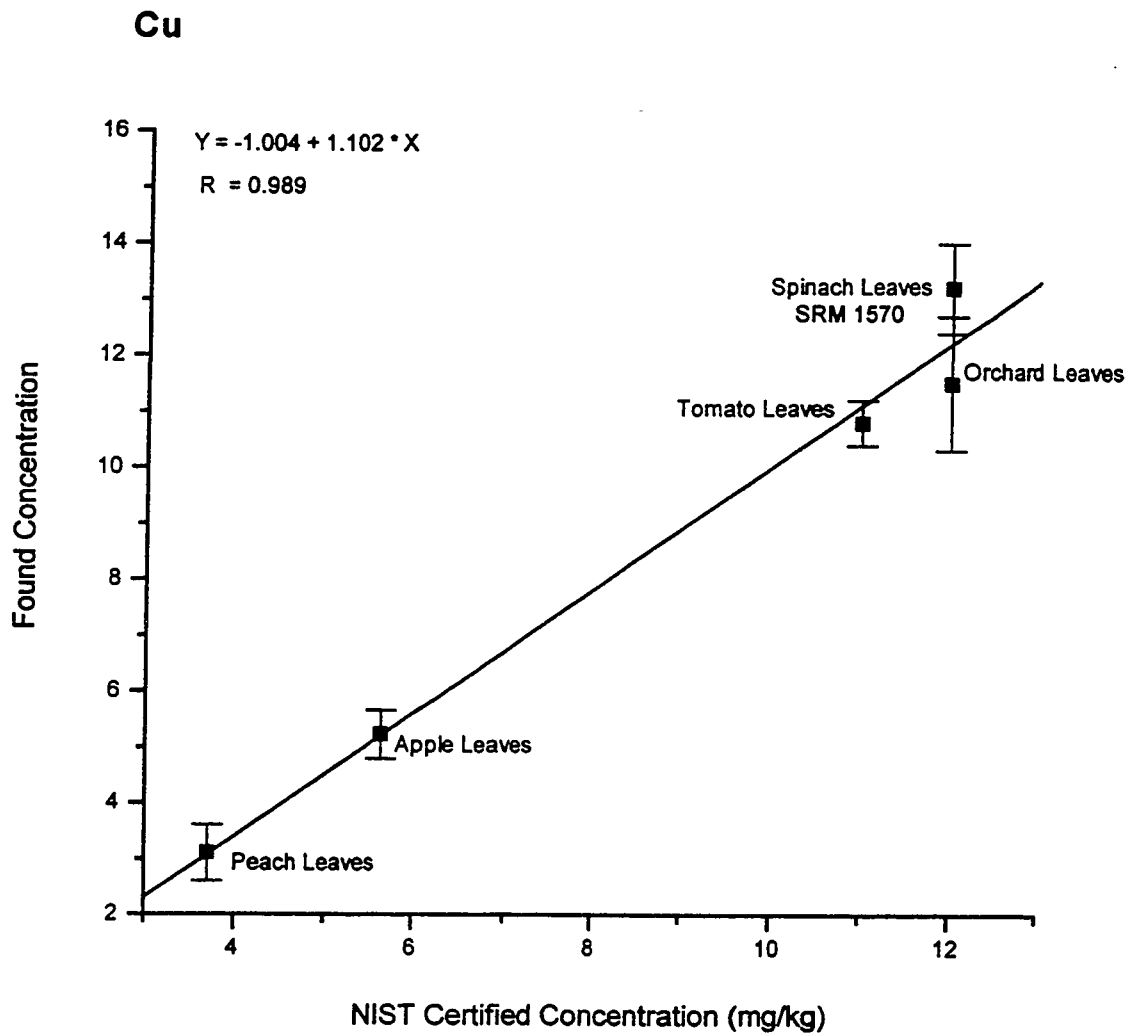


Figure 5.17 Cu concentrations in NIST Leaf SRMs

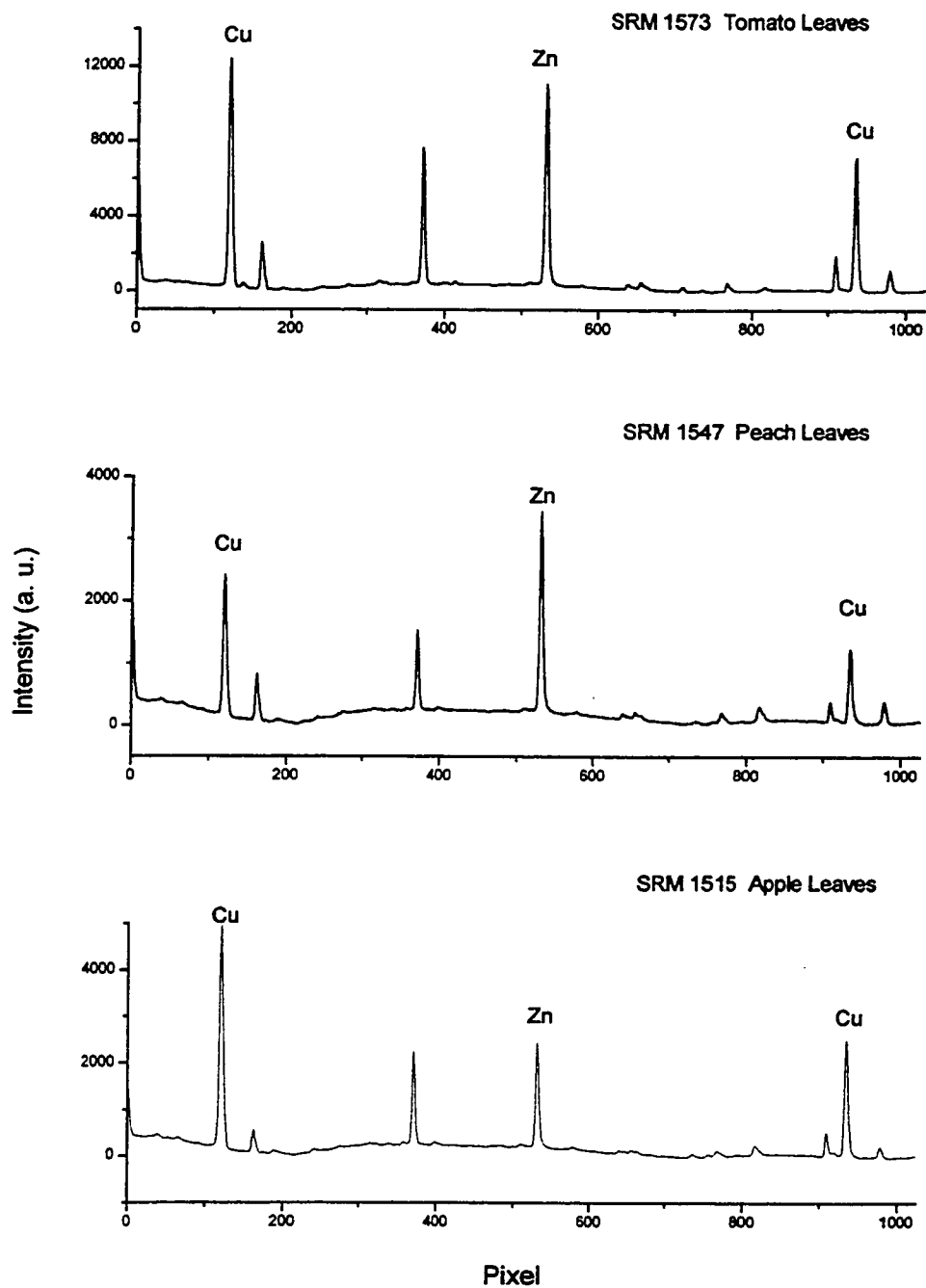


Figure 5.18 Zn and Cu spectra of NIST Leaf SRMs

The found results vs. certified values are plotted in Figures 5.16 and 5.17. The correlation coefficients were not as good as expected. The intercepts were also relatively high. The exact cause of the poor fit is not known. One reason may be the small concentration range. For Cu, the range is only from 4 ppm to 12 ppm. The spectra for SRMs 1573, 1547 and 1515 are presented in Figure 5.18. Cu and Zn were determined at the same time as spectral overlap was not a problem.

SRM 1570a Spinach Leaves is the replacement of the SRM 1570. It was felt that it would be interesting to test if the sample homogeneity was any different between these two materials.

5.5 Replicate Analysis of Spinach Leaves

Homogeneity refers to the spatial variation of the concentration of an element among different test portions taken from the material; good homogeneity is a prerequisite for the establishment of best estimate concentration values. The product is considered homogeneous with respect to the concentration of a given constituent if the measured concentration in a test portion of given mass is identical, within accepted uncertainty requirements, with the measured concentration in another test portion. Inhomogeneity reflects both natural variation and contamination introduced during preparation and handling. Although contamination, uniformly distributed throughout the bulk of the material, is generally of no consequence.

As homogeneity of one constituent does not imply homogeneity of another, each element must be separately characterized. Different masses of material should be taken in order to establish the minimum recommended mass and very precise analytical procedures must be employed. Multielement techniques such as instrumental neutron activation analysis (INAA) or atomic emission spectrometry (AES) as used for homogeneity estimations by Kratochvil et al. [22] and Griepink et al. [23] are efficient and desirable.

Replicate analyses of SRMs 1570 and 1570a are conducted. Variability of results of Zn and Cu in the leaves were presented in Figures 5.19 and 5.20. The RSDs of Zn and Cu for SRM 1570a were slightly higher than the RSDs for SRM 1570. By applying the

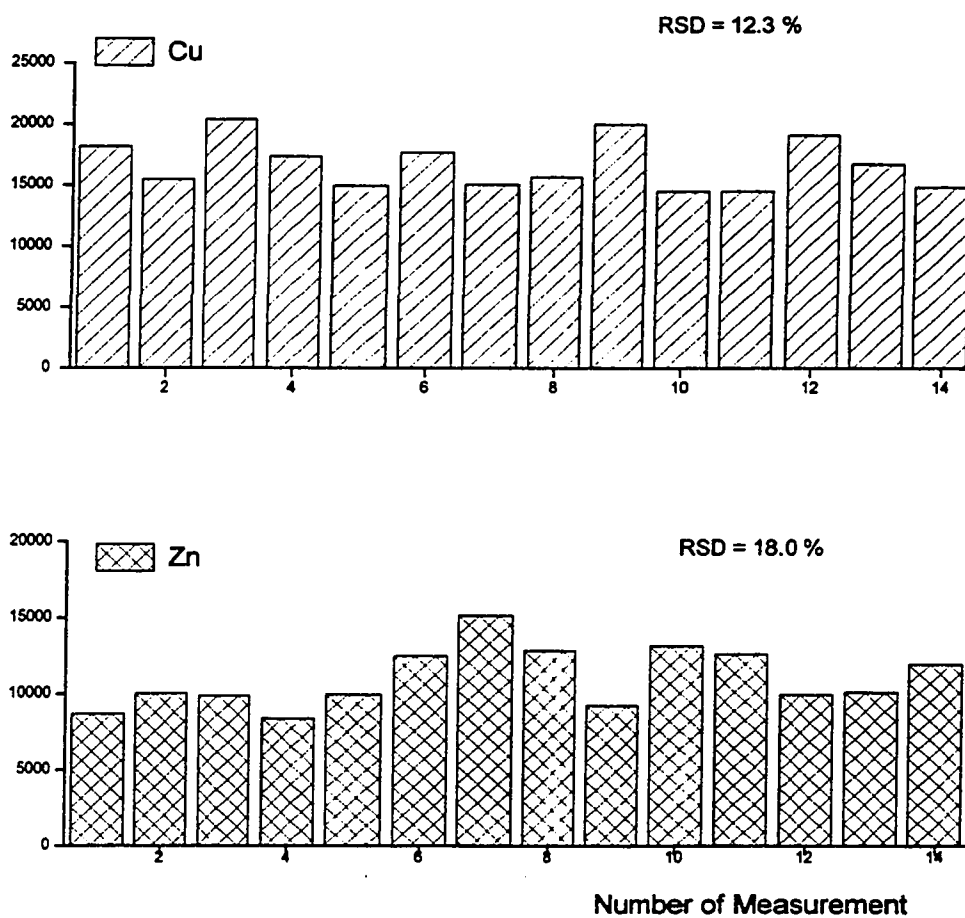


Figure 5.19 Variability of results for replicate determinations of Zn and Cu in NIST Spinach Leaves (SRM 1570a)

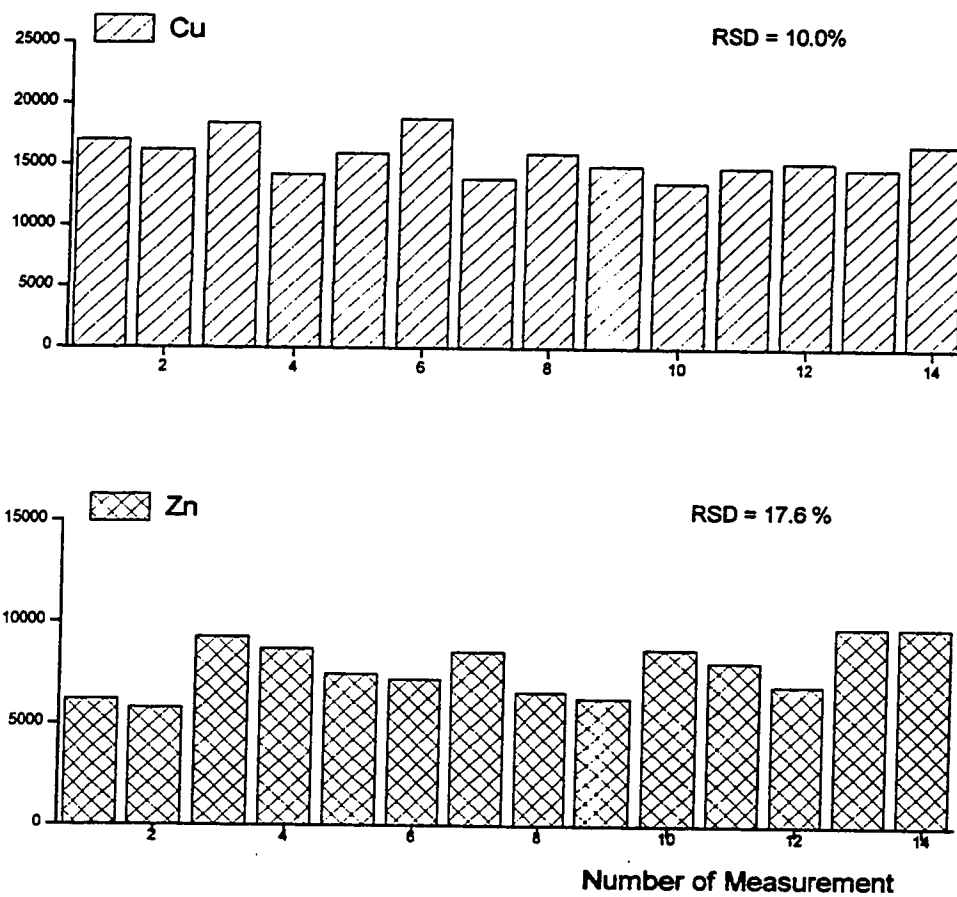


Figure 5.20 Variability of results for replicate determinations of Zn and Cu in NIST Spinach Leaves (SRM 1570)

F-test to the results, no significant differences (Variances) were found at 95% confidence level. The RSDs 10 -18% might be expected for such small test portion sizes (around 3 mg) in the spinach leaves. As discussed earlier, it is not expected that Zn and Cu would show heterogeneity in spinach leaves. This is because Zn and Cu usually do not exist in the grit while Cr, As and Al may concentrate in the grit.

5.6 Summary

During the course of this work, this automated direct sample insertion ICP has shown promise for volatile element determination in various sample matrices. Solution residues as an external calibration are applicable to the determination of volatile elements in many sample matrices. Although the precision and accuracy of the analysis results were not as good as the results obtained from solution nebulization, sample preparation, digestion and possible contamination were reduced or eliminated. The main limitation of the traditional nebulizer, inefficient sample introduction, has also been overcome. With an autosampler for handling the sample probes, it provides equivalent convenience for sample analysis as is found for normal solution analyses.

References:

1. C. W. Mcleod, P. A. Clarke and D. J. Mowthorpe, *Spectrochim Acta* **41B**, 63(1986).
2. M. Abdullah and H. Haraguchi, *Anal. Chem.* **57**, 2059 (1985).
3. M. Abdullah, K. Fuwa and H. Haraguchi, *Appl. Spectrosc.* **41**, 715 (1987).
4. Y. B. Shao and G. Horlick, *Appl. Spectrosc.* **40**, 386 (1986).
5. W. E. Pettit and G. Horlick, *Spectrochim. Acta* **41B**, 699 (1986).
6. V. Karanassios and G. Horlick, *Appl. Spectrosc.* **40**, 813 (1986).
7. W. T. Chan and G. Horlick, *Appl. Spectrosc.* **44**, 525 (1990).
8. G. Zaray, J.A. C. Broekaert and F. Leis, *Spectrochim. Acta* **43B**, 241 (1986).
9. X. R. Liu and G. Horlick, *J. Anal. At. Spectrom.* **9**, 833 (1994).
10. L. S. Ying, MS. Thesis, University of Alberta (1992).
11. R. R. Greenberg, J. S. Kane, T. E. Gills, *Fresenius J. Anal. Chem.* **352**,193(1995).
12. Certificate of Analysis, SRM 2689, 2690,2691, NIST, Gaithersburg, MD 20899, August 23, 1993.
13. Certificate of Analysis, SRM 2709, NIST, Gaithersburg, MD 20899, August 23, 1993.
14. Certificate of Analysis, SRM 2710, NIST, Gaithersburg, MD 20899, August 23, 1993.
15. Certificate of Analysis, SRM 2711, NIST, Gaithersburg, MD 20899, August 23, 1993.
16. M. Ihnat and M. S. Wolynetz, *Fresenius J Anal Chem* **345**, 185(1993).
17. J. Pauwels, U. Kurfurst, K. H. Grobecker, and P. Quevauviller, *Fresenius J Anal. Chem.* **345**, 478(1993).
18. D. A. Becker and T. E. Gills, *Fresenius J. Anal. Chem.* **352**,163(1995).
19. Certificate of Analysis, SRM 1570a, NIST, Gaithersburg, MD 20899, July 15, 1996.
20. Certificate of Analysis, SRM 1547, NIST, Gaithersburg, MD 20899, January 22, 1992.
21. Certificate of Analysis, SRM 1515, NIST, Gaithersburg, MD 20899, January 22, 1993.

22. B. Kratochvil, M. J. M. Duke and D. Ng, *Anal. Chem.* **58**, 102 (1986).
23. B. Griepink, H. Muntau and H. Gonska, *Fresenius J. Anal. Chem.* **319**,296(1984).

Chapter 6

Summary and Future Work

6.1 Summary

An Ar-O₂ mixed gas plasma with higher level of O₂ (20%) was studied with DSI-ICP for the determination of different elements in environmental samples. Satisfactory results were obtained for stack ash, kiln slag and landfill cell leachate. The Ar-O₂ mixed gas DSI-ICP-AES system could be readily used for a wide variety of applications in elemental analysis which are difficult and time consuming for other methods. Standardization for direct analysis of solid sample is always a challenging task. Partial matrix matched solution residue was found to be suitable for this application. The success of the experiment was mainly due to the usage of oxygen (20%) in the plasma operation. The amount of oxygen consumed the graphite cup along with the carried sample. As the result, the samples can be burned into the plasma efficiently to facilitate the direct determination of elements with different volatilities in hard to vaporize matrices. The samples used in the study included incineration kiln stack flyash, kiln slag, landfill cell leachate from a hazardous waste treatment plant. The results of these samples obtained from DSI-ICP were compared with the analyses results obtained from conventional solution nebulization ICP after microwave acid digestion. In general, the results were in good agreement between the two methods. Further, the O₂-Ar mixed gas DSI-ICP method was applied to analyze a series of standard reference soil and sediments. The experiment results indicated that four Canadian Reference Soil and several other NIST SRMs could be used as a solid calibration standards for analyzing samples with similar matrices. Linear calibration curves were obtained for Cr, Cu, Fe and Zn by using these reference materials. This method was applied to wear metal analysis in oil as well. Satisfactory results of Cr, Cu, Pb and V were also obtained from DSI-ICP as compared to the NIST certified value.

It is logistic to have a fully automated DSI-ICP to handle the sample analysis when a large number of analysis is required. As the sample cup can only hold milli-gram of sample each time, replicate analysis is often required if heterogeneity is present or

suspected. As the consequence, an automatic sample insertion system with a 24- sample holder tray was developed for the ICP in order to speed up the analysis and provide the consistency for each insertion. A simple car antenna was employed as an insertion driver. Insertion positions were controlled by a magnet and a Hall sensor. A dedicated computer with a window based custom made software was developed to control the autosampler sequences and synchronize data acquisition operation. Once the program is set, no attendant is required for the entire operation.

A dual use torch was developed to accommodate both conventional solution nebulization operation and direct sample insertion. By dropping or lifting a cap on the central tube of the torch, either solution or solid sample analysis could be performed on the single torch. The sensitivity and stability for the solution operation on the dual use torch are equivalent to the original set-up. The solution take up and wash out time are longer than the time required for conventional set-up. This could be further modified by optimizing the spray chamber position and the size of the cap.

It was soon found out that the new system could not handle high percentage of oxygen in the plasma due to the complicate electronic control system in the commercial instrument. The attention was then concentrated on the Ar plasma DSI operation for determination of volatile elements in various sample matrices. The system was optimized for observation position, power, ashing time etc. The multi-element capability of the spectrometer was limited by spectrum line leak though the mask. No more than five elements were determined simultaneously. Linear calibration curves for As, Cd, Cu, Mn, Pb and Zn were obtained. The average relative standard deviation for multiple analysis of solution residue was around 6% that showed good stability of the DSI operation.

The methodology was then used for determination of volatile elements in different matrices of NIST SRMs that included soil, ash, food and leaves. The analysis results indicated that the partial matched calibration solution residues could be valid for determination of volatile elements in these solid samples. In general, the results obtained from the DSI were in good agreement with NIST certified values. Multiple replicate analysis were done on the two spinach SRMs to access the sample homogeneity. No statistical differences were found for Zn and Cu in the leaves.

6.2 Future Work

One of the original goal of coupling an autosampler with Ar-O₂ mixed gas plasma was not accomplished here. This was mainly due to the modern electronically controlled torch box adapting the modification poorly. Therefore, the autosampler developed here has to be installed on the old type of torch box such as “Plasma-Thermo” torch box. With some work, it can be accomplished to fulfill the goal. However, the multi-element capability on the spectrometer is quite limited. Gain control for the data acquisition was also done manually. A better designed amplifier with on-board programmable gain amplifiers of wide range is needed for future work. Further development of software to combine the data acquisition and autosampler control is also necessary.

The PMT based simultaneous system has fixed wavelength and is difficult to do real time background correction. Solid-state detection system could be an ideal alternative to the PMT. Two type of the commercial systems are available. One is Perkin-Elmer’s Optima 3000 series, another is Thermo Jarrell Ash’s IRIS Advantage series. The difference between the two is in the type of CTD used for detection [1]. The Optima 3000 series instrument are equipped with a segmented-array CCD, which has fewer pixels than the IRIS, positioned only at the wavelengths of interest. The IRIS instruments have pixels at almost every wavelength, which allows them to read more than the Optima in any one sweep of the spectrum. Some DSI-ICP was done on the Optima 3000. It was found that the torch box could not handle high percent oxygen in the plasma either. It would be ideal to couple a old type of torch box to a cross dispersion echelle grating spectrometer with a CID array detector.

In ICP-AES, emission lines may suffer from spectral interferences, and selection of useful lines for trace analysis may be compulsory. In common practice, the presence of interferent lines is stated from tables of overlapping lines. However, with line-rich matrices at high concentration levels, or with analysis of high purities, weak lines from the matrix will show intensities comparable to the analyte signals. Many of these weak lines are not listed at all. As a consequence, tables are far from complete and it is dangerous to rely on table only. As a check for proper selection, it is good practice to measure at two analyte emission lines instead of one. Only if data from both lines results in equal concentration values within some acceptable limit (up to 10% difference), one can safely conclude to have full control over the interferences. With the new solid state detector, a lot of information is generated. An artificial intelligence expert system such as mathematical filter, neural network [2-4] would be very helpful to select lines and optimize the system.

ICP-MS has advantage of excellent sensitivity, nearly complete elemental coverage, isotopic information. It suffers isobaric interferences, sample matrix interference, and difficult with transient signals. Benefits of DSI in ICP-MS have been demonstrated by V. Karanassios and G. Horlick [5,6]. The absence of water and acids in the so-called dry plasma has resulted in a simplified background spectrum and a reduction in molecular species, particularly potentially interfering metal oxides. However, the rather slow scan speed with the current quadrupole mass spectrometer limited the multi-element capability. Recent advance of TOF-MS for the ICP could provide some benefits to couple the DSI-ICP with TOF-MS [7].

References

1. B. Erickson, *Anal. Chem.* **3**, 213A (1998)
2. E. H. van Veen, S. Bosch and M.T. C. de Looas-Vollebregt, *Spectrochim. Acta* **48B**, 1691, 1993
3. C. Schierle and M. Otto, *Fresenius J Anal Chem* **344**, 190 (1992)
4. W. Branagh, C. Whelan and E. D. Salin, *J. Anal. At. Spectrom.* **12**, 1307 (1997)
5. V. Karanassios and G. Horlick, *Spectrochim. Acta* **44B**, 1361 (1989).
6. V. Karanassios and G. Horlick, *Spectrochim. Acta* **44B**, 1387 (1989).
7. P. P. Mahoney, S. J. Ray, G. M. Hieftje, *Appl. Spectrosc.* **51**, 16A (1997).